To My Mother and Father

THE ELECTRONIC SPECTRUM OF CARBON DISELENIDE

THE ELECTRONIC SPECTRUM OF CARBON DISELENIDE

By

K. SRIKAMESWARAN, B.Sc., B.Sc.(Tech)., M.Sc.

A Thesis
Submitted to the Faculty of Graduate Studies
in Partial Fulfilment of the Requirements
for the Degree
Doctor of Philosophy

McMaster University
October 1968

DOCTOR OF PHILOSOPHY (1968)
(Chemical Physics)

McMASTER UNIVERSITY
Hamilton, Ontario.

TITLE: The Electronic Spectrum of Carbon Diselenide

AUTHOR: Srikameswaran Krishna Iyer,

B.Sc. (University of Bombay)

B.Sc (Tech)., (University of Bombay)

M.Sc. (University of Bombay)

SUPERVISOR: Professor G. W. King

NUMBER OF PAGES:

SCOPE AND CONTENTS:

The results of an investigation of the electronic absorption spectrum of carbon diselenide are presented. The synthesis of the compound from individual isotopes of selenium is described. Some new observations and results from a re-investigation of the infrared and Raman spectra are reported. The electronic absorption spectra of individual isotopic molecules were recorded and a detailed vibrational analysis of one of the observed systems in the spectrum has been made. The rotational structure of bands in this system has been examined. A preliminary study of two other systems are discussed. The spectra of carbon diselenide and the analogous carbon disulphide are compared and the similarity between the two spectra is shown.

ACKNOWLEDGEMENTS

I wish to express my thanks to Professor G. W. King for his advice, and gratitude for his encouragement during the course of my research work and the composition of this thesis.

I wish to express my thanks to Dr. A. E. Douglas of the National Research Council, Ottawa who made available invaluable experimental facilities for this research work.

I wish to express my thanks to Dr. W. J. Balfour, Mr. J. P. Bradford, Mr. E. J. Finn, Dr. J. L. Hencher, Dr. V. A. Job, Mr. K. G. Kidd, Mrs. H. E. Lock, Mr. J. O. P. McBride, Mr. P. R. McLean, Dr. D. C. Moule, Dr. A. W. Richardson and Mr. S. P. So and Mr. C. H. Warren who provided the necessary mental stimulation, experimental assistance and social climate during the period of my research work.

I am grateful to the Ontario Government for their grants of successive fellowships in the years 1966 to 1968.

I am grateful to Bhabha Atomic Research Centre, India for grants of special and extraordinary leaves of absence for the period 1964 to 1968.

I wish to express my thanks to Mrs. Michelle McLean and Mrs. Kamala Gurunathan for their arduous task of typing this thesis.

And finally, I wish to acknowledge the extraordinary efforts of my wife in pushing her husband through and past the pleasures and pains of a graduate student's life.

TABLE OF CONTENTS

Page

1. INTRODUCTION

2. EXPERIMENTAL

3. INFRARED AND RAMAN SPECTRA

4. ELECTRONIC ABSORPTION SPECTRA OF LINEAR SYMMETRIC TRIATOMIC MOLECULES :

Part A - THE R SYSTEM

LIST OF TABLES

LIST OF FIGURES

APPENDICES

CHAPTER 1

INTRODUCTION

1.1 General Theory

A polyatomic molecule consists of three or more nuclei and accompanying electrons held together predominantly by electrostatic interactions. The stationary states of this system, according to quantum mechanics, can be obtained from the time-independent Schroedinger equation

$$H_t \,|\Psi_t\rangle = E_t\, |\Psi_t\rangle \tag{1.1}$$

H_t represents the Hamiltonian operator for an isolated non translating molecule. If spin and relativistic effects are neglected, H_t is given by[1]

$$H_t = \frac{-\hbar^2}{2m}\sum_i \nabla_i^2 - \sum_\alpha \frac{\hbar^2}{2M_\alpha}\nabla_\alpha^2 + V_{ee} + V_{nn} + V_{ne} \tag{1.2}$$

The first two terms constitute the kinetic energy part of the Hamiltonian where ∇_i^2 is the Laplacian with respect to the i^th^ electron of mass m and ∇_α^2 is the Laplacian operator with respect to α^th^ nucleus of mass M . The remaining three terms V_{ee}, V_{nn} and V_{ne} constitute the internal potential energy of the molecule due to Coulombic interactions, and represent the inter-electronic repulsion, inter-nuclear repulsion and nuclear-electronic attraction terms respectively.

In principle, by solution of Schroedinger equation (1.1), energy eigenvalues E_t and corresponding eigenfunctions $|\Psi_t\rangle$ are obtained. The eigenfunctions represent the stationary states of the molecule. In practice, however, exact solutions are difficult to obtain and therefore, approximations are used. One such approximation was proposed by Born and Oppenheimer[2] and is based upon the large disparity between electronic and nuclear masses, m and M. In classical terminology, this disparity renders the heavy nuclei much slower in their movements with respect to those of the lighter electrons. For this reason the nuclei can be considered to be momentarily fixed, while the electrons are still in motion. Therefore the kinetic energy term due to the motion of the nuclei vanishes and V_{nn} is a constant. Under such conditions the electronic part of the Hamiltonian H_t can be written as

$$H_e = \frac{-h^2}{2m}\sum_i \nabla_i^2 + V_{ee} + V_{ne} \tag{1.3}$$

Its eigenvalues are represented by E_e and the corresponding eigenfunctions by $|\Psi_e(q_i, Q_\alpha)\rangle$, dependent on the coordinates of the electrons. Each $|\Psi(q_i, Q_\alpha)\rangle$ is also dependent on the nuclear coordinates Q_α as a parameter due to the V_{ne} term in H_e. The total Hamiltonian can now be written as the sum

$$H_t = H_e + H_n \tag{1.4}$$

where $H_n = -\sum_\alpha \frac{\hbar^2}{2M_\alpha}\nabla_\alpha^2 + V_{nn}$. In the zero order approximation of

Born and Oppenheimer[2], the total eigenfunction $|\Psi_t\rangle$ is written as a simple product

$$|\Psi_t\rangle = |\Psi_e(q_i, Q_\alpha)\Psi_n(Q_\alpha)\rangle \qquad (1.5)$$

where $|\Psi_e\rangle$ has been described above and $|\Psi_n\rangle$ is the nuclear component of the system depending only upon the coordinates of the nuclei. This product approximation has been shown to be valid under certain conditions[3,4]. One condition is that the ratio m/M should be small; another is that the functions which form the product should be nondegenerate[1]. By substitution of the product wavefunction in the Schrodinger equation (1.1), it can be shown[1,5] that

$$\left[H_n + E_e\ (Q_\alpha)\right]|\Psi_n\rangle = E_t|\Psi_n\rangle \qquad (1.6)$$

which is simply the Schrödinger equation for $|\Psi_n\rangle$. $|\Psi_n\rangle$ represents the stationary states of the nuclei. The Hamiltonian in this equation consists of the kinetic energy of the nuclei and the electronic energy of the molecule, at Q_α.

The total energy E_t of the system for a given state $|\Psi_t\rangle$ is given by the sum of the electronic energy E_e and the energy of nuclear motion E_n. That is,

$$E_t = E_e + E_n \qquad (1.7)$$

$|\Psi_n\rangle$, the nuclear wavefunction, is dependent only on the nuclear coordinates Q_α. If there are N nuclei in a polyatomic molecule, their positions are completely specified by

3N nuclear coordinates. By a proper 'choice' of 3N coordinates[6], the wavefunction $|\Psi_n\rangle$ can be approximated by the product of a vibrational wavefunction $|\Psi_v\rangle$, a rotational wavefunction $|\Psi_R\rangle$, and a translational wavefunction $|\Psi_{tr}\rangle$. The translational wavefunction can be ignored if the coordinates of the nuclei are defined relative to the centre of the mass of the molecule. The product is then given by

$$|\Psi_n\rangle = |\Psi_v \Psi_R\rangle \qquad (1.8)$$

It will be shown in section 3.1 that $|\Psi_v\rangle$ is a function of 3N-6 vibrational coordinates in a nonlinear molecule or of 3N-5 vibrational coordinates in a linear molecule. E_v represents the corresponding eigenvalue for this function $|\Psi_v\rangle$. It will be also shown that $|\Psi_R\rangle$ is a function of three rotational coordinates which describe the orientation in space of a set of rotating coordinate axes fixed in a nonlinear molecule. For a linear molecule $|\Psi_R\rangle$ is a function of two such coordinates. E_R represents the corresponding eigenvalue for $|\Psi_R\rangle$.

The total wavefunction for the molecule can therefore be approximated by

$$|\Psi_t\rangle = |\Psi_e \Psi_v \Psi_R\rangle \qquad (1.9)$$

and the total energy E_t is given by

$$E_t = E_e + E_v + E_R \qquad (1.10)$$

The 'spin' property[7] of electrons in the molecule has been neglected so far. When this property is taken into account, the electronic part[8] of the wavefunction can be approximated by the product $|\Psi_e \Psi_s\rangle$, where $|\Psi_s\rangle$ is a spin function dependent only upon coordinates in a hypothetical spin space. The product approximation $|\Psi_e\Psi_s\rangle$ is a valid approximation so long as there is no interaction between spin and orbital motion of the electrons. The total wave function now reads

$$|\Psi_t\rangle = |\Psi_e\Psi_s\Psi_v\Psi_R\rangle \qquad (1.11)$$

To obtain a better approximation to $|\Psi_t\rangle$ and E_t, additional terms should be added to the Hamiltonian in (1.1). Examples of these are terms due to spin-orbit interaction (H_{SO}), spin-spin interaction (H_{SS}) and interaction of the molecule with external fields (H_{ext}), etc. If these terms are small, standard methods due to perturbation theory[9] may be applied to obtain better approximation to $|\Psi_t\rangle$ and E_t.

1.2 Symmetry properties of eigenfunctions

In principle, each of the functions $|\Psi_e\rangle$, $|\Psi_v\rangle$ and $|\Psi_R\rangle$ and its corresponding eigenvalues E_e, E_v and E_R are obtained by solving an 'appropriate' wave equation[10]. In practice, the solutions $|\Psi_e\rangle$ of the 'electronic' waveequation (1.2) are difficult to obtain, except for simple molecules. However, for many problems in molecular spectroscopy, it is not necessary to know $|\Psi_e\rangle$ explicitly. From the symmetry properties of $|\Psi_e\rangle$, as well as those of $|\Psi_v\rangle$ and $|\Psi_R\rangle$, one can arrive at definite conclusions regarding some spectroscopic properties of the molecule. In the following chapters the use of symmetry properties of eigenfunctions in the classification of stationary states of the molecule and in the determination of selection rules for spectroscopic transitions will be illustrated.

The symmetry properties of eigenfunctions of a molecule are determined by the symmetry point group to which the molecule belongs. It is well known that each molecule can be classified under a symmetry point group according to the symmetry operations that can be performed upon its nuclei in their equilibrium positions. (For details of such classification, refer to, inter alia, King[7] and Hochstrasser[11]). That an eigenfunction of the molecule transforms as an irreducible representation of the symmetry point group, will be shown[1] presently. Since the total energy of a molecule in a stationary state must be invariant for any symmetry operation carried out on the molecule, the Hamiltonian must also be invariant. For any symmetry operator R, therefore, the following commutation rule holds

$$RH = HR \qquad (1.12)$$

which gives, for a nondegenerate state

$$HR|\Psi\rangle = RH|\Psi\rangle = RE|\Psi\rangle \qquad (1.13)$$

If $|\Psi\rangle$ is a normalized eigenfunction then this equation necessarily implies that

$$R|\Psi\rangle = \pm 1|\Psi\rangle \qquad (1.14)$$

The symmetry operation R, therefore, represents a one dimensional transformation matrix [1] or [-1]. This result holds for each symmetry operation R of the point group to which the molecule belongs. The eigenfunction must then transform as one of the one dimensional irreducible representations of the point group. Similar arguments could be used to show that degenerate eigenfunctions also transform as representations of higher dimension than unity. Each irreducible representation of a symmetry point group is denoted by a different symbol (Schoenflies notation)[1], in order to identify its transformation properties. This symbol, called the symmetry species, will be used hereafter to indicate the transformation properties of an eigenfunction of the molecule. Further, a general symbol $\Gamma(T)$ will also be used in this work to denote the representation (not necessarily irreducible) generated by the symmetry transformation of T, where T may be a function or a quantum mechanical operator. If the product resolution of (1.9) $|\Psi_t\rangle = |\Psi_e\Psi_v\Psi_R\rangle$ is valid, the symmetry species of each component function can be separately obtained. The overall symmetry of $|\Psi_t\rangle$ is given by the 'direct' product[1] representation which is written as

$$\Gamma(\Psi_t) = \Gamma(\Psi_e) \otimes \Gamma(\Psi_v) \otimes \Gamma(\Psi_R) \qquad (1.15)$$

The method of determining the symmetry species of $|\Psi_e\rangle$, $|\Psi_v\rangle$, and $|\Psi_R\rangle$ will be discussed in subsequent chapters with respect to a specific molecule. The direct product representation $\Gamma(\Psi_t)$, if reducible, can be written as a direct sum of irreducible representation[1]

$$\Gamma(\Psi_t) = n\Gamma_1 \oplus m\Gamma_2 \oplus l\Gamma_3 \oplus i\Gamma_i \oplus \qquad (1.16)$$

where i gives the number of times the irreducible representation Γ_i occurs in (1.16).

1.3 Origin and Intensities of Absorption Spectra

For each molecule, there exist a very large number possible stationary states $|\Psi_t\rangle$. If the molecule undergoes a transition from one state $|\Psi_i\rangle$ to another state $|\Psi_f\rangle$, there is a concomitant change in energy from E_i to E_f. This change can be expressed in terms of frequency thus,

$$\nu = \frac{E_i - E_f}{h} \qquad (1.17)$$

If $E_i > E_f$, electromagnetic radiation of frequency ν is spontaneously emitted by the molecule; if $E_i < E_f$, this radiation is absorbed. For such absorption, radiation of frequency ν must be incident on the molecule. Experimentally, this radiation is provided either by a source of radiation with a continuous range of frequencies or by monochromatic radiation of frequency ν. The absorbed radiation is observed as the absorption spectrum.

The transition from an initial state $|\Psi_i\rangle$ to a final state $|\Psi_f\rangle$ occurs by the interaction between the electromagnetic field associated with the incident radiation of frequency ν and the motion of electrostatic charges within the molecule. If the radiation field is included as a time dependent perturbation term in the Hamiltonian of equation (1.1) and applied to $|\Psi_i\rangle$ the probability of finding the molecule in the state $|\Psi_f\rangle$ can be determined[12]. Einstein[13] in 1917 expressed the probability of an absorption transition between two nondegenerate states in terms of a coefficient B_{if} which is given by

$$B_{if} = \frac{2\pi}{3\hbar^2} |R|^2 \qquad (1.18)$$

Here $|R|^2$ is called the transition probability and R is called the transition moment. $\vec{R}$ is expressed as the integral

$$R = \langle\Psi_f | P | \Psi_i\rangle \qquad (1.19)$$

P is an electric dipole, magnetic dipole, electric quadrupole, or a higher moment operator. In molecular spectroscopy, P is encountered most often as an electric dipole moment operator. Classically, the electric dipole moment of a system of charged particles is given by

$$\vec{P} = P_x\vec{i} + P_y\vec{i} + P_z\vec{k} \qquad (1.20)$$

where $P_x = \sum e_n x_n;\ P_y = \sum e_n y_n;\ P_z = \sum e_n z_n \qquad (1.21)$

$\vec{i}, \vec{j}, \vec{k}$ are unit vectors in Cartesian coordinates and e_n is the charge on the nth particle. The dipole moment operator is a polar operator[1] whose components transform as the x,y,z coordinates of the system. The magnetic moment operator is an axial vector[1] and transforms like a polar vector under rotations.

If $\vec{R}$ is nonzero at least for one of the components of $\vec{P}$, the transition between states $|\Psi_i\rangle$ and $|\Psi_f\rangle$ can occur. $\vec{R}$ therefore, represents the general selection rule for transitions between the two states. In the next section, specific selection rules are discussed in greater detail.

The intensity of a spectroscopic transition in absorption can be related to B_{if} above, the frequency ν of the incident radiation and the population of molecules N_i in the initial state $|\Psi_i\rangle$. If I^{if}_{abs} represents the intensity of absorption, this relationship is given by [14]

$$I^{if}_{abs} = I^{if}_{o} N_i B_{if} h \nu_{if} \Delta x \qquad (1.22)$$

Here, I^{if}_{o} is the intensity of incident radiation and Δx is the thickness of the absorbing layer of molecule in cm . B_{if} is determined by the transition probability $|\vec{R}|^2$. N_i, the number of molecules in a non degenerate state $|\Psi_i\rangle$ is given by the Maxwell-Boltzmann distribution law[15], thus

$$N_i = \frac{N \exp(-Ei/kT)}{\Sigma \exp(-Ei/kT)} \qquad (1.23)$$

where N is the total number of molecules, T is the absolute temperature and k is the Boltzmann constant.

For transitions between two 'electronic' states $|\Psi_n\rangle$ and $|\Psi_m\rangle$, the Einstein transition probability coefficient B_{nm} is related to a dimensionless function f_{mn} called the oscillator strength[7] by

$$f_{mn} = \frac{2\hbar mc\nu}{e^2} B_{nm} \qquad (1.24)$$

f_{mn} can be determined from experimental quantities. One of these quantities is the extinction coefficient ϵ_ν defined by the Beer-Lamberts' law[16]. The relationship between f_{mn} and ϵ_ν is given by[17]

$$f_{mn} = 4.317 \times 10^{-9} \times \int_{mn} \epsilon_\nu d\nu \qquad (1.25)$$

in absorption. In principle, f_{mn}, obtained from experimental quantities is substituted in equation (1.22) and B_{nm} is determined. The magnitude of the probability of transition i.e. $|\vec{R}|^2$ between states $|\Psi_m\rangle$ and $|\Psi_n\rangle$ is therefore obtained. For all possible transitions between an initial state m to a final state n that involve the excitation of a single electron, a sum rule defined by

$$\sum_{mn} f_{mn} = 1 \qquad (1.26)$$

holds.

1.4 Selection Rules

The probability of transition between any two states* $|\Psi''\rangle$ and $|\Psi'\rangle$ is determined by the square of the integral

---

*A' prime(') refers to the higher energy state and a double prime (") refers to the lower energy state of a transition.

$$\vec{R} = \langle \Psi' | \vec{P} | \Psi'' \rangle \tag{1.27}$$

If $\vec{R}$ is zero, the transition is forbidden. If $\vec{R}$ is nonzero the transition is allowed. Therefore the integral (1.27) determines the selection rule for transition between any two states $|\Psi'\rangle$ and $|\Psi''\rangle$. If $|\Psi'\rangle$ and $|\Psi''\rangle$ are explicitly known the integral can be evaluated and by substitution in equation (1.27) along with values of the other factors, the intensity of the transition can be determined. In practice, $|\Psi'\rangle$ and $|\Psi''\rangle$ are not often known explicitly. However, it can be established whether $\vec{R}$ is nonzero or not, from the symmetry properties of the two functions and those of the operator $\vec{P}$. For this purpose, the direct product of $\Gamma(\Psi')$, $\Gamma(\vec{P})$ and $\Gamma(\Psi'')$ is determined and reduced, if possible, to a direct sum of irreducible representations i.e.

$$\Gamma(\Psi') \otimes \Gamma(\vec{P}) \otimes \Gamma(\Psi'') = n_1\Gamma_1 \oplus n_2\Gamma_2 \oplus n_n\Gamma_n \oplus \tag{1.28}$$

It has been shown[1] that if at least one of the irreducible representations Γ_n in the direct sum is totally symmetric, $\vec{R}$ is nonvanishing. This condition can be used to determine whether a transition can occur between any two states $|\Psi'\rangle$ and $|\Psi''\rangle$. But, since the magnitude of $\vec{R}$ cannot be determined by this method, oscillator strengths f_{mn} determined experimentally are commonly used to assess the magnitudes of probabilities.

If $\vec{P}$ is assumed to be an electric dipole operator, and split into two parts[1], one due to the electron $\vec{P}_e$ and the other due to the nuclei $\vec{P}_n$ i.e.

$$\vec{P} = \vec{P}_e + \vec{P}_n \tag{1.29}$$

Therefore,

$$\vec{R} = \langle \Psi'_t | \vec{P}_e | \Psi''_t \rangle + \langle \Psi'_t | \vec{P}_n | \Psi''_t \rangle \tag{1.30}$$

If we also assume that the product resolution of (1.5) i.e., $|\Psi_t\rangle = |\Psi_e \Psi_n\rangle$ is valid, $\vec{R}$ can be written as

$$\vec{R} = \langle \Psi'_n | \Psi''_n \rangle \langle \Psi'_e | \vec{P}_e | \Psi''_e \rangle + \langle \Psi'_n | \vec{P}_n | \Psi''_n \rangle \langle \Psi'_e | \Psi''_e \rangle \tag{1.31}$$

For two different electronic states, $|\Psi'_e\rangle$ and $|\Psi''_e\rangle$ are orthogonal functions. Therefore $\vec{R}$ reduces to

$$\vec{R} = \langle \Psi'_e | \vec{P}_e | \Psi''_e \rangle \langle \Psi'_n | \Psi''_n \rangle \tag{1.32}$$

If, $|\Psi_n\rangle$ is written as a product of vibrational and rotational wavefunction i.e. $|\Psi_n\rangle = |\Psi_v \Psi_R\rangle$, the transition moment is given by

$$\vec{R} = \langle \Psi'_e | \vec{P}_e | \Psi''_e \rangle \langle \Psi'_v | \Psi''_v \rangle \langle \Psi'_R | \Psi''_R \rangle \tag{1.33}$$

When there is no transition between rotational states i.e. when $|\Psi'_R\rangle \equiv |\Psi''_R\rangle$

$$\vec{R} = \langle \Psi'_e | \vec{P}_e | \Psi''_e \rangle \langle \Psi'_v | \Psi''_v \rangle = \vec{R}_{e'e''} \langle \Psi'_v | \Psi''_v \rangle \tag{1.34}$$

The second factor in this integral is called the 'overlap' integral[14]. So, if $\vec{R}_{ee}$ is nonzero for at least one Cartesian component of $\vec{P}_e$ and the overlap integral is nonzero, a transition between $|\Psi'_e\rangle$ and $|\Psi''_e\rangle$ is possible. The transition is then an allowed electronic transition. The overlap integral determines the intensity distribution of the vibrational structure of the transition[14] and will be discussed in section (4.6). Sometimes, the molecule might change its symmetry on excitation. Then common symmetry species of $|\Psi'_e\rangle$ and $|\Psi''_e\rangle$ must be obtained with respect to the point group formed from elements in both states, before applying equation (1.34) for determination of selection rules.

If the product resolution i.e. $|\Psi_{ev}\rangle = |\Psi_e \Psi_v\rangle$ is not valid because of vibronic interaction, the transition moment reads

$$\vec{R} = \langle \Psi'_{ev} | \vec{P}_e | \Psi''_{ev} \rangle \neq \langle \Psi'_e | \vec{P}_e | \Psi''_e \rangle \langle \Psi'_v | \Psi''_v \rangle \quad (1.35)$$

Each state $|\Psi_{ev}\rangle$ is a vibronic state. Selection rules between vibronic states are determined by the direct use of equation (1.27). The symmetry species of each $|\Psi_{ev}\rangle$ i.e. $\Gamma(\Psi_{ev})$ is first determined by the product $\Gamma(\Psi_e) \otimes \Gamma(\Psi_v)$, (for justification of $\Gamma(\Psi_{ev}) = \Gamma(\Psi_e) \otimes \Gamma(\Psi_v)$, see reference 8). Then the direct product of $\Gamma(\Psi'_{ev}) \otimes \Gamma(\vec{P}) \otimes \Gamma(\Psi''_{ev})$ is determined to obtain the selection rule, as before. If a transition is not allowed electronically, it may be allowed as a vibronic transition. A transition allowed only by vibronic interaction is in general, less intense than an electronically allowed transition[18].

If each of the states $|\Psi'_t\rangle$ and $|\Psi''_t\rangle$ has a nonzero spin and if there is no spin-orbit interaction, then $|\Psi'_t\rangle = |\Psi'_e \Psi'_s \Psi'_n\rangle$ and $|\Psi''_t\rangle = |\Psi''_e \Psi''_s \Psi''_n\rangle$. The transition moment is given by

$$\vec{R} = \langle \Psi'_e | P_e | \Psi''_e \rangle \langle \Psi'_s | \Psi''_s \rangle \langle \Psi'_n | \Psi''_n \rangle \qquad (1.36)$$

$\vec{R}$ is zero unless $|\Psi'_s\rangle = |\Psi''_s\rangle$ due to the orthogonality of spin functions[8]. From this result, we get the selection rule $\Delta S = 0$. That is, the total spin does not change in an allowed electronic transition. But even if the spins are different in the two states, the transition may be allowed by spin-orbit interaction mechanism. In the presence of spin-orbit interaction, each function $|\Psi'_{es}\rangle$ and $|\Psi''_{es}\rangle$ may be written[8] in the form

$$|\Psi_{es}\rangle = |\Psi_e \Psi_s\rangle + \chi_{es} \qquad (1.37)$$

where χ_{es} represents a component function due to the interaction term. If this function is substituted in equation (1.27), $\vec{R}$ reduces to $\langle \Psi'_{es} | P_e | \Psi''_{es} \rangle$ The symmetry species of each $\Gamma(\chi'_{es})$ $[\equiv \Gamma(\Psi'_e) \otimes \Gamma(\Psi'_s)]$ and $\Gamma(\chi''_{es})$ $[\equiv \Gamma(\Psi_e) \otimes \Gamma(\Psi'_s)]$ are determined and the selection rule for the transition is determined from equation (1.8). If $\langle \chi'_{es} | P_e | \chi''_{es} \rangle$ is nonzero, then transitions between states with different spins i.e. $\Delta S \neq 0$ may be allowed. The intensity of transitions allowed because of spin-orbit coupling is also, in general, weaker than that of those allowed electronically without change of spin[18].

Selection rules for transitions between vibrational states and rotational states within the same electronic state (i.e. when $|\Psi'_e\rangle = |\Psi''_e\rangle$ are determined by the second term in equation (1.31). Since the first term is zero for $|\Psi'_n\rangle \neq |\Psi''_n\rangle$ in the same electronic state, $\vec{R}$ is given by

$$\vec{R} = \langle \Psi_n' | \vec{P_n} | \Psi_n'' \rangle = \langle \Psi_v' \Psi_R' | \vec{P_n} | \Psi_v'' \Psi_R'' \rangle \qquad (1.38)$$

where the product approximation $|\Psi_n\rangle = |\Psi_v \ \Psi_R\rangle$ of section 1.1 has been used. $|\Psi_v\rangle$ is a function of 3N-6 (or3N-5) molecule fixed vibrational displacement coordinates called normal coordinates, Q_k (discussed in Section 3.1) and $|\Psi_R\rangle$ is a function of 3 (or 2) space fixed coordinates X, Y, Z. The operator $\vec{P_n}$ cannot be separated completely into a space fixed coordinate component and a molecule fixed coordinate component. If P_X, P_Y, P_Z refer to the components of $\vec{P_n}$ along the space fixed axes X, Y, Z and P_x, P_y, P_z to the components of $\vec{P_n}$ along the molecule fixed axes x,y,z then we have the relation[19]

$$\begin{pmatrix} P_X \\ P_Y \\ P_Z \end{pmatrix} = \begin{pmatrix} \cos xX & \cos yX & \cos zX \\ \cos xY & \cos yY & \cos zY \\ \cos xZ & \cos yZ & \cos zZ \end{pmatrix} \begin{pmatrix} P_x \\ P_y \\ P_z \end{pmatrix} \qquad (1.39)$$

where the elements cos xX etc., are direction cosines between the two sets of axes. This relation can be written for each component of P thus

$$P_F = \sum \theta_{Fg} P_g \qquad (1.40)$$

where F = X, Y or Z and g = x, y or z. θ_{Fg} represents the direction cosines, and is a function of the vibrational coordinates.

If P_g is expanded in terms of the vibrational coordinates Q_k we have[19]

$$P_g = (P_g)_o + \sum_k^{3N-6} \left(\frac{dP_g}{dQ_k}\right)_{Q_k = 0} Q_k + \qquad (1.41)$$

Substitution of (1.41) and (1.40) into (1.38) gives the transition moment due to each component. (For details refer to Allen and Cross[19], 1963). For a transition between the same vibrational states i.e. for rotational transitions, the transition moment is written as

$$\langle \Psi'_v \Psi'_R | P_F | \Psi'_v \Psi''_R \rangle = \sum_g (P_g)_o \langle \Psi'_R | \theta_{Fg} | \Psi''_R \rangle \tag{1.42}$$

in which the orthogonality of the functions $|\Psi_v\rangle$ has been assumed. For simultaneous transition between pairs of vibrational and rotational states, the transition moment is given by

$$\langle \Psi'_v \Psi'_R | P_F | \Psi''_v \Psi''_R \rangle = \sum_g \langle \Psi'_v | P_g | \Psi''_v \rangle \langle \Psi'_R | \theta_{Fg} | \Psi''_R \rangle \tag{1.43}$$

Selection rules for rotational transitions and rotational-vibrational transition follow from expression (1.42) and (1.43) respectively. If the molecule has no permanent electric moment $(P_g)_0 = 0$ and therefore pure rotational transitions determined by expression (1.42) do not occur. But, if the molecule has a permanent moment selection rules for rotational transition are obtained[19] from the integral part of equation (1.42). Selection rules for vibrational transitions alone are determined by the first factor in expression (1.43). Let this factor be indicated by $R_{VV}^{'\,''}$. Therefore

$$R_{vv}^{'''} = \sum_{g} \langle \Psi_v^{'} | P_g | \Psi_v^{''} \rangle \qquad (1.44)$$

This integral can be established to be nonzero or zero by symmetry arguments which were discussed earlier.

In summary, methods of determining selection rules for electronic, vibronic, spin-orbit coupled, vibrational and rotational transition have been discussed in this section. These methods will be used subsequently in specific cases.

1.5 Types of Spectra

When molecules undergo simultaneous transitions between different pairs of stationary states, the absorption (or emission) spectrum consists of several frequencies. The pairs of stationary states participating in the transitions may be rotational, vibrational or electronic states; the pairs may also be combinations of these states (e.g. vibronic states). The resultant spectrum may be classified according to the type of states involved in the transitions. Three principal classes of spectra are briefly described below.

i) Rotational Spectra

Each molecule has three principal moments of inertia I_A, I_B and I_C which can be calculated from the bond distances and bond angles of the molecule. A molecule is classified as a spherical rotor, if all the three moments of inertia are equal; as a symmetric rotor, if two among the three moments of inertia are equal; and as an asymmetric rotor, if all three are unequal. A linear molecule is a particular case of a symmetric rotor, with the moment of inertia about the molecular axis equal to zero. The rotational states $|\Psi_R\rangle$ of each molecule may be approximated by 'appropriate' (spherical, symmetric or asymmetric)rotor functions. The eigenvalues E_R are expressed in terms of rotational constants A, B and C which are inversely proportional to I_A, I_B and I_C respectively, (see section 4.7). Selection rules between rotational states are determined by equation (1.42). Transitions between rotational states occur only if the molecule has a permanent dipole moment. Such transitions are accompanied by relatively small energy changes; the frequencies of radiation corresponding to the energy changes usually lie in the frequency range of 1000 - 300,000 megacycles/sec. In terms of wavelength, this range corresponds to 0.1-30 cm and is called the microwave region. The study of spectra of molecules in this region is termed microwave spectroscopy and yields data on rotational energy levels, moments of inertia and, in favourable cases, bond distances and bond angles of the molecule.

ii) Vibrational Spectra

The vibrational function $|\Psi_v\rangle$ of a molecule is a function of 3N-6 (or 3N-5) vibrational coordinates (section 1.2). It will be shown in section 3.1, that each $|\Psi_v\rangle$ can be approximated by a product of 3N-6 (or 3N-5) harmonic oscillator wavefunctions. The eigenvalues of each harmonic oscillator function is expressed in terms of a vibrational frequency ω_k and a vibrational quantum number v_k. Selection rules for transitions between vibrational states are determined by the first factor in equation (1.43); transitions between rotational states of each vibrational state occur simultaneously as determined by the second factor in the same equation. The observed spectrum therefore consists of frequencies corresponding to vibrational and superimposed rotational transitions. The frequencies in the spectrum are of relatively higher magnitude than those of pure rotational spectra. Experimentally, vibrational -rotational spectra of molecules are observed commonly in the 4000 - 40cm^{-1} region and are called infrared spectra. Analysis of the spectra gives the vibrational frequencies of the molecule. Because of restrictions imposed by selection rules (1.44) not all vibrational transitions can occur. Therefore, all the 3N-6 vibrational frequencies may not be obtained by a study of the infrared spectrum of the molecule. A complementary technique of observing vibration-rotation spectra is by Raman spectroscopy and will be discussed in section 3.5. In this technique, a monochromatic radiation of frequency ν_o is scattered by the molecule. In the scattered radiation, in addition to ν_o, frequencies $\nu_o \pm \nu_{vr}$ where ν_{vr} is the frequency corresponding to the energy difference between the two vibrational states, are observed. In favourable cases, by the analysis of both infrared and Raman spectra, all the 3N-6 (or 3N-5) frequencies of the molecule are obtained. These frequencies may be related to the strength of bonding (i.e. force constants) between the constituent atoms in the molecule.

iii) Electronic Spectra

The method of obtaining electronic eigenfunction $|\Psi_e\rangle$ and eigenvalues E_e will be discussed in section 4.1. Selection rules for transitions between any two electronic states are determined by equation (1.32). The energy difference between these electronic states have a wide range of values. The corresponding frequencies of transitions are of very large magnitude in comparison with those of either vibrational or rotational spectra. The observed spectrum for each transition may lie[16] in the infrared (25000 - 7500 Å), visible (7500- 4000 Å), ultra violet (4000 - 2000 Å) or in the vacuum ultraviolet (2000 - 20 Å) regions. In a given electronic transition, there are simultaneous transitions between vibrational and rotational states of each electronic state. From an analysis of the electronic spectrum, a variety of information, such as the shape of the molecule, vibrational frequencies, moments of inertia, etc., in both the combining states may be obtained. The data on vibrational frequencies and moments of inertia obtained in the ground state by the use of microwave, infrared and Raman techniques, are frequently very useful in analysing the electronic spectrum.

In the next section, an introduction to the spectroscopic problem dealt with in this thesis is given. Experimental techniques used in this work, are described in Chapter 2. Vibration-rotation spectra of carbon diselenide are dealt with in the Chapter 3 . In Chapter 4 and 5, the electronic spectrum of carbon diselenide is described.

1.6 Nature and Scope of the Present Work

Triatomic molecules are the simplest among polyatomic molecules. Extensive work has been done in the past in order to investigate their spectra, both experimentally and theoretically. A comprehensive list of such molecules which have been studied, as well as results obtained therefrom, has been compiled by Herzberg[8]. In this work, we shall confine our attention to one particular member of a group of triatomics represented by the molecular formula XCY. Here, C represents a carbon atom and X,Y either the same or different atoms (O, S, Se) belonging to the sixth group of the periodic table. Typical member of this group are CO_2 and OCS. Microwave spectra of OCS, OCSe and SCSe have been investigated by several workers[20,21,22,25,26]. CO_2 and CS_2 are symmetric linear molecules which do not have permanent dipole moments and therefore do not show pure rotational spectra. Infrared and Raman spectra of various XCY molecules of this type have been investigated[23]. One of the most frequently and thoroughly studied molecules is the Carbon dioxide (CO_2) molecule[27,28,29 & 30]. Similar investigations have been done on the SCS molecule also[27,31,32,33,34]. Wentink[23] studied the infrared and Raman spectra of not only CS_2 but also CSe_2, SCSe and SCTe molecules; furthermore, he predicted one of the vibrational frequencies in the unstable OCTe, SeCTe and CTe_2 molecules. The force constants in all these molecules have been reported[24]. A study of both vibrational and rotational spectra of these XCY molecules indicate that all of them are linear in their ground states. Internuclear distances r_{CX} and r_{CY} of some of these molecules, collected by Wentink[24] are given in Table 1-1 for further use.

The electronic spectra of OCO, SCS and OCS are well known. A general discussion of the spectra of the first two molecules has been presented by Herzberg[8] (1966). In each of these molecules, many spectral regions of absorption i.e. the so called 'systems', are known. Most of these systems lie in the vacuum ultraviolet and only a few of them have been investigated thoroughly. Very little is known about the spectra of three other members of the group i.e. OCSe, SeCSe and SCSe. The spectra of the first two molecules have been, however reported[35,36]. The spectra of other XCY molecules are not known.

In this work, a study of the spectra of carbon diselenide (i.e. CSe_2), one of the members of the XCY group, with X = Y, will be presented. The electronic absorption spectra of this molecule in the visible and ultraviolet regions were first reported by Callear and Tyerman[36,50]. During flash-photolysis studies on CSe_2 these authors observed and recorded the spectrum under low resolution. Four banded absorption systems were found. The first of these occurred in the far ultraviolet region at 2000Å. A second very strong one was observed at 2300Å region, and was reported to cause the decomposition of the CSe_2 molecule into CSe and Se fragments. The remaining two absorption systems were observed in the near ultraviolet at 3800Å and in the violet blue region at 4300Å. The latter system was also observed under somewhat higher resolution and found to consist of groups of line like heads. Callear and Tyerman[36] did not investigate the first, third and fourth of the above systems any further. The second system at 2300Å, however, was studied in detail in flash photolysis experiments. The spectral regions of absorption of CSe_2 mentioned above and those of CS_2 are indicated in Table 1-2. From this table it is seen that CS_2, an analogous member of the group, also has absorptions approximately in the same regions as those of CSe_2. Among these absorption spectra of CS_2, that at 4300 - 3300 Å has been analysed by Kleman[37],Liebermann[38], Douglas and Milton[39] and others[40,41]. The spectrum in the 3400 - 2900 Å region has not been analysed in as much detail as the 4300 Å system[37,40,42] and the spectrum in the 2200-1800 Å region has been investigated by Price and Simpson[43], Hauptman[44], Ramasastry and Rao[42] and Douglas and Zanon[45]. A comparison of the absorption systems of CS_2 and CSe_2 is discussed in Chapter 5. The purpose of the present work, given below, is to

i) synthesize CSe_2 from individual isotopes of selenium in order to obtain infrared, Raman and electronic absorption spectra;

ii) reinvestigate the infrared and Raman spectra and compare the results obtained with those of Wentink[23], whose work was limited by experimental difficulties;

iii) study in detail the electronic absorption system at 4300 Å and determine the nature of electronic states involved in the transition, the shape of the molecule in the excited state, the vibrational frequencies in both the states and any other information (Part 5.A)

iv) make a preliminary study on the absorption systems at 2300Å and 3800 Å,

v) compare the absorption systems of CSe_2 with those of CS_2 already investigated, and

vi) discuss the results on CSe_2 obtained in this work with respect to those obtained by Callear and Tyerman[36].

Other types of investigations have been made upon the CSe_2 molecule. Stiles et al[35] studied the effect of photolysis on CSe_2 by analysing its electron spin resonance spectra. They observed that solid phase CSe_2 samples reddened when irradiated with a Mercury lamp radiation (2537 Å), suggesting the formation of Se_2 molecules. The results of these irradiation studies showed that elemental selenium, selenium chains of the type $Se(Se)_nSe$, and polymers such as $(CSe)_n$ were formed. Brown and Whalley[46] studied the polymerization of CSe_2 and the structure of the polymer formed by infrared spectroscopy.

Table 1 - 1

INTERNUCLEAR DISTANCES (IN Å) IN SOME LINEAR XCY MOLECULES (GROUND ELECTRONIC STATE)

Molecule	*	r_{CO}	r_{CS}	r_{CSe}	r_{CTe}	r_{XY}	Ref.
CO_2	IR	1.162	-	-	-	2.324	47
OCS	M	1.164	1.559	-	-	2.723	20, 21
OCSe	M	1.160	-	1.711	-	2.871	22
CS_2	IR	-	1.555		-	3.109	32, 27
	UV	-	1.554		-	-	48
SCSe	A#	-	1.558	1.711	-	3.269	22
CSe_2	A	-	-	1.711	-	3.422	24
SCTe	M		1.557		1.904	3.461	49

*Method of measurement:

IR = Infrared spectrum
M = Microwave spectrum
UV = Ultraviolet Spectrum
A = Assumed value

Assumed value which gives the best calculated values of rotational frequencies; for details refer Wentink[24].

Table 1 - 2

ABSORPTION SYSTEMS IN CS_2 AND CSe_2

Designation	Region (Å)	
	CS_2	CSe_2
$\tilde{a} - \tilde{X}$	4300 - 3300*	4800 - 3900
-	3400 - 2900	4000 - 3500
$\tilde{A} - \tilde{X}$	2200 - 1800**	2600 - 2150
$\tilde{C} - \tilde{X}$	1780 - 2150	2150 - ?

* $\tilde{a}$ is a $^3A_2(B_2)$ state; the molecule is bent in this state[37].

** $\tilde{A}$ is a $^1B_2$ state; the molecule is bent in this state[45].

CHAPTER II

Experimental

2.1 Synthesis of Carbon diselenide from natural Selenium.

Two methods are available for the synthesis of carbon diselenide. The first method is the interaction of hydrogen selenide gas with carbon tetrachloride vapour in a hot pyrex tube at 500°C (Grimm et al,[51] 1936). The second method is the reaction of methylene chloride vapour with molten selenium at 550°C (Ives and Pittman,[57] 1947). The overall reactions are:

$$CCl_4 + 2H_2Se \xrightarrow{500\ ^\circ C} CSe_2 + 4HCl$$

$$CH_2Cl_2 + 2Se \xrightarrow{550\ ^\circ C} CSe_2 + 2\ HCl$$

Some properties of carbon diselenide, which are of importance in the present work, are given in Table 2-1.

Ives et al[52] reported that the yield (about 52%) of diselenide in the second method was much higher than that by the first method. Hence, the method of Ives et al was adopted in this work. Fig. 2-1 is a schematic illustration of the apparatus used in the synthesis of carbon diselenide. A stream of nitrogen gas was bubbled through methylene chloride (Fischer reagent grade) liquid at room temperature. The resultant mixture of nitrogen gas and methylene chloride vapour was passed over molten selenium (Analar Reagent grade) at red heat.

Table 2 - 1

PROPERTIES OF CARBON DISELENIDE

i)	Colour:	Golden yellow
ii)	Physiological:	Obnoxious odour; a few mg left exposed contaminates an entire room; reported to be lachrymatory and carcinogenic.
iii)	Melting point:	-45.5°C.
iv)	Boiling point:	125°C.
v)	Solubility:	Dissolves in carbon disulphide, carbon tetrachloride, methylene chloride, grease and hydrocarbon oils. Forms constant boiling mixtures with its solvents.
vi)	Other:	Reactive; decomposes on mercury surface; sensitive to light; turns brown and finally black on standing.
vii)	Vapour pressure[52]:	T °C 0 10 20 30 50 P mm 4.7 7.7 13.6 23.3 58.3

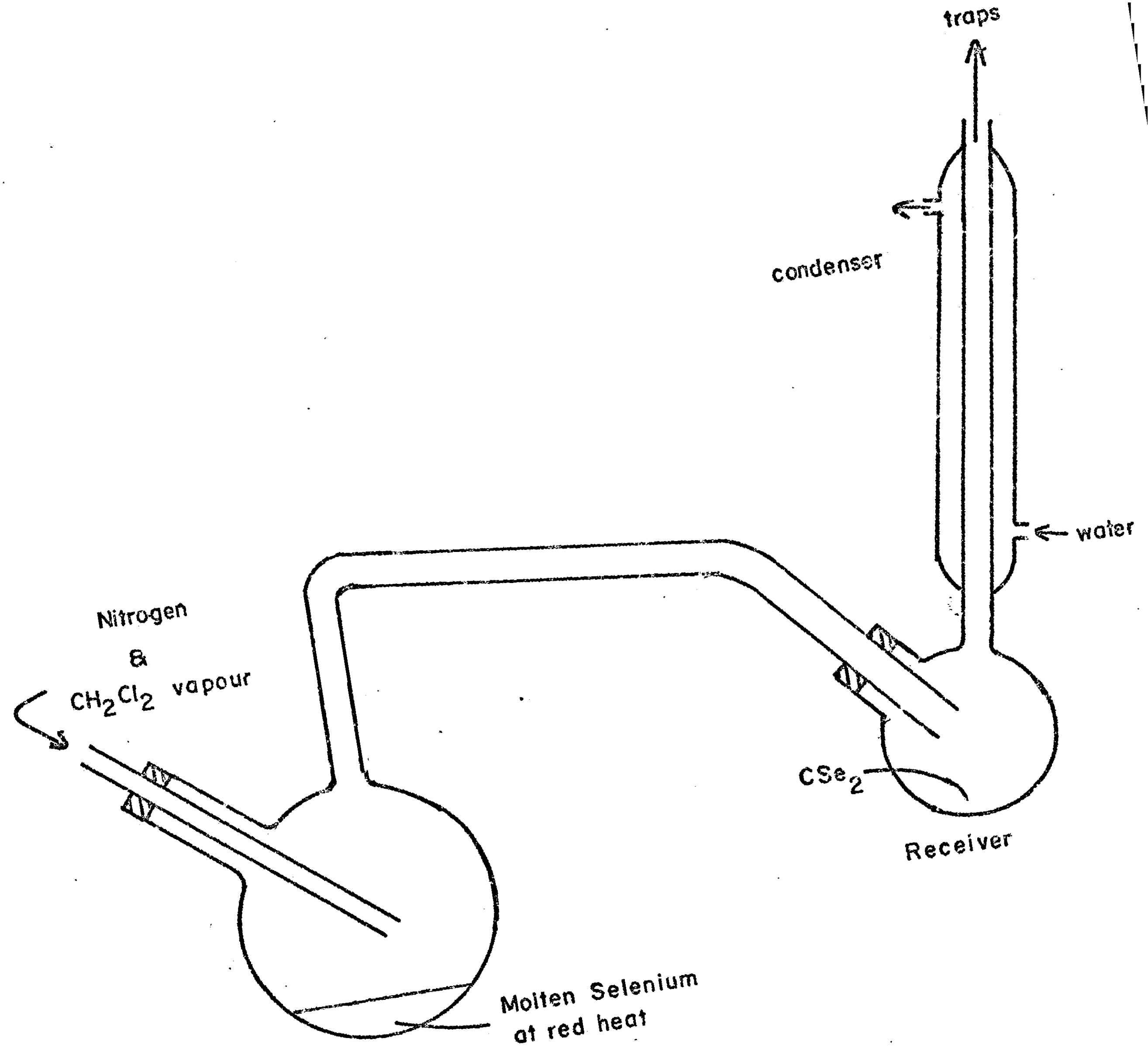

SYNTHESIS OF CSe_2 – FROM NATURAL SELENIUM

FIGURE 2.1

A solution of carbon diselenide in methylene chloride was condensed in the receiver. The solution was filtered to remove residual selenium and the filtrate was concentrated by fractional distillation at atmospheric pressure. Most of the methylene chloride distilled over at 42°C. The residual carbon diselenide fraction was stored at dry ice temperature (-78°C), for subsequent use.

2.2 Synthesis of Carbon Diselenide from Selenium Isotopes.

The method of Ives et al was used in the preliminary work but was modified subsequently for the following reasons: Firstly, it was necessary to synthesize CSe_2 from mg quantities of pure isotopes of selenium. The method of Ives et al, described earlier, was unsuitable not only because it required gram quantities of selenium, but also because substantial amounts of the element were lost in the form of a fine deposit all over the apparatus used.

Secondly, CSe_2 is toxic and has a penetrating offensive odor, (Table 2-1): it was therefore essential to work with the compound in completely closed systems. Apparatus equipped with stopcocks could not be used because CSe_2 dissolved in the stopcock grease and leaked out.

A new procedure was therefore devised for the synthesis and is described below.

Isotopes Se^{80}, Se^{78} and Se^{77} (obtained from Oak Ridge National Laboratory of the United States Atomic Energy Commision) were used in the synthesis; they had an isotopic purity of 97%, 96% and 87% respectively. Fig. 2.2 is a schematic illustration of the apparatus used. 15 mg of one of the selenium isotopes was introduced into each of the two thick walled pyrex reactor tubes shown. Methylene chloride (Fisher reagent grade) liquid, held in a reservoir, was solidified by surrounding it with a dewar containing liquid nitrogen. With stopcocks A and B open, the reactor tubes and the reservoir were evacuated. Stopcock A was then closed and the reservoir was allowed to warm up to room temperature. With stopcock B closed, the methylene chloride was transferred under vacuum into the reactor tubes which were surrounded by dewars containing liquid nitrogen. Each of the reactor tubes was then sealed off at the constrictions C shown, allowed to warm up to room temperature and then heated to redness at end D with a 'Meker' burner. Yellow droplets of CSe_2, along with selenium vapour were observed to condense on the cooler sides of the reactor near point E. After a few minutes of cooling, the reactor was heated at E to consume any of the deposited selenium. The process of heating the reactor at points where selenium is deposited was repeated till no red deposits of selenium were visible. The absorption cell was then evacuated through stopcock F and sealed off at constriction G. The break seals were destroyed with Teflon coated iron breakers. The side arm on the absorption cell was then immersed in liquid nitrogen; CSe_2 from the reactor tubes was thereby condensed in the side arm. The reactors were sealed off at constrictions H and disconnected from the cell.

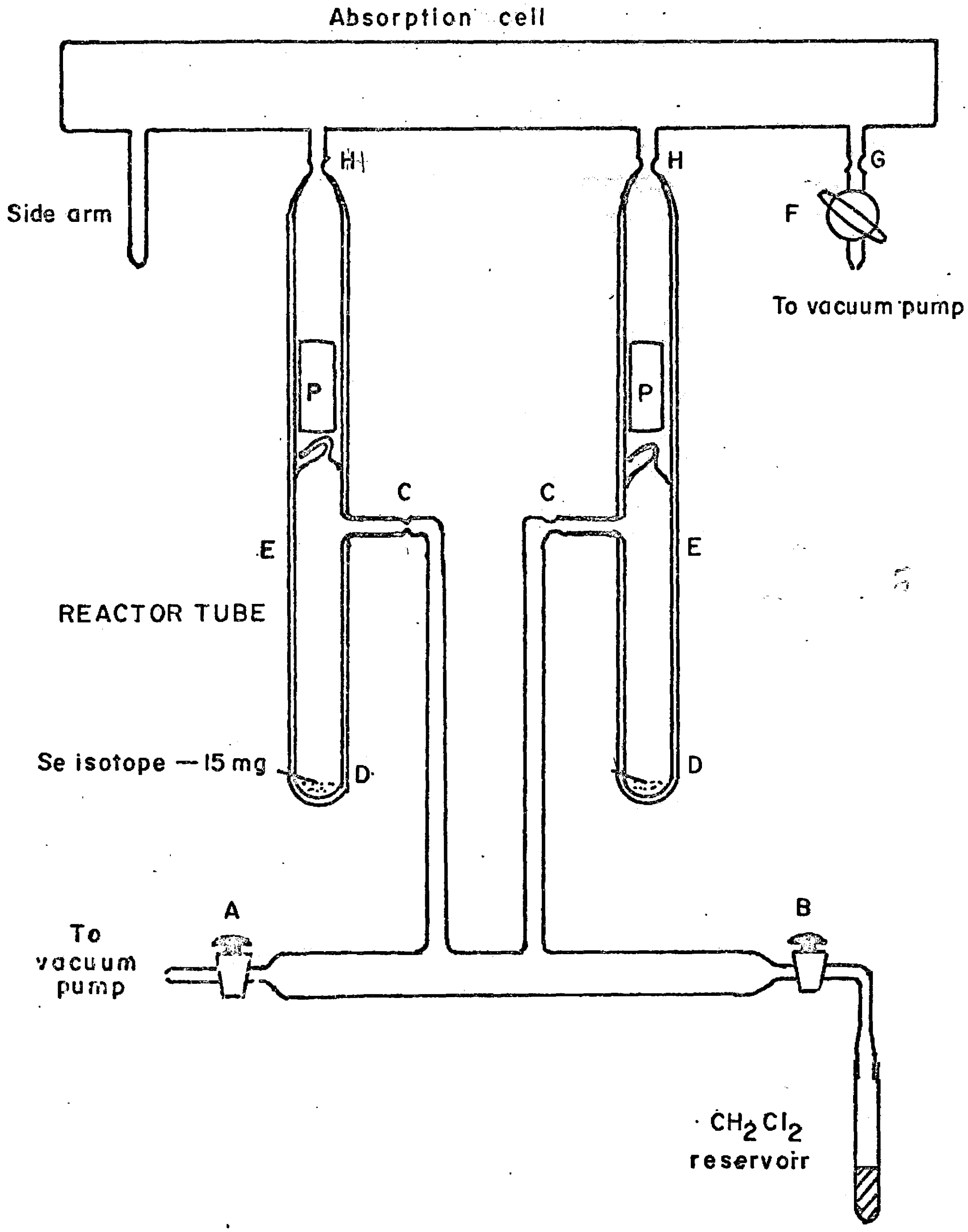

SYNTHESIS OF CSe_2 — FROM SELENIUM ISOTOPES

FIGURE 2.2

By this method, not even trace amounts of CSe_2 were released into the atmosphere. Odour and toxicity problems were entirely avoided. Milligram quantities of selenium isotopes were adequate to synthesize enough quantities of the compound for most of the present spectroscopic work. However, the exact amount of carbon diselenide formed in each reactor tube was unknown. From the quantity of selenium used (15 mg), volume of methylene chloride condensed in each reactor tube (.3 ml) and the efficiency of the reaction (52% yield), an estimate of the concentration of CSe_2 in CH_2Cl_2 solution was obtained. The maximum concentration of CSe_2 in the reaction was about 3g/ liter of CH_2Cl_2. The solution of CSe_2 obtained by this method was not purified or concentrated. The solvent CH_2Cl_2 was, as expected, the major impurity, as judged from infrared, Raman and ultraviolet spectra. It will be seen in sections 3.8 and Chapter 5 that the spectra of methylene chloride did not interfere with the interpretation of CSe_2 spectra.

Several types of cells, filled with vapour of CSe_2 (and CH_2Cl_2), were used in recording spectra;

i) Quartz cells 5 and 10 cm long and 2.5 cm diameter, provided with quartz windows.

ii) Pyrex cells 5 and 10 and 50 cm long and 2.5 cm diameter, with sealed-on pyrex windows.

iii) Pyrex cells 1.8 m long and 11 cm diameter, provided with ground flanges at either end. Flat pyrex windows were glued on to these ends with'Dekhotinsky' cement.

iv) Cells for infrared spectra, 10 cm long and 5 cm diameter provided with KBr windows or polyethylene windows.

The pressure of CSe_2 vapour in each cell was not measured. Mercury and oil manometers could not be used for measurement of pressure in the cells since CSe_2 attacked mercury and dissolved in oil. The partial pressure of CSe_2 in each cell (other than that in the 1.8 m cell) was assumed to be equal to its vapour pressure at room temperature, because some droplets of CSe_2 solution were always present in these cells at this temperature. The smaller cells were stored in a refrigerator (at3°C) when not in actual use. The larger 1.8 m cell was used immediately after filling it with the vapour of CSe_2.

Four isotopic CSe_2 molecules were studied in this work viz., $Se^{80} - C^{12} - Se^{80}$, $Se^{78} - C^{12} - Se^{78}$, $Se^{77} - C^{12} - Se^{77}$ and $Se^{78} - C^{12} - Se^{80}$. For convenience, these molecules will be indicated by the notations 80-80; 78-78; 77-77 and 78-80. The molecule obtained in the synthesis from natural selenium will be denoted by N-N. 78-80 was synthesized from a 1:1 w/w mixture of Se^{80} and Se^{78} isotopes and CH_2Cl_2 vapour, and therefore the product contained 80-80 and 78-78 also.

2.3 Infra Red Spectra

The infrared spectrum of carbon diselenide was examined with a Perkin Elmer Model 521 grating spectrophotometer in the region 4000 - 250 cm^{-1} and a Perkin-Elmer model 301 grating spectrophotometer in the 250 - 90 cm^{-1} region.

In the 4000 - 400 cm^{-1} region, the spectra of N-N, 80-80 and 78-78 molecules were obtained in 10 cm long cells with KBr windows. In the 400 - 90 cm^{-1} region, 10 cm long cells with polyethylene windows were used. Spectra of carbon tetrachloride, chloroform and methylene chloride vapour were also recorded with the same cells. These spectra were compared with the spectrum of carbon diselenide in order to ascertain whether these compounds were present as impurities in carbon diselenide. All spectra were recorded at room temperature.

The vacuum wavelengths of absorption bands were determined with respect to the vacuum wavelengths of absorption peaks due to a thin polystyrene film and atmospheric water vapour[53]. The uncertainty in measured frequencies is about 1 cm^{-1}.

2.4 Raman Spectra

Raman spectra of N-N, 80-80 and 78-78 were obtained with a Spex model 1400 - 11 Raman Spectrophotometer equipped with a 50 mW Spectra-Physics Model 125 Helium - Neon Laser source.

Solution samples of carbon diselenide, sealed in melting point tubes (2 mm dia), were used. Plane polarized laser radiation (at 6438 Å) was focused on the sample. Scattered radiation perpendicular to the incident beam was passed through a condenser lens into the Spex monochromator (a Czerny-Turner grating instrument). The output of the monochromator was detected by a photomultiplier (ITT Model FW-130); the response of the photomultiplier was amplified and recorded graphically as a function of wavelength on a linear scale and constituted the Raman spectrum. When necessary, an analyser which could be rotated by 90° about the optic axis was introduced in the path of the scattered beam between the sample and the monochromator. Spectra of the CSe_2 samples were recorded without the analyser, with the analyser oriented to transmit the incident plane polarized radiation and with the analyser perpendicular (90°) to this direction. After passing through the analyser, the radiation was completely depolarized by a "scrambler" before entering the slit of the monochromator.

Comparison spectra of liquid carbon tetrachloride, chloroform and methylene chloride were recorded. The wavelengths of each of the observed Raman bands were obtained from previously calibrated wavelength counter on the instrument. These wavelengths were converted to vacuum wavenumbers. The displacement in wavenumbers of each of these bands with respect to the wavenumber corresponding to 6438 Å was obtained. The uncertainty in wavelength measurements were about 1 Å and therefore the uncertainty in the wavenumber in this region was about $\pm$ 3 cm^{-1}.

2.5 Low Resolution Electronic Spectra

The absorption spectrum of CSe_2 vapour was recorded at room temperature on each of three low resolution instruments; a Cary (model 14) spectrophotometer, a Baush & Lomb 1.5 m concave grating (model 11) spectrograph and a Hilger Large Quartz (model 492) Prism spectrograph. With the Cary instrument, 5 and 10 cm quartz cells were used to scan the 2000 - 1850 Å region. The spectra of 80-80 solutions in liquid CH_2Cl_2 at 0.002 M concentration were also observed with this spectrometer in the 5000 Å - 3100 Å region. A 1 cm long pyrex cell, which could be sealed off to prevent the odour of CSe_2 from escaping and the solution from evaporating, was used. The solution was successively diluted with equal volumes of methylene chloride to record the spectrum at three different concentrations. Blank spectra of gas and liquid phase methylene chloride were also recorded.

The B & L and Hilger spectrographs were used to record spectra on photographic plates, with 5, 10 and 50 cm long pyrex and quartz absorption cells. Either a 250 W Xenon arc (Osram XBO high pressure lamp) in the ultraviolet or a tungsten filament lamp (6 watts) in the visible was used as sources of continuous radiation. Exposure times were of the order of 1 to 10 seconds. The B & L spectrograph was used in the 7600 - 3800 Å region, at a first order resolution of 30,000. The Hilger spectrograph was used for recording the spectra in the 4000 - 3400 Å and 2800 - 2200 Å regions.

2.6 High Resolution Electronic Spectra

In order to examine their vibrational and rotational structure in fine detail, the absorption bands of both natural and isotopic CSe_2 molecules were recorded on high resolution spectrographs in the 4800 - 3400 Å region. Pyrex cells, 10 and 50 cm long, were used to contain the vapour at room temperature.

One of the spectrographs used extensively was a 20 ft Ebert stigmatic plane grating spectrograph. The dispersion in the 4300 Å region was about 0.67 Å/mm and the resolving power in the first order was about 150,000. At slit widths of 30 μ to 50 μ, exposure times of the order of 15 sec to 3 minutes were necessary with a 250 W Xenon lamp source. Spectra were recorded on 35 mm Kodak SA - 1, Kodak Tri-X and Ilford FP-3 films. The alignment of the source absorption cell and the spectrograph optics was done using an OTT (model 170) 0.3 mW Helium-Neon Laser.

During the course of this work, certain bands were also photographed on a 35 ft astigmatic Eagle type concave grating spectrograph and a 35 ft Ebert spectrograph located at the National Research Council, Ottawa.* With the Eagle instrument, the 4800 - 3400 Å region was photographed in the 3rd order at a dispersion of 0.4 Å/mm and a resolution[54] of about 250,000. A Lyman flash discharge lamp and a tungsten filament lamp were used to record the spectrum, with a slit width of 20 μ. Exposure times ranged from 2 minutes to 15 minutes. Kodak I - 0 and II - 0 plates of dimension 18" X 2" were used.

---

*We are indebted to Dr. A. E. Douglas of the National Research Council of Canada, who permitted the use of these spectrographs.

A few selected bands of the 80-80 molecule were recorded* on the 35 ft Ebert spectrograph in the 13th, 14th and 15th orders with a Xenon lamp source at a slit width of 30 μ. The dispersion was approximately 0.1 Å/mm and the resolution about 600,000 in the 4300 - 3800 Å region.

2.7 Temperature work

The effect of temperature on the intensity of absorption bands in the 4800 - 3500 Å region was determined over a temperature range of - 42°C to 190°C.

In one typical set of experiments, the spectrum of 80-80 vapour was recorded at 22°C, 100°C and 190°C with a 20 ft Ebert spectrograph described in the last section. A 50 cm long absorption cell containing the compound was heated by a furnace made out of a 75 cm long, 40 mm diameter pyrex tube which was wound with nichrome wire and lagged with asbestos. The temperature of the interior of the furnace was measured with a mercury bulb thermometer.

In a second set of experiments, the spectrum of 80-80 vapour was obtained at - 78°C, -42°C, 22°C and 110°C with the Baush & Lomb and Hilger spectrographs. The vapour pressure of CSe_2 at -78°C and -42°C was too low to record a spectrogram from a 50 cm cell. The path length was therefore increased

---

*We thank Mr. F. A. Alberti of the National Research Council of Canada who photographed the bands using the absorption cells supplied by us.

using a 1.8 meter long cell provided with pyrex windows at either end. A White type multiple reflection system[55,56] was used external to the cell and a total path length of 22 meters was obtained. The 80-80 compound synthesized from 15 mg of Se^{80} was introduced in the cell along with helium gas at near atmospheric pressure. The helium was added to improve the thermal equilibrium between CSe_2 molecules and the cold cell walls. The exterior of the cell was then surrounded with powdered dry ice. The temperature of the outer cell surface was measured with a calibrated Iron-Constantan thermocouple. The spectrum was recorded when the temperature measured by the thermocouple reached a constant value. The external temperature of the cell could be raised above -78°C by passing a current through a lagged nichrome coil wound around the cell. Successive spectra at several temperatures were recorded on the same photographic plate using the Bausch and Lomb and Hilger spectrographs.

2.8 Zeeman Spectra

The effect of a superimposed magnetic field* (i.e. the Zeeman effect) on the fine structure of 80-80 absorption bands was studied in the 4800 - 3500 Å region. Magnetic fields of

---

*The equipment for generating a pulsed magnetic field was made available to us by Dr. A. E. Douglas.

10000, 15000 and 25000 gauss were used. The absorption cell (50 cm or 10 cm long) was axially supported within a cylindrical coil. The field was generated in pulses by discharging a large emf (of the order of 20 kV) through the coil with a bank of condensers. A Lyman flash discharge through a quartz capillary was used as the source of continuum for recording the spectra; it was triggered to emit at precisely the instant of maximum field strength. Initially, the spectrum of CS_2 in a field of 10000 gauss was recorded on the 35 ft Eagle spectrograph (section 2.6). The rotational lines of some bands in the CS_2 spectra are known to broaden in the presence of a magnetic field. The spectra of CS_2 was checked to see if this broadening did occur, before the spectra of CSe_2 was recorded. About 100 to 1000 flashes were used to record the spectra of CSe_2 on Kodak I-0 and II-0 plates.

2.9 Miscellaneous

On each photographically recorded spectrum, reference atomic spectral lines from a 110 V dc iron arc source or from a Jarrell-Ash Iron Hollow cathode lamp operated at 20 mA, were juxtaposed.

For recording spectra photographically, emulsions of types Kodak I-0, II-0, Tri-X, SA-1 and Ilford FP-3 were used. With the exception of Kodak Tri-X, all these emulsions were processed in a Kodak D-19 developer and a F-5 fixer. Kodak Tri-X emulsions were processed in Kodak Acufine developer and F-5 fixer.

The optical density of spectra recorded on these emulsions were measured with a Joyce-Loebl model 111C automatic recording microdensitometer. These values and visual estimates of intensities from photographic enlargements of spectra were utilized in the present work.

A travelling microscope (Mcpherson Instrument Co.) with a least count of 0.0001 mm was used to measure positions of band heads, rotational lines and other features in photographic spectrograms. The positions of the juxtaposed iron spectral lines were measured at the same time. Wavelengths of these lines were obtained from a table compiled by the molecular spectroscopy group of the National Research Council at Ottawa. The positions of band heads, etc., and the positions and wavelengths of iron lines were punched on computer cards. The data on these cards were analysed with a computer program written in Fortran IV language for an IBM 7040 computer[57]. In this program, the wavelengths and positions of iron lines were fitted to a quadratic by a least squares method; the wavelengths of the band heads and other features were obtained by interpolation from this quadratic, and, wavelengths obtained in this matter were converted to wavenumbers in vacuo by a formula derived by Edlen[58]. The uncertainty in wavenumbers was estimated to be $\pm$ 0.3 cm^{-1} for band heads and ± 0.03 cm^{-1} for rotational lines. Diffuse features had a larger uncertainty in their calculated wavenumbers.

Weak or obscure features which could not be measured directly with the microscope, were measured by interpolation from enlarged prints of the spectrum.

CHAPTER III

Infrared and Raman Spectra

3.1 Vibrational States and Energies

In section 1.2, it was shown that the nuclear wavefunction can be factored into a vibrational wavefunction $|\Psi_v\rangle$ and a rotational wavefunction $|\Psi_R\rangle$, by a proper choice of nuclear coordinates. In this section, a brief description of the nature of $|\Psi_V\rangle$ and associated energies is given. For details, reference to standard texts such as Wilson, Decius and Cross[6], Herzberg[48] and others [7,12] should be made.

Each free particle has 3 degrees of freedom corresponding to translations along three Cartesian axes. A polyatomic molecule is a system of N nuclei (which can be treated as particles) and therefore has 3N degrees of freedom. In a molecule, these nuclei are bound to each other by electrostatic forces and their motion is not independent of each other. But the molecule as a whole (like a single particle) has 3 translational degrees of freedom. It also has rotational degrees of freedom about Cartesian axes; if the molecule is nonlinear it has 3 rotational degrees of freedom and if the molecule is linear, it has only 2 such degrees of freedom. The remaining 3N-6 (or 3N-5 for a linear molecule) degrees of freedom correspond to intramolecular motions of the nuclei. 3N-6 (or 3N-5) coordinates are required to describe these motions.

By classical methods, it can be shown that the intramolecular motion can be resolved into 3N-6 (or 3N-5) distinct modes of harmonic oscillations, provided the amplitudes of these oscillations are small. Each non-degenerate oscillation is assigned a coordinate Q_k called the normal coordinate[6] and has a frequency ν_k. The Q_k can be related to either mass-weighted Cartesian displacement coordinates η_i or internal displacement coordinates R_i, by linear transformations. In terms of the normal coordinates Q_k classical expressions for the kinetic and potential energies have their simplest forms,

$$T = 1/2 \sum^{3N-6} \dot{Q}_k^2 \; ; \qquad V = 1/2 \sum^{3N-6} \lambda_k Q_k^2 \tag{3.1}$$

where $\dot{Q}_k$ is the time derivative of Q_k; $\lambda_k = 4\pi^2\nu_k^2$ is a constant. For an isolated molecule the sum T + V is a constant and gives the total classical energy of vibrations in the molecule.

According to Quantum Mechanics, the Hamiltonian for small vibrational displacements is given by

$$H_{vib} = \frac{-h^2}{8\pi^2} \sum_{k=1}^{3N-6} \frac{\partial^2}{\partial^2 Q_k^2} - \sum_{k=1}^{3N-6} \lambda_k Q_k^2 \tag{3.2}$$

in terms of normal coordinates. The wave equation is therefore given by

$$H_{vib} |\Psi_v\rangle = E_v |\Psi_v\rangle \qquad (3.3)$$

Since H_{vib} is a sum of 3N-6 (or 3N-5) independent Hamiltonians, one for each Q_k, (3.3) represents 3N-6 (or 3N-5) independent equations. The solution to each of these equations is a harmonic oscillator function, which is given by

$$|\Psi_{vk}(Q_k)\rangle = \mathcal{N}_k H_{v_k}(Q_k') \exp(-1/2 Q_k'^2) \qquad (3.4)$$

where $|\Psi_v(Q_k)\rangle$ represents the solution for the k^{th} normal coordinate, $\mathcal{N}_k$ is a normalizing factor, $H_{v_k}(Q_k')$ is a Hermite polynomial of degree v_k; and $Q_k' = Q_k \; (\lambda^{1/2}/\hbar)^{1/2}$. The eigenvalue of each function $|\psi_{vk}\rangle$ is given by

$$E_{v_k} = h\nu_k \, (v_k + 1/2) \qquad (3.5)$$

where v_k = 0, 1, 2 .... stands for the vibrational quantum number of the k^{th} vibrational mode. In the harmonic oscillator approximation, we can write the total wavefunction $|\Psi_v\rangle$ as a product of individual functions $|\psi_{v_k}\rangle$ i.e.

$$|\Psi_v\rangle = |\psi_{v_1}\rangle \psi_{v_2}\rangle \ldots |\psi_{v_k}\rangle \ldots |\psi_{v_{3N-6}}\rangle \qquad (3.6)$$

$$= \mathcal{N}_v H_{v_1}(Q_1') \; H_{v_2}(Q_2') \ldots H_{v_{3N-6}}(Q'_{3N-6})$$

$$\times \quad \exp\left[-1/2 \; (Q_1'^2 + Q_2'^2 + \ldots + Q'^2_{3N-6})\right] \qquad (3.7)$$

Each function $|\psi_{v_k}\rangle$ represents a component vibrational state. Two or more of these states may be degenerate i.e. have the same energy. The total vibrational energy is given by the sum of vibrational energies of each component vibrational state i.e.

$$E_v = \sum_{v_k} E_{v_k} = \sum_{v_k} h\,\nu_k(v_k + \frac{d_k}{2}) \qquad (3.8)$$

For nondegenerate component states $d_k = 1$; for doubly degenerate state $d_k = 2$; for triply degenerate state $d_k = 3$ ....etc.

3.2 Symmetry of vibrational states

The symmetry of each vibrational state $|\Psi_v\rangle$ may be determined according to principles developed in section 1.2. Each state $|\Psi_v\rangle$ must transform as one of the irreducible representations, degenerate or nondegenerate, of the symmetry point group of the polyatomic molecule. Consider equation (3.7). The exponent has the same form as the potential energy $\sum \lambda_k Q_k^2$ in equation (3.2) and like potential energy, it must be invariant to all the symmetry operations R of the molecular point group. Therefore, it is the product of Hermite polynomials alone that determines the symmetry of $|\Psi_v\rangle$. Assume that the molecule is in its ground vibrationless state. Then all quantum numbers v_k are zero. i.e

$$v_1 = v_2 = \ldots v_k = \ldots v_{3N-6} = 0 \qquad (3.9)$$

The Hermite polynomial of zero^th degree $H_o(Q_k')$ is unity. The product in (3.7) is also unity. Therefore $|\Psi_v\rangle$, which is a product of the totally symmetric exponential function with

Hermite polynomials of zeroth degree, must be totally symmetric. Thus the vibrational ground state of a polyatomic molecule is always symmetric.

The symmetry of excited vibrational states $|\Psi_v\rangle$ is obtained from the symmetry of the component states $|\Psi_{v_k}\rangle$ in the following way. Let the mth vibration alone be excited by one quantum i.e. $v_m = 1$ and $v_{k \neq m} = 0$. H_1 (Q_m') is a linear function of Q_m. Hence, the representation generated by $|\Psi(Q_m)\rangle$ would be the same as the representation generated by the normal coordinate Q_m. It can be shown that each normal coordinate Q_k necessarily belongs to one of the irreducible representations of the symmetry point group of the molecule. The symmetry species of each of the first excited states (with $v_k = 1$) must therefore correspond to one of these irreducible representations. The overall symmetry of $|\Psi_v\rangle$ is obtained from the direct product of irreducible representations of functions $|\Psi_v\rangle$, by the use of expression (1.15).

In the present work, we are interested only in the vibrations of triatomic molecules of the XCX type described in section 1.6. The method of obtaining symmetries of vibrational states and normal coordinates for triatomic molecules is described in the standard texts[59] and will not be repeated here. The method of obtaining these symmetries will be assumed. A linear symmetric triatomic molecule of the XCX type belongs to the $D_{\infty h}$ symmetry point group. If the molecule is bent, it belongs to the C_{2v} point group. Symmetry elements such as centre of inversion, rotation axes and reflection planes for the XCX molecule are shown in Figs. 4.3(a) and 4.3(b) for the molecule in both point groups. Irreducible representations indicated by Schonflies symbols and the 'character's (for definition, see ref. 60) of each irreducible representation are given in the character tables of Appendix A. Direct products of irreducible representations are given in Appendix B.

If the XCX molecule is linear, it has 3N-5 = 4 genuine vibrational modes and hence, 4 normal coordinates. The normal modes of vibration are[61]: a nondegenerate totally symmetric stretching vibration, ν_1 along the molecular axis corresponding to a coordinate Q_1; a doubly degenerate bending vibration ν_2 in the plane of the molecule corresponding to coordinates Q_2^a and Q_2^b; and a nondegenerate antisymmetric stretching vibration ν_3 along the axis of the molecule corresponding to a coordinate Q_3. Q_1 transforms as a σ_g^+ representation; $Q_2{}^a$ and $Q_2{}^b$ as a Π_u doubly degenerate representation and Q_3, as a σ_u^+ representation. The symmetries of states with $v_1 = 1$ ($v_2=0$, $v_3=0$); $v_2=1$ ($v_1=0$, $v_3=0$) and $v_3=1$ ($v_1=0$, $v_2=0$) is the same as those of Q_1, Q_2 and Q_3 respectively. The species of a state with $v_1=0$, $v_2=0$ and $v_3=0$ is σ_g^+. Let only one vibrational mode be excited. Then, the species of states with $v_1 > 0$ are always σ_g^+ and those of $v_3 > 0$ are σ_g^+ or σ_u^+ depending upon whether v_3 is even or odd respectively. The species of states for the degenerate

Π_u vibration with $v_2 > 1$ is obtained by the symmetric direct product method [59,62]. Symmetric products are shown in parenthesis in the direct product table of Appendix B. For $v_2 = 2$ two species of stages σ_g^+ and δ_g, which are degenerate in the harmonic oscillator approximation, are obtained; for $v_3 = 3$. two species Π_u and ϕ_u are obtained; for $v_3 = 4$, three species σ_g^+, δ_g and Π_g are obtained; etc. The symmetry species of some vibrational states are given in the fifth and seventh columns of Table 3-2[63].

If the XCX molecule is bent, it has 3N-6 = 3 genuine vibrational modes and hence three normal coordinates. All modes of vibration are nondegenerate[61]. They are: a symmetric stretching vibration ν_1 corresponding to a coordinate Q_1, a bending vibration ν_2 in the plane of the molecule, corresponding to a coordinate Q_2 and an asymmetric stretching vibration ν_3 corresponding to a coordinate Q_3. Q_1 and Q_2 transform as a_1 representations and Q_3, as a b_2 representation. Therefore the symmetries of states with v_1 or v_2 or $v_3 = 1$, follows. Excited states with $v_1 > 0$ and $v_2 > 0$ and $v_c = 0$ are always of a_1 symmetry. Excited states with $v_3 > 0$ are of a_1 symmetry, if v_3 is even and of b_2 symmetry, if v_3 is odd. In Figure 3.1, the vibrational modes of linear and bent XCX molecules are illustrated. In this figure, mass weighted cartesian coordinates on each atom are schematically shown.

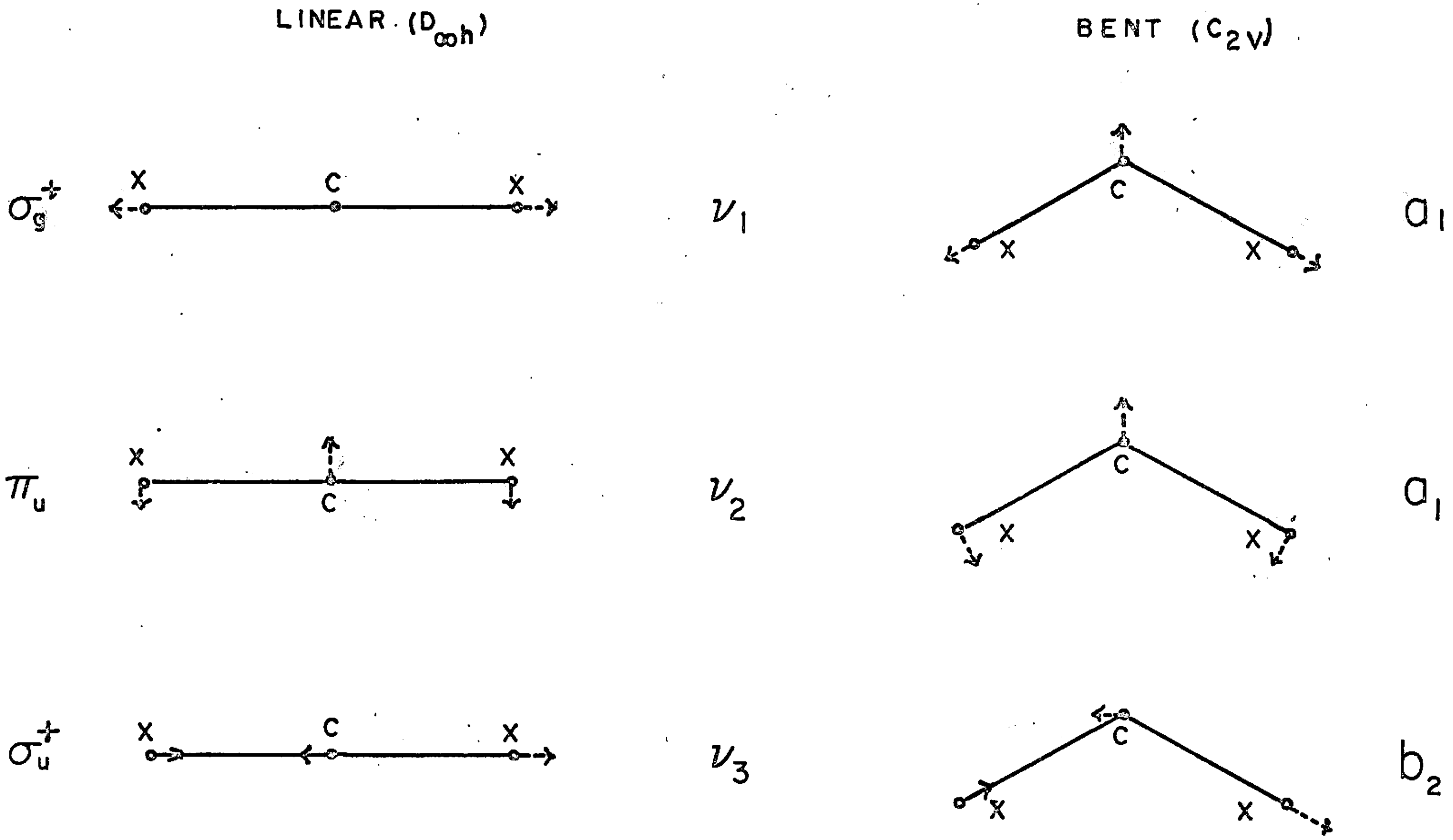

NORMAL MODES OF VIBRATION IN XCX MOLECULES

FIGURE 3.1

3.3 Vibrational angular momentum

The wavefunction for the excited vibrational state $|\Psi_{v_2}\rangle$ of the doubly degenerate π_u bending vibration of the linear XCX molecule can be written[64] as

$$|\Psi_{v_2}\rangle = N\, H_{v_{2a}}(Q'_{2a})\, H_{v_{2b}}(Q'_{2b})\, \exp -1/2[(Q'^{2}_{2a} + Q'^{2}_{2b})] \tag{3.10}$$

which is a part of Equation 3.7. The exponent represents the potential energy of a two dimensional oscillator along two orthogonal coordinates Q_2^a and Q_2^b. When these normal coordinates are expressed in polar form, it can be shown that an equivalent function

$$|\Psi v_2\rangle = f\,(v_2)\,\exp\,[\pm\, i l \phi] \tag{3.11}$$

is obtained. Here v_2 is the number of quanta of the degenerate vibration excited: $v_2 = v_{2a} + v_{2b}$. ϕ measures the angle of rotation in the (Q_2^a, Q_2^b) plane, $f(v_2)$ is a function independent of ϕ, and l the vibrational angular momentum quantum number, which takes the values

$$l = v_2,\ v_2 - 2,\ v_2 - 4,\ \ldots\ 1 \text{ or } 0 \tag{3.12}$$

For $v_2 = 2$, $l = 0$ or 2; for $v_3 = 3$, $l = 3$ or 1 etc.
The vibrational levels are classified as σ_g^+, πu, δg etc. according to the value of $l = 0, 1, 2$ etc. This classification procedure yields the same species as those obtained in section 3.2 for the excited states of the π_u vibration.

3.4 Energy levels of vibrational states

For a triatomic molecule, the total energy E_v given by expression (3.8) reduces to

$$E_v = h\nu_1 (v_1+1/2) + h\nu_2 (v_2+\frac{d}{2}) + h\nu_3 (v_3+1/2) \qquad (3.13)$$

d = 1 for a bent molecule and d = 2 for a linear molecule. In terms of wavenumbers (units of cm^{-1}) (3.10) may be written as

$$\frac{Ev}{hc} = G(v_1, v_2, v_3) = \omega_1 (v_1 + 1/2) + \omega_2 (v_2 + \frac{d}{2}) + \omega_3 (v_3+1/2) \qquad (3.14)$$

where $G(v_1, v_2, v_3)$ is called the term value of a vibrational state with quantum numbers v_1, v_2 and v_3 and where $\omega_i = \frac{\nu_i}{c}$ is the frequency in wavenumber units.

E_v, given by (3.13) is correct only in the harmonic oscillator approximation; that is, only when the potential energy term in the Hamiltonian (3.2) is quadratic in the coordinate Q_k. In a higher order approximation, cubic, quartic, etc., anharmonic terms in Q_k are included in the potential energy; these terms are treated as perturbation terms H' and added to the Hamiltonian (3.2) and the perturbed wavefunctions obtained. The form of the corrected wavefunction is not given here. It can be shown however, that these functions retain the symmetry of the zeroth order wavefunctions. Term values in the anharmonic oscillator approximation are given empirically[65] by the expansion

$$G\ (v_1, v_2, v_3) = \sum^{3} \omega_k (v_k + \frac{d_k}{2}) + \sum_{k \neq j} x_{kj} (v_k + \frac{d_k}{2})\ (v_j + \frac{d_j}{2})$$

where x_{kj} is an anharmonicity coefficient and d_k is the degeneracy of the kth vibration.

The effect of anharmonicity not only alters the energy of each state obtained in the harmonic approximation but also removes some of the degeneracies present in these vibrational states. As shown in the last section, each excited state of the bending vibration with $v_2 > 1$ has component states with different values of l. In the harmonic oscillator approximation all these components are degenerate. It can be shown that states of the same symmetry can interact due to anharmonicity, therefore states of the same l, but different v_2 (which have the same symmetry), can interact due to anharmonicity. Due to this interaction, states with different l but the same v_2, have different energies. When this difference in energies between the l components is also taken into account, the term values are given by[66]

$$G\ (v_1, v_2^{l}, v_3) = \sum \omega_k\ (v_k + \frac{d_k}{2}) + \sum x_{kj} (v_k + \frac{d_k}{2})\ (v_j + \frac{d_j}{2}) + g l^2 \tag{3.16}$$

where g is a small constant of the same order as x_{kj}. Each state with $l > 0$ is still doubly degenerate but this degeneracy is not removed by anharmonicity interaction.

Even if two states are not degenerate in the harmonic oscillator approximation, they could interact due to anharmonicity, provided that both states are of same symmetry. If the states have nearly the same energies in the harmonic oscillator approximation, the interaction between the states is large (as can be shown by perturbation theory) and therefore the perturbed energies differ considerably from their zeroth order values. This type of perturbation is known as Fermi resonance[67] and could occur between any two vibrational states in the molecule. The term values for these states cannot be given explicitly. Transitions involving such perturbed states give rise to bands with anomalous frequencies and anomalous intensities.

3.5 Selection Rules for Vibrational Spectra

i) Infrared Spectra:

Selection rules for electric dipole transitions between vibrational states of triatomic molecules are well known[68] and will not be re-established here. These rules are obtained from the symmetry species of the two vibrational states (given in section 3.2) involved in the transition, and those of the dipole moment operator $\vec{P}$ (given in the character tables of Appendix A), by use of expression (1.15), and with the aid of direct product table of Appendix (B). Selection rules for vibrational transitions in triatomic molecules are summarized in Table 3-1.

Some basic notations and definitions will be given here for subsequent use. Each vibrational state of a linear molecule will be denoted by (v_1, v_2^{l}, v_3) where v_1, v_2 and v_3 are the vibrational quantum numbers and l is the vibrational angular momentum quantum number. The ground state is therefore represented by $(0, 0^\circ, 0)$. Each band due to transition from $(0, 0^\circ, 0)$ to any one of the states $(1\ 0^\circ\ 0)$, $(0\ 1^1\ 0)$, $(0\ 0^\circ\ 1)$ is called a fundamental; to any one of the states $(n\ 0^0\ 0)$ $(0\ m, 0)$ or $(0\ 0^0\ p)$ where n, m or p is greater than 1 is called an overtone; and to any other state is called a combination band. If the initial state is not the ground state, then the observed frequency corresponding to the transition is called a 'hot' band. For bent molecules, the same notation and definitions apply with one exception; in these molecules, l is not defined and is therefore dropped from (v_1, v_2^{l}, v_3).

For a linear XCX molecule, if the transition moment given by (1.44) is nonzero for that component P_g which is parallel to the molecular axis, the resulting transition is called a parallel transition; if the transition moment is nonzero for components perpendicular to this axis, the resulting transition is called a perpendicular transition.

ii) Raman Spectra:

Raman spectra may be observed when a molecule scatters incident radiation. Selection rules for transitions between vibrational states are also determined by the transition moment integral given by (1.27). However for Raman transitions, the operator $\vec{P}$ in this integral is not an electric dipole moment operator. Placzek and Teller[69] showed that the correct operator to be used is a 'polarizability' tensor $[\alpha]$. The transition moment therefore reads as

$$R_{v'v''} = \langle \Psi_v' | [\alpha] | \Psi_v'' \rangle \qquad (3.17)$$

$[\alpha]$ is a 3 x 3 symmetric matrix with elements α_{xx}, α_{yy}, α_{zz}, α_{xy}, α_{yz} and α_{xz}. The matrix relates the electric field vector $\vec{E}$ of the incident radiation to a vector $\vec{\mu}$, which represents the dipole moment induced in the molecule. In matrix notation, $[\alpha]$ is defined by

$$[\vec{\mu}] = [\alpha] \quad [\vec{E}] \qquad (3.18)$$

Selection rules may be determined as before by the use of expression (1.15) from the symmetry species of $|\Psi_v'\rangle$, $|\Psi_v''\rangle$ and those of $[\alpha]$ given in the character table of Appendix A. The method of determination will not be given here since selection rules for Raman transitions in triatomic molecules are well known. These rules along with those for infrared transitions are summarized in Table 3-1.

An experimental quantity, available in the study of Raman spectra, is the depolarization ratio ρ_1. It is defined as the ratio of the scattered intensity which is polarized perpendicular to the plane of polarization of the incident radiation to the intensity parallel to the same plane. When plane polarized radiation is used for scattering and intensities are measured in a direction perpendicular to this plane

Table 3 - 1

SUMMARY OF SELECTION RULES FOR VIBRATIONAL TRANSITIONS FROM THE GROUND STATE ($^1\Sigma_g$) OR ($^1A_1$) OF XCX MOLECULES

LINEAR#

SPECIES OF $\lvert\Psi'_v\rangle$	SPECIES OF $\lvert\Psi''_v\rangle$	SELECTION RULE and BAND TYPE	
		Infrared	Raman
σ_g^+	σ_g^+	F	A.P
π_u	σ_g^+	A, $\perp$	F
σ_u^+	σ_g^+	A $\parallel$	F
δ_g	σ_{g+}	F	A.d
π_u	π_u	F	A.d
δ_g	π_u	A $\perp$	F
π_g	π_u	A $\parallel$	F
π_u	δ_g	A $\perp$	F

BENT

SPECIES OF $\lvert\Psi'_v\rangle$	SPECIES OF $\lvert\Psi''_v\rangle$	SELECTION RULE and BAND TYPE	
		Infrared	Raman
A_1	A_1	A, $\parallel$	A,P
B_2	A_1	A,	A,d

A.	allowed transition	F.	forbidden transition
$\parallel$	parallel band	$\perp$	perpendicular band
P	polarized band	d	depolarized band

Ref. to 68, pp. 271, 274, for a more detailed listing

($I_\perp$) and parallel to this plane ($I_\parallel$), ρ_l is given by

$$\rho_l = \frac{I_\perp}{I_\parallel} \qquad (3.19)$$

This ratio can be shown to be 3/4 for nontotally symmetric Raman active vibration when plane polarized radiation is used for excitation. For totally symmetric vibrations the ratio lies between 0 and 3/4.

As a corollary of selection rules (given in Table 3-1) for vibrational transitions in linear XCX molecules, the following rule is obtained. For a molecule with a centre of symmetry, transitions that are allowed in the infrared spectrum are forbidden in the Raman spectrum, and conversely, transitions that are allowed in the Raman spectrum are forbidden in the infrared. This rule is called the mutual exclusion rule and applies to all molecules with a centre of symmetry.

3.6 Rotational Structure of Infrared Bands

The rotational eigenfunctions and eigenvalues of a linear XCX molecule are similar to those of homonuclear diatomic molecule and have been described in standard texts[70]. The following is a condensation of such material for future use.

The term values (or energy levels) $F_V(J)$ of rotational states of a linear molecule are given by

$$F_V(J,l) = B_V\,[J(J+1) - l^2] - D_V[J(J+1) - l^2]^2 \qquad (3.20)$$

where J is the rotational quantum number, ℓ is the vibrational angular momentum quantum number. B_v is the rotational constant in the v^{th} vibrational level and D_v is a constant which represents the effect of centrifugal stretching.

In a first approximation, the total energy T of vibration and rotation of the molecule is given by

$$T = G(v_1, v_2, v_3) + F_v (J) \qquad (3.21)$$

Substitution of (3.20) and (3.16) in (3.21) gives

$$T = \sum^{3} \omega_k \left(v_k + \frac{d_k}{2}\right) + \sum_{k \neq j} x_{kj} \left(v_k + \frac{d_k}{2}\right) \left(v_j + \frac{d_j}{2}\right) + g\ell^2$$
$$+ B_v[J(J+1) - \ell^2] - D_v[J(J+1) - \ell^2]^2 \qquad (3.22)$$

Here, all the symbols have the same significance as before. B_v, the rotational constant, is different for different vibrational levels due to interaction of rotation with vibration. The relationship between B_v and v_i is given by

$$B_v = B_e - \sum_{k}^{3} \alpha_k \left(v_k + \frac{d_k}{2}\right) \qquad (3.23)$$

Here α_k is a constant and is small compared to B. B_e is the value of B at the equilibrium position of the nuclei and is related to the equilibrium internuclear distance r_{CX} in the following way.

$$B_e = \frac{h}{8\pi^2 c I_B} = \frac{27.9889 \times 10^{-40}}{I_B} \text{ in cm}^{-1} \qquad (3.24)$$

where I_B, the moment of inertia, is given by

$$I_B = \sum_{i}^{3} m_i r_i^{2} = 2\, m_X\, r_X^{2} \qquad (3.25)$$

m_X is the mass of the X atom in a m.u.

Selection rules are determined by the transition moment $\vec{R}_{V'K'V''R''}$ given by (1.43)

$$\vec{R}_{V'R'V''R''} = \sum_g \langle \Psi'_V | P_g | \Psi''_V \rangle \langle \Psi'_R | \theta_{F_g} | \Psi''_R \rangle \qquad (3.26)$$

The first factor in (3.26) has been dealt with in section (3.5). The second factor gives the matrix elements of the direction cosines θ_{Fg} between molecule fixed axes (g) and space fixed axes (F); and determines selection rules for transition from rotational states of one vibrational state to the rotational states of the other. The method of obtaining these selection rules from the matrix elements have been described by Allen and Cross[19]. Selection rules so obtained for a linear molecule, are given below.

a) For parallel transitions

$\ell = 0 \qquad \Delta\ell = 0 \qquad \Delta J = \pm 1$

$\ell \neq 0 \qquad \Delta\ell = 0 \qquad \Delta J = 0, \pm 1 \qquad (3.27a)$

b) For perpendicular bands

$\Delta\ell = \pm 1 \qquad \Delta J = 0, \pm 1 \qquad (3.27b)$

The method of obtaining the relative values of the transition probability $\left|\vec{R}_{R'R''}\right|^2$ i.e. the so called line strengths A_{lJ} between states of different quantum numbers l and J, are also given in the same reference above[19]. For a linear molecule, which is a symmetric top molecule with $I_A = 0$ and $I_B = I_C$ (and for symmetric top molecules) expression for A_{lJ} are called Hönl - London formulae. These formulae are tabulated in Appendix C.

Frequencies (expressed in cm^{-1}) corresponding to transitions between rotational states are given by

$$\sigma = F'(J', l') - F''(J'', l'') \qquad (3.28)$$

If equation (3.20) and selection rules (3.27) are substituted in (3.27), three types of expressions for σ result, and are given by

$$\begin{aligned} P(J) &= F'(J-1, l') - F''(J, l'') = \sigma_0 - (B_V' + B_V'')J + (B_V' - B_V'')J^2 \\ Q(J) &= F'(J, l') - F''(J, l'') = \sigma_0 + (B_V' - B_V'')J + (B_V - B_V'')J^2 \\ R(J) &= F'(J+1, l') - F''(J, l'') = \sigma_0 + 2B_V' + (3B_V' - B_V'')J + \\ &\quad (B_V' - B_V'')J^2 \qquad (3.29) \end{aligned}$$

Terms due to D in (3.20) have been neglected in the substitution. σ_0 is called the band origin. The selection rule in l gives a constant term and has been included in σ_0. The double degeneracy in l (section 3.4) has been assumed to persist. Observed frequencies corresponding to P(J), Q(J) and R(J) are called P,Q and R branches respectively.

From the selection rules in Table 3-1, we note that the $(0\ 0^{\circ}\ 1) \leftarrow (0\ 0\ 0)$ transition corresponding to the fundamental is a parallel transition in the infrared spectrum. Therefore selection rules for rotational transitions are , $\Delta \ell = 0$ and $\Delta J = \pm 1$. This fundamental should have P and R branches only. For vibrational states of the same electronic state, B_V' and B_V'' are usually nearly equal. It can then be shown[71] that in the spectrum, these branches have to two intensity maxima (which look like 'wings' on either side of σ_o. The $(0\ 1^{1}\ 0) \leftarrow (0\ 0^{\circ}\ 0)$ fundamental is a perpendicular transition. Therefore the selection rules are $\Delta \ell = \pm 1$ $\Delta J = 0, \pm 1$. All three branches occur in this case. It can be shown that the Q branch is the most intense branch. The frequencies of the Q branch are all nearly equal and the spectra lines corresponding to these frequencies lie almost on top of another since $B_V' \sim B_V''$. Therefore the band appears to have a single intense maximum (which looks like a spike when unresolved).

3.7 Isotope Effect

Since isotopic atoms have the same electronic structure, substitution of an atom by its isotope in a molecule does not alter the potential function under which the nuclei move.[71] However, nuclei of isotopic atoms have different masses. Therefore the vibrational frequencies ω_k which are mass dependent, are altered.

A theorem of fundamental importance in studying the alteration of vibrational frequencies of a molecule, by isotopic substitution, has been given by Teller and Redlich[73]. This theorem relates the vibrational frequencies of two isotopic molecules in terms of masses of the constituent atoms, and the moments of inertia. For a symmetric triatomic molecule XCX, the ratio of frequencies between pairs of isotopic molecules such as XCX and X^iCX^i; or XCX and XC^iX; or XCX and $X^iC^iX^i$ derived from Teller and Redlich relationship is given by

$$\rho_3^2 = \left(\frac{\omega_3^i}{\omega_3}\right) = \frac{m_C m_X}{m_C^i m_X^i}\left(\frac{m_C^i + 2m_X^i \sin^2 \alpha}{m_C + 2m_C^i \sin^2 \alpha}\right) \tag{3.30}$$

$$\rho_{12}^2 = \left(\frac{\omega_1^i \omega_2^i}{\omega_1 \omega_2}\right) = \frac{(2m_X^i + m_C^i)(m_X^2\ m_C)}{(2m_X + m_C)(m_X^i\ 2\ m_C^i)} \tag{3.31}$$

where $\omega_1, \omega_2, \omega_3$ are the zero order frequencies. m_X and m_C are the masses of X and C atoms respectively. The superscript i stands for one of the two isotopic molecules and 2α is the angle between XCX bonds. These expressions are expected to hold approximately if observed frequencies of fundamentals are used, instead of ω_k.

For linear XCX molecules, the bond angle $2\alpha = 180°$. With this value (3.30) reduces to

$$\rho_1^2 = \left(\frac{\omega_1^i}{\omega_1}\right) = \frac{m_X}{m_X^i} \qquad \rho_2^2 = \left(\frac{\omega_2^i}{\omega_2}\right) = \left(\frac{\omega_3^i}{\omega_3}\right) = \frac{m_X(1 + 2m_X^i/m_C^i)}{m_X^i\ (1 + 2\ m_X/m_C)} \tag{3.32}$$

If only one of the X atoms in an XCX molecule is replaced by an isotope, these relations do not hold. The exact relationships between frequencies ω_i for such an unsymmetric substitution have been given by Rosenthal (see reference 74) . However, provided that the mass difference $\Delta m_X = m_X{}^i - m_X$ is small compared to m_X, the isotope shifts $\Delta\omega_k = \omega_k^i - \omega_k$ for XCX and XCX^i molecules is approximately given by half the shift for XCX and X^iCX^i molecules.

3.8 The present work

a) Observations and results:

Wentink[23] obtained the infrared spectrum of CSe_2 both in the gas and liquid phases in the 4000 - 400 cm^{-1} region with a Perkin Elmer (model 21) spectrophotometer. He also obtained the Raman spectrum of CSe_2 in the liquid phase with the 5461Å spectral line of Hg as the exciting radiation. Two experimental limitations in his work were: 1) the infrared spectrophotometer used could not record infrared spectra below 400 cm^{-1}. Therefore bands, predicted (by Wentink) to occur in the region below 400 cm^{-1}, were not experimentally observed. 2) It was found by Wentink[23] that samples of CSe_2 decomposed when irradiated with radiation from a mercury lamp. Therefore, the scattered radiation from these samples could not be photographically recorded over long periods in order to observe weak bands.

In the present work, the first limitation was overcome by the use of Perkin-Elmer model 521 and model 301 spectrophotometers, by which the infrared spectrum of CSe_2 could be examined in the wider 4000 - 90 cm^{-1} range. The second limitation was overcome by obtaining the Raman spectrum with a laser Raman spectrophotometer, described in section 2.4. Relatively short periods of time were required to record spectra on this instrument and decomposition of samples was not observed during these periods. Observation of bands below 400 cm^{-1} in the infrared spectrum, and observation of a more complete Raman spectrum in this work, therefore represent extensions of Wentink's observations. Furthermore, the spectra of the 78-78 and 80-80 isotopic molecules were also obtained in addition to the spectra of the N-N molecule.

Since CH_2Cl_2 is always present as an impurity in CSe_2, all observed spectra have bands due to the former molecule. CH_2Cl_2 forms a constant boiling mixture with CSe_2 and could not be removed from CSe_2 by simple fractional distillation. Wentink surmounted this difficulty by distilling CSe_2 (N-N) solution in CH_2Cl_2, with CS_2; by this procedure CH_2Cl_2 was completely replaced by CS_2 as a solvent for CSe_2. Then he compared the spectrum of CSe_2 in CH_2Cl_2, with the spectrum of CSe_2 in CS_2 in order to distinguish bands of CSe_2 from those of either of CH_2Cl_2 or CS_2. This procedure could not be adopted for mg quantities of the 80-80 and 78-78 compound.

In this work, the infrared and Raman spectra of 80-80, 78-78 and N-N molecules were compared with those of CH_2Cl_2,

$CHCl_3$, CCl_4 and H_2O molecules. By such a comparison, bands of the former could be distinguished from those of the latter molecules. In the first column of Table 3-2, the infrared and Raman bands of CSe_2 which were observed in the work are listed in order of decreasing wavenumbers (cm^{-1}) and the phase in which the band was obtained is shown in parenthesis. In the third column, symbols are given to indicate the method (infrared or Raman) by which the band was observed, the relative intensities among these bands, and whether a band was polarized or not in the Raman spectrum. Symbols used are explained at the bottom of the same table. In the second column of this table the wavenumbers given by Wentink for these bands are given.

In the infrared spectrum, two strong bands are observed. One at 1303 cm^{-1}, which has two intensity maxima on either side of a central minimum, is the strongest band in the spectrum; the separation between the two maxima is 6.5 ± 0.5 cm^{-1}. The other band at 313 cm^{-1}, which has only one intensity maximum, is the next strongest band. These two bands are shown in Fig. 3.2. Other weak bands are observed at 1666, 1260, 940 and 667 cm^{-1}. The band at 940 cm^{-1} seems to be similar in appearance to the 1303 cm^{-1} band. The remaining three bands are much weaker and are almost overlapped by bands due to either CH_2Cl_2 or H_2O. A strong band was observed at 794 cm^{-1} in the spectrum of the N-N molecule and not in those of 80-80 or 78-78. This band was also observed by Wentink who attribu-

Table 3 - 2

INFRARED AND RAMAN BANDS OF CARBON DISELENIDE

Observed Bands (cm^{-1})			Upper State				Lower State				Molecule
This work	Wentink		v_1	v_2^l	v_3	Species	v_1	v_2^l	v_3	Species	
1666(g)#	1666	I^{+} vw**	1	0^0	1	σ_u^+	0	0^0	0	σ_g^+	
1606(l)	n.o.	R. vvw	0	1^1	1	π_g	0	0^0	0	σ_g^+	
1303(g)	1303	I. vs.	0	0^0	1	σ_u^+	0	0^0	0	σ_g^+	
940(g)	930	I. w.	0	0^0	1	σ_u^+	1	0^0	0	σ_g^+	
667(g)	673	I vw.	1	1^1	0	π_u	0	0^0	0	σ_g^+	
667(l)	n.o.	R. vw	0	3^3	0	ϕ_u	0	1^1	0	π_u	
647(l)	n.o.	R. vw	0	2^2	0	δ_g	0	0^0	0	σ_g^+	
636(l)	n.o.	R. vvw	0	3^1	0	π_u	0	1^1	0	π_u	
631(l)	n.o.	R. vvw	0	2^0	0	σ_g^+	0	0^0	0	σ_g^+	
369(l)	n.o.	R.s.pol	1	0^0	0	σ_g^+	0	0^0	0	σ_g^+	78-78
364(l)	366	R.s.pol	1	0^0	0	σ_g^+	0	0^0	0	σ_g^+	N-N

Table 3 - 2 (continued)

364(l)	n.o.	R.s.pol	1	0^0	0	σ_g^+	0	0^0	0	σ_g^+	80-80
313(g)	n.o.	I.s	0	1^1	0	π_u	0	0	0	σ_g^+	

*1260 cm^{-1} I.vw. Unassigned. Observed by Wentink at 1253 cm^{-1} and Assigned to $(0\ 0^0\ 1) \longleftarrow (0\ 0^0\ 0)$ of $C^{13}Se_2$

795 cm^{-1} R.vvw. Unassigned

**v.s.	very strong	s.	strong	w.	weak	vw.	very weak
vvw.	very very weak						
I	Infrared band	R.	Raman band	n.o.	Not observed.		
l	liquid phase	g.	gas phase.				

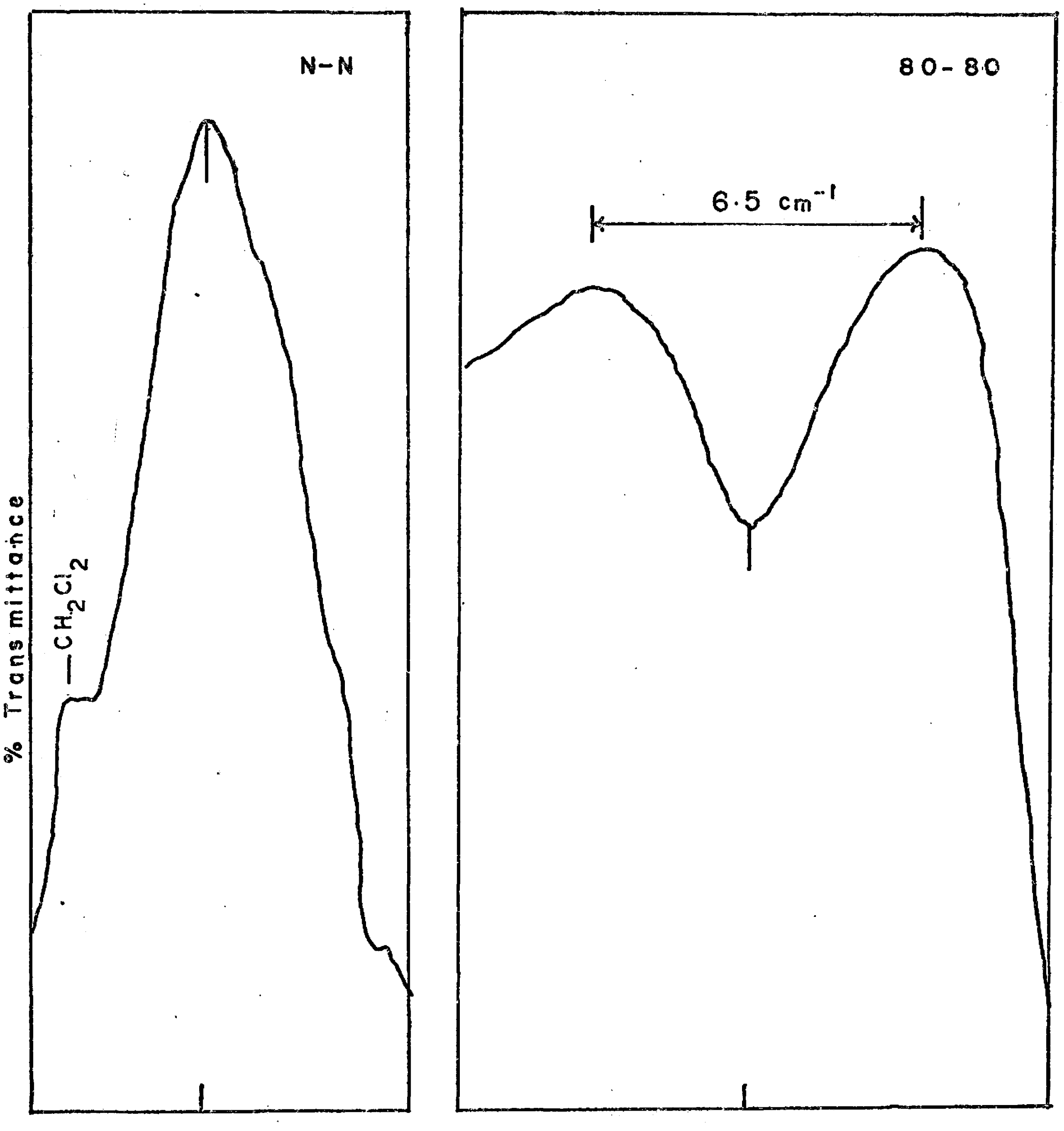

a. 313 cm^{-1} b. 1303 cm^{-1}

Vapour phase

FUNDAMENTALS IN THE INFRARED SPECTRUM OF CSe_2

FIGURE 3.2

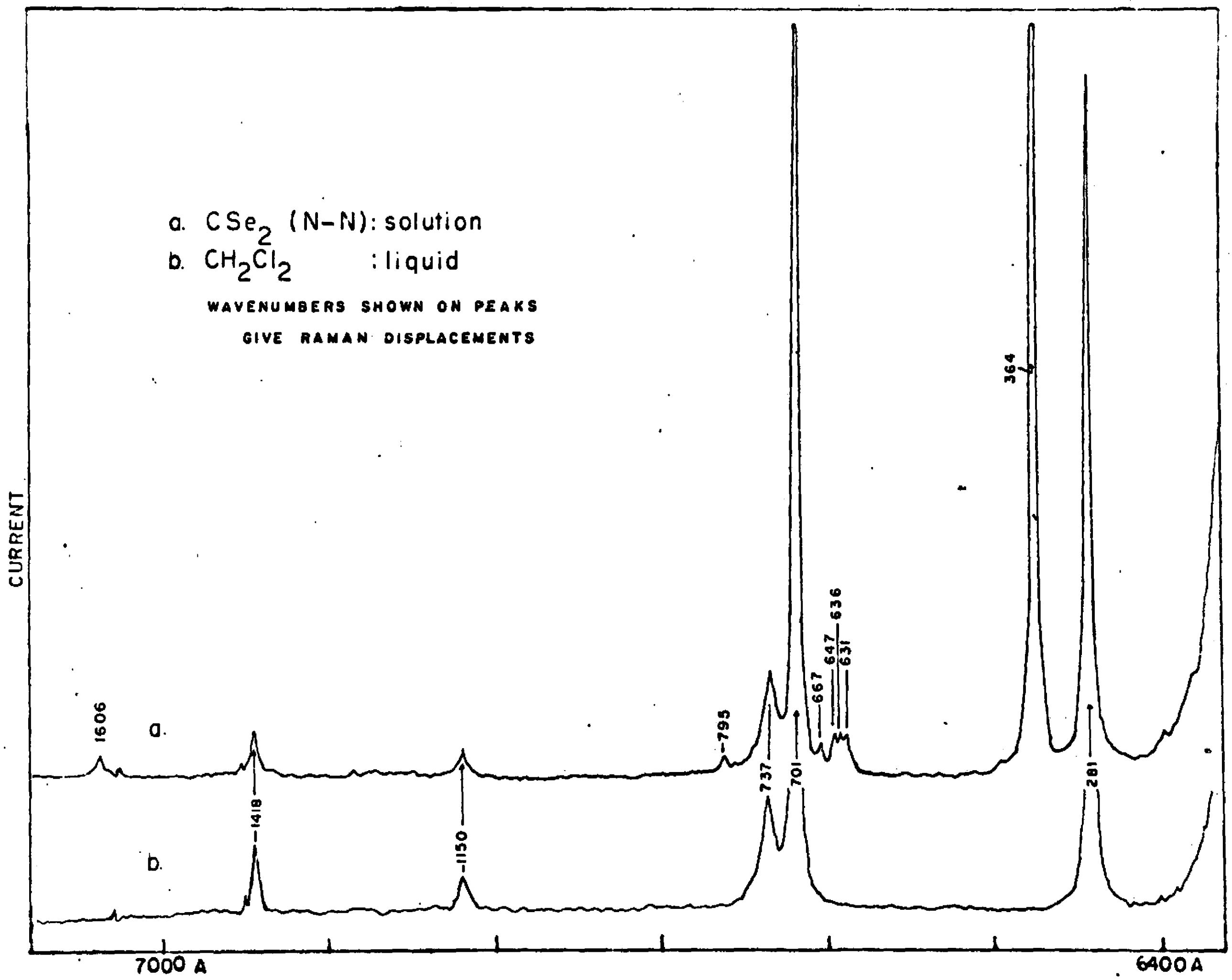

RAMAN SPECTRA OF CSe_2 AND CH_2Cl_2

FIGURE 3.3

ted it to some unknown volatile impurity. We found that the strongest infrared band of CCl_4 vapour occurs at 794 cm^{-1} and that the shape of this band and the band in the N-N spectrum are comparable. This 794 cm^{-1} band was therefore assigned to the CCl_4 molecule. Since in the spectra of 80-80 and 78-78 molecules, a band is not observed at 794 cm^{-1}, it was concluded that the band is not due to CSe_2. This difference between the spectra of N-N and the other two isotopic molecules is probably due to the difference in the procedure adopted for their synthesis. Comparison of infrared spectra of 80-80 and 78-78 molecules does not indicate any measurable isotopic shifts.

The Raman spectrum of CSe_2(N-N) which was concentrated by fractional distillation is shown in Fig. 3.3A. The Raman spectrum of CH_2Cl_2 is also shown in Fig. 3.3B. Apart from the bands of CH_2Cl_2, only one strong band is observed in the spectrum. This band occurs at 364 cm^{-1} for N-N, at 364 cm^{-1} for the 80-80 and at 369 cm^{-1} for the 78-78 molecules. The difference in wavenumbers between these two bands of 80-80 and 78-78 is 5 cm^{-1} and represents the isotopic shift $\Delta\sigma = \omega^{80} - \omega^{78}$. It was found that these bands at 364 and 369 cm^{-1} are reduced in intensity almost completely, when an analyser is placed in the Raman scattered beam with its optical axis oriented perpendicular to the plane of polarization of the incident beam. Wentink not only observed a Raman band of the N-N molecules at 366 cm^{-1} but also another band at 300 cm^{-1}. No band is observed in this work at this latter frequency. But an intense band of CH_2Cl_2 is however observed at 281 cm^{-1}. Since CH_2Cl_2 is always present as an impurity in CSe_2, it is possible that Wentink misconstrued this band at 281 cm^{-1} as a CSe_2 band. In addition to the band at 364 cm^{-1}, a few previously unreported weak bands at 795, 667, 647, 636 and 631 cm^{-1} observed in this work, are listed in Table 3-2.

b) Interpretation and Discussion

It is inferred from Table 3-2 that bands which occur in the infrared spectrum do not occur in the Raman spectrum and vice-versa (except for one very weak band at 667 cm^{-1}, see paragraph 3). The mutual exclusion rule, mentioned in section 3.5, therefore applies in the present case. The molecule must therefore have a centre of symmetry and this requirement is fulfilled only if the XCX molecule is linear and not bent.

Three fundamentals are expected in the spectrum of an XCX molecule; two of them should be active in the infrared spectrum and one in the Raman (Table 3.1). The strong infrared bands observed at 1303 cm^{-1} and 313 cm^{-1} were assigned as the two infrared active fundamentals. The former has two intensity maxima on either side of a single minimum. Such a shape is expected for a parallel band of a linear molecule (section 3.7). This band at 1303 cm^{-1} was assigned to the σ_u^+ asymmetric stretching fundamental i.e. to the parallel $(0\ 0^0\ 1) \leftarrow (0\ 0^0\ 0)$ transition. The second band at 313 cm^{-1} has a single maximum, as expected for a perpendicular transition in a linear molecule (sec. 3.6). This band was assigned to the Π_u bending fundamental i.e. to the perpendicular $(0\ 1^1\ 0) \leftarrow (0\ 0\ 0)$ transition. The intense Raman active band at 364 cm^{-1} is strongly polarized with a depolarization ratio $\rho_l < 3/4$. This value is much lower than the value of 3/4 expected for a nontotally symmetric fundamental. This band at 364 cm^{-1} was assigned to the σ_g^+ symmetric stretching fundamental i.e. to the $(1\ 0^{\circ}\ 0) \leftarrow (0\ 0^{\circ}\ 0)$ transition.

Weaker bands observed in the Raman spectra for the first time, could be assigned as the overtones and hot bands in the Π_u bending vibration. The band at 631 cm^{-1} was attributed to the $(0\ 2^{\circ}\ 0) \longleftarrow (0\ 0^{\circ}\ 0)$ transition and the band at 647 cm^{-1} to the $(0\ 2^2\ 0) \longleftarrow (0\ 0^{\circ}\ 0)$ transitions. The bands at 636 cm^{-1} and 667 cm^{-1} were attributed to the $(0\ 3^1\ 0) \longleftarrow (0\ 1^1\ 0)$ and $(0\ 3^3\ 0) \longleftarrow (0\ 1^1\ 0)$ transitions respectively. A very weak band observed at 795 cm^{-1} was not assigned; it could be due to an impurity. A very weak band at 1606 cm^{-1} was assigned to $(0\ 1^1\ 1) \longleftarrow (0\ 0^{\circ}\ 0)$. In the infrared spectrum, two weak bands were observed at 1666 cm^{-1} and 667 cm^{-1}. These were assigned as combination bands and attributed to $(1\ 0^{\circ}\ 1) \leftarrow (0\ 0^{\circ}\ 0)$ and $(1\ 1^1\ 0) \longleftarrow (0\ 0^{\circ}\ 0)$ transitions respectively. It may be noted that the occurence of a band at 667 cm^{-1} in both the infrared and Raman spectra is explained without violation of the mutual exclusion rule since it is assigned to different transitions. The infrared band at 940 cm^{-1} is similar in shape to the 1303 cm^{-1} and was attributed to the parallel transition, $(0\ 0^{\circ}\ 1) \longleftarrow (1\ 0^{\circ}\ 0)$. A weak band occurs at 1260 cm^{-1}

in the infrared and will be discussed later. In Table 3-2 the quantum numbers and symmetry species of the final and the initial states are given.

All the above assignments could be made on the assumption that the XCX molecule is linear. If the molecule were bent, all bands must be active both in the infrared and Raman spectra (Table 3-1) and this activity is not observed. Wentink observed additional bands in the liquid phase spectra also. These bands were also assigned by him on the basis that the molecule is linear. We therefore conclude that on the basis of the current experimental evidence that CSe_2 molecule is linear. This conclusion is in accordance with the observation of other workers that other molecules of the XCY group are also linear.

An isotopic shift of 5 cm^{-1} was observed in the σ_g^+ fundamental. It is possible to verify by calculation whether the shift is of the right order of magnitude from the reduced Teller-Redlich expression (3.32). For $\omega_1 = 364$ cm^{-1}, $m_{Se} = 80$ and $m_C = 12$, we get

$$\omega_1^{78} = \omega_1^{80} \times \sqrt{m_{Se}^{80}/m_{Se}^{78}} = 368.6 \text{ cm}^{-1} \tag{3.33}$$

Therefore $\Delta\omega_1 = \omega_1^{78} - \omega_1^{80} = 4.6$ $cm^{-1} \approx 5$ cm^{-1}. It is seen that there is good agreement between the observed and calculated isotopic shifts. A similar calculation for the $\nu_2(\pi_u)$ and $\nu_3(\sigma_u^+)$ fundamentals shows that there should be very little isotopic shifts for these fundamentals. The weak band observed at 1260 cm^{-1} was interpreted by Wentink as the $\nu_3(\sigma_u^+)$ fundamental of the $C^{13}Se_2$ molecule. Substitution of $\omega_3(C^{12}Se_2) = 1303\ cm^{-1}$, $m_C = 12$, $m_C^i = 13$ and $m_{Se} = 80$ in equation (3.32) gives $\omega_3(C^{13}Se_2) = 1255\ cm^{-1}$. This calculated value is in reasonable agreement with the observed value of 1260 cm^{-1}. But the observed intensity ratio of $\nu_3(C^{13}Se_2)$: $\nu_3(C^{12}Se_2) = 0.05$ is five times larger than the molecular ratio of $C^{13}Se_2$: $C^{12}Se_2 = 0.01$ calculated from isotopic abundances. This latter ratio is the expected intensity ratio for the isotopic bands. Therefore, even though there is agreement in wavenumbers, there is no agreement in intensities. Wentink has indicated that Plyler and Humphreys[75] observed the $\nu_3(C^{13}S_2)$ band in the infrared spectrum and has quoted this observation in support of the assignment of the 1260 cm^{-1} band. Our conclusion is that more experimental evidence is needed to establish that the 1260 cm^{-1} band is an isotopic band. However, this band cannot be accounted for in any other way. The present observations on the fundamentals of 80-80 and 78-78 are given (in cm^{-1}) below, in comparison with those of Wentink on the N-N molecules.

	Wentink		This work		Shift	
	$C^{12}Se_2$	$C^{13}Se_2$	80-80	78-78	obs	calc
1	368	-	364	369	5	4.6
2	not observed		313	313	0	0
3	1303	1260	1303	1303	0	0

From the separation of the P and R branch maxima in the 1303 cm^{-1} band an approximate value of B was calculated with the formula[76]

$$\sigma_M^R - \sigma_M^P = \sqrt{\frac{8kTB}{hc}} = 2.358\sqrt{TB} \qquad (3.34)$$

Where T = Temperature in °K, the value of $\sigma_M^R - \sigma_M^P$ was 6.5 ± 0.5 cm^{-1} as measured from the band maxima. At a temperature of 300°C, the B value was found to be 0.025 ± 0.008 cm^{-1}. An alternative way of calculating B, is from the expressions for the moment of Inertia I_B (equation 3.24) and B (equation 3.25) which are given below

$$I_B = 2\, m_{Se}\, r^2_{CSe}; B = \frac{h}{8\pi^2 c I_B}$$

With $m_{Se} = 80$ and $r_{CSe} = 1.711$ Å (Table 1-1), it was found that B = 0.0360 cm^{-1}. The agreement between the two values of B is not satisfactory. This disagreement could arise from two causes. Firstly, the formula for B values given by equation (3.34) is only approximate and in addition, there is some error in locating the exact positions of the P and R maxima (Fig. 3.2). Secondly, the value $r_{CSe} = 1.711$ Å quoted by Wentink is not an experimental value; it was transferred from the corresponding value in the OCSe molecule. This transference of the r_{CSe} value may not be justified. We have no way of finding the exact value for B; it could not be determined from an analysis of the rotational structure of the 1303 cm^{-1} band. The rotational lines were not resolved by the spectrophotometer used in this work. In order to find a better value of B, the contour of the band at 1303 cm^{-1} was calculated. A band contour program written for a 7040 IBM computer was used for this purpose (see section 5.6). It was found that the band contour was not sufficiently sensitive to changes in the B value and good fits could be obtained for B values in the 0.025 - 0.030 cm^{-1} range. From the value of $B = 0.025\ cm^{-1}$, we find that $r_{CSe} = 2.05$ Å.

From the data in Table 3-2, force constants and anharmonicity constants were calculated. Results of these calculations are given in Table 3-3.

Table 3 - 3

GROUND STATES CONSTANTS IN CARBON DISELENIDE

A. Fundamentals:

$\omega_1(\sigma_g^+) = 364 \pm 3$ cm^{-1}

$\omega_2(\pi_u) = 313 \pm 1$ cm^{-1}

$\omega_3(\sigma_u^+) = 1303 \pm 1$ cm^{-1}

B. Force Constants (units - 10^{-5} x dynes/cm)*

		This Work	Wentink
Stretching force constant k_1	=	5.91	5.94#
Bending force constant $\frac{k\alpha}{r_{12}^2}$	=	0.161	0.158
Stretch-stretch interaction constant k_{12}	=	0.33	0.36

C. Anharmonicity Constants+

$x_{22} = 1 \pm 0.5$ cm^{-1}

$g = 4 \pm 1.5$ cm^{-1}

---

* Calculated from equation (D.3) in Appendix for the values of ω_1, ω_2 and ω_3 above

\+ Calculated from Raman bands in Table 3-2 and equation (5.3) x_{12} and x_{23} were assumed to be zero.

CHAPTER 4

ELECTRONIC ABSORPTION SPECTRA OF LINEAR XCX MOLECULES:

4.1 Electron Configurations and the Ground State

Exact solutions $|\Psi_e(q,Q_d)\rangle$, for the electronic part of the time independent Schrödinger equations $H_e|\Psi_e\rangle = E_e|\Psi_e\rangle$ are obtained only for very simple molecules such as H_2^+. For other molecules, approximate solutions are usually obtained. One method of successive approximation by which these latter solutions are determined is called the variational method.[79] In this method, a trial wavefunction $|\Phi_e\rangle$ which is an approximation to some $|\Psi_e\rangle$ is constructed from a set of known basis functions $|\Phi_i\rangle$. A particularly important form of the trial wavefunction is the linear combination given by

$$|\Phi_e\rangle = \sum_i^M C_i |\Phi_i\rangle \qquad (4.1)$$

Where M is the number of basis functions used and the C_i are constants. The eigenvalue corresponding to $|\Phi_e\rangle$ is then calculated by the relation

$$E_{\Phi_e} = \frac{\langle\Phi_e|H_e|\Phi_e\rangle}{\langle\Phi_e|\Phi_e\rangle}$$

E_{Φ_e} will be, in general, higher than E_e, the exact value[80]. Therefore Φ_e is improved successively by varying the parameters C_i until the energy E_{Φ_e} is as close to E_e as possible. The variational method is usually applied to calculate ground state $|\Phi_e\rangle$

Each member $|\Phi_i\rangle$ of the basis set is usually expressed in terms (as described below) of single electron wavefunctions ϕ_is, called molecular orbitals (MO's). These wavefunctions are obtained by assuming that each electron in a molecule can be assigned a wavefunction ϕ_i which is a function of the coordinates (x_i, y_i, z_i) of that electron only and has corresponding orbital energy ϵ_i. For each electron moving in the field of the (fixed) nuclei and the field of all the other electrons, the wave equation is given by[81]

$$\nabla^2\phi_i + \frac{2m}{\hbar^2}\left(\epsilon_i - V_{ni} - \sum_{k\neq i} V_{ik}\right)\phi_i = 0 \tag{4.2}$$

Here, V_{ni} is the potential produced by the nuclei on the ith electron and V_{ik} is the potential produced by electron k on electron i and ϵ_i is the orbital energy. A general solution of this single electron wave equation is not available and therefore, an approximate solution must be used for each ϕ_i. If each electron is also assigned a spin function α or β, the product function $\phi_i\alpha$ on $\phi_i\beta$ is called a (molecular) spin orbital. Each $|\Phi_i\rangle$ is now expressed as an antisymmetric product function of the spin orbitals of every electron. The form of the product function is expressible as a Slater determinant[82] with spin-orbitals as elements so that the Pauli principle can be satisfied.

If each electron in the molecule is assigned to a molecular orbital ϕ_i, then a configuration is said to be defined for the system. As a variety of MO's s are available for each electron, different electron configurations for the molecule can be defined. Among all these configurations that, for which the molecule has the lowest energy, is the ground state configuration. Any other configuration is called an excited state configuration. A given electron configuration may generate one or more electronic states Φ_e. In this work, the symmetry properties of MO's and of the electronic states resulting from different electron configurations will be examined and used to determine selection rules for transitions between their states.

For a linear molecule, the single electron functions ϕ_i s are of the form[81]

$$\phi_i = R_i(z_i, \rho_i)\exp(\pm i\lambda_i \varphi) \qquad (4.3)$$

where z_i, ρ_i, φ_i are cylindrical coordinates of the i^{th} electrons and R_i is a radial function in z_i and ρ_i, λ_i is a quantum number representing the angular momentum in units of $\hbar$, along the internuclear axis. Each MO ϕ_i transforms as one of the irreducible representations of a $C_{\infty h}$ or $D_{\infty h}$ point groups, according to whether the molecule has not, or has a centre of symmetry and is designated by the symbols σ, π, δ,.....etc., depending upon the value of $|\lambda_i| = 0, 1, 2$...etc.

As a linear XCX molecule belongs to the $D_{\infty h}$ point group, each M O can be further classified as a symmetric (g) or antisymmetric (u) with respect to inversion of the wavefunctions ϕ_i at the coordinate centre of symmetry in the molecule.

For a bent CX_2 molecule, no simple form of ϕ_i is known, as in linear molecules. However, it can be shown that each MO can be constructed to transform as an irreducible representation of the C_{2v} point group.

In general, each single electron wavefunction ϕ_i may be approximated by a linear combination of atomic orbitals[83], (LCAO) centred on each of the constituent atoms of the molecule. The LCAO/MO is written as

$$\phi_i = \sum a_{ip} \chi_p \tag{4.4}$$

Here p is a summation index over the number of atomic orbitals (AO's) chosen and a_{ip} are unknown coefficients to be determined. For mathematical simplification[83], instead of atomic orbitals, 'symmetry' orbitals may be used in forming ϕ_i. Each symmetry orbital is itself constructed as a linear combination of AO's centred on equivalent (for definition, refer to 6) nuclei; it transforms as an irreducible representation of the molecular point group. Then, each set of MO's is formed as a linear combination of those symmetry orbitals which have the same transformation properties under the group operations. The coefficients $|a_{ip}|^2$ determine the proportion of each AO in each MO, and may themselves be determined by a variational method.

There are 22 electrons in the CO_2 molecule; 6 are from the $(1s_C)^2$ $(2s_C)^2$ $(2p_C)^2$ atomic orbital configuration of the carbon atom and 8 each from the $(1s_O)^2$ $(2s_O)^2$ $(2p_O)^4$ configurations of the oxygen atoms. If the 6 K shell (s) electrons are neglected we are left with 16 electrons in the molecule. From the AO's on the C atoms and the pair of equivalent O atoms, symmetry orbitals can be built. Fig. 4.1, schematically illustrates the MO's of the CO_2 molecule and the symmetry orbitals from which the MO's were formed. Each orbital is represented by a horizontal line. On the right, the species of symmetry orbitals and the linear combination of AO's used are given for the oxygen atoms. On the left, the symmetry orbitals and the AO's of the carbon atom are given. Lines are drawn to indicate the type of symmetry orbitals that contribute most in forming each molecular orbital.

The relative ordering of the energies ϵ_i for the CO_2 MO's have been calculated by Mulligan (1951), who also obtained the coefficients a_{ip} determining the proportion of the component AO's in each MO . His data is presented in Table 4-1. The symbols B, b, N, a, A in that table respectively mean strongly bonding, weakly bonding, nonbonding, weakly antibonding and strongly antibonding, following the notation used by Mulliken (1958). The same symbols have been used to label the MO's of Fig. 4-1. We note from the figure that the bonding (B) MO's are lower in energy then either of the symmetry orbitals

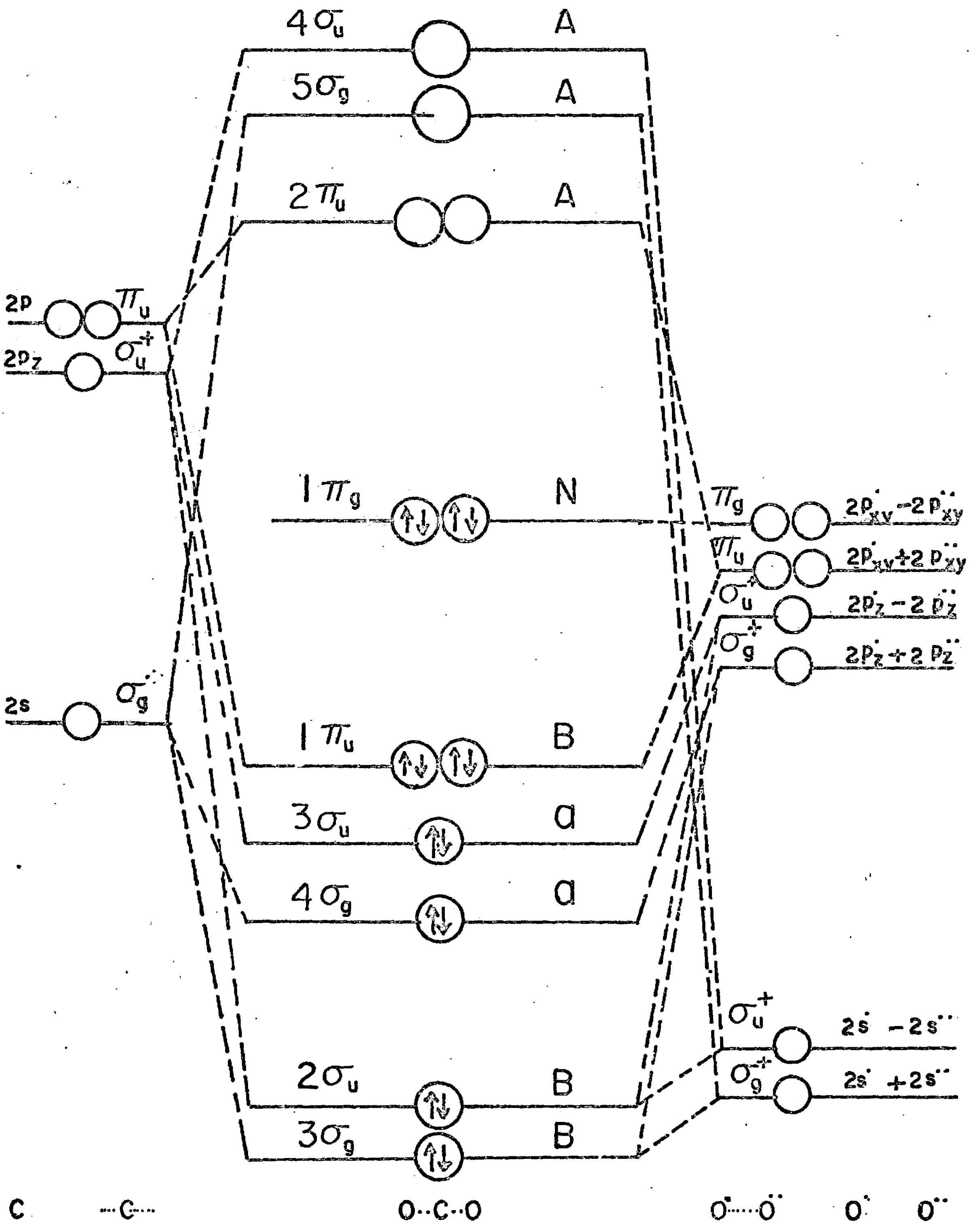

MOLECULAR ORBITALS (SCHEMATIC)

FIGURE 4.1

from which the MO's are formed whereas the corresponding antibonding (A) MO's are higher in energy with respect to their symmetry orbitals. For nonbonding (N) MO's no relative energy change is indicated.

The occupation of the lowest energy MO's by the 16 electrons of CO_2 are also shown schematically in the centre of Fig. 4.1. Each nondegenerate (σ) orbital is doubly occupied by electrons of opposite spins whereas each twofold degenerate (π) orbital is occupied by four electrons. The ground state configuration of CO_2 is therefore given by

$$(3\sigma_g)^2\ (2\sigma_u)^2\ (4\sigma_g)^2\ (3\sigma_u)^2\ (1\pi_u)^4\ (1\pi_g)^4 \tag{4.5}$$

Since all the MO's are fully occupied, (4.5) represents a closed shell configuration. Only one electronic state can result from this configuration and this state transforms as a totally symmetric representation, Σ_g^+. The ground state of CO_2 is thus denoted by $\tilde{X}\,{}^1\Sigma_g^+$ where $\tilde{X}$ is the notation generally used to specify the ground state of molecules.

If the inner closed AO configurations on the S atom (i.e. K, L shells) and on the S_e atom (i.e. K, L & M shells) are neglected, both these atoms have the same type of valence (outer) shell configuration as an O atom. Hence it is reasonable to assume initially that the molecular orbitals of CS_2 and CSe_2 molecules are similar to those of CO_2 both in their symmetry behaviour and relative ordering of orbital energies.

Table 4-1

MOLECULAR ORBITALS OF CARBON DIOXIDE°

MO#	FORM°°	ORBITAL ENERGY		*
		Computed	Observed	*
$4\sigma_u$	$0.85(s-s')+0.84(z+z')+1.55z_c$	-4.8	2	A
$5\sigma_g$	$0.55(s+s')-1.32s_c+0.64(z-z')$	-3.1	2	A
$2\pi_u$	$0.57(x+x')-0.92x_c$	2.5	5	A
$1\pi_g$	$2^{-1/2}(x-x')/2^{-1/2}(y-y')$	11.5	13.73	N
$1\pi_u$	$0.49(x+x')+0.53x_c;..(y+y')+..y_c$	18.8	17.30	B
$3\sigma_u$	$-0.64(s-s')+0.37(z+z')-0.65z_c$	17.9	18.07	a
$4\sigma_g$	$-0.51(s+s')+0.40s_c+0.46(z-z')$	19.4	19.38	a
$2\sigma_u$	$0.38(s-s')+0.11(z+z')-0.51z_c$	42.4		B
$3\sigma_g$	$0.48(s+s')+0.32s_c+0.21(z-z')$	44.9		B

*. Symbols A, a, N, b, B denote antibonding, slightly antibonding, nonbonding, slightly bonding, and bonding respectively.

\# The lowest energy orbital of each species is given the prefixing number 1. The higher energy orbitals are successively numbered.

° Table adapted from Mulliken[89].

°° LCAO/SCF/MO's given by Mulligan[90].

s, s', s_c are the 1s orbitals of O, O' and C

$x, y, z;\ x', y', z';\ x_c, y_c, z_c$ are the p_x, p_y, p_z orbitals of O, O' and C respectively.

The electron configurations with lowest energy of CO_2 and CSe_2 should therefore be closed shells, giving rise to $^1\Sigma_g^+$ states. For CO_2 and CS_2, an $^1\Sigma_g^+$ ground state has been established by analysis of their electronic absorption spectra[8,37].

4.2 Excited States

In the excited state of a molecule in which one or more electrons are promoted to higher energies, there is usually a rearrangement of electrons and nuclei with respect to their coordinates in the ground state. If, in this excited state, maximum stability (lowest energy) is achieved by a change in the nuclear conformation, the molecule has a different shape and may belong to a different symmetry point group classification. For a symmetric triatomic molecule, there are two possible equilibrium conformations of the nuclei. In one of these conformations the molecule remains linear ($D_{\infty h}$ group) and in the other, it is bent (C_{2v} group).

An excited state configuration of the linear CO_2 molecule may be obtained by promoting an electron from the ground state configuration. From Fig. 4.1 and Table 4-1, we see that the unoccupied orbitals of lowest energy are the $2\pi_u$, $5\sigma_g$ and $4\sigma_u$. By promoting an electron from the $1\pi_g$ orbital to these orbitals, the following configurations and electronic states are obtained.

Configuration	States	
............$(1\pi_g)^3\ (2\pi_u)$	- $^1\Sigma_u^+\ ^1\Sigma_u^-\ ^3\Sigma_u^+\ ^3\Sigma_u^-\ ^1\Delta_u\ ^3\Delta_u$	
............$(1\pi_g)^3\ (5\sigma_g)$	- $^1\Pi_g\ ^3\Pi_g$	
............$(1\pi_g)^3\ (4\sigma_u)$	- $^1\Pi_u\ ^3\Pi_u$	(4.6)

Completely filled orbitals can be neglected in determining the symmetry of states and have therefore been omitted in (4.6). The method of determining the symmetry of excited states from the above configurations are well known[84] and will not be repeated here. Alongside each configuration, the symmetry species of states generated from each configuration are shown.

If the molecule is bent in the excited state, configurations of electrons in MO's that transform as the irreducible representations of the C_{2v} point group, must be used to determine the resultant excited states. In order to build up such configurations, the symmetry and ordering of these MO's must be known. This information is available for simple bent molecules such as O_3 (Fischer-Hjalmars, 1958)[85] and may be used qualitatively to obtain configurations for the bent CO_2 molecule. Walsh[86] showed that the MO's of a bent triatomic molecule can be correlated with MO's corresponding to its linear conformations, both by symmetry and orbital energy. Qualitative curves of orbital energy versus bonding angle $X\hat{C}X$ obtained by him, have long been in use. Peyerimhoff and Buenker[87] obtained such curves for the N_3^- ion, on the basis of quantitative calculations. These curves are presented in Fig. 4.2, and are

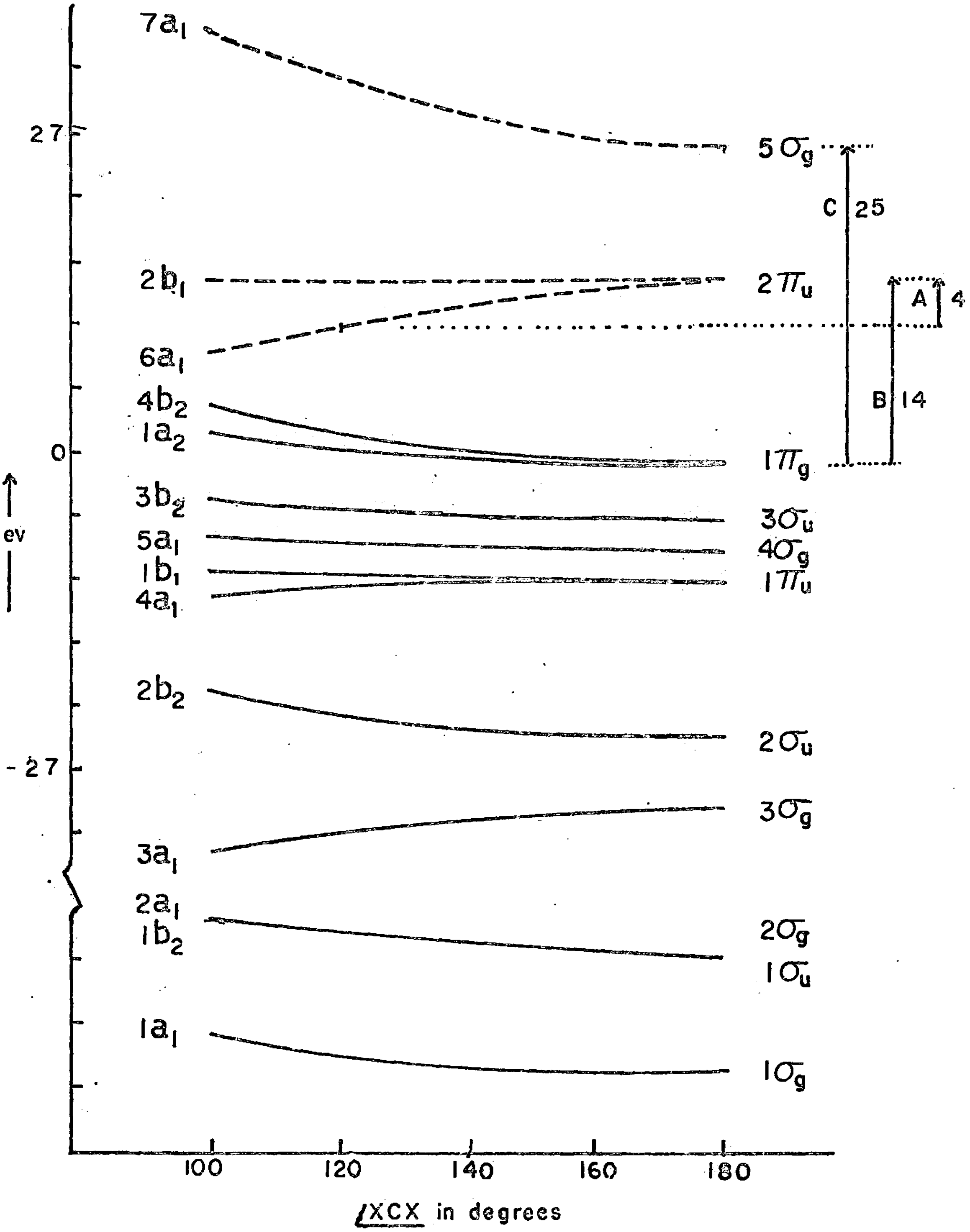

WALSH TYPE DIAGRAM FOR N_3^-

FIGURE 4.2

expected to apply qualitatively to the isoelectronic CO_2 molecule. The ordinate in Fig. 4-2 gives the orbital energy in electron-volts and the abscissa represents the bending angle $\widehat{XCX}$ in the 100°-180° range. The extreme left corresponds to the bent conformation of the molecule and the extreme right to its linear conformation. From the figure, it is seen that each doubly degenerate (π) orbital correlates with two nondegenerate orbitals of the bent molecule. Thus, the $2\pi_u$ orbital correlates with the $6a_1$ and $2b_1$ orbitals, the $1\pi_g$ with the $4b_2$ and $1a_2$ orbitals and the $1\pi_u$ with the $5a_1$ and $1b_1$ orbitals. In addition to correlations by symmetry, we see that there are changes in energy for each correlating orbital as the bonding angle is varied adiabatically. For example, the $6a_1$ orbital decreases in orbital energy with increasing $\widehat{XCX}$ angle, whereas the energies of $4a_1$ and $1b_1$ orbitals increase with it.

From the figure, we see that the drop in orbital energy for the $6a_1$ orbital is going from 180° to 120° is about 4eV (see arrow A). A bent molecule with its valence shell electrons in the $6a_1$ orbital has therefore greater stability than a linear molecule with a $2\pi_u$ valence shell configuration. Another use of the diagram is to obtain excitation energies for electron promotion from one orbital to another. For example, the energy required to promote one electron from the $1\pi_g$ orbital to the $2\pi_u$ orbital is of the order of 14 eV (see arrow B in Fig. 4.2)

Promotion to a $5\sigma_g$ orbital requires an excitation energy of about 26 eV (arrow C). Comparison of these numbers indicate that if transitions corresponding to both excitations are observable, then the lower energy transition should correspond to a $2\pi_u \longleftarrow 1\pi_g$ electron promotion. As a result of this transition the equilibrium configuration of the molecule is expected to be bent since a further lowering in energy is achieved by the occupation of the $6a_1$ orbital (by the electron). The discussion above is based upon a Walsh type diagram for the N_3^- ion but the same arguments are expected to apply in the case of the isoelectronic CO_2 molecule and the analogous CS_2 and CSe_2 molecules.

From the lowest energy MO's on the left of Fig. 4.2 the following electron configurations for the bent molecule may be obtained:

	Configuration	States
Ground State......	$(1a_2)^2(4b_2)^2$	$^1A_1$
Excited States....	$(1a_2)^2(4b_2)(6a_1)$	$^1B_2, {}^3B_2$
....	$(1a_2)(4b_2)^2(6a_1)$	$^1A_2, {}^3A_2$
....	$(1a_2)(4b_2)^2(2b_1)$	$^1B_2, {}^3B_2$
....	$(1a_2)^2(4b_2)(2b_1)$	$^1A_2, {}^3A_2$ (4.7)

The symmetry of excited electronic states arising from each configuration has been obtained from the direct product (Appendix B) of orbital species in partially occupied shells. Both singlet and triplet states result and are shown alongside each configuration.

Electron configurations and the symmetry species of electronic states obtained from these configurations, for both bent and linear CO_2 molecules are given in Table 4-2. Excitation energies quoted by Mulliken[89] for each state and the expected shape of the molecule in that state, are also given in the same table.

4.3 Selection rules for absorption spectra

The principles developed in sections 1.3 and 1.4 will be now used to determine the selection rules for transitions between a ${}^1\Sigma_g^+$ ground state and any one of the excited states of Table 4-2.

For this purpose, we recollect that the transition moment integral (1.27) is

$$\vec{R} = \langle \Psi | \vec{P} | \Psi \rangle \tag{4.8}$$

If $\vec{R}$ is to be nonzero, the direct product of symmetry species of Ψ, $\vec{P}$ (i.e. P_x, P_y, or P_z) and Ψ'' must contain at least one totally symmetric component. $|\Psi\rangle$ could represent an electronic state $|\Psi_e\rangle$, a singlet or a triplet electronic state $|\Psi_{es}\rangle$ or a vibronic state $|\Psi_{ev}\rangle$. The symmetry species in the first two types of states are given in Table 4-2. The species of the electric dipole operators P_x, P_y and P_z are given below

	$D_{\infty h}$	C_{2v}
P_x	Π_u	B_1
P_y		A_1
P_z	σ_u^+	B_2

(4.9)

Table 4-2

ELECTRON CONFIGURATIONS AND ELECTRONIC STATES[+] OF CO_2

Linear				Bent			
Configuration	$\Gamma(\Psi_e)$	E(eV)[#]	$\Gamma(\Psi_e\Psi_s)$	Configuration	$\Gamma(\Psi_e)$	$\Gamma(\Psi_e\Psi_s)$	Form
$(1\pi_g)^3(5\sigma_g)$	$^1\Pi_g$	14.6	Π_g	$..(1a_2)(4b_2)^2(6a_1)$	$^1A_2$(f)[*]	A_2	Linear
				$..(1a_2)^2(4b_2)(6a_1)$	$^1B_2$	B_2	
	$^3\Pi_g$	14.6	Π_g Δ_g Σ_g	$..(1a_2)(4b_2)^2(6a_1)$	$^3A_2$	B_2,A_1,B_1	Linear
				$..(1a_2)^2(4b_2)(6a_1)$	$^3B_2$	A_2,B_1,A_1	
$..(1\pi_g)^3(2\pi_u)$	$^1\Sigma_u^+$	22.1	Σ_u^+	$..(1a_2)(4b_2)^2(2b_1)$	$^1B_2$	B_2	Linear
	$^1\Delta_u$	9.5	Δ_u	$..(1a_2)^2(4b_2)(2b_1)$	$^1A_2$(f)	A_2	Linear
				$..(1a_2)^2(4b_2)(6a_1)$	$^1B_2$	B_2	Bent
	$^3\Sigma_u^-$	9.2	$\Sigma_u^+ + \Pi_u$	$..(1a_2)^2(4b_2)(2b_1)$	$^3A_2$	B_2,A_1,B_1	Linear
	$^1\Sigma_u^-$	9.2	Σ_u	$..(1a_2)(4b_2)^2(6a_1)$	$^1A_2$(f)	A_2	Bent

Table 4-2 (Contd.)

Linear				Bent			
Configuration	$\Gamma(\psi_e)$	E(eV)#	$\Gamma(\psi_e\psi_s)$	Configuration	$\Gamma(\psi_e)$	$\Gamma(\psi_e\psi_s)$	Form
$..(1\pi_g)^3(\pi_u)$	$^3\Delta_u$	8.4	Π_u	$..(1a_2)(4b_2)^2(2b_1)$	$^3B_2$	A_2,B_1,A_1	Linear
			Δ_u	$..(1a_2)(4b_2)^2(6a_1)$	$^3A_2$	B_2,A_1,B_1	Bent
			Φ_u				
	$^3\Sigma_u^+$	7.6	$\Sigma_u^- + \Pi_u$	$..(1a_2)^2(4b_2)(6a_1)$	$^3B_2$	A_2,B_1,A_1	Bent
$..(1\pi_g)^4$	$^1\Sigma_g^+$	0.00	Σ_g^+	$..(1a_2)^2(4b_2)^2$	$^1A_1$	A_1	Linear

*f Transition is forbidden electronically from the ground state to this state.

\+ The table has been adapted from reference[89].

\# Energies of states as calculated by Mulligan[90].

The correlation of the Π_u species above with an A_1 and a B_1 species has been obtained from the data of Appendix E. The change in the molecule fixed axes systems between the linear and bent conformations of the molecule can be seen from a comparison of Fig. 4.3 a) and b). It is seen therein that if the molecule is bent in the excited state, the z axis of the linear molecule becomes the y axis of the bent molecule and that the x axis is perpendicular to the molecular axis (σ_{yz}) in both conformations. Note that x, y, z axes of both molecules pass through the centre of mass. From the symmetry species of $|\Psi'\rangle$, P_x, P_y or P_z and $|\Psi''\rangle$, direct products are obtained from the data in Appendix B and selection rules are determined.

In the discussion to follow transitions allowed electronically will be dealt with in i), transitions allowed because of spin orbit coupling in ii) and, vibronic transitions in iii).

i) The selection rules for an electronically allowed transition is determined by the integral product (equation 1.34)

$$\vec{R} = \langle\psi_e|\vec{P}|\psi_e\rangle\langle\psi'_v|\psi''_v\rangle \qquad (4.10)$$

The first factor is non-zero if the direct product

$$|(\Psi_e') \otimes (P_x, P_y \text{ or } P_z) \otimes (\Psi_e'')$$

generates a totally symmetric component.

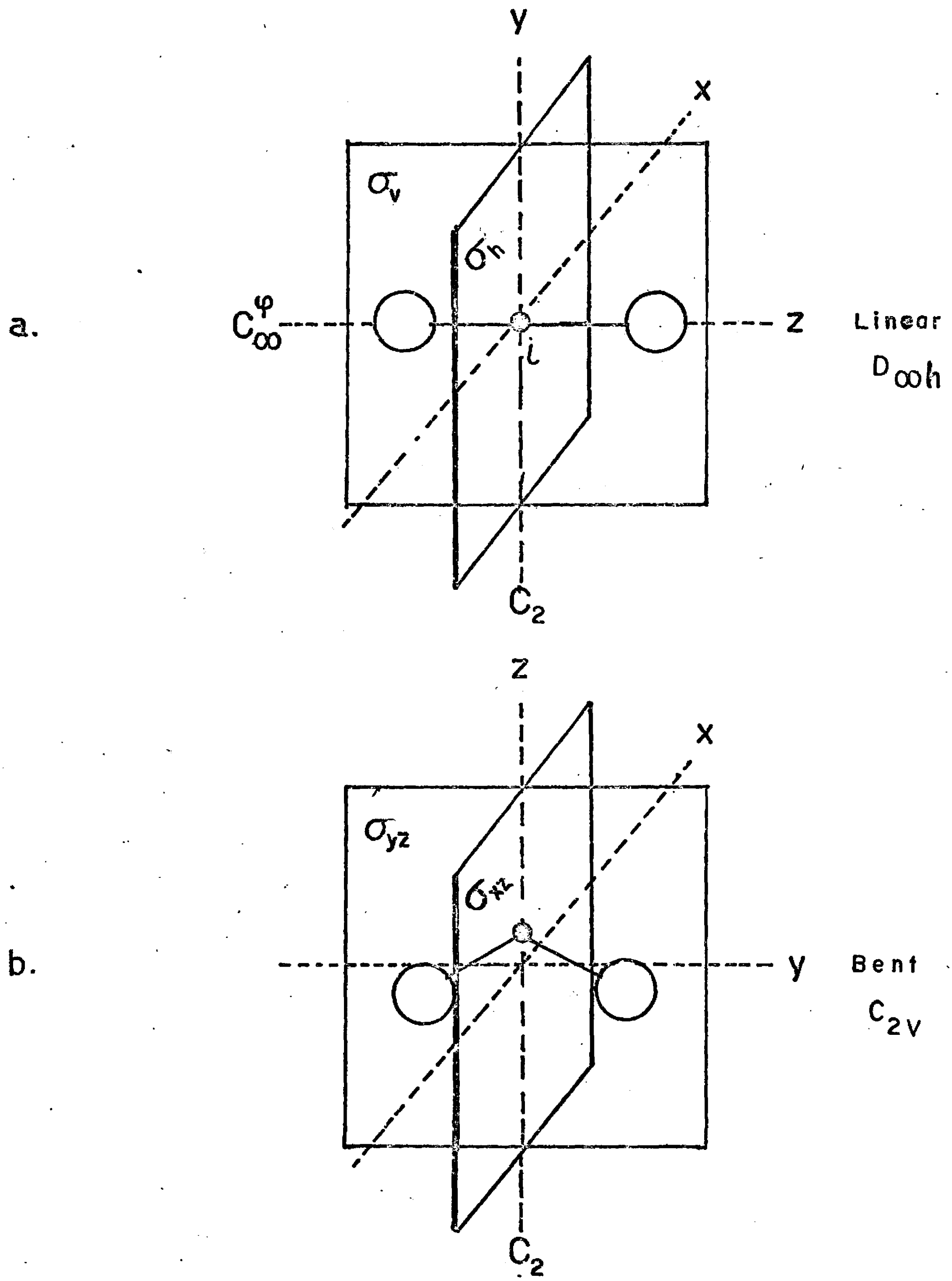

SYMMETRY ELEMENTS OF XCX MOLECULES

FIGURE 4.3

By the use of Appendices A and B, it can be shown that for a linear XCX molecule, this integral factor is nonzero only for the following transitions

$$
\begin{aligned}
& {}^1\Sigma_u^+ \longleftarrow \tilde{X}\,{}^1\Sigma_g^+ \\
\text{and}\quad & {}^1\Pi_u \longleftarrow \tilde{X}\,\Sigma_g^+ \qquad (4.11a)
\end{aligned}
$$

From Table 4-2 it is seen that whereas a ${}^1\Sigma_u^+$ is a possible excited state for the molecule, ${}^1\Pi_u$ state does not occur among the manifold of excited states. It can also be shown that the first transition in (4.11a) is a parallel type transition[88], since $\vec{R}$ is nonzero for the P_z component which is parallel to the symmetry axis z of the linear molecule (Fig. 4.3) and that the second transition is a perpendicular transition since $\vec{R}$ is nonzero for the P_x and P_y components which are perpendicular to the same z axis. Transitions to all other linear states in Table 4-2 are forbidden electronically.

If the molecule is bent in the excited state, then the symmetries of $|\Psi_e'\rangle$ P_x, P_y and P_z and $|\Psi_e''\rangle$ in the C_{2v} point group must be used to determine the direct product. From Appendix E, it is seen that the ${}^1\Sigma_g^+$ ground state correlates with a ${}^1A_1$ state; it is also seen that a ${}^1\Sigma_u^+$ excited state correlates with a ${}^1B_2$ state, if the change in the axis systems of Fig. 4.2 is assumed. The correlations of Π, Δ etc. states are also given in the same appendix. By a determination of the direct product, it can be shown that the following is an allowed electronic transition

$$ {}^1B_2 \longleftarrow \hat{x}\ {}^1A_1\left({}^1\Sigma_g^+\right) \qquad (4.11b) $$

It can also be shown that the transition is of the parallel type. From Table 4-2 it is seen that a ${}^1B_2$ state is a possible excited state for the molecule. Transitions from the ground state to the excited ${}^1A_2$ states can be shown to be forbidden.

The second integral factor of (4.10) (i.e. the overlap integral) determines vibrational selection rules for the electronic transition; for the overlap integral to be nonzero, $|\Psi_v'\rangle$ and $|\Psi_v''\rangle$ must transform as the same irreducible representations.

For the linear XCX molecule, transitions from its σ_g^+ ground ($v_1=v_2=v_3=0$) vibrational state, are therefore possible only to vibrational states of σ_g^+ symmetry in the ${}^1\Sigma_u^+$ excited electronic state. Since all vibrational levels of the σ_g^+ (symmetric stretch) vibration, and at least one component of alternate excited levels in the π_u (bending) and the σ_u^+ (antisymmetric stretching) vibrations are of σ_g^+ species, transitions to all these states are allowed from the ground state. According to statistical mechanics[15] (Appendix F), a fraction of all the molecules populate excited vibrational levels ($v_i''>0$) of the ground electronic state. Transitions from these v_i'' levels to excited state vibrational levels (v_i') of the same symmetry are possible. The vibrational selection rules for an allowed linear-linear electronic transitions can therefore be summed up by writing

$\Delta v_1 = 0, \pm 1, \pm 2, \pm 3 \ldots$ for the σ_g^+ vibration

$\Delta v_2 = 0, \pm 2, \pm 4, \pm 6 \ldots$ for the π_u vibration

and $\Delta v_3 = 0, \pm 2, \pm 4, \pm 6 \ldots$ for the σ_u^+ vibration (4.12)

where $\Delta v_i = v_i' - v_i''$, refers to the change in the vibrational quantum number of the ith vibration. For a bent $\longleftarrow$ linear transition, the same type of argument gives the vibrational selection rules for the two totally symmetric $\nu_1(a_1)$, $\nu_2(a_2)$ and the one antisymmetric $\nu_3(b_2)$ modes in a $^1B_2 \longleftarrow {}^1A_1({}^1\Sigma_g^+)$ electronic transition. Thus we have

$\Delta v_1, \Delta v_2 = 0, \pm 1, \pm 2, \pm 3 \ldots$ for the ν_1 and ν_2 and

$\Delta v_3 = 0, \pm 2, \pm 4, \ldots\ldots$ for the ν_3 vibrations

(4.13)

The observed vibrational spectrum of an electronic transition may be grouped into progressions and sequences. We define a progression as that collection of transitions from a given vibrational level of one electronic state, to a set of successive levels of the same vibration, in a second electronic state. We define a sequence as that series of transitions having the same value of Δv_i. Thus, those transitions from the $v_1'' = 0$ level of the $\tilde{X}\,{}^1\Sigma_g^+$ state to the set of $v_1' = 0, 1, 2\ldots$etc. levels of the ${}^1\Sigma_u^+$ excited state form a v_1' progression; and those transitions with $\Delta v_1 = v_1' - v_2'' = 0$ forms a sequence in the ν_1 vibration.

ii) Transitions from the $\tilde{X}\,{}^1\Sigma_g^+$ state to the triplet states of Table 4-2 can occur because of spin-orbit interaction discussed in section 1.4. The symmetry species of spin functions in the $D_{\infty h}$ and C_{2v} point groups are given in Appendix E. For S=1, these species are,

$$\begin{tikzcd} D_{\infty h} & C_{2v} \\ \Sigma_g^- & A_2 \\ \Pi_g \arrow[r, dash] \arrow[dr, dash] & B_1 \\ & B_2 \end{tikzcd} \qquad (4.14)$$

The irreducible representation generated by the spin-orbit function $|\Psi_{es}\rangle$, as obtained from the direct product of each spin species in (4.14) with orbital species of each triplet state, are listed in the 4th and 7th columns of Table 4-2. These spin orbit species are used in determining selection rules from equation (1.27).

The probability of transitions which occur only because of spin-orbit coupling, depends upon the magnitude of this coupling. In each of the doubly degenerate ${}^3\Delta$ or ${}^3\Pi$ states of Table 4-2 the magnitude of spin-orbit interaction can be large or small and each triplet state may be separated into component (multiplet) states of different energy. The energy splitting is determined by the magnitude of the spin-orbit interaction. The species of the multiplet components for each orbitally degenerate state is also shown in Table 4-2. Selection rules for transitions from the $\tilde{X}\ {}^1\Sigma_g^+$ state to these component states are also determined by the integral (1.27). It can be shown that among the multiplet components shown in Table 4-2, only the Π_u component can 'combine' with the ground state (in a transition). The vibrational structure of the corresponding $\Pi_u \longleftarrow \tilde{X}\ {}^1\Sigma_g^+$ transition is the same as that of a ${}^1\Sigma_u^+ \longleftarrow \tilde{X}\ {}^1\Sigma_g^+$ electronic transition discussed earlier; however, the rotational structure (section 4.7) of each vibrational 'band' would be of the perpendicular type.

In Table 4-2, the multiplet component species of triplet states, in which there is very little orbital angular momentum, that is ${}^3\Sigma^-$ of the linear molecule and ${}^3A_2$ and ${}^3B_2$ states of the bent molecule are also given. Transitions between the ${}^1\Sigma_g^+$ ground state to any of these triplet states could occur by the intensity 'borrowing' mechanism. If the excited triplet state and some other singlet state which are not very much separated in energy interact due to spin-orbit coupling, then the wavefunction of the triplet state and this singlet state 'mix'. If a transition between this singlet state and the ${}^1A_1$ (${}^1\Sigma_g^+$) state is allowed, then a transition between the triplet state and the ground state is not strictly forbidden. Therefore a nonzero probability for the triplet ⟵ singlet transition is possible.

iii) Transitions from the $\tilde{X}\ {}^1\Sigma_g^+$ (${}^1A_1$) state to the ${}^1A_2$, ${}^1\Sigma_u^-$, ${}^1\Delta_u$ and ${}^1\Pi_g$ states of Table 4-2 are electronically forbidden. To determine whether transitions from the vibronic levels of the $\tilde{X}\ {}^1\Sigma_g^+$ (A_1) state to the vibronic levels of the nondegenerate ${}^1A_2$ and ${}^1\Sigma_u^-$ are allowed, we first obtain the respective vibronic species in each state. If the molecule is in the bent ${}^1A_2$ state, alternate levels (v_2=1, 3, 5, 7...) of the antisymmetric stretching vibration are of b_2 species, the corresponding vibronic species are therefore of $b_2 \otimes A_2 = B_1$ symmetry in the ${}^1A_2$ state and of $b_2 \otimes A_1 = B_2$ symmetry in the ground ${}^1A_1$ state. Perpendicular transitions to any of the B_1 vibronic levels of the excited states are allowed from the B_2 and A_1 vibronic levels of the ground state, (this statement can be verified by the use of equation 1.27). Similar considerations can be used to show even though the ${}^1\Sigma_u^- \longleftarrow \tilde{X}\ {}^1\Sigma_g^+$ transition is forbidden electronically, vibronic transitions of the type $\Pi_g \leftarrow \Pi_u$: $\Delta_u \leftarrow \Delta_g$ are allowed by symmetry.

Transitions between vibronic levels of the degenerate ${}^1\Delta_u$ or ${}^1\Pi_g$ electronic states and those of the ${}^1\Sigma_g^+$ ground state are discussed in the next section; since an important vibrational-electronic type of interaction can occur when degenerate vibrations are excited in degenerate electronic states, this interaction must be considered before examining rules for vibronic transitions any further.

4.4 The Renner Effect

The twofold orbital degeneracy of Π, Δ....etc. (i.e. $\Lambda > 0$) electronic states of diatomic molecules is removed by interaction with the rotational motion of the nuclei (see section 4.7). But in a polyatomic molecule, such a degeneracy may be removed by interaction with degenerate bending vibrations. This type of interaction was first recognized by Teller[91] and was subsequently applied by Renner[92] to evaluate the splitting of Π electronic states of the linear CO_2 molecule. The consequences of such vibronic interactions in linear molecules is called the Renner (-Teller) effect.

In the absence of vibronic interaction, the Born-Oppenheimer approximation can be used to write the total wavefunction $|\Psi_t\rangle$ in the product form $|\Psi_e\ \Psi_v\ \Psi_R\rangle$. If the rotational part is neglected, the product wavefunction $|\Psi_e\ \Psi_v\rangle$ for a linear molecule is given explicitly by the function[93]

$$|\Psi(\Lambda, v, l)\rangle = |\Psi_e\ \Psi_v\rangle = \exp\ (\pm\ i\Lambda\theta) \times \rho_{v|l|}(r)\exp\ (\pm\ il\varphi) \tag{4.15}$$

In Fig. 4-4, the bending coordinate r, the azimuthal angle θ of the electron from a fixed plane P containing the linear molecule, and the angle φ between the plane of bending motion and the fixed plane P, have been indicated. $\rho_{v|l|}(r)$ in the wavefunction (4.15) above is the radial part of the vibrational wavefunction. The definition of the quantum numbers Λ, l and v has been given in sections 3.2 and 3.3.

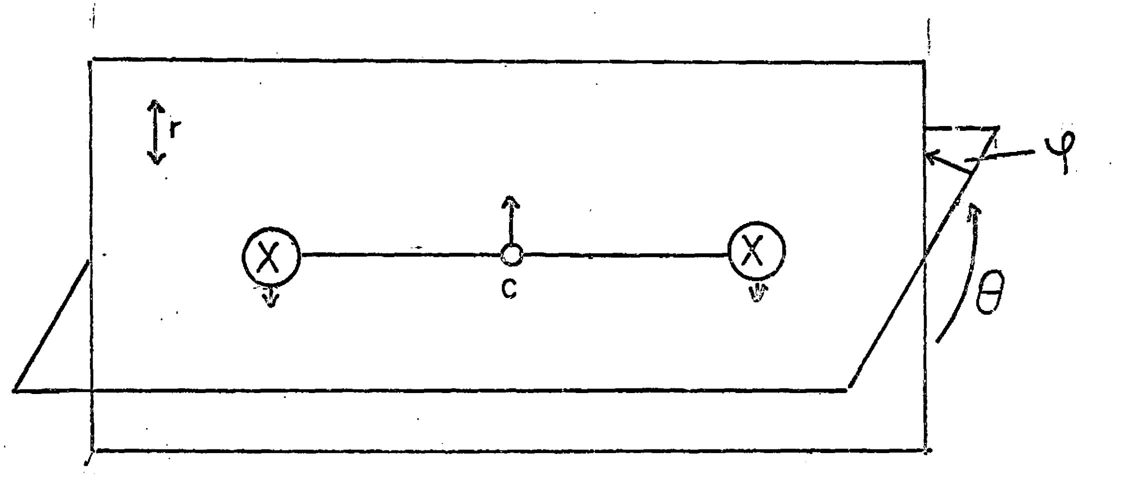

$$\bar{\alpha} = \theta - \varphi$$

BENDING VIBRATION OF XCX MOLECULES

FIGURE 4.4

When there is an interaction between the bending motion and electronic motion, the product function $|\Psi_e \Psi_v\rangle$ is not a good approximation. The effect of the electronic-vibrational interaction on the product function and the zero order eigenvalues can be calculated by perturbation methods, provided the interaction is small and known explicitly. Pople and Longuet-Higgins[94] represented the perturbation due to vibronic interaction as an expansion in r and $\alpha = \theta - \varphi$, and gave it the following form.

$$\begin{aligned} V' = V_o(r) &+ V_1(r)\,[\exp(i\alpha) + \exp(-i\alpha)] \\ &+ V_2(r)\,[\exp(2i\alpha) + \exp(-2i\alpha)] \\ &+ V_3(r)\,[\exp(3i\alpha) + \exp(-3i\alpha)] \\ &+ V_4(r)\,[\exp(4i\alpha) + \exp(-4i\alpha)] \\ &\ldots\ldots\ldots \\ &+ V_m(r)\,[\exp(mi\alpha) + \exp(-mi\alpha)] \\ &+ \\ &+ \ldots\ldots \end{aligned} \tag{4.16}$$

where $V_m(r)$ is of the order of r^m. The matrix element which determines the corrections to the zero order energies and eigenfunctions is given by[95]

$$\langle \Psi_p(\Lambda, v, l) \,|\, v' \,|\, \Psi_q(\Lambda, v, l) \rangle \tag{4.17}$$

For a given pair of states $|\Psi_p\rangle$ and $|\Psi_q\rangle$ of the molecule, those terms in V' which give a nonzero value for (4.17) may be determined from the requirement that the product in the bracket must be totally symmetric. It can be shown that this requirement is fulfilled in the following cases.

a) $|\Psi_p(\Lambda, v, l)\rangle$ and $|\Psi_q(\Lambda, v, l)\rangle$ are identical.

In this trivial case, it can be shown that the integral is nonzero only for the $V_o(r)$ term. As $V_o(r)$ is a constant, all integrals (4.17) have the same value.

b) $|\Psi_p(\Lambda, v, l)\rangle$ and $|\Psi_q(\Lambda, v, l)\rangle$ are not identical.

If both functions are the degenerate components of an electronic state, they may be distinguished from each other by the signed value (if greater than zero) of the quantum no. $K = |\pm\Lambda \pm l|$. It can be shown that all odd terms in V' (of 4.16) such as $V_1(r)[\quad]$, $V_3(r)[\quad]$...etc. give vanishing matrix elements (4.16) between the two component states. It can also be shown that only those even terms $V_m(r)[\quad]$ where $m = |K \pm \Lambda - (K \mp \Lambda)|$ give nonvanishing matrix elements. For example in a Π state, $\Lambda = \pm 1$. Therefore $m = |(K\pm 1) - (K\mp 1)| = |2|$ or $|-2|$. Between the two components of a Π electronic state, only the $V_2(r)[\quad]$ term therefore gives a nonzero matrix element. Similarly, it can be shown[94] that only the $V_4(r)[\quad]$ term gives a nonzero matrix element for the components of a Δ state.

From the discussion in a) and b) above, it is evident that the perturbation expression V' reduces to the following forms for Π and Δ states:

Π states: $\Lambda = \pm 1$ $\quad V' = V_o(r) + V_2(r)\ \exp(2i\alpha) + \exp(-2i\alpha)$

Δ states: $\Lambda = \pm 2$ $\quad V' = V_o(r) + V_4(r)\ \exp(4i\alpha) + \exp(-4i\alpha)$

(4.18)

As a result of the perturbation, two component states are obtained for each of the Π and Δ states; one of the components is symmetric and the other antisymmetric with respect to reflection in the molecular plane. Furthermore these two components are of different energy; the degeneracy of the Π and Δ states is removed. In the new zero order wavefunctions, Λ and l are not good quantum numbers since the electronic and vibrational angular momenta are not independently conserved and must be replaced by $K = |\pm\Lambda\pm l|$.

For Π electronic states, Pople and Longuet-Higgins[94] obtained the potential function of each component state in terms of the bending coordinate r. For the higher energy component the potential function is given by

$$U^{+} = 1/2r^{2} + hr^{4} \qquad (4.19)$$

$$U^{-} = (1/2-f)r^{2} + g'r^{4} \qquad (4.20)$$

Here, the quantities $g' > 0$ and h are anharmonic constants for the lower and upper states respectively and f is a constant measuring the strength of the vibronic coupling. For Δ electronic states, Merer and Travis[96] obtained the potential functions of the two components in the following form

$$U^{\pm} = (k \pm 1/2\eta')r^{4} \qquad (4.21)$$

Here η' and k are quartic coefficients for the Δ state.

The potential functions U^{+} and U^{-} for each electronic state may be plotted as a function of the bending coordinate r.

The forms of these functions are given in Fig. 4-5a), b) and c) for the U^+ and U^- components for a Π state and in Fig. 4-5 d) and e) these components in a Δ state. It can be seen from the expression for U^- in (4-20) that if $f < 1/2$, U^- has the form in Fig. 4-5b) with two minima at +r and -r. At these values of the bending coordinate, the molecule has a lower energy than at $r = 0$. Therefore, a molecule in the lower component state should be stable in the bent conformation. In b), the upper component U^+ is quadratic in r and has a minimum corresponding to the linear conformation. A molecule in the upper component state should be stable in the linear conformation. It was shown by Dixon[96] that if the vibronic interaction is sufficiently large, the upper state may also have a double minimum potential and this curve is given in c). Therefore U^+ and U^- effectively represent the potential functions of two non degenerate states, each of which may belong to a different symmetry point group. This separation of potential curves illustrated by b), c) and e) represents a Static Renner effect. It can be seen from (4-20) that $f > 1/2$, both U^+ and U^- are anharmonic oscillator functions of r. The potentials have the form of Fig. 4-5a). For Δ states, the potential functions U_-^+ given by (4-21) are represented in Fig. 4-5d). In both a) and d) the molecule remains linear, even though the degenerate state has been split into component states. Both a) and d) represent small vibronic interaction. The separation of potential curves actually occurs only during a degenerate vibration (and

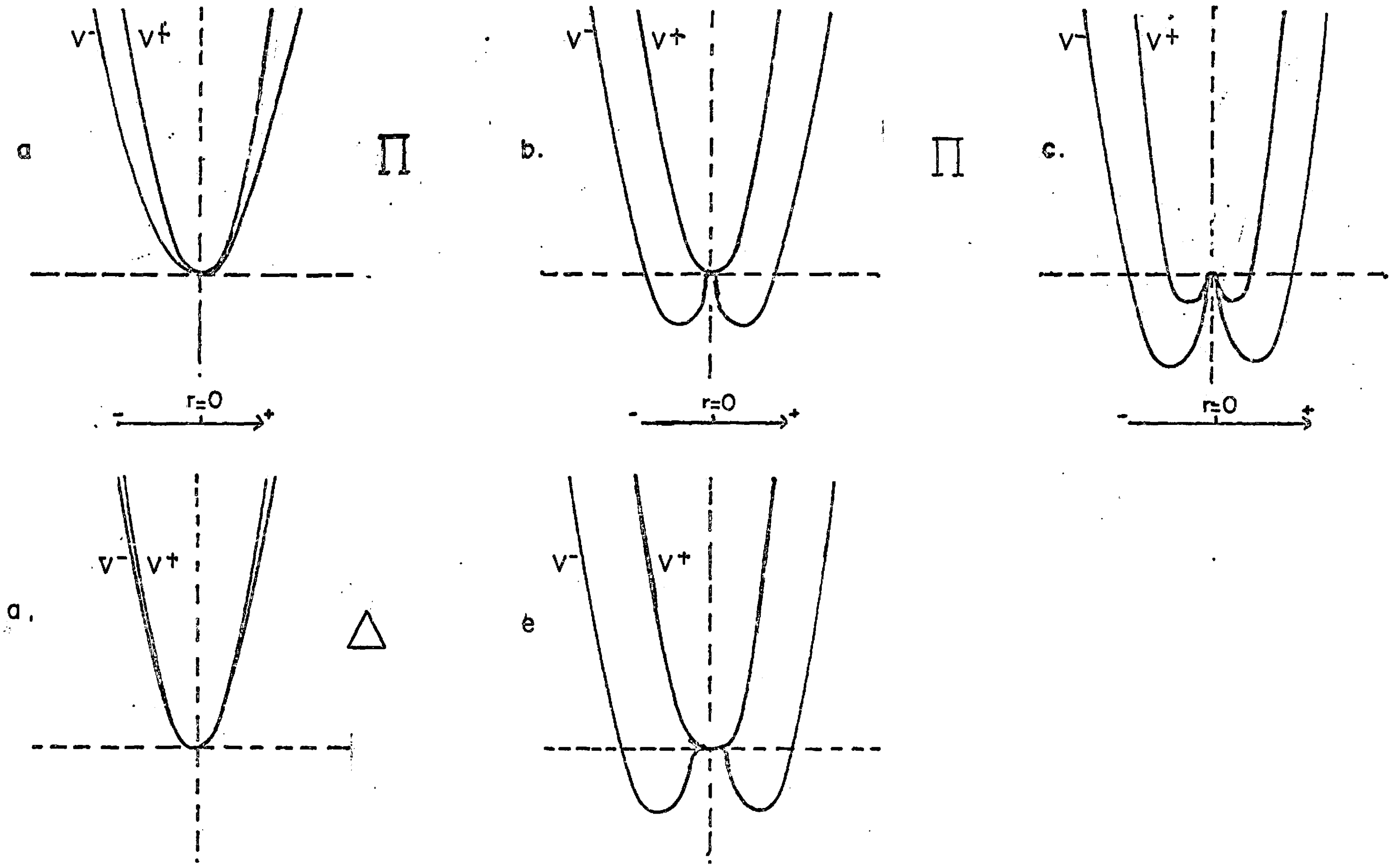

THE RENNER-TELLER EFFECT

FIGURE 4.5

therefore strictly static potential curves U^+ and U^- cannot be drawn). Fig. 4-5e) shows the potential functions of a Δ state for a static Renner effect and is similar to b).

The eigenvalues of the vibronic levels of a $^1\Pi$ state were obtained by Renner for small interaction and by Pople and Longuet-Higgins for small and larger interactions. No such calculation is available for those of a $^1\Delta$ state. However, the eigenvalues of vibronic states of a $^2\Delta$ state have been calculated by Merer and Travis[97] for small Renner-Teller interaction.

The symmetry of the (Renner-Teller) component states has been indicated before; one of them must be symmetric and the other antisymmetric with respect to reflection in the molecular plane. In the extreme case, the XCX molecule is bent in both states and therefore each state can be classified according to the irreducible representations of the C_{2v} point group. For a strong vibronic interaction, two component states, one of A_2 symmetry and another of B_2 symmetry, are obtained from the doubly degenerate $^1\Pi_u$ and $^1\Delta_g$ excited states of the CO_2 molecule. In general, it is not possible to state which of the vibrational states of the components belong to U^+ and which to U^-. Each vibronic level is identified by the quantum number K. The selection rules for transitions from the vibronic levels of the ground state to the vibronic levels of the two component states are determined as before in section 4.3

if the symmetries of these vibronic levels are known. The spacings between vibrational bands can be determined from the formulae of Merer and Travis for Δ states and from the formulae of Renner or Pople and Longuet-Higgins for Π states, provided the vibronic interaction is small.

If the excited state is a $^3\Delta_u$ or $^3\Pi_g$ state, spin orbit coupling and Renner-Teller coupling must both be taken into account. When both interactions are of comparable magnitude the energies of vibronic levels are given by complicated expressions. Hougen[97] calculated these expressions for $^3\Pi$ (as well as $^2\Pi$) states in XYX molecules. For $^3\Delta$ states, no such calculations are available.

If vibronic interaction is large, the molecule will be stable in the bent conformation (of the 'static' approximation). The energy levels of the vibronic states will then be similar to those of the vibrational states of a bent molecule. In the next section, we examine the energy structure of vibrational levels in a bent molecule.

4.5 Vibrational energy levels in bent and linear states

According to equation 3.15, the vibrational energy levels of a bent molecule are expressed as term values G^b thus,

$$G^b(v_1,v_2,v_3) = \omega_1^b\,(v_1 + 1/2) + \omega_2^b\,(v_2 + 1/2) + \omega_3^b\,(v_3 + 1/2) \tag{4.22}$$

where terms due to anharmonicity have been neglected. Similarly, from equation 3.16, the vibrational energy levels of a bent molecule which is in a nondegenerate electronic state are expressed as term values G^l thus,

$$G^l (v_1,v_2,v_3) = \omega_1^l (v_1+1/2) + \omega_2^l (v_2+1/2) + \omega_3^l (v_2+1/2) \tag{4.23}$$

where terms with anharmonicity coefficients have been neglected. The term, $\omega_2^l(v_2+1)$, in the latter expression (4.23) represents the energy levels of the doubly degenerate (π_u) bending vibration. Two degrees of freedom are associated with this vibration. The corresponding terms $\omega_2^b(v_2 + 1/2)$ in the first expression (4.22) represents the energy levels of the non-degenerate bending vibration. Only one degree of freedom is associated with the bending vibration of a bent molecule. Therefore, one 'bending' vibrational degree of freedom is 'lost' by the linear molecule if it bends; this lost degree of freedom appears as a rotational degree of freedom about the y axis (which is a principal axis) of the bent molecule (Fig. 4.3). If the term values given by equations 4.22 and 4.23, are to be compared for the same number of degrees of freedom, an additional term has to be added to 4.23, corresponding to the rotational energy levels of the bent molecule about its y axis.

The rotational energy levels of a bent XCX molecule are those of an asymmetric rotor with unequal principal moments of inertia I_A, I_B and I_C. These moments of inertia can be calculated from the bond distance r_{cx}, the bond angle $\widehat{XCX}$ and the masses of X and C atoms. It can be shown by calculation

(Appendix H) that the moment of inertia about the y axis of the bent CSe_2 molecule is the smallest principal moment of inertia I_A and that I_B is nearly equal to I_C. In terms of rotational constants A, B and C where,

$$A = \frac{h}{8\pi^2 cI_A} \qquad B = \frac{h}{8\pi^2 cI_B} \qquad C = \frac{h}{8\pi^2 c\, I_C}$$

these relationships are given by

$$A > B \simeq C$$

which is a characteristic property of a near prolate asymmetric rotor. In the case of CSe_2 for example, if the angle $\widehat{SeCSe}$ is 120° and r_{CSe} = 1.711Å then A = 2.0 , B = 0.048 and C = 0.047, in cm^{-1} units. It is seen from Appendix H, that $A > B \simeq C$, even if the bond angle is large. The asymmetry parameter κ is nearly equal to -1 which is the value of κ for a prolate symmetric rotor. Hence, we assume that the rotational energy levels of the bent molecule can be represented by expressions similar to those of a prolate symmetric rotor. These expressions are given in Appendix G. The energy levels for the rotational motion about the y axis alone is given by the term $A_{v_2}K^2$ where $K = |\pm\Lambda \pm l|$ is the angular momentum quantum number given before and A_{v_2} is the rotational constant for the vibrational state with quantum number v_2. If this $A_{v_2}K^2$ term is added to 4.23 , we get

$$G^b\ (v_1,v_2,v_3) = \omega_1^b(v_1+1/2) + \omega_2^b(v_2+1/2) + \omega_3^b(v_2+1/2) + A_{v_2}K^2 \qquad (4.23\ a)$$

This expression gives the term value of rovibrational levels with quantum number v_1, v_2, v_3 and K.

The correlation between the vibrational levels of a linear molecule and the rovibronic levels of the bent molecule is illustrated by Figs 4-6 a), b) and c). In b), successive vibrational levels of the degenerate $\nu_2(\pi)$ mode of the linear $^1\Sigma$ state are shown by horizontal lines within the potential curve. The l (=K) sublevels are also indicated therein. The potential function of a bent XCX molecule, with two minima at +r and -r values of the bending coordinate in the linear molecule, is shown in Fig 4-6 a). The illustration at the top of this figure shows the 'bending' of the linear molecule. It is seen that this potential function resembles the lower component functions represented in Fig 4-5 b) and e). The molecule is stable in the bent configuration at the +r and -r values of the bending coordinate. The hump at r=0 represents a finite potential barrier for the molecule to change over from a +r to -r configuration or vice-versaby the bending motion. However, this barrier does not exist for a change of configuration by rotation about the y axis of the bent molecule. Each curve in Fig 4-6 represents a planar section of a cylindrically symmetric potential curve. Horizontal lines representing vibrational levels have been drawn both near the minima and the central hump in Fig 4-6 a). Fig c) and a) are the same curves except for the expansion of the vertical energy scale in the former. In c), the first three vibrational levels i.e.

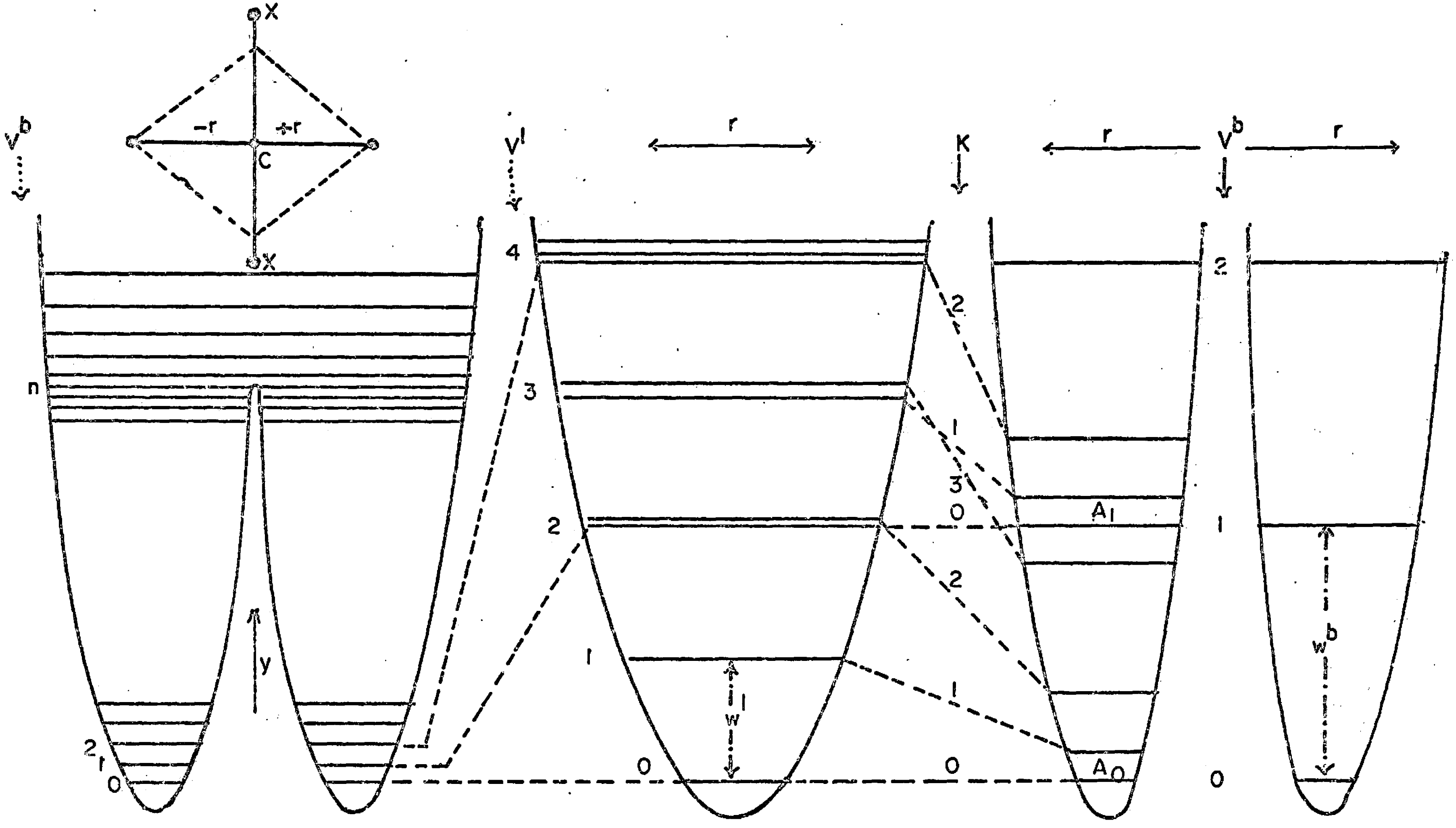

a. Bent b. Linear c. Bent

CORRELATION OF ENERGY LEVELS IN XCX MOLECULES

FIGURE 4.6

v_2^b = 0, 1, and 2 are shown. Quadratically spaced rotational sublevels with K = 0, 1, 2 and 3 are also shown for the v_2^b=0 level. The energy spacing between K=0 and 1 has been denoted by A_0. A_1, corresponding to a similar spacing in the v_2^b=1 vibrational level, is also indicated. Pairs of lowest energy levels with the same K have been connected by dashed lines.

From Fig 4-6a), we note that if the vibrational quantum v_2^b exceeds the value at the top of the hump (i.e. $v_2^b > n$) the molecule is effectively linear; because, the amplitude of bending vibration in the 'bent' molecule is large enough to 'freely' change the molecular configuration from +r to -r. Secondly, the width of the potential function above the hump is larger than that below the hump. For this reason, the vibrational frequency (ω_2^1) of the linear molecule must be smaller than that (ω_2^b) of the bent molecule. Thirdly, comparison of b) and c) in the figure indicates that the constant A_o of the bent molecule is correlated with that of the vibrational frequency ω_2^1. That is, A_o will approximately become equal to ω_2^1 when the molecule changes its configuration from bent to linear.

The variation in energy of the K levels as the molecule changes its conformation has been investigated by Dixon[98], Johns[99] and Thorson and Nakagawa[100]. Each of them considered the potential function of a linear molecule as that of a two dimensional isotropic harmonic oscillator, and introduced a perturbation in the function to produce the central 'hump' shown in Fig 4-6a). Thorson and Nakagawa assumed the potential function to be

$$V = 1/2r^2 + K_B/(C^2 + r^2) \qquad (4.24)$$

where C, K_B are constants. It is seen that if $r = 0$, $V = K_B/C^2$ gives the hump height. Dixon used a function of the form

$$V = 1/2r^2 + \alpha \exp(-\beta r^2) \qquad (4.25)$$

where α, β are constants. It is seen that if $r = 0$, $V = \alpha$ gives the hump height. The first of the two summation terms in (4.24) and (4.25) is the potential function of a two dimensional harmonic oscillator for which eigenvalues and solutions are known[101].

The method of applying these functions (4.24) and (4.25) to calculate the energy levels of the molecule has been discussed by Johns and will not be repeated here. However, some of the conclusions arrived at by Johns and other workers on the basis of their calculations, are summarized below with the aid of Fig. 4.7.

1. Fig. 4.7 a shows the variation in the value of ΔG i.e. $G(v_2+1,K) - G(v_2,K)$ of the bent molecule, with respect to an average term value $\bar{G}$, given by $1/2\,[G(v_2+1,K)+G(v_2,K)]$. It is seen that each $\Delta G(K)$ curve decreases to a minimum and then increases again. This minimum is most pronounced for K=0 and less so for higher K values. Such a behaviour of ΔG values has been observed experimentally for some triatomic molecules[99,102] and has been attributed to the potential hump in the potential function discussed earlier. The minimum in ΔG occurs at an

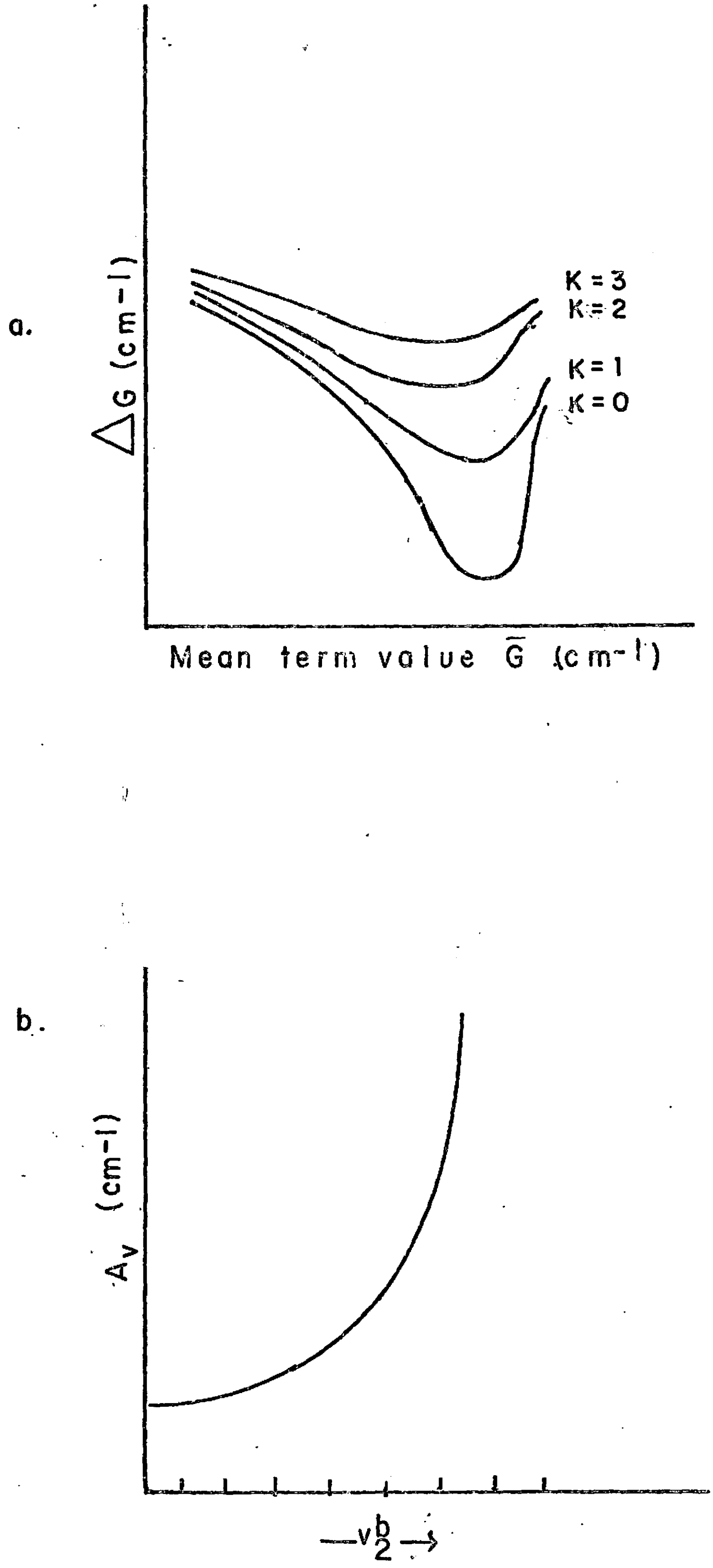

FIGURE 4.7

energy corresponding to that near the top of the hump[99]. The decrease in ΔG values up to the minimum can be attributed to a negative value of the anharmonicity coefficient x_{22} in expression (3.16) and the increase ΔG after the minimum to a positive value of the anharmonicity coefficient.

II. Fig. 4.7b shows the variation to the value of $A_{v_2}^{b}$ with respect to v_2^b. It is seen that A_{v_2} increases slowly for small values of v_2^b and then increases rapidly for larger values of v_2^b. Experimental evidence for such a behaviour of A_{v_2} has been found[99].

If, from an experimentally observed spectrum, evidence is obtained in support of these two conclusions above, it can be inferred that a bent state is involved in the transition.

In order to determine selection rules for transitions from the vibronic levels of the ${}^1\Sigma_g^+$ electronic state to the vibronic levels of the bent XCX molecule, the symmetry species of the latter levels must be known. It is convenient to assume that the symmetry of each of these vibronic levels is the same as that of the correlating vibronic levels in (the limiting case of) the linear molecule. Selection rules are then determined by the use of (1.27).

4.6 The Franck - Condon Principle

In section 4.3 selection rules for electronic transitions and for transitions between vibrational states of each 'combining' electronic state have been discussed. The selection rules for such vibrational transitions in the product wavefunction approximation $|\Psi_e \Psi_v\rangle$ are determined by the overlap integral

$$R_{v'v''} = \langle \Psi_{v'} | \Psi_{v''} \rangle \qquad (4.26)$$

which is one of the factors of $\vec{R}$ in equation 4.10. $|R_{v'v'}|^2$ determines the relative intensities of the vibrational bands in an electronic transition, and is the basis of the quantum mechanical formulation of the Franck-Condon principle[103]. The classical approach to the Franck-Condon principle will not be discussed here. For the present purpose we shall just use the criterion that larger the magnitude of the overlap integral, more intense will be the observed transition between the states $|\Psi_{v'}\rangle$ and $|\Psi_{v''}\rangle$ Therefore (4.26) becomes

$$R_{v'v''} = \langle \psi_{v_1'} / \psi_{v_1''} \rangle \langle \psi_{v_2'} / \psi_{v_2''} \rangle \langle \psi_{v_3'} / \psi_{v_3''} \rangle$$

$$= R_{v_1'v_1''} \times R_{v_2'v_2''} \times R_{v_3'v_3''} \qquad (4.27)$$

for the vibrational wavefunctions of the linear triatomic molecule. Each of these factors is considered separately below with the aid of Figs. 4-8 a), b), c) and d).

The potential energy curves for the symmetric stretching coordinate Q_1 [in (a) and (b)] and for the bending coordinate Q_2 [in (c) and (d)] are shown schematically in the figures. The curves in a) have each of their potential minima, corresponding to the excited and ground state equilibrium configurations,

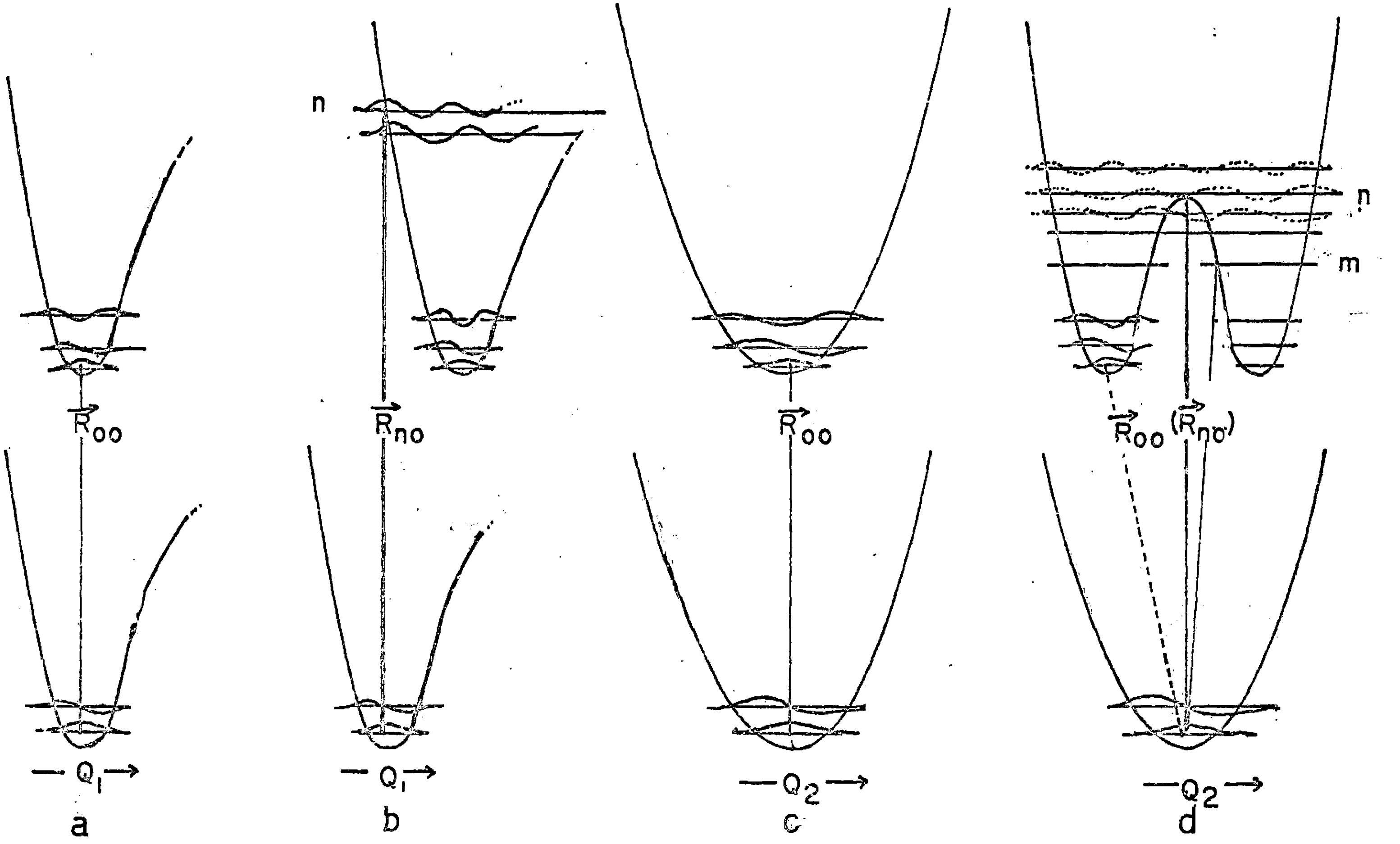

THE FRANCK—CONDON PRINCIPLE

FIGURE 4.8

at the same coordinate positions. In b), these minima are displaced. The curve at the top half of c) gives the potential energy curve for the bending coordinates for a linear molecule; that of d) gives the potential energy curve for the bending coordinate for a XCX molecule with energy minima at two values of the bending coordinates. The ground state potential curve is also shown in c) and d). The form of the wavefunctions for a few vibrational levels are also indicated in each of these curves. Vertical or sloping lines are drawn from $v''_i = 0$ levels to excited state vibrational levels.

The intensity distribution among the vibrational transitions for a given electronic transition will be considered with respect to each of the cases a), b), c) and d) in Fig. 4-8. Case a): There is very little change in the equilibrium value of the bond length r_{CX} between the two electronic states. Therefore, the potential curves of ground and excited states for the symmetric stretching mode Q_1 are almost the same; $|\psi_{v'_1}\rangle$ and $|\psi_{v''_1}\rangle$ are nearly orthogonal. Hence, the overlap integral $R_{v'v''}^{v'_1 v''_1}$ is large only for vibrational transitions with $\Delta v_1 = v'_1 - v''_1 = 0$. In cold absorption, most of the molecules are in the $v''_1 = 0$ level. Therefore, if $\Delta v_1 = 0$ applies, only the 0 - 0 band will be observed. At higher temperatures, levels with $v''_1 > 0$ are also populated sufficiently and sequence bands with $\Delta v_1 = 0$ from excited vibrational levels of the ground state may be observed. In case a), therefore, sequence bands in the symmetric stretching vibration will be the most intense.

Case b): There is a very large change in the equilibrium value of r_{CX}. The potential functions are not identical for the symmetric stretching vibrational mode Q_1 in the ground and excited electronic states. Hence, the overlap integral between states with quantum numbers v_1' and $v_1'' \neq v_1'$ can be nonzero because $|\psi_{v_1'}\rangle$ and $|\psi_{v_1''}\rangle$ are not necessarily orthogonal. Let us consider only these vibrational transitions from the state with $v_1'' = 0$ to v_1' states (i.e. absorption transitions at very low temperatures). It is found that the maximum value of $R_{v_1'v_1''}$ is obtained, not between states with identical vibrational quantum numbers as in case a), but between states with $v_1' = n$ (where $n > 0$) and $v_1'' = 0$; n is a large integer if the change in r_{CX} is large. Nonzero values of overlap integrals may also be obtained between states with $v_1' > n$ or $v_1' < n$, and $v_1'' = 0$. Therefore, bands corresponding to transitions from $v_1'' = 0$ to states with $v_1' = \ldots\ldots n+1, n, n-1 \ldots$ etc. (which represents a v_1' progression) are observed in cold absorption. Among the bands of this progression, that which corresponds to the $v_1' = n \leftarrow v_1'' = 0$ transition will be the most intense. At higher temperatures, progressions in v_1' from the initial vibrational level $v_1'' > 0$ are also observed. In case b) therefore, progressions in the symmetric stretching vibration will be the most intense.

Case c): This case is analogous to case a) except that the potential functions are plotted for the bending coordinate Q_2 (or 'r' as in section 4.5). The molecule is linear in both the ground and excited electronic states and therefore there is no change in the coordinate Q_2. By arguments similar to those used in case a), it can be shown that in cold absorption the 0-0 band is the most intense and that at higher temperatures, sequence bands in the bending vibration may be observed.

Case d): In this case, vibrational transitions from the ground electronic state of a linear molecule to a excited electronic state of a bent molecule are examined. Since the XCX molecule is stable in the bent configuration of the excited state at $Q_2' = r$, the equilibrium value of the bending coordinate $Q_2'' = 0$ in the ground state is necessarily altered on excitation. The potential functions are quite dissimilar and the upper state function resembles that in Fig 4.6 a) or the bent component of the function in Fig. 4.5 b) or e). Whereas the schematic representation of vibrational wavefunctions is correct near the minima of this potential function (Fig. 4.8 d), it is not strictly correct for the wavefunctions near the hump; because if there is strong vibronic interaction, the product resolution $|\Psi_{e'}\Psi_{v'}\rangle$ is not a good approximation to the total $|\Psi_t\rangle$. In spite of this limitation, these wavefunctions represented by dotted curves are given in Fig. 4.8 (d), in order to explain qualitatively, the distribution of intensities in vibrational transitions. The overlap integral $R_{v_2'v_2''}$ (if $R = R_{e'e''} \times R_{v'v''}$ is assumed to be valid) will be a maximum for states with $v_2'' = 0$

and $v_2' = 0$ and $v_2' = n$ where n is a value of the quantum number near the hump. This transition between $v_2'' = 0$ to $v_2' = n$ level is represented in the figure by a vertical line. $R_{v_2' v_2''}$ will decrease from this maximum value to a minimum value for states with $v_2'' = 0$ and $v_2' = 0$. This transition between $v_2'' = 0$ to $v_2' = 0$ level is represented by a dashed dotted line. The value of $R_{v_2' v_2''}$ for a transition between states with $v_2'' = 0$ and $v_2'' = m$, where $n > m > 0$ lies between these maximum and minimum values. Such a transition is represented by a full line. If an electronic transition from the ground state to the excited state is allowed for a linear conformation of the XCX molecule in both states, (i.e. for $r' = 0 \leftarrow r'' = 0$) then, in cold absorption, a progression of bands in the bending vibration due to transition from $v_2'' = 0$ to $v_2^{b'} = \ldots.\ n+1,\ n,\ n-1\ \ldots.$ etc. may be observed. The band due to $v_2' = n \leftarrow v_2'' = 0$ transition should be the most intense, and the intensity of bands on either (frequency) side of this band should decrease successively. On the other hand, an electronic transition from the ground state to the excited state may be allowed only if the molecule is bent in the excited state (i.e. $R_{e'e''}$ is zero for $r' = r \leftarrow r'' = 0$ transition). Even then, a progression of bands in the bending vibration may be observed; but in this case, transition from $v_2'' = 0$ occur, not to levels near $v_2' = n$ but to $v_2^{b'} = \ldots.\ m+1,\ m,\ m=1\ldots.$ etc. levels, where m is a quantum number between $v_2^{b'} = 0$ and $v_2^{b'} = n$. Transitions to v_2' levels near m have the highest probability, because $R_{e'e''} \times R_{v'_2 v''_2}$ has a minimum value for these levels. This product is zero at $r' = 0$ because $R_{e'e''}$ is zero and is very small at $r' = r$ because $R_{v'v''}$ is very small. It is concluded therefore, that if the XCX molecule is bent in the excited state, progressions in the bending vibration may be observed.

It can be shown, by similar arguments as above, that, in principle, progressions in the antisymmetric stretching vibration should occur, if in its equilibrium configuration in the excited state, the XCX molecule is linear but has unequal r_{CX_1} and r_{CX_2}.

4.7 Rotational Structure of vibronic transitions

Transitions from vibronic states of a linear XCX molecule in its ground ($^1\Sigma_g^+$) electronic state to those of the linear or bent XCX molecule in its excited (singlet or triplet) electronic state have been discussed in the previous sections. Transitions between rotational states accompanying each vibronic transition are discussed in this section.

The vibronic states of the linear XCX molecule can be classified by the quantum number $K = |\pm\Lambda \pm l|$. The symmetry species of these states are denoted by symbols Σ, Π, Δ ... etc. depending upon the value of K. In the ground $^1\Sigma_g^+$ electronic state, $\Lambda = 0$ and hence, $K = l$. In the excited state, Λ can be greater than zero, as is evident from Table 4-2. The energies of rotational states in each of these vibronic levels are analogous to those in electronic states of a homonuclear diatomic molecule. The symmetry of each rotational level is given by its parity + or - and nuclear exchange symmetry 's' or 'a'. The term values of rotational levels are given by expression (3.20) where K replaces l. Each of these rotational levels is doubly degenerate for Π, Δ.... etc. vibronic states, in which K > 0. For the ground Σ_g^+ (or any excited Σ electronic state) this degeneracy is l-type degeneracy discussed in section 3.4; interaction of rotation and vibration removes this degeneracy and the resultant splitting of levels with the same J is called 'l' type doubling. The magnitude of this splitting for π vibrational levels is approximately given by

$$\delta = q_{\pi} J(J+1) \qquad (4.28)$$

where, for XCX molecules, q_{π} is given by

$$q_{\pi} = \frac{B_e^2}{\omega_2} \left(1 + \frac{\omega_2^2}{\omega_3^2 - \omega_2^2} \right) (v_2+1) \qquad (4.29)$$

For Δ vibrational states δ is given by

$$\delta = q_{\Delta} J^2 \; (J+1)^2 \qquad (4.30)$$

where q_{Δ} is much smaller than q_{π}. For excited singlet electronic states such as $^1\Pi$, $^1\Delta$ etc. in which $\Lambda > 0$ there is an electronic double degeneracy for each J level. The splitting of this degeneracy, i.e. the so called Λ-type doubling, is caused by interaction between electronic and rotational motions of the molecule and has been discussed extensively in literature[104].

For Π electronic states, δ is again given by equation (4.28) but q is given by

$$q \backsimeq \frac{2B_e^2}{\sigma_e} \qquad (4.31)$$

where σ_e =T'-T" (see equation 4.40)

For vibrational levels with $l > 0$ in these degenerate electronic states the total twofold degeneracy in K has to be considered. The splitting of this degeneracy i.e. the so called K-type doubling occurs by the interaction of rotational electronic motion as well as by that of rotation and vibration[105]. The magnitude of this splitting is proportional to J(J+1) for Π vibronic states and $J^2(J+1)^2$ for Δ vibronic states. The symmetries of rotational levels in each vibronic state such as Σ_g, Σ_u, Π_g, Π_u etc., are the same as those of homonuclear diatomic molecules and will not be discussed here. (For details refer to 106).

In section 4.5, it was indicated that the bent CSe_2 molecule is a near prolate symmetric top. Rotational energy levels can therefore be represented by expressions similar to those of a prolate symmetric top. In terms of an asymmetry parameter defined by[107]

$$b = \frac{C_v - B_v}{2\left[A_v - 1/2(B_v + C_v)\right]} \qquad (4.32)$$

where A_v, B_v and C_v are rotational constants in the vibrational state, the term values $F_v(J,K)$ for the rotational levels are given by[108]

$$F_v(J,K) = 1/2\ (B_v + C_v)J(J+1) + [A_v - 1/2(B_v + C_v)]$$
$$+ (1 - 3/8\ b^2 - 51/512\ b^4 - \ldots)K^2$$
$$+ \Delta B^K_{eff}\ J(J+1)$$
$$+ \Delta D^K_{eff}\ J^2(J+1)^2$$
$$+ \Delta H^K_{eff}\ J^3(J+1)^3 + \ldots \qquad (4.33)$$

These formulae are expected to be valid as long as J and b are not too large. In these expressions ΔB_{eff}, ΔD_{eff} and ΔH_{eff} are coefficients related to b and are given in Appendix G. For $K > 0$, each of these coefficients have two values, because of the ± signs in equation (G.1), (G.2) (G.3) and (G.4). Therefore, if $K > 0$, each J level splits into two levels of different term values. This splitting represents a K-type doubling of each J level and increases with the value of b, the asymmetry parameter. In other words, the greater the deviation from linearity and therefore, from a symmetric top, the greater is this K-type doubling. This doubling is a maximum for K = 1 and decreases for increasing values of K.

Selection rules for rotational transitions are given by

a) For parallel transitions:

$K' = K'' = 0 \qquad \Delta K = 0 \qquad \Delta J = \pm 1$

$K > 0 \qquad \Delta K = 0 \qquad \Delta J = 0, \pm 1$

b) For perpendicular transitions:

$\Delta K = \pm 1 \qquad \Delta J = 0, \pm 1$

and in addition, by symmetry, the selection rules

$+ \longleftrightarrow -$ $\qquad + \nleftrightarrow +$ $\qquad - \nleftrightarrow -$

$s \longleftrightarrow s$ $\qquad a \longleftrightarrow a$ $\qquad s \nleftrightarrow a$

These selection rules apply whether the XCX molecule is linear or bent (to a near prolate symmetric top) in the excited state. If the molecule is linear in both the ground and excited states, the rotational structure of vibronic transitions are very similar to those of homonuclear diatomic molecules and will not be discussed here in detail (refer to 106). If the molecule is bent, in the excited state, the rotational structure of vibronic transitions are similar but not the same. Transitions between the vibronic levels of the ground state and the vibronic levels of the bent excited state are illustrated with the help of Fig. 4.9. In this figure, K sub-levels and their symmetry species in the ground $^1\Sigma_g^+$ electronic state and in excited B_2 and B_1 electronic states are shown. The symmetry species of K sublevels are given in parenthesis and correspond to those of the linear molecule in the limiting case. As mentioned earlier in section 4.3, the transition $^1B_2 \leftarrow {}^1\Sigma_g^+$ is a parallel transition and the $^1B_1 \longleftarrow {}^1\Sigma_g$ transition is a perpendicular transition (so is a $^1A_1 \longleftarrow {}^1\Sigma_g^+$ transition). Possible transitions between K sublevels of the former pair of states, as determined by the selection rule $\Delta K = 0$, are represented schematically by vertical lines in the left half of the figure. Possible transitions between the K sublevels of the latter pair of states, as determined by the selection rules $\Delta K = \pm 1$, are represented similarly in the right half of the

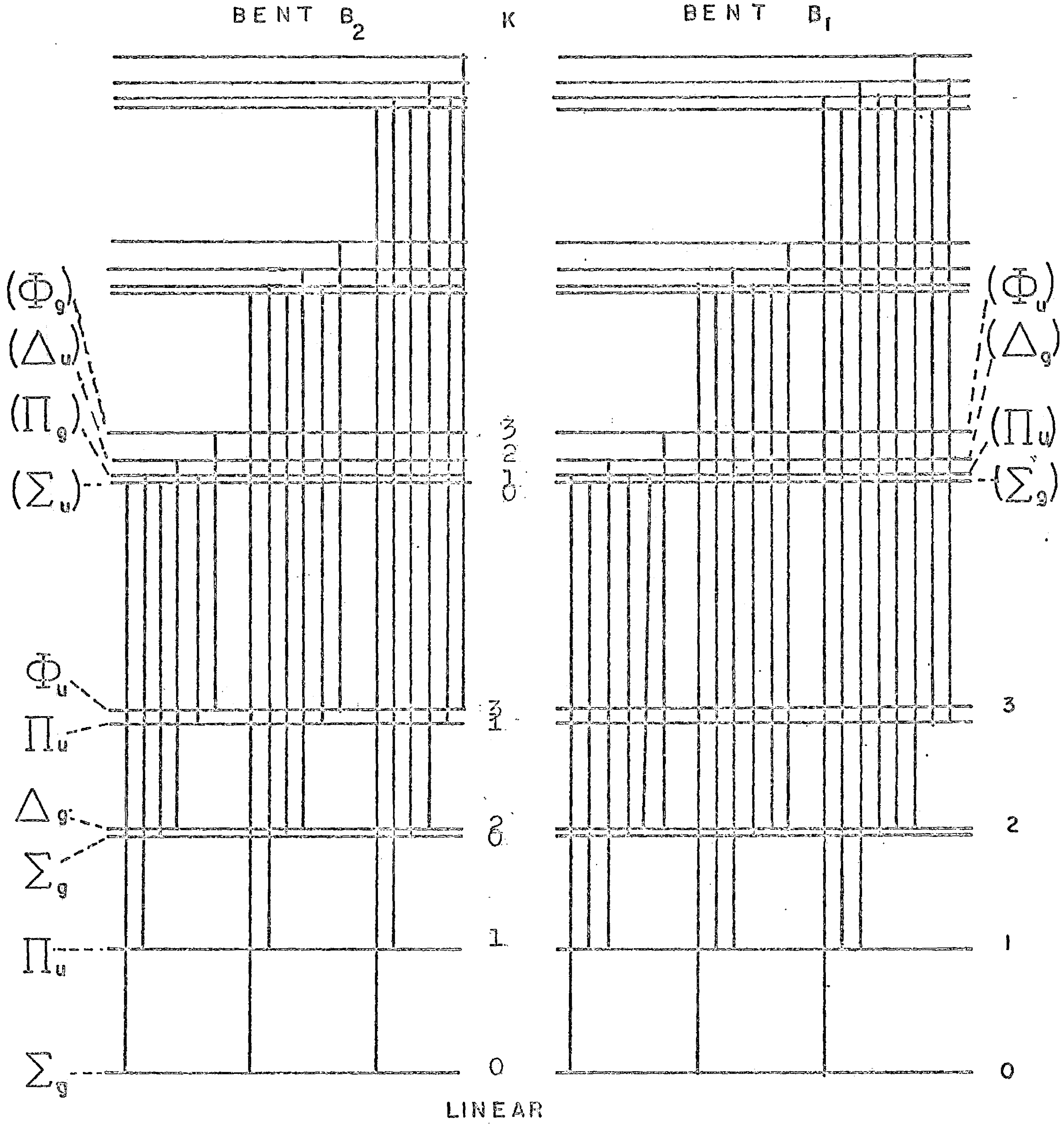

XCX MOLECULE

K - SUBLEVELS AND EFFECTIVE SYMMETRIES

FIGURE 4.9

figure. It can be shown that for parallel transitions the rotational structure of vibronic bands resembles $\Sigma_u - \Sigma_g$; $\Pi_g \longleftarrow \Pi_u$; $\Delta_u \longleftarrow \Delta_g$ etc. type transitions of a homonuclear diatomic molecule whereas for perpendicular transitions $\Pi_u \longleftarrow \Sigma_g$; $\Sigma_g \longleftarrow \Pi_u$; $\Delta_g \longleftarrow \Pi_u$;... etc. type transitions. As shown in section (3.6), the selection rules in J give rise to three main series of rotational lines called P, Q and R branches in each of these vibronic transitions. In a $\Sigma - \Sigma$ type transition, however, the Q branch is absent; in other parallel type transitions, the Q branch lines are relatively weaker than P or R branch lines; and in perpendicular transitions, Q branch lines are relatively stronger than P or R branch lines. It can be shown that if the nuclei of XCX molecule have a zero spin, alternate rotational lines in each branch are absent in $\Sigma_u \longleftarrow \Sigma_g^+$ and $\Pi_u \longleftarrow \Sigma_g^+$, type vibronic bands. It can also be shown that if the spin of the equivalent X nuclei is 1/2, then the intensities of successive rotational lines in each branch of the latter two band types are expected to be in the ratio of 3:1.

Since both bent ← linear and linear ← linear transitions discussed above have very similar rotational structure, some properties must be found in order to distinguish between the two types. Such properties are enumerated below.

(1) The ΔD_{eff} coefficient (Appendix G) of the excited vibronic state, has the largest value for K = 0 and is proportional to the square of the asymmetry parameter b. If a rotational

analysis of a $\Sigma - \Sigma$ band is carried out, the value of D', the centrifugal distortion constant, in the upper state can be determined. If the upper state is bent then $D' = \Delta D_{eff}$ is expected to have an anamolously large value[109] compared to the D' value of the linear XCX molecule.

(2) The upper state can be judged to be bent or linear from the magnitude of the K-type doubling in the excited state. If the molecule is bent considerably, the deviation of the molecule from a symmetric top is relatively large. Therefore K-type doubling is expected to be large[109], when compared to the K-type doubling in a linear XCX molecule or when compared to the K-type doubling in the ground state.

The magnitude of the K type doubling δ in the upper state is

$$\delta(J) = 1/2\ (B_v - C_v) J(J+1) \qquad (4.34)$$

This $\delta(J)$ may be obtained from a rotational analysis of $\Pi - \Sigma$ type vibronic bands, by the use of the following relationship between the rotational lines

$$\begin{aligned}[R(J) - Q(J)] - [Q(J+1) - P(J+1)] &= \delta(J+1) + \delta(J) \\ &= (B_v - C_v)\ (J+1)^2\end{aligned} \qquad (4.35)$$

If there were no K-type doubling, the right hand side of (4.35) would be zero; if there is doubling, the right hand side is nonzero and is called a 'combination' defect. If the magnitude of the combination defect is large, it is a good indication of a bent upper state, provided that the ℓ - type doubling is not anamolously large in the ground state.

(3) In vibronic transitions of the parallel type, the effect of large K-type doubling on the rotational structure may be observed directly. In $\Pi - \Pi$ transitions, for example, because of ℓ - type doubling in the ground ($^1\Sigma_g^+$) state and the K-type doubling in the excited state, three pairs of rotational branches $P_c(J)$, $P_d(J)$, $Q_c(J)$, $Q_d(J)$, and $R_c(J)$, $R_d(J)$ occur. If the K-type doubling is as large as in a considerably bent molecule, each branch in a pair is separated widely from the other with increasing J value. The most prominent heads in the $\Pi \leftarrow \Pi$ band are formed by either the P_c and P_d pair of branches or the R_c and R_d pair of branches. Q_c and Q_d branches are weaker and may not be observed. If the separation between P_c and P_d or R_c and R_d is large, then two band heads which are well resolved are observed. Such a large separation is not expected, if the molecule is linear in both the upper and lower states, since the ℓ or K-type doubling for these states are usually small. In $\Delta - \Delta$, $\Phi - \Phi$, ...etc. type parallel transitions, the splitting between the heads formed by P_c, P_d or R_c, R_d is expected to be relatively smaller than that for $\Pi \leftarrow \Pi$ type transitions.

From a rotational analysis of the J structure of vibronic bands of bent linear transitions, an effective rotational constant for the upper state $B'_{eff} = 1/2\ (B'_v + C'_v)$ (refer to equation 4.33) can be obtained. From a vibrational analysis of these transitions, term values of rovibronic levels defined by v_2 and K may be obtained from the wavenumbers of the bands observed in the transition. From (4.33) it is seen that if J=0 and K=0, 1, or 2, the following relationships are obtained.

$$F_V'(0,1) - F_V'(0,0) = A_V' - 1/2\,(B_V' + C_V') \qquad (4.36)$$

and for K' = 0 and K' = 2

$$F_V'(0,2) - F_V'(0,0) = 4A_V' - 2\,(B_V' + C_V') \qquad (4.37)$$

Hence, by substitution of experimentally obtained values of $F_V(0,0)$, $F_V(0,1)$ in (4.36) and (4.37) and from $B_{eff}' = 1/2(B_V'+C_V')$ and (4.35) the individual constants A_V, B_V and C_V may be obtained.

The discussion so far has been restricted to singlet-singlet electronic transitions. Transitions from the singlet ground state of the linear molecule to triplet states may be allowed due to spin-orbit interaction in the excited state. If the molecule is linear in the excited state, then spin orbit interaction in this state is treated in the same way as in diatomic molecules. When the interaction is small[110] (Hund's case b), a triplet ← singlet transition is relatively forbidden; if it is large (Hund's cases a) or c)), each triplet state is split into component multiplet states (section 4.3). The symmetry species of such component states is given in Table 4.2. Selection rules for transitions from the $^1\Sigma_g^+$ ground state to these component multiplet states are obtained as usual. Selection rules for vibronic and rotational transitions in these component states are also determined as before. If the molecule is bent in the excited triplet state then transitions from the singlet ground state to this triplet state could occur by the intensity 'borrowing' mechanism described in section 4.3. The rotational structure of the triplet singlet transitions should resemble that of a transition from the singlet ground state to the singlet state from which intensity is 'borrowed' by the triplet state. In Table 4.2 the multiplet component states for each triplet state of the bent molecule are also given; if a large spin-orbit interaction is possible then the three component states are widely separated in energy. Transitions from the ground state to these states should be very similar to the bent-linear transitions discussed earlier.

4.8 Zeeman Effect

Application of a magnetic field to a polyatomic molecule introduces an external perturbation term into the total Hamiltonian. The function of the magnetic field is to destroy the isotropy of space. When this field is applied the 2J + 1 fold degeneracy of each rotational level J is removed in the molecule. This effect is called the Zeeman effect[111]. For atoms, the perturbation term due to the magnetic field is given by $H_Z = -\mu.H = \beta (L_Z + g_s S_Z)H$ where z is the field direction, μ is the magnetic moment of the atom, $\beta = eh/4\pi m_e c$ the Bohr magneton; L_Z and S_Z are the components of the orbital and spin angular momenta in units of h and g_S is a constant for the state.

If the molecule has a magnetic moment μ, the 2J + 1 states of different M_J will have different energies and observed spectra of transitions involving these J levels should exhibit a fine structure in the magnetic field.

Three types of Zeeman effect are known in linear molecules[112]. The first of these types occurs in electronic states which have magnetic moments due to the orbital angular momenta of electrons. Examples of such states are $^1\Pi$, $^1\Delta$ ... etc. (i.e. states with $\Lambda > 0$) of linear molecules. It has been shown that in this type of Zeeman effect, the overall splitting (i.e. the difference in energy) $\Delta\sigma(J, - J)$ between the M = +J and M = -J levels of each J level, decreases inversely as J + 1. Each line of an observed rotational spectrum, if resolved, appears as several lines because of the splitting in energy of each J level. In the first of the three types of Zeeman effect, the separation between these component lines decreases rapidly with increasing J and may be observed only for small values of J. The second type of Zeeman effect occurs in states where a magnetic moment arises from electron spin. Such a typical state is the $^3\Sigma$ state of linear molecules. It has been shown that the overall splitting $\Delta\sigma(J, - J)$ in this state is nearly independent of J for higher values of J. Therefore, the Zeeman splitting of rotational lines in the spectrum arising from transitions between $^3\Sigma$ electronic states should be of equal magnitude for higher rotational levels. This type Zeeman effect is expected in Hund's case b) states where spin is weakly coupled to the orbital angular momentum. The third type occurs in nondegenerate singlet $^1\Sigma$ electronic state. In this state, the magnetic moment of the molecule due to nuclear rotation is effectively compensated by that of the accompanying movement of the electrons. However, it has been found that in spite of this compensation, this state does have a small magnetic moment which usually arises from an interaction with some other state. The magnitude of the interaction ΔE has been given by Townes and Schawlow[113] in the following form

$$\Delta E = \sum_{n} \sum_{s} \sum_{s} \mu_0 \frac{\hbar^2 J_s H'_s}{I_s} \frac{\langle 0 | L_s | n \rangle \langle n | L_{s'} | 0 \rangle}{E_0 - E_n} \tag{4.38}$$

Here H'_{s}, is a perturbation term due to the magnetic interactions and has been defined by the authors[113].

$|0\rangle$ represents the wavefunction of the observed state with energy E_0.

$|n\rangle$ represents the wavefunctions of an interacting state with energy E_n.

n is the summation index over all such states.

s is the summation index over the cartesian coordinates of the electrons of the molecule.

J_s is the component of angular momentum (in units of $\hbar$) about each principal axis.

I_s is the moment of inertia about each principal axis.

μ_0 is the nuclear magneton.

L_s represents the orbital angular momentum of the electrons.

It is seen from (4.38) that if $E_o - E_n$ is small, ΔE is large and the Zeeman effect is large and proportional to J. The Zeeman splitting of observed rotational lines should therefore show a corresponding dependence on J.

Therefore, by application of an external magnetic field and by examination of the rotational structure under high resolution the magnitude of the Zeeman splitting can be evaluated as a function of the quantum number J. From the dependence of the splitting on J, the type of state viz., an orbitally degenerate state, or a spin multiplet state or a $^1\Sigma$ state, involved in the transition may be inferred.

4.9 Isotopic Shifts

Equations (3.30), (3.31), (3.32) derived from the Teller-Redlich product rule, were used in the last chapter to calculate the fundamental frequencies ω_k^i of an 'isotopic' triatomic molecule from those ω_k of a 'normal' molecule. If the two sets of frequencies ω_k and ω_k^i are known in both the states of an electronic transition, the isotopic shifts in the vibrational spectrum can be calculated. Thus, if σ^i and σ represent the frequencies of the iso-vibronic transitions (refer to footnote in section 5.3) in the two molecules, the isotopic shift is simply

$$\Delta\sigma = \sigma - \sigma_i \qquad (4.39)$$

Each σ is given by:

$$\sigma = (T'-T'') + (G'-G'') + (F'-F'')$$
$$\sigma_i = (T_i'-T_i'') + (G_i'-G_i'') + (F_i'-F_i'') \qquad (4.40)$$

where T, G and F are the electronic, vibrational rotational term values respectively. 'i' refers to the heavier isotope. If we assume that the potential functions of both isotopic molecules in the upper and lower electronic states are very nearly the same, then $T=T_i$ in both the upper and lower states. Therefore, $T'-T'' = T_i'-T_i'' = \sigma_e$. If the rotational term values F and F_i are neglected, the expressions (4.40) reduce to:

$$\sigma = \sigma_e + G'(v_1' \; v_2' \; v_3') - G''(v_1'' \; v_2'' \; v_3'')$$
and
$$= \sigma_e + G_i'(v_1' \; v_2' \; v_3') - G_i''(v_1'' \; v_2'' \; v_3'') \qquad (4.41)$$

where v_1, v_2, v_3 are the vibrational quantum numbers in the triatomic molecules (as described in section 3.3).

For transitions between linear states of XCX molecules an approximate expression for $\sigma = \sigma - \sigma_i$ is obtained by substituting the expression for $G(v_1, v_2, v_3)$ from equation (3.14) in (4.41) above. The result is

$$\sigma - \sigma_i = (\omega_1' - \omega_1'^{i})(v_1'+1/2) - (\omega_1'' - \omega_1''^{i})(v_1''+1/2)$$
$$(\omega_2' - \omega_2'^{i})(v_2+1) - (\omega_2'' - \omega_2''^{i})(v_2''+1)$$
$$(\omega_3' - \omega_3'^{i})(v_3'+1/2) \; \omega_3'' - \omega_3''^{i})(v_3''+1/2)$$
$$(4.42)$$

where $\omega_1, \omega_2, \omega_3$ are the three zero order vibrational frequencies. Terms in x_{ik} and g of (3.16) have been neglected under the assumption that these constants do not influence $\Delta\sigma$ very much by isotopic substitution. Each frequency ω_k is related to the corresponding isotopic frequency ω_k^i by the relations given by equation (3.32) and $\omega_k^i = \rho_k \omega_k$.

For transitions in which the excited state is bent and the ground state is linear, $\Delta\sigma$ is obtained by the substitution of $G^b(v_1, v_2^K, v_3)$ from (4.23) for G' and $G^l(v_1, v_2^l, v_3)$ from (4.23) for G" in equation (4.41). The result is:

$$\begin{aligned}\sigma - \sigma_i &= (\omega_1' - \omega_1'^{i})(v_1'+1/2) - (\omega_1'' - \omega_1''^{i})(v_1''+1/2) \\ &+ (\omega_3' - \omega_3'^{i})(v_3'+1/2) - (\omega_3'' - \omega_3''^{i})(v_3''+1/2) \\ &+ (\omega_2' - \omega_2'^{i})(v_2'+1/2) - (\omega_2'' - \omega_2''^{i})(v_2''+1) \\ &+ (A' - A'^{i})K'^2 \end{aligned} \qquad (4.43)$$

If (4.42) and (4.43) are combined, we get

$$\begin{aligned}\sigma - \sigma_i &= \Delta\omega_1' \ (v_1'+1/2) - \Delta\omega_1'' \ (v_1''+1/2) \\ &+ \Delta\omega_2' \ (v_2'+d\ /2) - \Delta\omega_2'' \ (v_2''+1) \\ &+ \Delta\omega_3' \ (v_3'+1/2) - \Delta\omega_3'' \ (v_3''+1/2) \\ &+ [A' - A_i']K^2 \end{aligned} \qquad (4.44)$$

where d' = 2 for a linear excited state; d' = 1 for bent state and $\Delta\omega_k = \omega_k - \omega_k^i$. A and A^i are the rotational constants for the 'normal' and isotopic molecule respectively. If K' = 0, as in the case of $\Sigma - \Sigma$ transition, the expression for $\Delta\sigma$ is very similar to that for linear-linear transitions. If

$K' > 0$, then $\sum - \sum$ increases or decreases quadratically with K' depending on the sign of $(A'-A_i')$. For a bent XCX molecule the relationship between vibrational frequencies between isotopic species X^iCX^i and XCX cannot be simply written as $\omega_k^i = \rho\omega_k$. The relationships among ω_k and ω_k^i are (equation 3.30 and 3.31):

$$\omega_3^i = \rho_3\,\omega_3 \quad \text{and}$$

$$\omega_1^i\omega_2^i = \rho_{12}\,\omega_1\omega_2 \tag{4.45}$$

where ρ_3 and ρ_{12} are defined by equation (3.30) and (3.31). At least one of the two isotopic frequencies $\omega_1^{i'}$ or $\omega_2^{i'}$ must be known to evaluate the other from relation (4.44).

It is seen from equation (4.44) that $\Delta\sigma$ is a linear function of each v_k. This linear relationship is illustrated in Fig. 4.10 and will be used subsequently in section 5.4 . Each plot represents $\Delta\sigma \propto v_k$, with the restriction that all $v_j \neq v_k$ are constants or zero. K has also been assumed to be zero. $\omega_1^{i''}$ and $\omega_2^{i''}$ obtained in section 3.8 for the (80-80) molecule and the corresponding frequencies ω_1'', ω_2'' for the (78-78) molecule were used to calculate $\Delta\sigma$. These values are quoted in Fig. 4.10. Assumed values of $\omega_1^{i'}$ and $\omega_2^{i'}$ (based on data in section 5-3) for the 80-80 molecule and ω_1' and ω_2' for the 78-78 molecule are also given. Since 80-80 is a heavier molecule than 78-78, $\omega_k > \omega_k^i$. Some inferences may be drawn by examination of Fig. 4.10. They are:

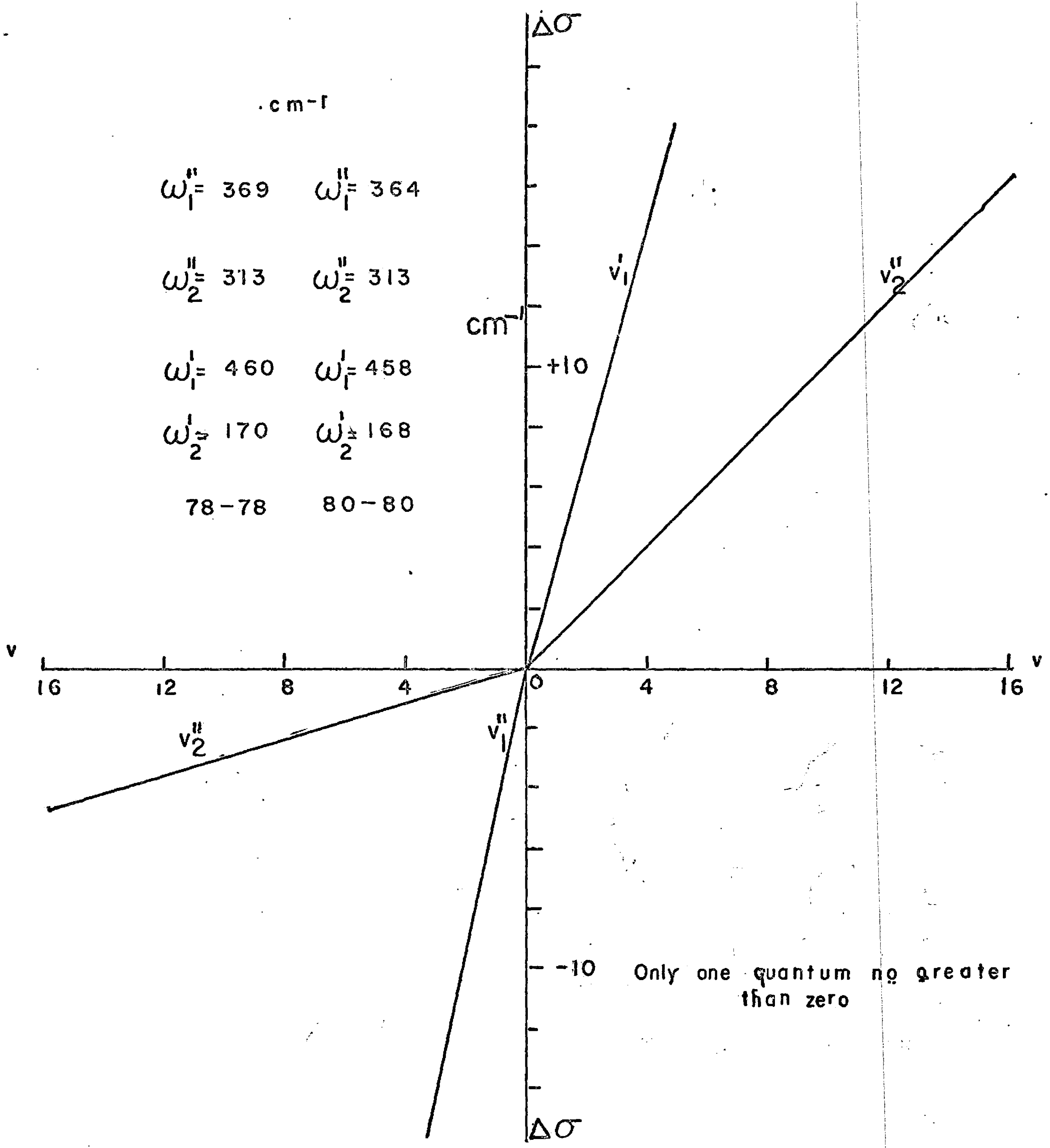

CALCULATED ISOTOPIC SHIFTS $\Delta\sigma$ VS V_i

FIGURE 4.10

(a) The isotopic shift $\Delta\sigma$ for the origin band i.e. for a $(0,0^0,0) \longleftarrow (0,0^0,0)$ transition is nearly zero.

(b) Isotopic shifts are positive if $v_k' > 0$ and if all other quantum numbers $v_j \neq v_k$ are zero.

(c) Isotopic shifts are negative if $v_k'' > 0$ and if all other quantum numbers $v_j \neq v_k$ are zero.

These conclusions are expected to apply generally, even though specific values of ω_k have been used. The expressions used in calculating $\Delta\sigma$ are valid only in the harmonic approximation.

Chapter 5

DESCRIPTION AND ANALYSIS OF CARBON DISELENIDE SPECTRUM

The vapour phase electronic absorption spectrum of carbon diselenide, observed under low resolution on the Cary 14 spectrophotometer, is shown in Fig. 5.1. Four regions of absorption are indicated therein, by the symbols R, V,[*] A and C. These absorptions correspond to those observed by Callear and Tyerman[36] on low resolution Hilger and 3 m concave grating spectrographs. Each absorption has a discrete structure. Some preliminary observations on the four absorptions are given below.

Absorption	Region (Å)	Remarks
R	4500-4000	very weak
V	4050-3450	weak
A	2600-2100	very strong
C	2100-	strong

It was mentioned in section 2.2 that methylene chloride constituted the major impurity in CSe_2 and that it could not be removed. The electronic absorption spectrum of pure methylene chloride vapour was compared with the spectrum of CSe_2. It was found that among the four absorptions shown in Fig. 5-1, the absorption C is apparently superimposed on an absorption

---

[*] The nomenclature R and V have been chosen to correspond to those of Kleman[37] for the absorptions in the CS_2 spectrum. The absorption (R) of CS_2 has been identified as an $\tilde{a} \longleftarrow \tilde{X}$ transition; and the absorption A and C of CS_2 as $\tilde{A} \longleftarrow \tilde{X}$ and $\tilde{C} \longleftarrow \tilde{X}$ transitions respectively[8].

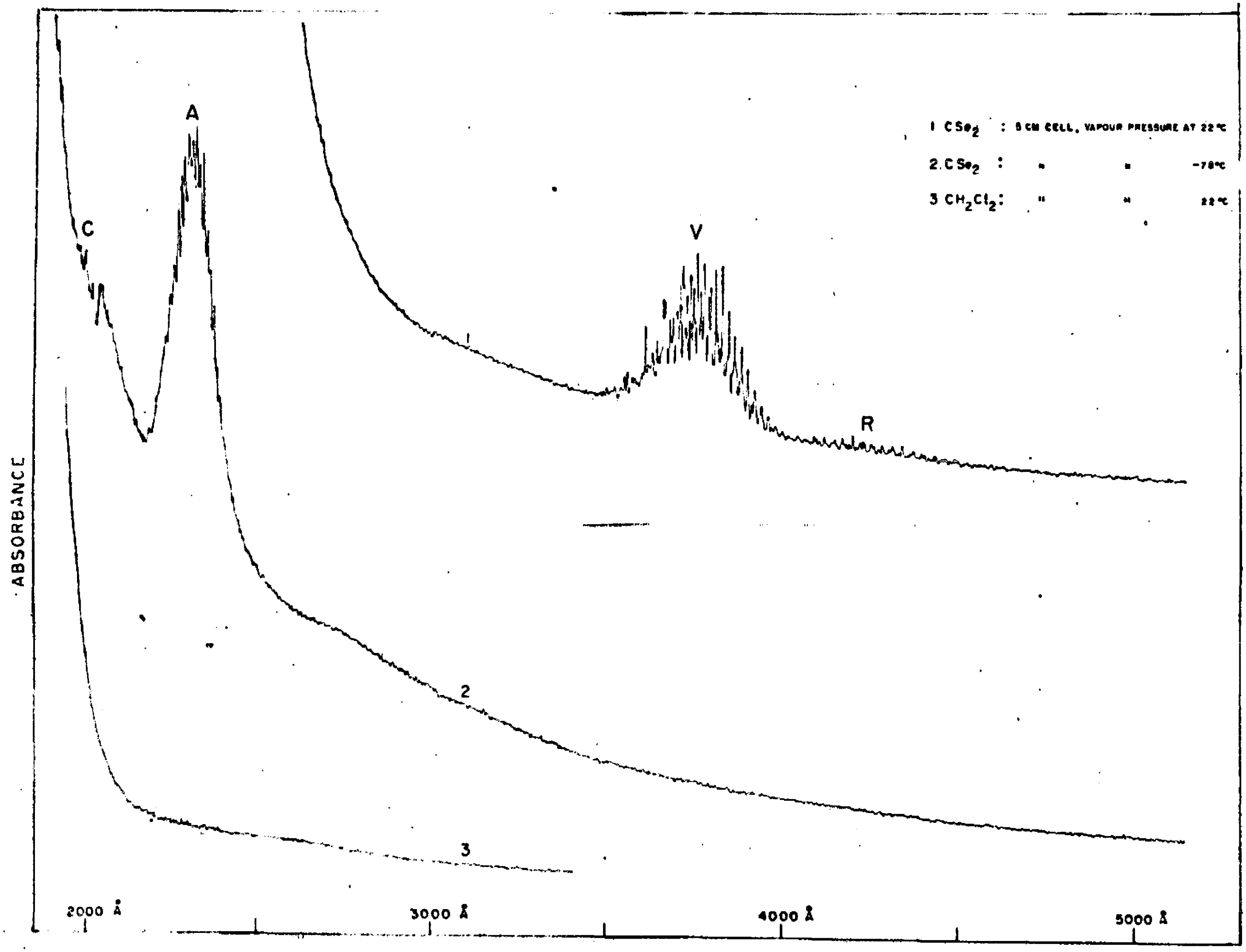

LOW RESOLUTION ABSORPTION SPECTRUM OF CARBON DISELENIDE

FIGURE 5.1

due to methylene chloride vapour (compare curves 2 and 3 in Fig. 5.1) and lies almost in the vacuum ultraviolet spectral region. This region was not examined in the present work. The remaining absorptions R, V and A are not observed in methylene chloride vapour.

5.1 Comparison of Oscillator strengths

The oscillator strength f_{nm} for each of the three systems was calculated from their respective absorbance values measured from low resolution Cary 14 spectrograms. The details of the method used to calculate f_{nm} are given in Appendix I.

The spectral regions of absorption of CSe_2 has been shown below in (5.1). Analogous absorption systems of CS_2 (reported by Kleman[37]) also occur in similar regions and their wavelength ranges are also shown in (5.1). The oscillator strengths of the CSe_2 absorption systems are given in the third column and those of CS_2 in the sixth column. The absorption pressure-path (in units of mm of Hg for p and in m for ℓ), needed to observe each of the three absorption systems in CSe_2 and CS_2 are also given below.

	CSe_2			CS_2		
System	Region (A)	f_{nm}	pxl	Region (A)	f_{nm}	pxl
R	4500-4000	10^{-4}	9	3800-3400	$<10^{-4}$	160
V	4050-3450	10^{-3}	1	3300-2900	10^{-4}	3.2
A	2600-2100	10^{-1}	0.01	2100-1900	-	0.05

(5.1)

Since the amount of CSe_2 present in the synthesized mixture is not known exactly (section 2.2), f_{nm} values could be inaccurate by a factor of 10 (see Appendix I). Kleman observed the R and V systems of CS_2 on a 35 ft Eagle spectrograph similar to the one used in this work for recording the R and V systems of CSe_2. The absorption pressure-path length data for CS_2 are quoted from his work. A value for f_{nm} for the A system of CS_2 is not available. The estimate given in (5.1) of the absorption pressure path length for this system has been obtained from the data of Tyerman.[119]

The probability of the transition is proportional to f_{nm}. From the data in (5.1) above, we note that the oscillator strengths for the R:V:A systems of CSe_2 are in the ratio of 10^{-3}: 10^{-2}: 1. Hence, we conclude that the R and V absorptions result from relatively forbidden transitions in comparison with the A system transition and that between the R and V absorptions, the latter results from a transition which is more 'allowed' than the former. The relative oscillator strengths and absorption pressure-path lengths among the CS_2 systems apparently have a similar relationship as those of CSe_2. However, the value of f_{nm} and pxl for each system of CS_2 is smaller and larger respectively than that of the corresponding systems of CSe_2.

Since the f_{nm} values in CSe_2 is greater than the f_{nm} values expected for magnetic dipole (10^{-5}) or electric quadrupole (10^{-8}) allowed transitions, it is likely that the R, V and A systems arise from electric dipole transitions (for which f_{nm} = 1 to 10^{-4})[115]. Further, the $f_{nm} = 10^{-1}$ value of the A system is closer to that of an allowed electronic transition (for which f_{nm} = 1 to 10^{-1}); and the f_{nm} values 10^{-3} and 10^{-4} of the V and R systems respectively are closer to those of many vibronically allowed transitions (for which $f_{nm} = 10^{-2}$ to 10^{-4}). Therefore, it is possible that V and R systems arise from forbidden electronic transitions which 'become' allowed by vibronic interactions. This argument does not preclude the possibility that these systems result from transitions between the singlet ground state and triplet excited states in Table 4.2.

5.2 Spectra of isotopic species of CSe_2

Naturally occuring elemental selenium contains six of its stable isotopes in relatively large abundances (Table 5-1). The presence of these isotopes complicates the observed spectrum of CSe_2 synthesized from natural selenium considerably, as discussed below.

It can be shown (Appendix J) that, if six stable isotopes are present, twenty-one different species of isotopic CSe_2 molecules are formed during the synthesis. The notation used to identify each of these species is given in section 2.2. From the percentage natural abundances given in Table 5-1 for each isotope, the molecular ratios among the isotopic species present in CSe_2(N-N) may be obtained. The method of calculating their molecular ratio is shown in Appendix J. From these ratios, the number of molecules of each isotopic species relative to 100 molecules of the 80-80 species can be obtained. Their relative values are given in Table 5-1, and can be used to calculate the relative intensities among bands of isotopic molecules. The intensity of a band corresponding to a given electronic transition is directly proportional to the number of molecules N_i in the initial state of the transition (equation 1.22). Hence, from the data in the above table, we see that, if a band due to the 80-80 molecule has an intensity of 100, that due to the 78-78 molecule should have relative intensity of 25 for the same transition. Therefore, the numbers in the last six columns of Table 5-1 represent the relative intensities for bands due to isotopic molecules, in a given transition. Only eleven out of the twenty-one species in the table have bands whose relative intensity values exceed 4. Bands of these eleven species are the ones expected to be seen experimentally.

The complexity of the observed spectrum of CSe_2 (N-N), due to the presence of isotopes of selenium, is illustrated with the aid of Fig. 5.2. a) shows the spectrum of the R system of the N-N species photographed on a Bausch and Lomb 1.5 m grating spectrograph. Under the resolution of this instrument, most absorption bands are diffuse, with a few showing line-like structure. In b) one of the bands, as it appears under the higher resolution of a 20 ft Ebert spectrograph is shown. Ten line like heads which belong to this band, are marked by arrows in the figure [Band heads, not marked by arrows do not belong to the band under discussion]. Callear and

Table 5-1

ISOTOPIC SPECIES OF CARBON DISELENIDE

Mass No.	Natural % Abundance of Se^i	Relative Number# of Isotopic molecules in (N-N)					
		82	80	78	77	76	74
82	8.84	4					
80	49.96	40	100				
78	23.61	20	100	25			
77	7.50	4	35	20	4		
76	9.12	4	40	20	4	4	
74	0.96	1	1	1	1	1	1

Refer to Appendix J for calculations

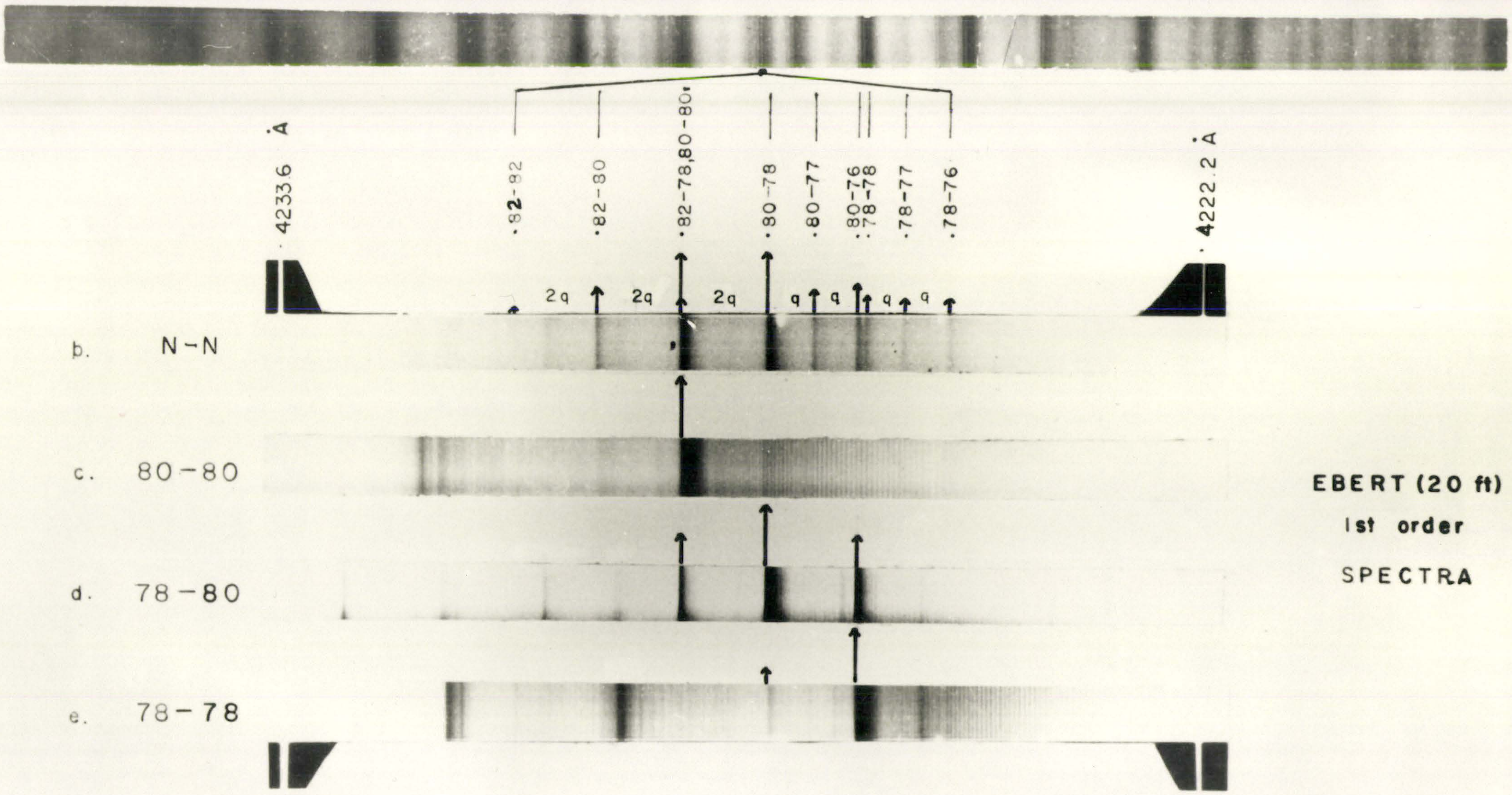

ISOVIBRONIC BANDS IN THE 23641 cm^{-1} REGION

FIGURE 5.2

Tyerman[36] observed these line like heads, and concluded that their bands are different in structure from those of the R system in the CS_2 spectrum. In this investigation, it was found that these heads could be explained satisfactorily as bands due to different isotopic CSe_2 molecules. The correct assignment of each band head to a specific isotopic molecule can be arrived at by comparing the spectrum in b) with the spectra of 80-80, 78-80 and 78-78 molecules shown in Fig. 5-2 c), d) and e) respectively. One strong band, marked by the arrow, is seen in c). This band is due to the 80-80 molecule and has a discrete rotational structure which is degraded to the violet. Two bands, one weak and the other strong are observed in the spectrum of the 78-78 molecule. The stronger band is due to the 78-78 molecule and has a violet degraded rotational structure, like the band in c). Three bands are observed in the spectrum of the 78-80 species. It can be observed that the intensity of the middle band is nearly twice that of the other two (as indicated by the relative heights of the arrows). The band at the left is due to the 80-80 molecule and the band at right due to the 78-78 molecule and the band in the middle due to the 78-80 molecule. The bands of 80-80 and 78-78 molecules occur in the absorption spectra because the 78-80 component was synthesized from a 1:1 w/w mixture of Se^{80} and Se^{78}. (The presence of three bands, incidentally, proves that there are two atoms of Se in the absorber. Refer to Appendix J). The bands of 80-80, 78-80 and 78-78 molecules can be readily identified in b) by their positions; the juxtaposed arrows which indicate these bands, bear the 80-80, 78-80 and 78-78 labels. The two intervals between these three bands are equal; the interval between 80-80 and 78-80 have been given the symbol "2q". The remaining seven band heads in b) can be identified in the following way. As shown in section 3.7, the isotopic shift between bands of XCX and X^iCX^i molecules is expected to be approximately double that between bands of XCX and XCX^i molecules. Here, the interval between 80-80 and 78-78 bands is '4q' and that between 80-80 and 80-78 bands is '2q' which justifies this expectation. Hence, we assume that if there is a mass change of two in one selenium atom between two isotopic CSe_2 molecules, the interval between the bands of the species should be '2q' and if there is a mass change of two in each of the selenium atoms, the interval should be '4q'. With this interval rule as basis, the band heads of 82-82, 82-80, 78-76 etc. could be satisfactorily located with respect to the bands of 80-80 and 78-78. In Fig. 5-2 b), the ten band heads of isotopic species, identified by this interval rule, are marked by arrows and labelled according to species. The intervals between band heads are shown in units of 'q'. By the interval rule, the bands of 80-80 and 82-78 must coincide. This coincidence is indicated by superimposed arrows. Similarly, the bands of 80-76 and 78-78 must coincide; however, these appear to be separate. The heights of the juxtaposed arrows are proportional to the relative intensity value given in Table 5-1 for each species. The intensities of band heads in the spectrum in b) are observed to be approximately in the same ratio as the heights of the arrows. We conclude, therefore, that each of the ten like heads can be accounted for as band heads of isotopic species and that the presence of these isotopic heads is a primary reason for the apparent complexity of the observed spectrum of CSe_2^{nat}(N-N)

Since the spectrum of the N-N species is complex it was not investigated in detail in this work. The spectrum of the R, and V systems were, however, recorded under high resolution. Most of this investigation on the R and V absorption systems of CSe_2 was carried out with the 80-80 and 78-78 species, because Se^{80} and Se^{78} were most readily available with relatively greater isotopic purity (∽97%). The spectra of 77-77 and 78-80 species were also recorded for specific purposes. The rest of this chapter is divided into four parts. In part A, the description and analysis of the R systems is presented and in parts B and C a preliminary investigation of the V and A systems respectively is given. Part D is a summary of this work.

PART A

THE R SYSTEM

5.3 General Description

The absorption bands of the R system were recorded using 50 cm long absorption cells each containing the vapor of 80-80, 78-78, 77-77, 78-80 and N-N compounds at room temperature.

The R system of N-N was also recorded with an 1.8 m White type multiple reflection cell containing the vapour at a pressure of 23 mm., at room temperature (27°C). Isotopic compounds were not used in the 1.8 m long path length cell because sufficient amounts of these compounds for filling such a cell were not available. The effect of temperature on the intensity of the R system was studied by taking spectra at - 42°C, 22°C, 100°C and 200°C. The vapour pressure of CSe_2 was too low at temperatures below - 42°C and a spectrum could not be observed even with the use of the multiple reflection cell. At and above 200°C, CSe_2 either decomposed or polymerized, producing deposits on the inner surfaces of the absorption cell. Experimental details of recording spectra are discussed in section 2.6.

At room temperature and with a path length of 50 cm the observed R system absorption lies in the range of 3950 to 4550 Å. At 100°C and 200°C, weaker bands at the red end of the spectrum increase in intensity and hot bands are observed above 4550 Å. When the path length is increased to 20 m at room temperature, the R system could be observed up to 4800 Å. Many bands observed in this additional region of the red end of the spectrum occur at the same wavelength as the bands observed when the shorter path length cells were heated. Callear and Tyerman[36] also observed such an extension of the R system, in the high temperature absorption of N-N vapour.

Altogether about 300 bands were observed in the high resolution spectrum of both 80-80 and 78-78 vapour. Most of these are weak, showing a profile that is sharp and line like without any associated rotational structure. Some of the bands are diffuse, broad or multiple headed. The structure of the band heads is more difficult to determine at the higher energy end (4000 Å) of the spectrum since weaker bands of the V system overlap the bands of the R system in this region. All strong bands of the system, whose rotational structure is discernible, are degraded to the violet. Many of them have sharp resolved rotational lines, a few wavenumbers away from the wavenumber of the band head. The rotational structure of many of these bands of CSe_2 resemble that of the violet degraded bands of the CS_2 (R) system. Most of the CSe_2 bands are apparently single headed. However, in the red end of the spectrum several bands with double heads are also observed. Many of the bands observed for each isotopic spectrum partially overlap each other so that often, it is difficult to determine whether a weak head is genuine or an intense rotational line of another band.

The spectrum of 80-80 and 78-78 in the 3950 - 4600 Å region is shown in Appendix K. The wavenumbers of all the observed band heads in 80-80 and 78-78 in the 3950 - 4800 Å region are given in Appendix L. Band heads, listed by wavenumbers in the same row of the table in Appendix L, do not necessarily belong to isovibronic* transitions. However, in those rows where differences in wavenumbers (i.e., isotopic shifts) are also given in addition to wavenumbers, band heads have been judged to belong to isovibronic transitions. The estimated intensity of each 80-80 and 78-78 band head is also given relative to a value of 100 for the most intense band. The intensity estimates are based on visual judgement of spectra, and of their microdensitometer traces. The letters c, mc, mh, h alongside intensity values of 80-80 bands indicate cold, possibly cold, possibly hot and hot bands respectively. Such data was not obtained for every band in the system.

Both the 80-80 and 78-78 spectra contain a large number of bands. Therefore, it was not always possible to decide just by a comparison of the two spectra whether a band in the 80-80 spectrum and another band in 78-78 result from isovibronic transitions. Because of this difficulty isotopic shifts for all the observed bands could not be unambiguously determined. For the stronger bands in the spectra, the method outlined below and illustrated by Fig. 5-3 b) for the band at 22744 cm^{-1} was used to determine isotopic shifts. In this figure, the spectrum at the top is that of 80-80, the middle one is that of 78-78 and the bottom one is that of CSe_2 synthesized from a 1:1 w/w mixture of Se^{78} and Se^{80}. The band heads of each

---

* For convenience, those transitions which have the corresponding number of vibrational excited quanta in the ground and upper states have been termed as isovibronic transitions.

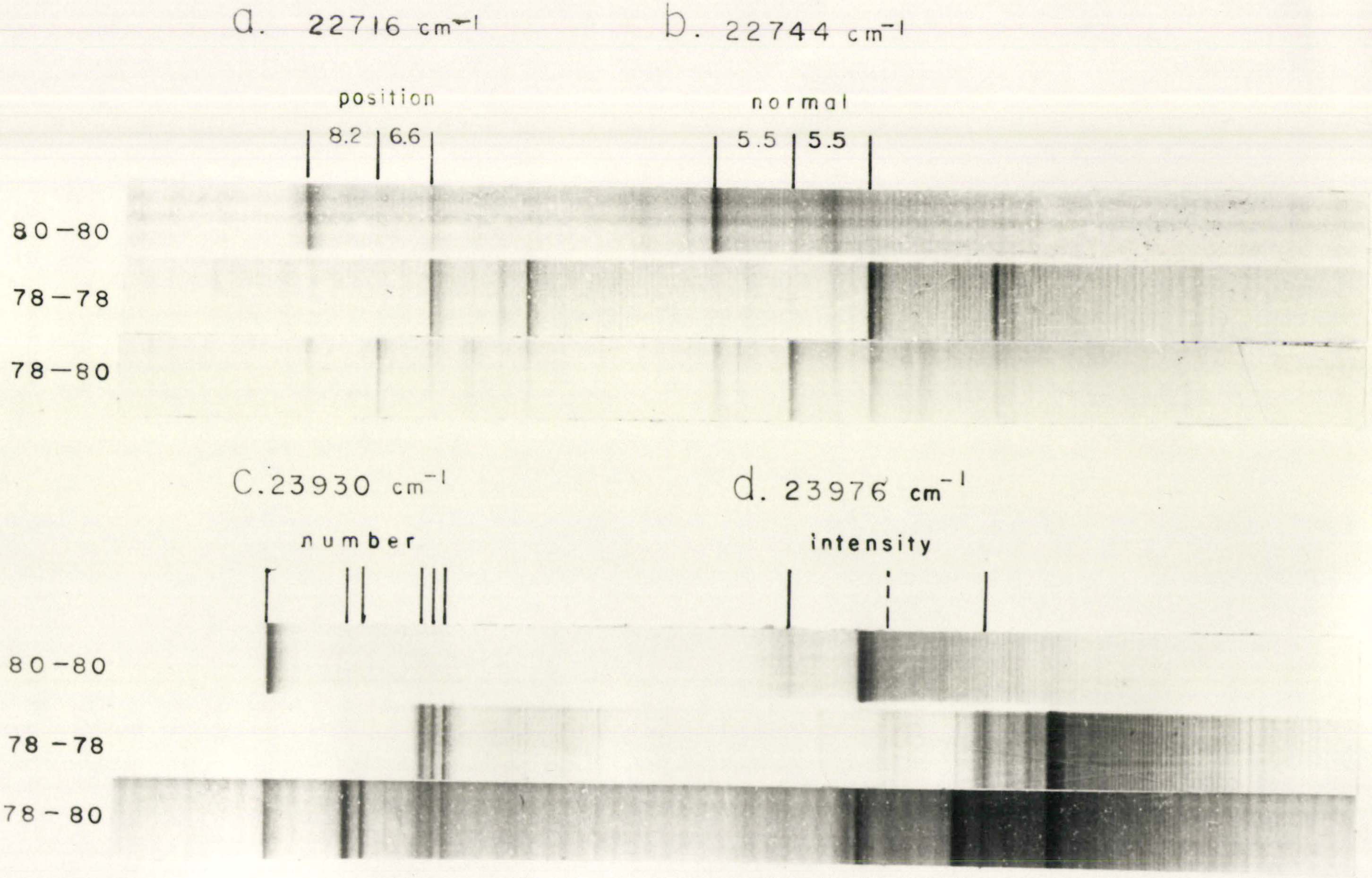

OBSERVED IRREGULARITIES IN BAND HEAD STRUCTURE

FIGURE 5.3

isotopic species are indicated by leading lines. It was mentioned earlier in section 5-2, that the band heads of isovibronic transitions in the 80-80, 78-80 and 78-78 molecules are separated by equal energy intervals (in this case, each interval is 5.5 cm^{-1} in wavenumber units) and also have an intensity ratio of 1:2:1. These requirements are fulfilled for the 78-78 and 80-80 bands shown at 22744 cm^{-1} and therefore we conclude that these two bands result from 'isovibronic' transitions. Similarly, other isotopic bands in 78-78 and 80-80 were compared with those of 78-80; if the two criteria mentioned above are satisfied for all three bands in the 78-80 spectra the transitions were identified as isovibronic. The intervals between isovibronic bands i.e. isotopic shifts were recorded. However, this method of identification could not be used for low intensity bands in the isotopic spectra or for those bands which are overlapped or perturbed, as shown below.

Perturbations are observed in various parts of the spectrum. Many band heads are displaced from their 'normal' positions in the energy spectrum. Several have anamolous intensities and structure. It can be shown that these effects are present in the system by a comparison of isotopic spectra. Fig. 5-3 b) has been discussed in the earlier paragraph and represents the 'normal' case of energy and intensity relationships among the isotopic band heads of 80-80, 78-80 and 78-78 species. Fig. 5-3 a) shows the band at 22716 cm^{-1}. Here the wavenumber intervals between the 80-80, 78-80 and 78-78 band heads are in the ratio of 8.2 : 6.6 whereas the expected ratio is 1:1. Therefore either one, or two, or all band heads are not in their normal position in the spectrum. An example of an intensity anomaly is seen in Fig. 5-3 d) for the bands at 23976 cm^{-1} where the intensity of the 80-80 band is much less than that of the 78-78 band and therefore the expected intensity ratio of 1:2:1 for the 80-80, 78-80 and 78-78 bands does not agree with the observed ratio. A third case of apparent perturbation is seen in the band at 23930 cm^{-1} reproduced in Fig. 5-3 c). Here, the band in 80-80 appears to be single, that in 78-78 seems to be triple, and that in 78-80, double headed. The explanation, that the band in 78-78 is a triply overlapped band, was subsequently found to be reasonable. Perturbations are also evident in the rotational structure of strong bands. Members of series of lines forming a branch in the rotational structure are often seen to be displaced from expected positions or reduced in intensity. Examples of such rotational perturbations are not illustrated here.

5.4 Evidence in favour of a bent excited state

A. Occurence of progressions in the bending vibration -

Many strong bands and a large number of weak bands occur throughout the observed range of the R system absorption. Even in the spectrum of a single isotopic species such as 80-80, no regularity or repetitive patterns among these bands is obvious. It is possible that a part of this irregularity is caused by the presence of perturbations discussed in the earlier section.

Some examples of frequency differences among the strongest bands are approximately 40, 125, 170, 295, 465, 630, 770, 930...etc. cm^{-1}. However, among these values, series of bands with successive intervals of $\backsim$170 and $\backsim$465 cm^{-1} could be identified.

The members of series, which have successive but irregular intervals of 170 cm^{-1}, form the most prominent groups. Within each group, the intensity of each successive band increases with its frequency and reaches a maximum at the second or third member of the group. The relative intensities among the bands within each group varies slowly. If the bands were member of a sequence then the intensity variation among them should be much more pronounced and show a different distribution (Appendix F). Furthermore, spectra observed at low temperatures indicate that the member of the most intense group of these bands are cold bands, suggesting that all these bands originate on the vibrationless ground state ($v_1'' = v_2'' = v_3'' = 0$). Therefore it is assumed that each of these groups form a progression rather than a sequence. The frequency interval of 170 cm^{-1} is too small to be any of the ground state vibrational frequencies (obtained in section 3.8) viz. $\omega_1'' = 364$ cm^{-1}, $\omega_2'' = 313$ cm^{-1} and $\omega_3'' = 1303$ cm^{-1}. Further, it will be shown in section 5.4 B, that the excited state symmetric stretching frequency ω_1 in a linear state cannot be smaller than its value of 364 cm^{-1} in the ground state. Hence, the interval of 170 cm^{-1} is also too small to be the excited state symmetric stretching mode in the linear CSe_2 molecule. Hence we assume that these groups of bands with a frequency intervals of 170 cm^{-1} form a progression in the bending vibration. Such an observation of progressions in this bending vibration according to Franck-Condon principle implies that the molecule is bent in the excited state. (section 4.6).

Alternatively, the strongest bands can also be arranged into groups with a frequency interval of about 460 cm^{-1} between successive bands. The number of members in each group is fewer than the number in the progression (in bending vibration) described in the previous paragraph. These groups were assumed to be progressions in the symmetric stretching mode; the magnitude of the excited state stretching frequency i.e. 460 cm^{-1} is compatible with that derived from arguments presented in section 5.4 B. Since the intensities of successive members of the group are fairly constant they cannot be attributed to sequence bands.

If the transition by which the R systems absorption occurs, is between electronic states of the linear CSe_2 molecule (i.e. a linear $\longleftarrow$ linear transition) progressions in the symmetric stretching mode should be observed provided there is a change in the internuclear distance r_{CSe}. When there is very little change in r_{CSe}, sequences should be observed (refer discussion on the Franck-Condon principle 4.6). In either case, alternate members of a progression in the nontotally symmetric vibration i.e. Δv_2 or $\Delta v_3 = 0, \pm 2, \pm 4$...etc. should be observed with low intensity. The observation of progressions in the symmetric stretching mode satisfies the first of the above requirements for a linear-linear transition. The requirement that alternate members of a progression in the bending vibration occur is not satisfied because the interval of 170cm^{-1} is probably too small to be two quanta of the bending frequency ω_2 for the linear CSe_2 molecule.

For a bent ⟵ linear transition, however, progressions should be observed both in the symmetric stretching modes as well as in the bending modes (section 4.6). The observation of both types of progression is consistent with this requirement. It is therefore likely that the excited state corresponds to that of a bent molecule.

B. Rotational structure

The rotational structure of the bands in the R system provides more evidence in favour of a bent excited state. As mentioned in the earlier section, strong bands in the systems are violet degraded and reveal sharp rotational lines. These lines appear to be regularly spaced; the intervals between successive lines suggest only a small value (see section 5.6) for the difference in rotational constants between the ground and excited state vibrational levels. If the molecule is linear in both states, then the intervals between rotational lines must be a function of $\triangle B$ and the observed rotational structure must be the J structure. It is known from basic theory (sections 3.6 and 4.8) that the rotational structure of vibronic bands can be violet degraded only if the rotational constant in the upper vibronic state (B') is greater than that in the lower vibronic state (B"). If the molecule is linear in both states, $B' > B''$ implies that $r'_{CSe} < r''_{CSe}$, since B is inversely proportional to the moment of inertia $I_B = 2\ m_{Se} \times r^2_{CSe}$ (Equation 3.25). If the internuclear distance in the excited state (r'_{CSe}) is smaller than that in the ground state (r''_{CSe}), it means that there is a greater bonding in the excited state of the linear molecule than in the ground state. This conclusion is contrary to expectation; since from arguments presented in section 4.2, it would imply that an electron promotion has occured from the nonbonding $1\pi g$ orbital to a bonding orbital rather than to an antibonding orbital. If the molecule is bent in the upper state however, an excited state B' value larger than its value in the ground state can be obtained even for a $r'_{CSe} > r''_{CSe}$. This argument is illustrated in Appendix H, where in the first column of the table several values of r'_{CSe} are given. For the sake of argument r''_{CSe} may be assumed to be equal to 1.711 Å from the data of Wentink[23] In the second column, bond angles $\widehat{SeCSe}$ are given. The third, fourth and fifth columns show the calculated rotational constants A, B, C in cm^{-1} for the corresponding geometry and the last column shows the value of the asymmetry parameter. It is found that $\kappa \simeq -1$ for all the rows and therefore the molecule is approximately a prolate symmetric top for any angle of bending in the given range. It is also shown in the table that even if the r_{CSe} is larger in the excited state, B' can be larger than B". Hence, violet degraded vibronic bands are possible even if the internuclear distance r_{CSe} is larger than that in the ground state, provided the molecule is bent in the excited state. Therefore, the rotational structure of the bands also suggests a bent excited state. In section 5.6 the rotational structure of these bands is examined in greater detail.

C. Isotopic shifts

The values of isotopic shifts $\Delta\sigma = \sigma^{78} - \sigma^{80}$, for the bands of the R system are given in Appendix L. From this isotopic shift data, the following observations and references (based upon the discussion in section 4.10) can be made:

1. None of the bands, for which isotopic shifts could be determined, have zero or near zero isotopic shifts. Such a small shift is expected for an origin band (see Fig. 4.10). Hence it is tentatively assumed that the origin band corresponding to the $(0,0,0)' \longleftarrow (0,0,0)''$ transition is not observed in the spectrum.
2. All observed isotopic shifts are positive and lie in the range of 3 to 16 cm^{-1}. Smaller shifts are observed at the low energy end of the spectrum and large shifts at the high energy end of the spectrum. Most of the intense cold bands (which were observed in temperature work) lie in the latter region. Large isotopic shifts for cold bands indicate that these bands result from transitions between the vibrationless ($v_1''=v_2''=v_3''=0$) ground state to the excited vibrational levels (v_1', v_2' and v_3' where one or more v_i' may be nonzero) of the upper state.

The absence of an observable origin band and the presence of bands due to $(v_1, v_2, v_3)' \longleftarrow (0,0,0)''$ transitions, indicates that there is a change in the equilibrium geometry of the molecule in the excited state (refer to discussion of the Franck-Condon principle in section 4.6). This change in geometry could be due to changes in the internuclear distance r_{CSe} or a change in the bond angle SeCSe. Since progressions in the bending vibration are observed, it is likely that there is a change in the bond angle in the excited state.

Small isotopic shifts in the lower energy end of the spectrum can be accounted for under the assumption that there is a change in equilibrium geometry on excitation. Transitions in this region are from excited vibrational levels v_i'' of the ground state to lower vibrational levels v_i' of the excited state. It can be shown from equation (4.44) by substitution of approximate quantum numbers v_i' and v_i'', that isotopic shifts are indeed small in this case.

5.5 Detailed Vibrational Analysis of the R_1 System

The vibrational levels of a linear $\sum_g^+$ state and the rovibronic levels of a bent excited state have been discussed before in section 4.5 (the symmetries of these levels are given in Fig. 4.9). It has been shown (section 4.7) that for $\Delta K=0$ (i.e. parallel type) transitions, $\Sigma-\Sigma$, $\Pi-\Pi$, $\Delta-\Delta$, etc. type bands result whereas for $\Delta K = \pm 1$ (i.e. perpendicular type) transitions, $\Sigma-\Pi$, $\Pi-\Sigma$, $\Delta-\Pi$, etc. type bands result. In the present work, violet degraded bands with sharp rotational structure are observed (section 5.3) in the spectrum and the rotational structure of many of these bands resemble that of the $\Sigma - \Sigma$ type bands in the R system of CS_2. In Fig. 5.7, an example of such a $\Sigma - \Sigma$ band in the R system of CSe_2 is shown. In addition to these bands, several $\Pi - \Pi$ bands are also observed in the present work. These bands were identified as $\Pi - \Pi$ type bands by their rotational structure; this method of identification is discussed in section 5.6. Bands of $\Pi - \Sigma$, $\Pi - \Delta$...etc. types are not observed. A classification of bands by their rotational structure into $\Sigma - \Sigma$, $\Pi - \Pi$, $\Delta - \Delta$...etc. types determine directly the value of the quantum number K for each of these bands in the ground and excited states.

As mentioned in section 5.4.A, progressions are observed with a separation of about 170 cm^{-1} between successive members. At room temperature $\Sigma - \Sigma$ type bands are the strongest bands observed in the spectrum and many of them form these (170 cm^{-1}) progressions. A typical progression of bands has members with wavenumbers 23295.2, 23471.6, 23641.5, 23807.7, 23976.2 and 24151.3 cm^{-1}. The successive intervals between these bands are 176.4, 169.9, 166.2, 168.5 and 175.3 cm^{-1}. These intervals apparently decrease to a minimum before increasing again. Such a uniform behavior was not always observed. In some progressions of $\Sigma - \Sigma$ bands, successive intervals were staggered.

Since the frequencies of all three fundamentals in the ground state, viz. $\omega_1 = 364 \text{ cm}^{-1}$, $\omega_2 = 313 \text{ cm}^{-1}$ and $\omega_3 = 1303 \text{ cm}^{-1}$ are known, intervals between band heads corresponding to these frequencies were sought in the spectrum. None of these intervals occured frequently enough for unambigous identification.

However, a wavenumber difference of 631.4 cm^{-1} is obtained between two $\sum-\sum$ type bands at 23641.5* and 23010.1 cm^{-1}. This difference is in good agreement with 631 cm^{-1}, the wavenumber of the observed Raman active overtone band (section 3.8), corresponding to the $(0\ 2^\circ 0)'' \longleftarrow (0\ 0^\circ\ 0)''$ vibrational transition in the ground state bending vibration (for notation refer to section 3.5). In addition to the above two $\sum-\sum$ type bands, three pairs of $\prod-\prod$ type bands are observed at 23034.6 and 22398.9; 22870.1 and 22234.1; 22694.8 and 22059.0 cm^{-1}. The intervals between bands of each successive pair is 635.7, 636.0 and 635.8 cm^{-1} respectively. The mean value of the last three number i.e. 635.9 cm^{-1} is in good agreement with 636 cm^{-1}, the wavenumber of the observed Raman active overtone band, corresponding to the $(0\ 3^1\ 0)'' \longleftarrow (0\ 1^1\ 0)''$ transition in the ground state bending vibration.

It was assumed tentatively that the 23641.6 and 23010.1 cm^{-1} bands of the $\sum-\sum$ type occur due to transitions from the $(0\ 0^\circ\ 0)''$ and $(0\ 2^\circ\ 0)''$ vibrational levels of the ground state

---

* Unless otherwise stated, wavenumbers quoted in text, refer to those of the (80-80) isotopic species.

respectively to a common rovibronic level with K' = 0 of a bent upper state denoted by $(v_1\ v_2^0\ v_3)'$. The $\Pi - \Pi$ type bands at 23034.6 and 22398.9 cm^{-1} was assumed to be due to transitions from the $(0\ 1^1\ 0)''$ and $(0\ 3^1\ 0)''$ levels of the ground state respectively to a common rovibronic level (with K = 1) of a bent upper state. The successive intervals between the bands (of the previous paragraph) at 23034.6, 22870.1 and 22694.8 cm^{-1} are 164.5 and 175.3 cm^{-1} and those between the $\Pi - \Pi$ type bands at 22398.9, 22234.1 and 22059.0 cm^{-1} are 164.8 and 175.1 cm^{-1}. Each set of these three bands, therefore form progressions similar to that formed by the $\Sigma - \Sigma$ type bands mentioned earlier in this section.

For $v_3'' = 0$, the expression for the term values of the ground state for the bending vibrational levels can be shown (from equation 3.16) to have the following form.

$$G''(0, v_2^{l}) = \omega_2''(v_2 + 1) + x_{22}''(v_2 + 1)^2 + g l^2 + 1/2\ (x_{12}'' + x_{23}'') \times (v_2 + 1) + 1/4\ x_{13} \qquad (5.2)$$

It can be shown that if the term value $G''\ (0, 0^0) = 0$, then the expression (5.2) above reduces to (5.3) on the following

---

*Notation:- Same as section 3.5 except that the prime and double prime refer to upper and ground electronic states respectively; also, K is equal to l in the ground state and K represents the total angular momentum in the upper state. Since the quantum number v_3 is not encountered in this analysis the notation is reduced to $(v_1, v_2^l\ )$ in each state for convenience.

page.

$$G''(0,\ v_2^{l}) = \omega_2^{o''}(v_2 + 1) + x''_{22}\, v_2^{\,2} + g l^2 \qquad (5.3)$$

where $\omega_2^{o''} = \omega''_2 + 2x''_{22} + 1/2\ (x''_{12} + x''_{23}) + 1/4\ (x''_{13})$ has been substituted in (5.2). The interval of 631.4 cm^{-1} obtained in the last section corresponds to the wavenumber difference between $G''(0,0°)$ amd $G''(0,2°)$ term values and the interval of 635.9 cm^{-1} to the difference between $G''(0,3^1)$ and $G''(0,1^1)$ term values. By substitution of these intervals and appropriate term values $G''(o,\ v_2^{l}\ )$ it was found that $x_{22} = 1.2\ cm^{-1}$. With this value of x'_{22}, term value differences $G''[0,(v_2+2)^{l}\ ] - G''(0,\ v_2^{l})$ for $v_2 = 2,\ 3,\ 4$ .. etc. were calculated by the use of equation (5.3). Some of these calculated term value differences are given below in cm^{-1}.

$$\begin{aligned}
G''(0,2^o) &- G''(0,0^o) = 631.4\\
G''(0,3^1) &- G''(0,1^1) = 635.9\\
G''(0,4^o) &- G''(0,2^o) = 640.7\\
G''(0,4^2) &- G''(0,2^2) = 640.7\\
G''(0,5^1) &- G''(0,3^1) = 644.8\\
G''(0,5^3) &- G''(0,3^3) = 644.8
\end{aligned} \qquad (5.4)$$

Pairs of bands whose wavenumber intervals correspond to each of these calculated intervals were identified in the spectrum. The members of the pair were then assigned the corresponding quantum numbers $0,\ (v_2 + 2)^{l}$ and $0,\ v_2^{l}$ of the ground state and assumed to share a common upper rovibronic state in the transition.

In Fig. 5.4, a typical set of bands in each of the 80-80 and 78-78 spectra, resulting from (isovibronic) transition from ground state levels and K = 0,1,2,3 ... sublevels of one v_2' level in the excited state are represented schematically. The observed wavenumber differences between ground state levels of the same l (=K) which have the same symmetry, are shown. The agreement between these differences and the calculated differences in (5.4) may be verified. From the scheme in Fig. 5.4 it is seen that bands at 23178.2 and 22547.2 cm^{-1} must be of the $\Sigma-\Sigma$ type; and the bands at 22870.1 and 22234.1 cm^{-1} must be of the $\Pi-\Pi$ type. From an observation of their rotational structure and band head structure (see section 5.6) it was found that all the above four bands are of the correct types. Such agreements between expected and assigned band types were found for bands of the 78-78 molecule also. The relative intensities among the bands represented in Fig. 5.4 were also consistant with their assignment. The $\Sigma-\Sigma$ and $\Pi-\Pi$ bands arising from $v_2'' = 0$ and 1 levels respectively were the most intense bands (see Appendix L) in each of the isotopic molecules, as expected (see Appendix F) of bands arising from transitions from the ground and a low energy (313 cm^{-1}) excited vibrational state. For other bands of Fig. 5.4, there is a decrease in intensity with an increase in the value of the v_2'' level from which they originate. From temperature work it was found that the band at 23178.2 cm^{-1} is a cold band and that at 22870.1 cm^{-1} is relatively a hotter band (refer Appendix L). Such a temperature effect supports the assignment of the former band to a transition arising

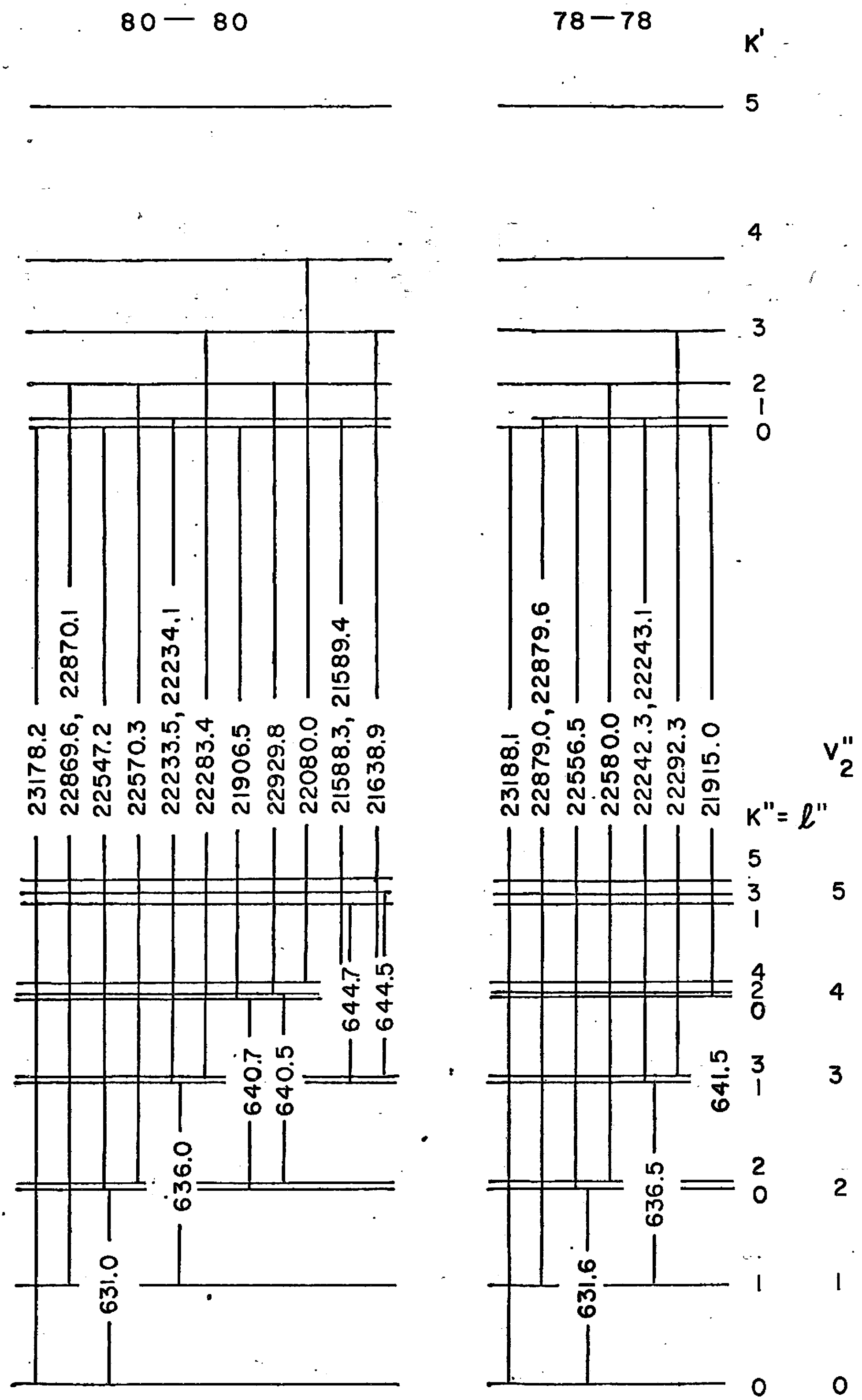

A typical v_2'' progression in the R system

FIGURE 5.4

from a v_2'' = 0 initial state. The quantum numbers v_1'' and v_3'' for this state should be zero for the same reason. Several such sets i.e. transitions from the ground state vibrational levels to K sublevels of each successive v_2'' level in the excited state, could be picked out. Five or six sets could be arranged into progressions with successive intervals of approximately 170 cm^{-1} (between corresponding members in each set). Five progressions of such sets are observed. Four of these are schematically shown in Fig. 5.5. Each vertical line in this diagram represents the first member of a set (of Fig. 5.4) i.e. a $\Sigma - \Sigma$ type band. The wavenumber of this band and, in parenthesis, the isotopic shift $\Delta\sigma$, are given. The members of each progression are believed to be transitions from the ground state v_1'' = 0 level to successive v_1' levels. The successive intervals (mean values of 4644, 4613 and 4657) between v_1' levels are shown. Each vibrational level has been numbered in Fig. 5.5; these numberings are justified in section 5.7. The wavenumbers of all those bands which have been assigned are given in Table 5.2. Table 5.2 a) lists $\Sigma - \Sigma$ type bands; 5.2 b) lists $\Pi - \Pi$ type bands; 5.2 c) lists $\Delta - \Delta$ bands; etc. The assignments of vibrational quantum numbers for $\Sigma - \Sigma$ and $\Pi - \Pi$ type bands are shown in the spectrograms of Appendix K.

In each isotopic spectrum, about 100 bands can be assigned to transitions from the vibronic levels of a linear ground state to those of the same bent excited state. The strongest bands in the spectrum, with a few exceptions, are

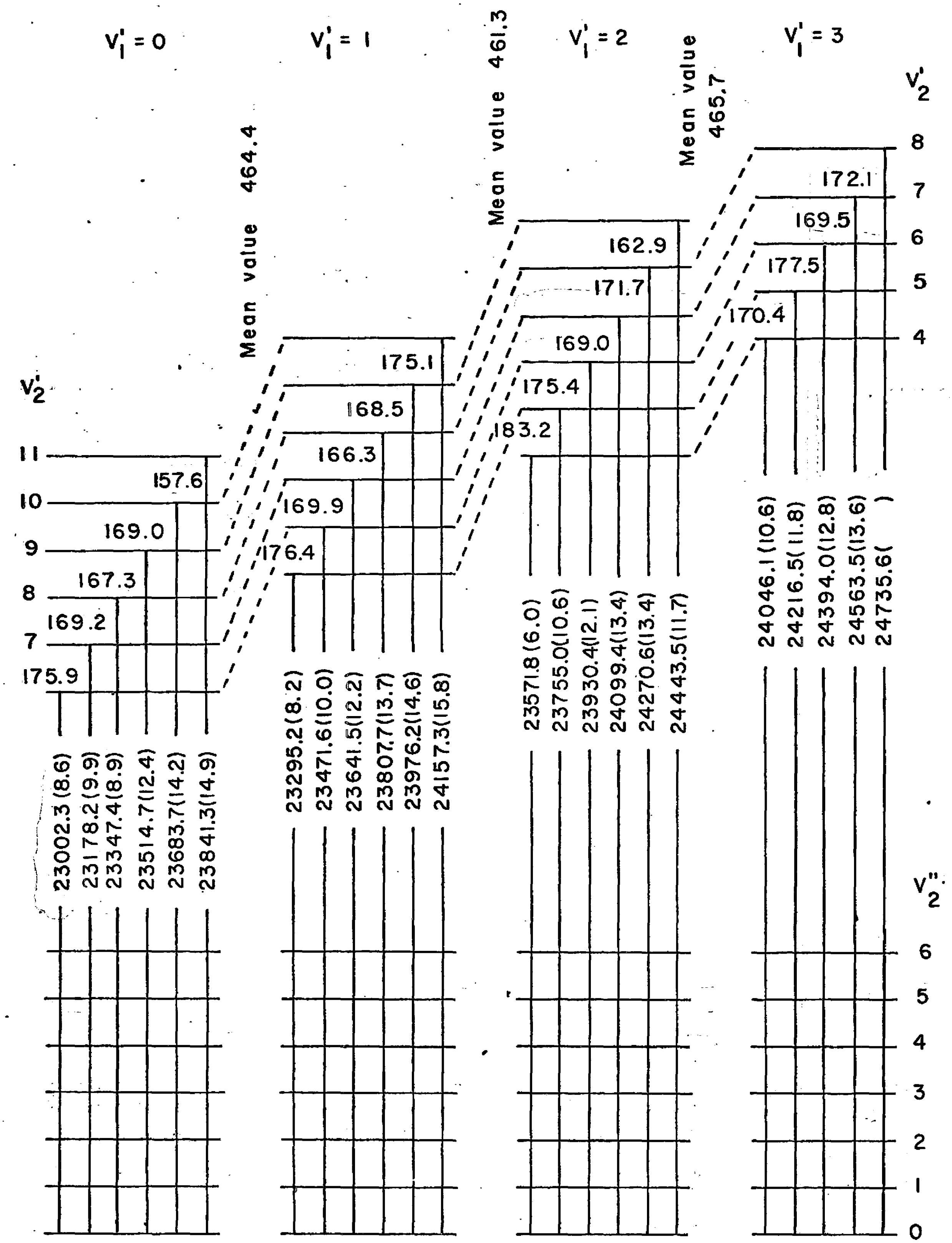

v_1' and v_2' progressions in the (80 – 80) species

FIGURE - 5.5

assigned without difficulty in this analysis. The combination differences $G''[0, (v_2 + 2)^K] - G''(0, v_2^K)$ were used as basis for checking the correctness of assignments. All pairs of bands which are transitions from $[0, (v_2 + 2)^K]''$ and $(0, v_2^K)''$ levels to any common excited state rovibronic level are expected to have the same value of $G''[0, (v_2 + 2)^K] - G''[O_2, v_2^K]$, within limits of experimental error. These differences were evaluated from the wavenumbers of assigned band heads in Table 5-2 and mean values are given below in cm^{-1}.

	80-80	78-78
$p_1 = G(0, 2^0) - G(0,0^0) =$	631.3	631.7
$p_2 = G(0, 3^1) - G(0,1^1) =$	636.0	636.6
$p_3 = G(0, 4^0) - G(0,2^0) =$	640.7	641.5
$p_4 = G(0, 4^2) - G(0,2^2) =$	640.1	640.9
$p_5 = G(0, 5^1) - G(0,3^1) =$	644.8	646.8
$p_6 = G(0, 5^3) - G(0,3^3) =$	645.1	

(5.5)

Since the strongest bands of the system are $\Sigma - \Sigma$ and $\Pi - \Pi$ bands the maximum number of individual 'p_i' values were obtained for the first two differences (p_1 and p_2) above. The largest deviation from the mean value of 631.3 cm^{-1} was 0.4 cm^{-1} and from the mean value of 631.7, it was ± 0.6 cm^{-1}. Similar satisfactory agreements were obtained for the p_i values of 636.0 and 636.6 cm^{-1}. These agreements support the vibrational analysis.

Table 5-2 a)

$\Sigma - \Sigma$ BANDS OF THE R SYSTEM (in cm^{-1})

$v_1', v_2' - v_1'', v_2''$	I (80-80)	σ 80-80	σ 78-78	I (78-78)
0,6 - 0,0	10	23002.3	23010.9	15
0,7 - 0,0	75	23178.2	23188.1	75
0,8 - 0,0	95mc	*23347.4	23356.3	80
0,9 - 0,0	100c	23514.7	23527.1	100
0,10 - 0,0	70m	*23683.7	23697.9	90
0,11 - 0,0	10	23841.3	23856.2	10
0,6 - 0,2	25h	22371.6	22379.3	30
0,7 - 0,2	60h	22547.2	22556.5	55
0,8 - 0,2	50	22716.4	22724.6	40
0,9 - 0,2	40	22883.5	22895.5	50
0,10 - 0,2	55	23052.2	23063.6	55
0,6 - 0,4	h	21730.1	21738.2	
0,7 - 0,4	h	21906.5	21915.0	
0,8 - 0,4	h	22075.6		
1,5 - 0,0	15	23295.2	23303.4	15
1,6 - 0,0	70	23471.6	23481.6	50
1,7 - 0,0	90mc	23641.5	23653.7	80

---

*overlapped;

c=cold, mc=possibly cold, m=cold or hot, mh=possibly hot
h=hot

Table 5-2 a) (in cm^{-1}) (continued)

$v_1', v_2' - v_1'', v_2''$	I (80-80)	σ 80-80	σ 78-78	I (78-78)
1,8 - 0,0	100c	23807.7	23821.4	100
1,9 - 0,0	100	23976.2	23990.8	70
1,10 - 0,0	20	24151.3	24166.7	10
1,5 - 0,2	20	22664.0	22671.4	15
1,6 - 0,2	45	22840.2	22849.4	55
1,7 - 0,2	65m	23010.1	23021.9	70
1,8 - 0,2	95	23176.5	23189.6	75
1,9 - 0,2	95mc	*23347.4	23359.2	25
2,4 - 0,0	20	23571.8	23577.8	10
2,5 - 0,0	25	23755.0	23763.9	20
2,6 - 0,0	70c	*23930.4	23943.3	50
2,7 - 0,0	90m	24099.4	24112.5	80
2,8 - 0,0	60mc	24270.6	24284.0	25
2,9 - 0,0	20mc	24443.5	24455.2	10
2,4 - 0,2	10	22938.9	22945.9	10
2,5 - 0,2	10	23124.1	23132.4	10
2,6 - 0,2	15	23298.8	23311.9	25
2,7 - 0,2	50	23468.0	23480.6	25
3,4 - 0,0	10	24046.1	24056.7	15
3,5 - 0,0	15	24216.5	24228.3	10
3,6 - 0,0	40	24394.0	24405.2	30
3,7 - 0,0	40c	24563.5	24575.3	50
3,8 - 0,0	10	24735.6		

Table 5-2 a) (in cm^{-1}) (continued)

$v_1', v_2' - v_1'', v_2''$	I (80-80)	σ 80-80	σ 78-78	I (78-78)
3,6 - 0,2	10	23762.3	23771.3	10
3,7 - 0,2	40	23932.7	23944.2	50

Table 5-2 b)

$\Pi - \Pi$ BANDS OF THE R SYSTEM

$v_1', v_2' - v_1'', v_2''$	I	σ 80-80	σ 78-78	I
0,6 - 0,1	45	22694.5 694.8	22702.1 701.9	50
0,7 - 0,1	85	22869.6 870.1	22879.6 22879.0	90
0,8 - 0,1	100m	*23034.6	23044.3 044.7	90
0,9 - 0,1	50	23219.6 220.1	23226.3 226.8	30
0,10 - 0,1	70mh	23388.4	23399.9 400.7	90
0,6 - 0,3	30	22058.4 059.0	22065.1 065.7	30
0,7 - 0,3	50	22233.5 234.1	22242.3 243.1	45
0,8 - 0,3	55	22398.9 399.1	22408.1 409.1	60
0,9 - 0,3	20	22583.7		
0,10 - 0,3	30	22752.2	22763.1	35
0,6 - 0,5	h	21413.5		
0,7 - 0,5	h	21588.3 589.4		
0,8 - 0,5	h	21754.6	21761.3	
1,5 - 0,1		22986.7 987.4	22994.1 994.9	
1,6 - 0,1	90m	23160.8 161.3	23170.8 171.3	90

Table 5-2 b) (continued)

$v_1',v_2' - v_1'',v_2''$	I	σ 80-80	σ 78-78	I
1,7 - 0,1	60	23340.9	23350.8 351.8	80
1,8 - 0,1	90mc	23499.4	23513.4	100
1,9 - 0,1	70m	23683.7	23697.9	90
1,10 - 0,1	20	23858.4	23873.2	20
2,4 - 0,1	25	23267.5	23276.8	15
2,5 - 0,1	50m	23474.5	23487.5	35
2,6 - 0,1	50mc	23623.3 624.5	23637.4	60
2,7 - 0,1	70	23803.2	23816.1	80
2,8 - 0,1	10	23969.9	23985.8	25
2,9 - 0,1	15	24151.3	24167.1	25
1,5 - 0,3	15	22351.1	22360.4	15
1,6 - 0,3	40	22525.2 525.8	22533.9 534.3	25
1,7 - 0,3	10	22705.2	22714.9	10
1,8 - 0,3		22863.8	22876.9	15
2,6 - 0,3		22986.7 987.4	23000.6	10
2,7 - 0,3	20	23167.4	23179.1	10
3,4 - 0,1	25	23755.0	23765.6	20
3,5 - 0,1	70c	23932.7	24942.5	60
3,6 - 0,1	15	24103.4	24114.9	80
3,7 - 0,1	60mc	24264.9	24284.0	80

Table 5-2 b) (continued)

$v_1', v_2' - v_1'' v_2''$	I	σ_{80-80}	σ_{78-78}	I
3,4 - 0,3	50	23468.0		

Table 5-2 c)

$\Delta - \Delta$ BANDS OF THE R SYSTEM

$v_1', v_2' - v_1'', v_2''$	I	σ 80-80	σ 78-78	I
0,5 - 0,2	10	22225.8		
0,6 - 0,2	30	22395.4	22402.2	20
0,7 - 0,2	80	22570.3 570.8	22580.0	75
0,8 - 0,2	50	22744.0	22755.3	60
0,9 - 0,2		22910.1	22924.1	30
0,10 - 0,2	10	23096.2	23104.2	15
0,5 - 0,4		21585.9		
0,6 - 0,4	h	21754.6	21761.3	
0,7 - 0,4	h	21929.8		
0,8 - 0,4		22103.6		
1,5 - 0,2	25	22687.7	22695.3	20
1,6 - 0,2		*22863.8	22870.5	
1,7 - 0,2	10	*23033.0	23041.2	20
1,8 - 0,2	20	23211.9	23218.9	20
1,9 - 0,2	15	22377.9		
2,5 - 0,2	15	23149.7	23166.0	15
2,6 - 0,2	35	23329.8	23340.9	15
2,7 - 0,2	10	23497.2	23507.0	5

Table 5-2 d)

$\Phi - \Phi$ BANDS OF THE R SYSTEM

$v_1', v_2' - v_1'', v_2''$	I	σ 80-80	σ 78-78	I
0,8 - 0,3	10	22455.9	22464.1	20
0,7 - 0,3	30	22283.4	22292.3	25
0,6 - 0,3		22100.0	22107.5	10
0,8 - 0,5	h	21809.0	21816.4	
0,7 - 0,5	h	21638.9		
0,6 - 0,5	h	21454.9		
1,7 - 0,3		22754.8	22763.8	
1,6 - 0,3	25	22581.0		
1,6 - 0,5	h	21934.7		

A plot of p_i (given in 5.5) against v_2 is shown in Fig. 5.6. From this plot, $\omega_2^{o''}$ and x_{22} were obtained, as indicated in the figure, and are given below.

For 80-80 $\omega_2^{o''} = 313.4\ \mathrm{cm}^{-1}$ $x_{22} = 1.1\ \mathrm{cm}^{-1}$

For 78-78 $\omega_2^{o} = 313.5\ \mathrm{cm}^{-1}$ $x_{22} = 1.2\ \mathrm{cm}^{-1}$

The respective values are equal within limits of experimental errors.

Term values in the ground state:

From these numbers, and the value of p_i is given in (5.5) the term values of $G''(0, v_2^K, 0)$, for K = 0 and K = 1 were calculated with respect to the $(0\ 0^o\ 0)''$ level, as shown below.

For K = 0

cm^{-1}

	$G(0,0^o,0)$	p_1	$G(0,2^o,0)$	p_3	$G(0,4^o,0)$
80-80	0	631.3	631.3	640.7	1272.0
78-78	0	631.7	631.7	641.5	1273.2

(5.6)

For K = 1

cm^{-1}

	$G(0,1^1,0)$	p_2	$G(0,3^1,0)$	p_5	$G(0,5^1,0)$
80-80	313.4	636.0	949.4	6448	1594.2
78-78	313.5	636.6	950.1	646.8	1596.9

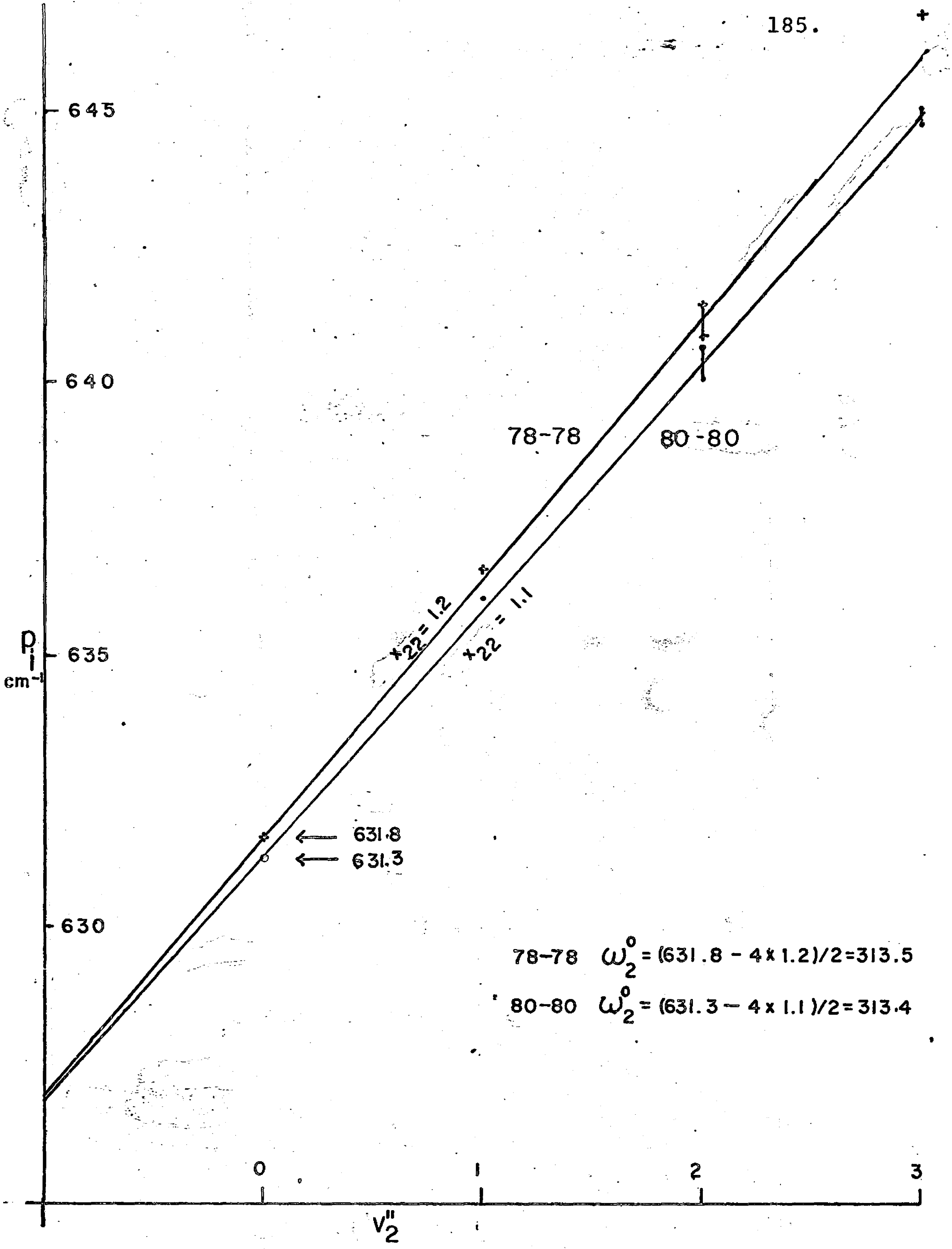
645
640
635
630
p_i
cm^{-1}
78-78
80-80
$x_{22} = 1.2$
$x_{22} = 1.1$
631.8
631.3
78-78 $\omega_2^0 = (631.8 - 4 \times 1.2)/2 = 313.5$
80-80 $\omega_2^0 = (631.3 - 4 \times 1.1)/2 = 313.4$
0
1
2
3
v_2''

FIGURE 5.6

If 'g' in equation (5.3) is known then the term values $G''(0,v_2^K,0)''$ for K = 2, 3 .... etc. levels may be calculated. In the present work 'g' was found to be equal to 4 (± 1.5) cm^{-1}, from the data on liquid phase Raman spectra (refer to Table 3-3) and was judged to be relatively inaccurate to be used for calculations of $G''(0, v_2^K)''$ values.

Term Values in the Upper State:

From these $G''(0,v_2^K)''$ values and the wavenumber of assigned bands in Table 5.2, the term values of the upper state levels $T(v_1, v_2^K)'$ were next calculated. These term values are defined by

$$T'(v_1, v_2^K)' = \sigma_H(v_1, v_2^K)' + G''(0,v_2^K)'' \quad (5.6)$$

where σ_H is the wavenumber of the band head (formed by the J structure) corresponding to the transition from $(o, v_2^K)''$ level to $(v_1, v_2^K)'$ level. Mean term values T' so obtained are given in Table 5-3 for both isotopic molecules (80-80 and 78-78). Isotopic shifts $T^{(78-78)} - T^{(80-80)} = \Delta\sigma$ are also given in the last two columns of the same table.

Rovibronic levels in the upper state which have same vibrational quantum numbers v_1, v_2 (and v_3) but which have different values K = 0 and K = 1 are separated by wavenumber interval given by (equation 4.36)

$$T'(v_1,v_2^l)' - T'(v_1,v_2^0)' = F_v'(J,l) - F_v'(J,0) \quad (5.7)$$

Table 5-3 a

TERM VALUES, $\Delta G'$ VALUES, A CONSTANT AND ISOTOPIC SHIFTS $\Delta\sigma_H = T^{78} - T^{80}$ in CM^{-1} IN IN THE UPPER STATE

v_1', v_2'	80-80			78-78			K=0	K=1
	K=0	K=1	$\bar{A}$	K=0	K=1	$\bar{A}$	$\Delta\sigma_H$	$\Delta\sigma_H$
0,6	23002.9	23008.3	5.4	23011.1	23015.7	4.6	8.2	7.4
ΔG	175.7	175.2		177.1	177.5			
0,7	23178.6	23183.5	4.9	23188.2	23193.2	5.0	9.6	9.7
ΔG	169.4	164.8		168.1	165.5			
0,8	23348.0	23348.3	0.3	23356.3	23358.7	2.4	8.3	10.4
ΔG	166.9	185.0		170.8	181.6			
0,9	23514.9	23533.3	18.4	22527.1	23540.3	13.2	12.2	7.0
ΔG	169.1	167.4		169.5	173.4			
0,10	23684.0	23701.7	17.7	23696.6	23713.7	17.1	12.6	12.0
ΔG	157.3			159.7				
0,11	23841.3			23856.3			15.0	

Table 5-3 b

TERM VALUES T", ΔG" VALUES, A CONSTANT AND ISOTOPIC SHIFTS $\Delta\sigma_H = (T_H^{78} - T_H^{80})$ IN (CM^{-1}) IN THE UPPER STATE

v_1' v_2'	80-80			78-78			K=0	K=1
	K=0	K=1	$\overline{A}$	K=0	K=1	$\overline{A}$	$\Delta\sigma_H$	$\Delta\sigma_H$
1,5	23295.3	23300.7	5.4	23303.2	23308.4	5.4	7.9	7.7
ΔG	176.2	174.3		178.1	176.2			
1,6	23471.5	23475.0	3.5	23481.3	22484.6	3.3	9.8	9.6
ΔG	170.0	179.1		172.4	180.5			
1,7	23641.5	23654.4	12.9	23653.7	23665.1	11.4	12.2	10.7
ΔG	166.3	158.6		167.7	161.8			
1,8	23807.8	23813.0	5.2	23821.4	23826.9	5.5	13.6	13.9
ΔG	169.8	184.0		169.5	184.5			
1,9	23977.6	23997.1	19.5	23990.9	24011.4	20.5	13.3	14.3
ΔG	171.7	174.8		175.8	173.3			
1,10	24151.3	24171.8	20.5	24166.7	24184.7	18.0	15.4	12,9

Table 5-3 c

TERM VALUES $\Delta G'$ VALUES, A CONSTANT AND ISOTOPIC SHIFTS

$\Delta\sigma = (T_H^{78} - T_H^{80})$ IN (CM^{-1}), IN THE UPPER STATE

v_1' v_2'	80-80			78-78			K=0	K=1
	K=0	K=1	$\bar{A}$	K=0	K=0	$\bar{A}$	$\Delta\sigma_H$	$\Delta\sigma_H$
2,4	23571.0	23580.9	9.9	23577.7	23590.3	12.6	6.7	9.4
ΔG	184.2	207.0		186.0	210.7			
2,5	23755.2	23787.9	32.7	23763.7	23801.0	37.3	8.5	13.1
ΔG	175.0	147.4		179.8	149.6			
2,6	23930.2	23937.3	7.1	23943.5	23950.6	7.1	13.3	13.3
ΔG	169.1	179.4		168.9	178.8			
2,7	24099.3	24116.7	17.4	24112.4	24129.4	17.0	13.1	12.7
ΔG	171.3	166.6		171.6	169.9			
2,8	24270.6	24283.3	12.7	24284.0	24299.3	15.3	13.4	16.0
ΔG	162.9	181.4		174.2	181.3			
2,9	24443.5	24464.7	21.2	24458.2	24480.6	22.4	14.7	15.9

If J = 0, then this (5.7) reduces to

$$F'(0,1) - F'(0,0) = A_v' - 1/2\ (B_v' + C_v') = \bar{A}_v \qquad (5.8)$$

where A_v', B_v' and C_v' are rotational constants in the upper state with quantum numbers v_1' and v_2' and $\bar{A}_v$ is used as a convenient symbol. Values of $\bar{A}_v$ are given in Table 5-3 for each isotopic species.

The assignment of vibrational quantum numbers v_1', and v_2' to the bands of Table 5-2 are tentative. The bands of that progression shown at the extreme left of Fig. 5.5, were assigned the quantum number $v_1' = 0$ for the final state of the corresponding transitions; no progressions which could arise from still lower energy v_1' levels were observed with certainty. The assignment of quantum numbers v_2' for bands of each progressions was done by the use of isotopic shifts. Isotopic shifts given in Table 5-3 were used for this purpose. These shifts, for bands whose quantum numbers are $v_1' = 0$, $v_1'' = 0$, $v_2'' = 0$ and $K' = 0$, were plotted against a running number, and this plot is shown in Fig. 5.11. The closest integral intercept of the curve at $\Delta\sigma = 0$ was assumed to be zero and the number axis is renumbered to obtain a better (but not necessarily exact) numbering of v_2' since the isotopic shift for the origin band cannot be exactly predicted for each band. The values of v_2' given in Tables 5-2 and 5-3 for the $(0,v_2)'$ levels are the suggested values based on Fig. 5.11 The numberings of v_2' levels for each of the remaining $v_1' = 1, 2, 3$ levels is dependent

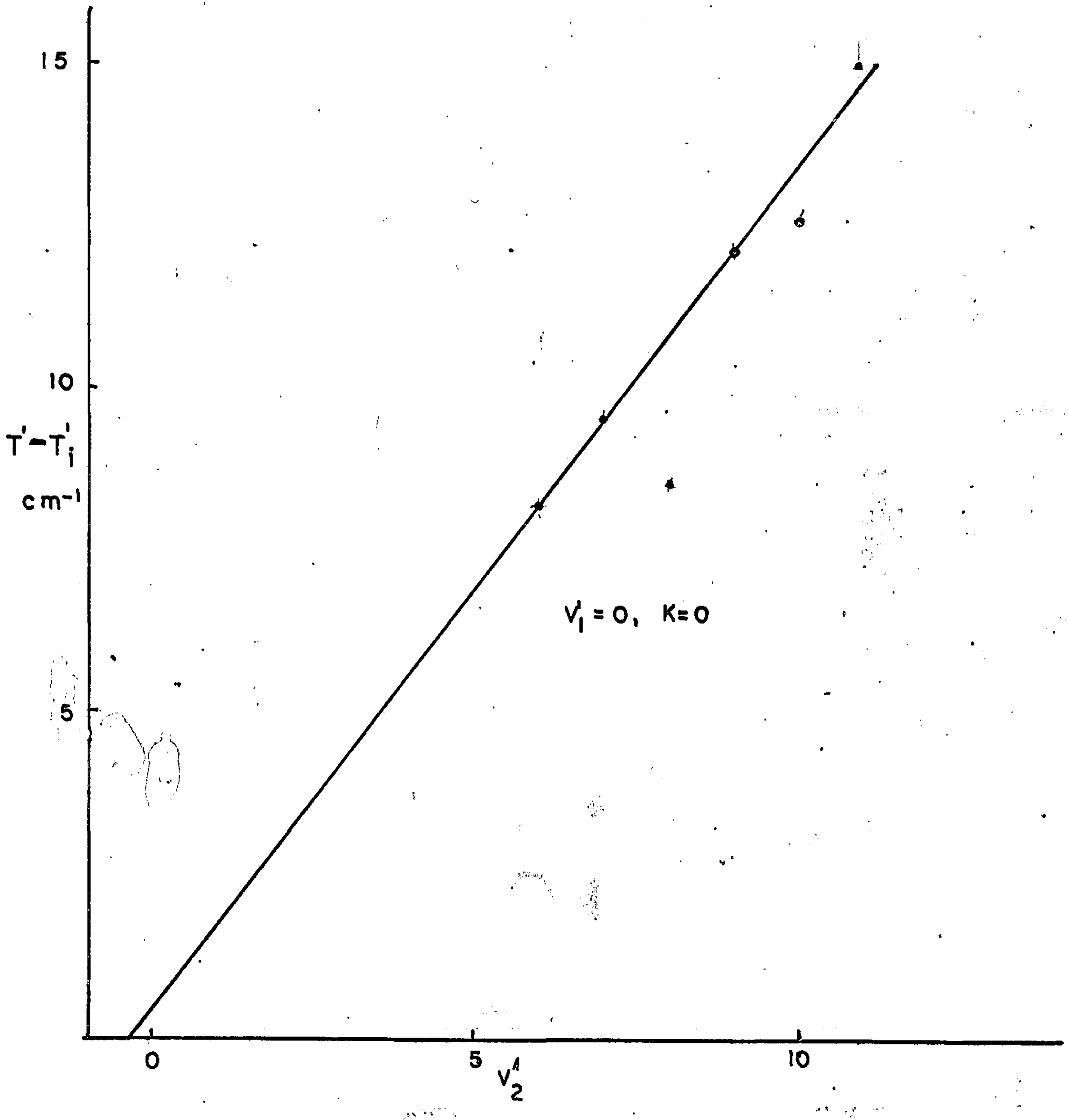

FIGURE 5.11

upon the choice of ω_1', the symmetric stretching frequency in the excited state. If $\omega_1' \approxeq 460$ cm^{-1}, then the numberings for v_2' given in the above tables are correct, relative to the $v_1' = 0$, v_2' progression. If $\omega_1' \backsimeq 630$ cm^{-1} (see section 5.7) each v_2' level in successive progressions has its current numbering decreased by one, two and three successively. Since the linear relationship between isotopic shifts and v_2' , anticipated from equation (4.44) seems to hold only approximately the values of v_2' could be in error by ± 2. Plots of $\Delta\sigma \propto v_2'$ for all progressions observed in the spectrum are not shown in Fig. 5.11 In general, isotopic shifts for bands of these progressions are irregular. Neglect of anharmonicity effects in the isotopic shift formula is not expected to give rise to such irregularities. The only available explanation seems to be the presence of large perturbations (section 5.2). In his work on CS_2, Kleman[37] reported that the isotopic shifts for the higher quantum number levels could not be predicted by the simple isotopic shift formula. This statement appears to be true for carbon diselenide also.

From Tables 5-3 a) , b) and c), it is seen that $\bar{A}$ values in general, increase with an increase in v_2'. Fig./5.8 gives the plots of $\bar{A}$ against v_2' in each of the $v_1' = 0$, 1 and 2 levels. The shape of these curves resemble qualitatively, those given in Fig. 4.7 (by Johns)[99] , but points in the plot show considerable deviations. By extrapolating the curve of $\bar{A}$ against v_2' to $v_2' = 0$ an intercept of $\bar{A}_0 = 1.5$ cm^{-1} is obtained. This value is expected to have an estimated error of ± 1.0 cm^{-1} or even

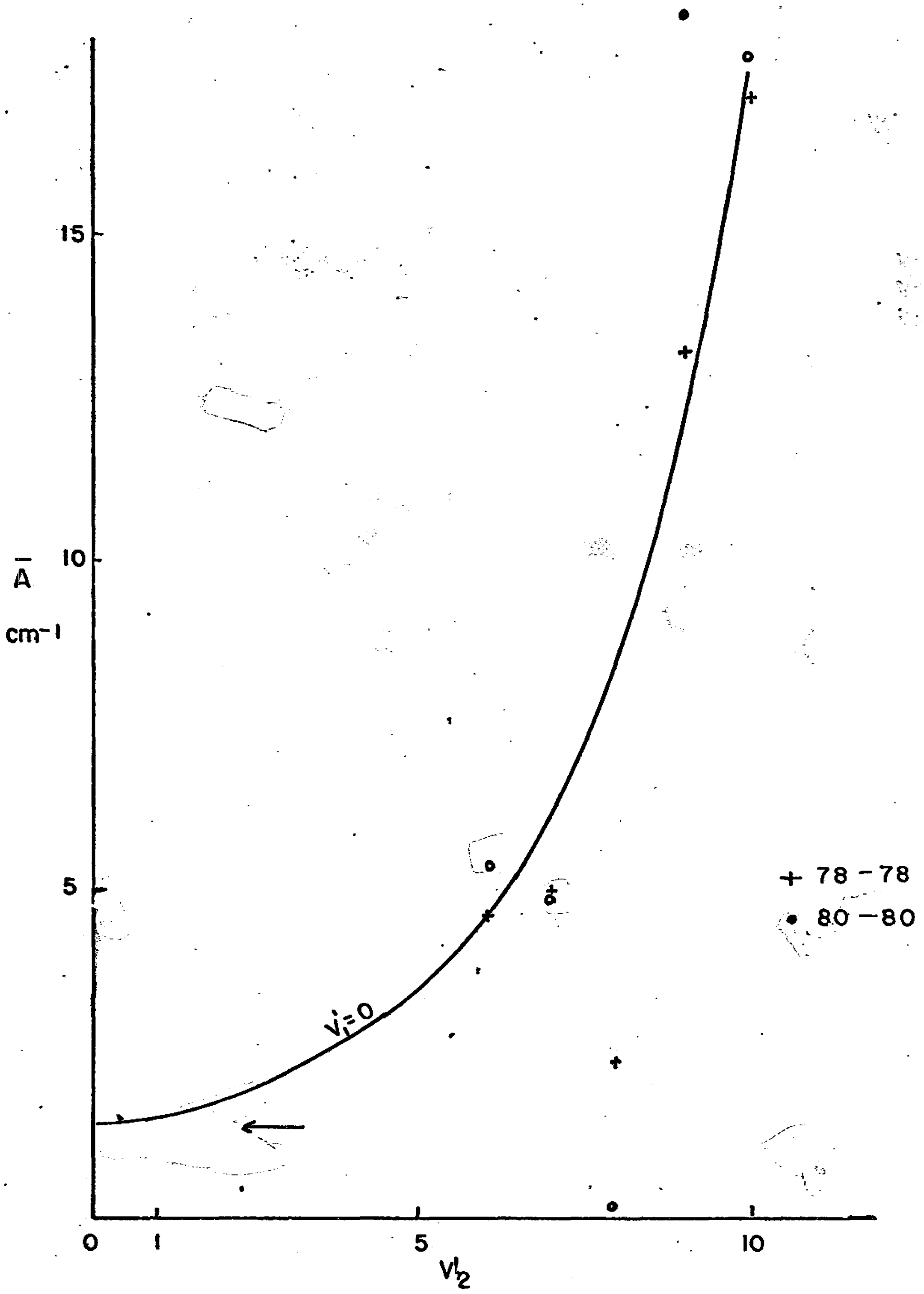

FIGURE 5.8

a higher positive value. Since the A values obtained are erratic, the quadratic relationship (section 4.7)

$$G'(v_1, v_2^K) = \text{constant} + \bar{A}\,K^2 + .. \qquad (5.9)$$

could not be established between the term values of the K" = 0, 1, 2 .. etc. sublevels of each v_2' level. If such a relationship could be established, it will be additional proof of a bent excited state.

In Fig. 5.5, $G'[v_1, (v_2+1)^K] - G'[v_1, v_2^K] = \Delta G'$ values are marked, for the K = 0 sublevels in the excited state. Fig. 5.9 shows the curves obtained from plots of $\Delta^{G'}$ values of Table 5-3 against $v_2' + 1/2$. A qualitative resemblance of these curves to that given by Johns[99] is evident (compare Fig. 4.7). However, it cannot be established whether the agreement in shape is fortuitous or not because of the occurence of perturbations in the system. If the minima in the $\Delta G'$ curves are genuine, their observation is an additional proof for a bent excited state as discussed in section 4.5. Each curve in the figure has been extrapolated to $v_2' = 0$ to obtain some indication of the magnitudes of $\Delta G'$ for the $v_2' = 0$ and $v_2' = 1$ levels. If anharmonicity effects are neglected $\Delta G' \approx \omega_2'$; from the figure, $\Delta G'$ is seen to be in the range of 210 to 185 cm^{-1}. A more reliable value of the excited state bending vibration frequency ω_2' could not be obtained with the present work.

5.6 Rotational Structure

Liebermann[38], by a detailed rotational analysis, showed that many bands of the R system of CS_2 are of the $\Sigma - \Sigma$ type.

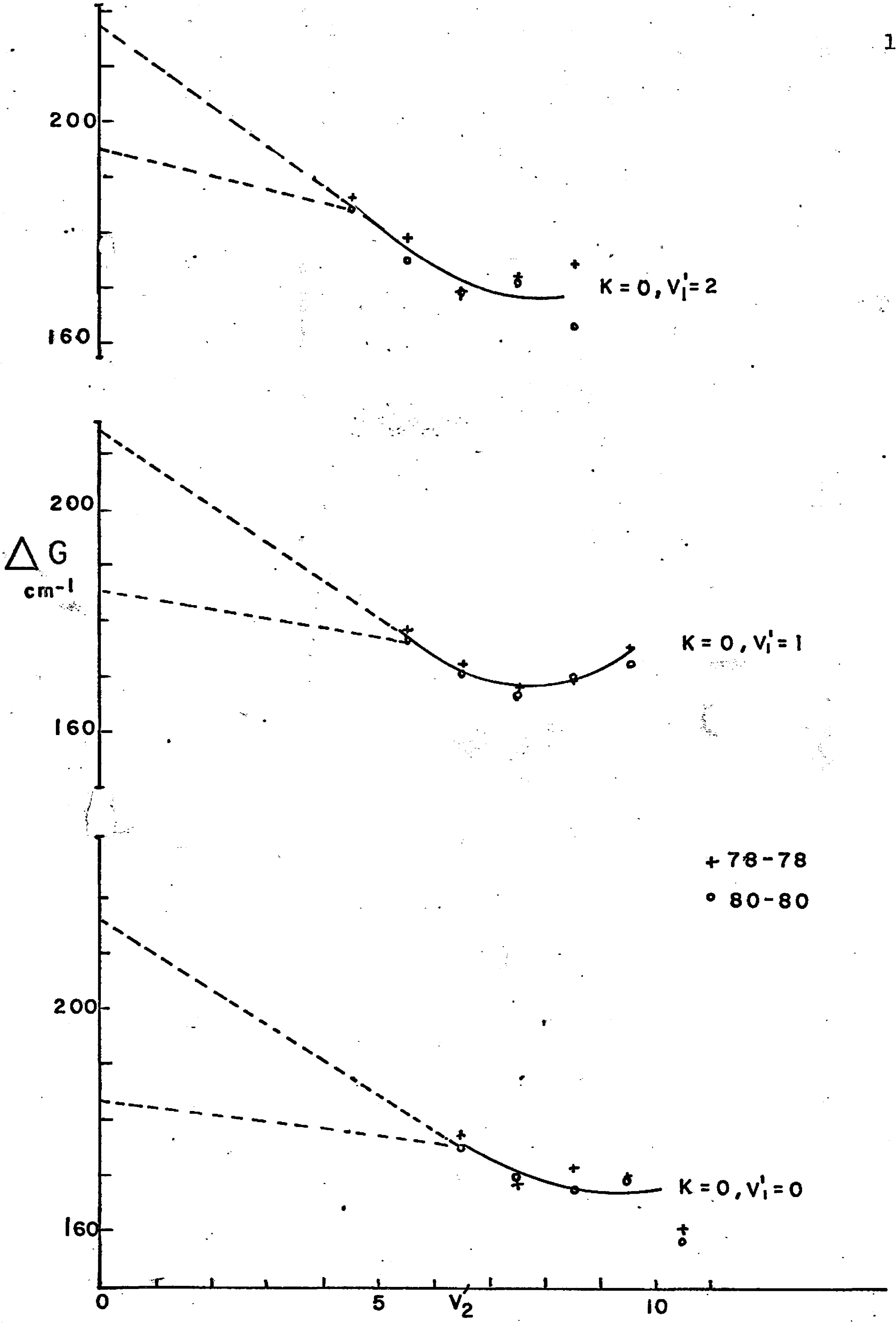
200
160
K = 0, V_1'= 2
200
ΔG
cm-1
K = 0, V_1'= 1
160
+ 78-78
○ 80-80
200
K = 0, V_1'= 0
160
0
5
V_2
10

FIGURE 5.9

Kleman observed that, in addition to these $\Sigma-\Sigma$ type bands $\Pi-\Pi$, $\Delta-\Delta$., etc type bands are also present in the system. Such a classification of bands by their rotational structure enabled Kleman to arrive at a satisfactory vibrational analysis of the R system of CS_2.

In this work, a similar classification was attempted with the same purpose in view. $\Sigma-\Sigma$ type bands were identified easily. These bands are single headed, have a simple sharp line like rotational structure which is degraded to the violet and resemble the $\Sigma-\Sigma$ type bands of CS_2. The rotational lines apparently form a single R branch; and are resolved beyond 2 or 3 cm^{-1} from the band head. A few of these bands were photographed on a high resolution 35 ft spectrograph; one of the bands in which the rotational structure is very well resolved is shown in Fig. 5.7. Displacements of rotational lines from their expected wavenumber positions in the branch were observed in several bands. These irregularities were attributed to perturbations.

The $\Pi-\Pi$, $\Delta-\Delta$, etc types of bands in the CSe_2 R system could not be identified by inspection or by comparison of the bands of the R system of CS_2. In the latter spectra $\Pi-\Pi$ bands were observed to be double headed with a separation of 4 to 5 cm^{-1} between the two heads; $\Delta-\Delta$ bands were also double headed with a separation of about 1 cm^{-1} between the heads. Kleman identified these bands by their appearence alone in the lower energy end of the CS_2 spectrum.

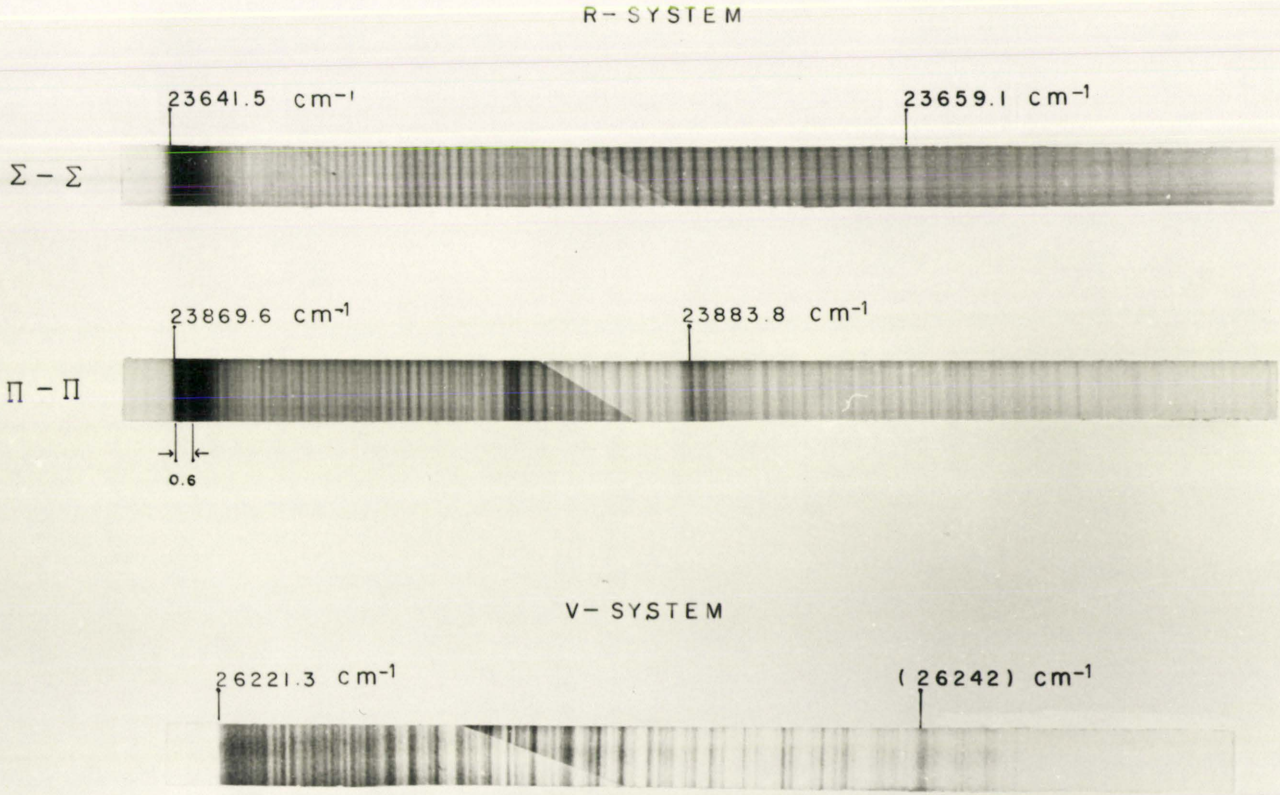

BAND TYPES IN THE ABSORPTION SPECTRUM OF CSe_2 (80-80)

AS OBSERVED ON A 35 FT EBERT SPECTROGRAPH

FIGURE 5.7

In the CSe_2 spectrum some double headed bands with a spacing of less than 1 cm^{-1} between the heads were observed at the lower energy end of the spectrum. It was, however, difficult to assign these bands to either $\Pi \leftrightarrow \Pi$ or $\Delta \leftrightarrow \Delta$ types by inspection alone. One such double headed band in the CSe_2 spectrum is shown in Fig. 5.7 and has been classified as a $\Pi - \Pi$ band. The method by which the identification was arrived at is discussed below.

A band contour program in Fortran IV language was formulated for an IBM 7040 computer. With the program, the band contours of $\Sigma - \Sigma$, $\Pi - \Pi$, and $\Delta - \Delta$ type bands due to parallel transitions as well as those of $\Pi - \Sigma$ $\Delta - \Pi$ etc type, due to perpendicular transitions, could be calculated. In the first stage of the program the rotational energy levels of the ground state, which are very similar to those of a diatomic molecule were calculated for a given B value. In this calculation, Λ - type or l -type doubling were also taken into account by the use of expression (4.28). In the second stage, the rotational energy levels of the bent excited state were calculated from the formulae of Polo[108] (given in Appendix G) for given values of the constants A,B and C. The wavenumbers corresponding to transitions allowed by selection rules in K, J and parity, between the two sets of levels were calculated. Hönl-London formulae for line strengths, statistical weights of J levels, and the distribution of molecules in each J level at a given temperature are taken into account in order to calculate the relative intensities among rotational lines corresponding to each transition. The mechanics of producing a calculated rotational band contour for a given spectroscopic resolution was adopted from the asymmetric rotor contour program of Parkin.[121]

The program was initially used to calculate the contours of Σ-Σ, Π-Π and Δ-Δ bands of the R system of CS_2. A,B and C constants given by Lieberman and Kleman were used for the calculation. The contours obtained were found to match qualitatively, the rotational line structure of these Σ-Σ, Π-Π, Δ-Δ bands, illustrations of which are given by Kleman. The separation between the two heads of a Π-Π or Δ-Δ type band head is determined by the asymmetry parameter 'b' given in Appendix G. It was observed from band contour calculations that the appearance of each of these Π-Π and Δ-Δ bands in the CS_2 spectrum is not unique; a band contour of a Π-Π band with a small 'b' value resembles the band contour of a Δ-Δ band with a large 'b' value. Therefore a better guide to the assignments of Π-Π and Δ-Δ bands in the R system of CS_2 is obtained from the wavenumber of the bands in the spectra rather than on their characteristic appearance.

The band contour program was used next to calculate the contours of Σ-Σ, Π-Π, Δ-Δ as well as Σ-Π,... etc type bands for the CSe_2 molecule. The rotational constant A_v was assumed to be equal to the $\bar{A}_v$ values in Table 5-3. A wide range of $\bar{A}_v$ values can apply as seen from this table, and therefore this constant was varied in the range of 3 to 20 cm^{-1}.

B'_v and C'_v were estimated from the resolved part of the rotational structure of $\Sigma-\Sigma$ type bands in the R system of CSe_2. The difference in wavenumbers of successive rotational lines $R(J) - R(J-2)$ were plotted against a running number. From the slope of these curves, $\Delta B = 1/2(B'_v + C'_v) - B''_v$, (this relationship may be verified from equations 4.33, 3.20 and 3.23) were calculated. It was found that ΔB lies in the range of 0.0005 to .002 cm^{-1}. For each assumed value of B'' in the range of 0.025 and 0.036 cm^{-1} (section 3.8), $1/2(B'_v + C'_v)$ was obtained and used for calculating the band contour. It was assumed that B'_v is nearly equal to C'_v and the difference between the two constants and A_v served as a paramter for calculating b. The contours are determined by the asymmetry parameter 'b' as well as the difference ΔB rather than the individual values of rotational constants. In general, the value of 'b' is much smaller than for CS_2. In Fig. 5.8 typical $\Sigma-\Sigma$, $\Pi-\Pi$ and $\Delta-\Delta$ contours calculated in this way are shown. By a comparison of Fig. 5.10 with the spectrogram of Fig. 5.7, it can be seen that the calculated contour of $\Sigma-\Sigma$ and $\Pi-\Pi$ type bands show a qualitative resemblance to the observed bands in the latter figure. From Fig. 5.10, it may be observed that $\Delta-\Delta$ bands are not double headed. It was found that in the range of A_v, B_v and C_v values used for calculating contours only $\Pi-\Pi$ bands are double headed; $\Sigma-\Sigma$ bands are single headed and are distinguishable from $\Delta-\Delta$ bands by the simpler rotational structure of the former. The contours of $\Sigma-\Pi$ and

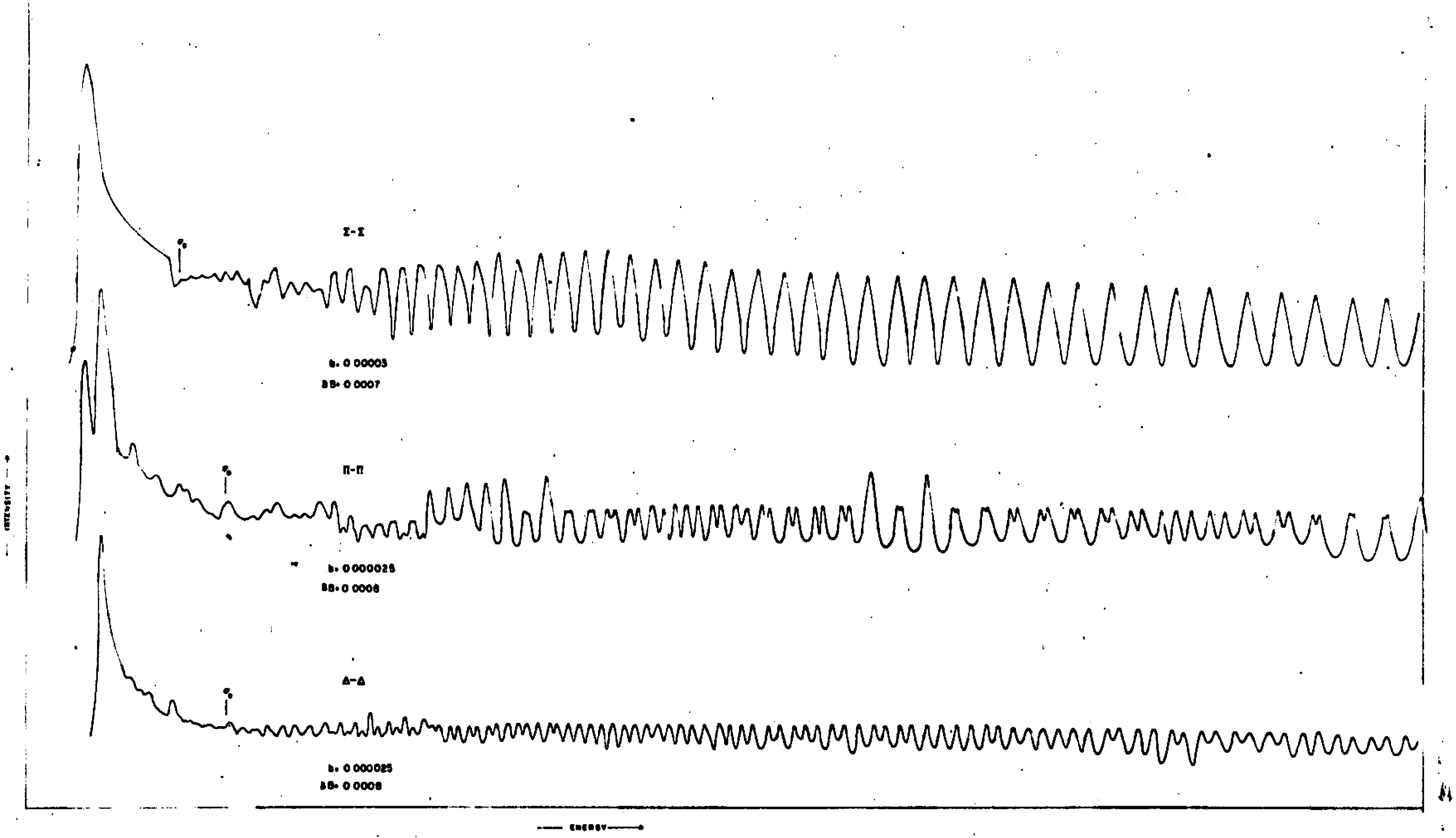

CALCULATED CONTOURS OF BAND TYPES IN THE R-SYSTEM OF CARBON DISELENIDE

FIGURE 5.10

$\Pi-\Sigma$ type bands were calculated to be double headed but the calculated contours did not match those of observed bands.

In order to pick out $\Sigma-\Sigma$ bands from other band types in the R system, the spectrum of the (77-77) molecule was observed on a high resolution 21 ft Ebert spectrograph. Since Se^{77} has a nuclear spin of I = 1/2, the intensity of alternate rotational lines in $\Sigma-\Sigma$ bands must be in the ratio of 3:1; whereas since Se^{80} has a nuclear spin of I = 0, alternate rotational lines, in $\Sigma-\Sigma$ bands of the (80-80) molecule should be missing. This difference in the structure of $\Sigma-\Sigma$ type bands of the two isotopic molecules was looked for in order to identify these bands unambigously. However, this method was not successful; the rotational structure of the bands of (77-77) species was not resolved by the spectrograph. The only evidence for the presence of alternate rotational lines in the (77-77) bands which must be missing in the (80-80) bands, seems to be the apparent loss of resolution of rotational lines in the levels of the former molecule in comparison with the resolution of line into the bands of the latter molecule.

5.7 Calculations

A. Bond angle :

If the rotational constants A and B at the equilibrium position of the bent molecule are known, the bond angle 2α can be calculated from the relation[120].

$$\tan^2 \alpha = \frac{m_C}{m_C + 2\, m_{Se}} \times \frac{A}{B} \qquad (5.10)$$

where m_C is the mass of the Carbon atom and m_{Se} is the mass of the Selenium atom. It is assumed that the rotational constant $A = \bar{A}'_{00} = 1.5 \pm 1$ cm^{-1} (from Fig. 5.8) and that B'' lies in the range of 0.025 cm^{-1} to 0.036 cm^{-1} (section 3.8). According to section 5.6, B' values are not greater than B'' by more than 0.002 cm^{-1}. Therefore the approximation $B' = B''$ can be used. This approximation is not in greater error than is the uncertainty in the value of A. By substitution of these values of B and A in (5.10) it is found that $2\alpha = 105^\circ$ to 140°.

B. Origin band of the R system :

As mentioned in section 5.3, the σ_{000} band (i.e. the origin band) has not been positively identified in the spectrum. It is possible that the origin band transition has a very small probability and that all the observed bands at the low energy end (where the origin band is expected) of the spectrum are due to transition from excited v_2'' levels.

An approximate value for σ_{000} was obtained from the isotopic displacements of term values $\Delta\sigma$ given in Table 5-3. $\Delta\sigma$ values for the levels $(0\ v_2^0\ 0)'$ were plotted against the term values; the intercept on the term value axis for $\Delta\sigma = 0$, gives a very approximate value for σ_{000}. It was found by this method that

$$\sigma_{000} = 21900 \text{ cm}^{-1}$$

with a large estimated uncertainty of ± 400 cm^{-1}.

C. Upper state vibrational frequencies :

An approximate range of values for the bending vibrational frequency in the upper state i.e. 180 to 215 cm^{-1} has been given in section 5.5. A value of the asymmetric stretching frequency in the upper state ω_3' was not found.

It was mentioned in section 5.3, that progressions were also observed in the symmetric stretch corresponding to wavenumber intervals of about 460 cm^{-1} between members of each progression. This value could be close to the correct value of the symmetric stretching frequency in the upper state. In Fig. 5.5, these intervals are marked and are obtained from wavenumber differences between bands arising from transitions between a common ground state to successive v_1' levels in the excited state. The mean interval between successive bands $v_1' = 0,1,2,3$ are given at the top of the figure. These values are 464.9, 461.3 and 465.7 cm^{-1} (refer to Fig. 5.5). It is interesting to note that these intervals do not increase or decrease uniformly. However, other possible differences between corresponding bands of each v_2' progression are 293, 630, 805, 972, .. etc cm^{-1}, and, in principle, one of these values could correspond to the symmetric stretching frequency.

Kleman, in the case of CS_2, chose the most reasonable value of ω'_1 from a similar set of possible frequencies, by a determination of the stretching force constants k_1' in the upper bent state. For this purpose, he used equations (D.2) in which the bond angle $\widehat{SCS}$ and ω_2', determined by the analysis of the R system of CS_2 were substituted. He chose that ω_1' as the correct frequency which gave a positive value of k_1' as well as a value smaller than k_1'' in the linear ground state. Such a procedure could not be used satisfactorily in this work because of the uncertainties in the bond angle and ω_2'. Therefore it has been assumed that the value of 465 cm^{-1} is close to the correct value. The values 805, 972 ...etc. cm^{-1} are felt to be too high and the value of 293 cm^{-1} too low. The possibility that ω_1' could be close to 630 cm^{-1} is not entirely eliminated.

PART B

THE V SYSTEM

5.8 A brief description and some preliminary remarks on the V system absorption of CSe_2 is given in this section. A detailed analysis of this system has not been attempted at the present time.

A. Observations:

10 and 50 cm cells which contained the vapour (at room temperature) of 80-80 and 78-78 molecules were used for recording spectra on low and high resolution spectrographs. A very large number of bands, some strong and many weak, were observed in the 4050-3450 Å region of the absorption spectrum. The higher wavelength end of the spectrum just overlaps the lower wavelength end of the R system. In this region of overlap, there are several weak bands which could not be

assigned to one system on the other. The last panel in Appendix K shows this region of the spectrum.

Bands at the higher wavelength (lower energy) end of the spectrum are violet degraded and have sharp heads. Some of the heads in the 80-80 spectrum are double headed with a separation of 3 to 4 cm^{-1} between the heads; in the 78-78 spectrum, double heads are not as evident, and each band head appears slightly diffuse. The number of intense bands in this region of the spectrum are relatively smaller, and the wavenumber intervals between these bands are larger, than at the higher energy region of the spectrum. The most intense bands lie in this latter region. Many bands in this region do not show a marked violet degradation; they appear as broad patches, with intensity maxima occuring within each patch. For such bands, wavenumbers of band heads could not be obtained accurately, since band heads are not well defined. These bands could be similar in appearance to those observed in the V system of CS_2 by Kleman[37].

One of the violet degraded bands observed at 26221 cm^{-1} is shown at the bottom of Fig. 5-7. It is seen, by a comparison of this band with the $\Sigma - \Sigma$ and $\Pi - \Pi$ type bands of the R system given in the same figure, that the rotational structure of the V system band appears to be more complex. The rotational lines in this band are not broadened in the presence of a magnetic field (up to 25000 gauss).

Many of the intense bands could be arranged into progressions with an interval of about 360 cm^{-1} between successive bands. These bands are shown schematically in Fig. 5.12. Wavenumbers and estimated intensities (in parenthesis) of each band in the 80-80 molecule are given on each vertical line representing the band. Isotopic shifts $\Delta\sigma = \sigma_H^{78} - \sigma_H^{80}$ are also given next to the intensity value. Double headed bands are indicated by the symbol d.h. and single headed bands by s.h.; all other bands are more complex in appearance. The intervals between successive bands of each progression are given. Other possible intervals between the intense bands are about 125, 245, 485, 830 ...etc. cm^{-1}. These intervals are found between bands of one progression and those of another.

It is observed from the figure that the intensity of each band within each progression increases with wavenumber. It is also observed that isotopic shifts are large for bands at higher wavenumbers and decrease regularly by about 5 cm^{-1} for successive bands.

B. Discussion:

The oscillator strength and spectral region of the V system of CSe_2 are similar to those of the V system of CS_2 (section 5.1). It is possible that these systems are analogous.

Several workers have observed the V system of CS_2 which appears to have a complex vibrational and rotational structure. A complete vibrational analysis of the system is not available. A detailed discussion and a tentative analysis

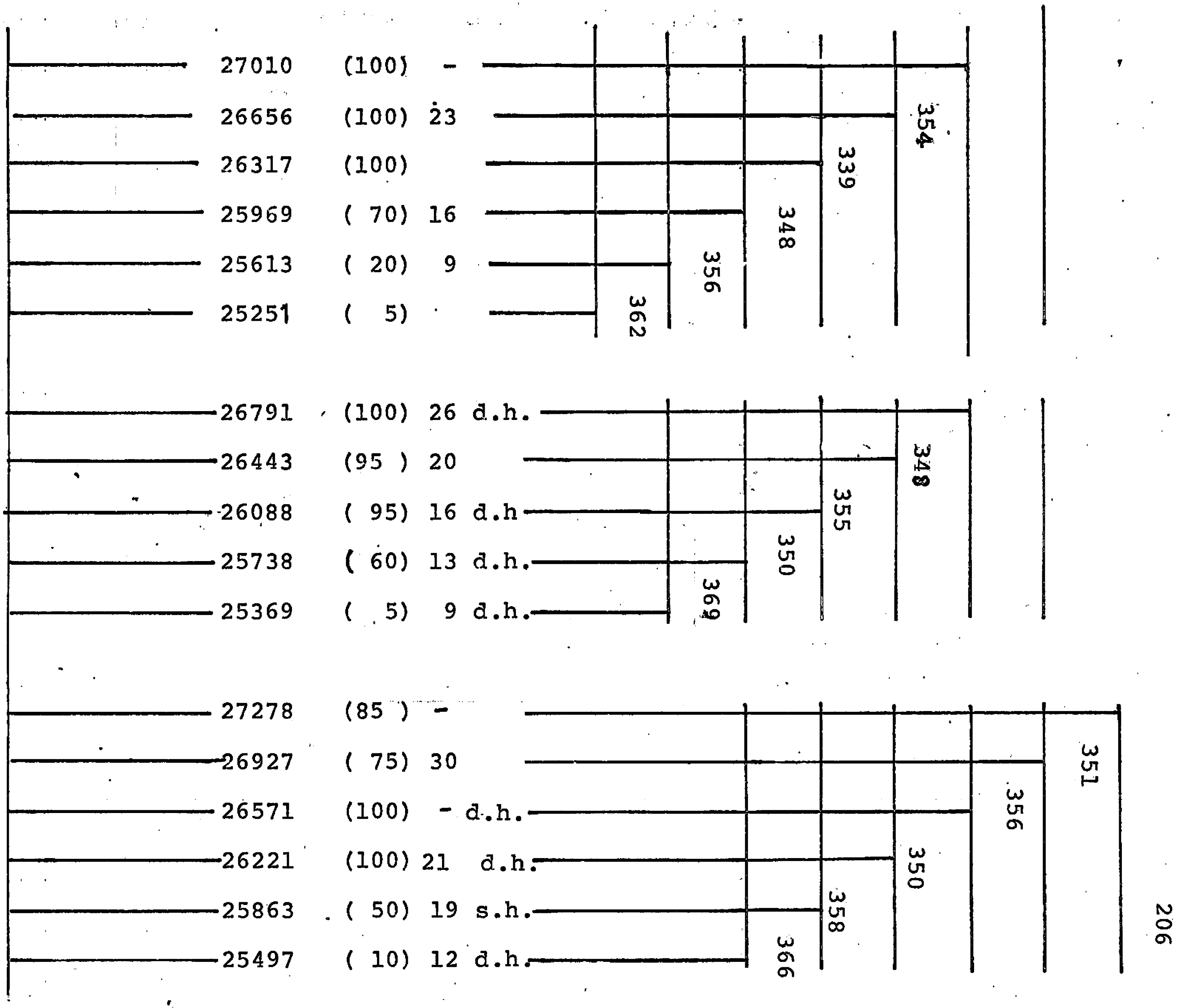

Observed progressions in the V system of 80-80 species

FIGURE 5.12

has been given by Ramasastry and Rao[42]. These authors observed progressions which they attributed to the symmetric stretching frequency of the CS_2 molecule in a slightly bent excited state. They proposed that this excited state is a ${}^1A_2$ electronic state to which a transition from the ${}^1\Sigma_g^+$ ground state occurs, and that this ${}^1A_2$ state is one of the (Renner-Teller) split component states of a ${}^1\Pi_g$ excited state (refer to Table 4-2) of the linear molecule.

Callear and Tyerman observed the analogous V system of CSe_2 for the first time but did not propose an analysis. In this work, the same system was observed with the 80-80 and 78-78 molecules. The violet degradation of bands at the low energy regions of the spectrum indicates that the corresponding transitions are probably from a linear ground state to a bent excited state (section 5.4B); since such a distinct degradation is not observed in bands at the higher energy region of the spectrum, it is probable that the transitions in the latter region are from a linear ground state to a linear excited state. Both these observations may be explained on the basis that the excited electronic state is that of a 'slightly' bent molecule; since, the upper state vibrational levels for the first kind of transition could correspond to those of the molecule in the bent conformation and for the second kind of transitions they could correspond to excited vibrational levels (of the same upper electronic state) in which the molecule has changed over to a linear conformation.

Few of the observed intervals between intense bands correspond to 313.5 or 631.3 cm^{-1} which are the wavenumbers corresponding to one and two quanta respectively of bending vibration in the ground state. If the molecule is indeed bent in the excited state, it is difficult to understand the reason why these intervals are not observed, as in the case of the R system.

However, if the electronic transition which corresponds to the V system absorption is an allowed transition (if the molecule is linear or even slightly bent in the excited state), progressions in symmetric stretching vibrations ω'_1 and ω''_1 should be observed. It is possible that the intervals of about 360 cm^{-1} shown in Fig. 5.12 correspond to the symmetric stretching vibration in the excited state. The observation of large changes in isotopic shifts for successive members of the progressions is consistent with this assignment (section 4.10). It was found that these progressions could not be accounted for as those of the ground state symmetric stretching frequency because of the small changes in relative intensities between bands in each progression. Among other observed wavenumber differences the interval of 485 cm^{-1} between progressions could be two quanta of the upper state bending frequency.

For an allowed electronic transition, the oscillator strength may be much higher than the value of 10^{-3} observed for the V system. This observation is therefore not consistent with the proposition that the transition is an allowed transition. But, it is possible to account for both observations viz. a low value of oscillator strength, as well as progressions in the symmetric stretching frequency in the excited state, if the possibility of spin-orbit interaction in the excited state is taken into account.

It is therefore suggested that the excited state is a triplet state to which transition from the ground state is allowed, predominantly due to spin-orbit interaction rather than vibronic interaction. Such a large spin orbit interaction is possible for molecules such as CSe_2, two constituent atoms of which are quite heavy. Further work is necessary to establish with certainty the nature of the excited state.

PART C

THE A SYSTEM

5.9 This system of CSe_2 which is observed in the 2600-2100Å regi has an analogue in the $\tilde{A}^1B_2 \longleftarrow \tilde{X}^1\Sigma_g^+$ system of CS_2 as mentioned in section 5.1. The upper state of the latter system was established by Douglas and Zanon[45] by a partial rotational analysis of a few bands in the system. The vibrational structure of this system is not understood completely, but these workers state that this structure is similar to that of the R system of CS_2. It is possible that the A system of CSe_2 arises from a similar transition as the A system of CS_2.

In the present work, the A system of CSe_2 was recorded only under low resolution on the spectrophotometer.

The wavelengths and wavenumbers of the observed intensity peaks from the (Cary) spectrograms are given in Table 5-4. The uncertainty in the wavenumber data is of the order of 15 - 20 cm^{-1}. The absorption spectrum must be recorded at higher resolution to obtain more accurate data for a vibrational analysis. The only evidence available at present to establish that this system is similar to that of CS_2 is the comparable intensities and regions of occurence of both systems.

PART D

SUMMARY AND CONCLUSIONS

The objectives of this work were listed in section 1.6. Among these objectives, the following have been achieved.

i. Milligram quantities of CSe_2 have been synthesized from individual isotopies of selenium viz. Se^{80}, Se^{78} and Se^{77} by a previously unreported method (section 2.2). These isotopic molecules were used for recording absorption spectra.

ii. The infrared and Raman spectra of N-N, 80-80, and 78-78 molecules were investigated. The vapour phase infrared spectrum of the molecules have been investigated in the range of 4000-90 cm^{-1}, thereby extending the range previously examined by Wentink[23]. The reported fundamental at 308 cm^{-1}, due to the bending vibration of CSe_2, has been observed experimentally at 313 cm^{-1}. A more complete Raman spectra of N-N, 80-80 and 78-78 molecules have been recorded. The symmetric

Table 5-4

WAVELENGTHS, WAVENUMBERS AND ABSORBANCE READINGS OF SYSTEM Å

Å $\pm$ 1	σ (air) cm^{-1}	Absorbance
2402.5	41623	0.60
2389	41858	0.68
2381	41999	0.77
2377	42069	0.77
2375	42105	0.76
2370	42194	0.87
2367	42247	0.94
2356.5	42435	1.02
2346	42625	1.22
2334	42844	1.47
2332.5	42872	1.47
2324	43029	1.50
2321	43084	1.48
2313	43233	1.72
2302.5	43431	1.76
2299	43497	1.68
2294.5	43582	1.75
2290.5	43658	1.84
2281	43840	1.83
2279.5	43869	1.85
2270	44052	1.81
2259.5	44257	1.73

Table 5-4 (contd.)

Å ±1	(air) cm^{-1}	Absorbance
2252	44405	1.42
2248.5	44474	1.48
2242	44603	1.33
2240	44642	1.33
2230	44843	1.16
2226.5	44913	1.14
2221	45024	1.05
2217.5	45095	1.03

stretching fundamental and overtones of the bending vibration were observed experimentally for the first time. Results of these investigations indicate that the molecule is linear in the ground state, as expected (section 3.8).

iii. The electronic absorption spectra of N-N, 80-80 and 78-78 molecules in the vapour phase were observed under low and high resolution in the 4500 - 3450 Å region. The R system absorption in the 4600 - 4000 Å region has been investigated in detail. A satisfactory vibrational analysis has been obtained on the basis that the transition for the R system is from a linear ground state to a bent B_2 state. Approximate frequencies of the symmetric stretching and bending vibration in the excited state have been found. The bond angle in the excited state conformation of the molecule seems to be in the range of 105 - 140°.

iv. A brief report on the V system absorption of 80-80 molecule in the 4050-3450 Å region is given. Preliminary studies show that the molecule could be slightly bent in the excited state of the transition corresponding to the V system. Further work is necessary to establish the nature of the excited state (section 5.B).

v. The absorption spectra of CSe_2 in the 2300 Å region, at low resolution was observed. It is tentatively assumed that the corresponding transition is a $\tilde{A}\,{}^1B_2 - \tilde{X}\,{}^1\Sigma_g^+$.

Some conclusions may be drawn regarding the electronic states involved in the observed transitions of the CSe_2

molecule by a consideration of the electron configuration of CO_2. These configurations have been given in section 4.1. If it is assumed that these configurations are acceptable approximations to those of the CSe_2 molecule, we can write the following for the latter molecule

Configuration Symmetry

$$\begin{array}{lll} \ldots\ldots\ldots & (\pi_g)^3(\pi_u)^1 & - \; {}^1\Sigma_u^+ \; {}^3\Sigma_u^+ \; {}^1\Sigma_u^- \; {}^3\Sigma_u^- \; {}^1\Delta_u \; {}^3\Delta_u \\ \text{Excited state}\ldots\ldots\ldots & (\pi_g)^3(\sigma_g)^1 & - \; {}^1\Pi_g \; {}^3\Pi_g \\ \ldots\ldots\ldots & (\pi_g)^3(\sigma_u)^1 & \;\; {}^1\Pi_u \; {}^3\Pi_u \end{array} \qquad (5.11)$$

The relative energies of the resultant states given for CO_2 in Table 4-2 are expected to apply here also.

The R system is the lowest energy absorption observed so far. It must therefore correspond to a transition from the ${}^1\Sigma_g^+$ state to one of the relatively low lying states given above. The choice of the upper state of the R system is discussed below.

i) The oscillator strengths of 10^{-4} (section 5.1) for the system indicates that the transition is not an allowed electric dipole (magnetic dipole or electric quadrupole) transition. Therefore, we eliminate the possibility that the transition is from the ${}^1\Sigma_g^+$ to the ${}^1\Sigma_u^+$ state which results from the $(\pi_g)^3\pi_u$ configuration; a transition to one of the triplet electronic states or orbitally degenerate singlet electronic states seems likely.

ii) The correct choice of the upper state may be obtained from a comparison of the R system of CSe_2 with that of the R system of CS_2 for which the transition has been established to be a $B_2 \longleftarrow {}^1\Sigma_g^+$ type transition. There are many 'areas' of similarity between these two CS_2 and CSe_2 spectra and are listed below:

a) Oscillator strengths f_{nm} have comparable magnitudes.

b) The vibrational structures of the two systems are remarkably similar. Both systems are transitions of the bent-linear type.

c) The rotational structure of bands in the two systems are also quite similar and have a singlet-singlet type rotational structure. All assigned bands are of the parallel type.

d) Both systems occur in very similar spectral regions, which indicates that the transition energies are of the same order of magnitude. Hence, it is possible that the upper states are from very similar electronic configurations.

e) It was found that, in addition to the bands of the R system, several intense bands were present at the higher energy end of the spectrum which could be assigned to progressions of 170 cm^{-1} intervals. These bands could not be assigned as members of the R system. The frequencies of members of one such progression are (24367.6, 24529.9, 24709.1, 24875.7 cm^{-1}). Kleman[37] found similar progressions of bands which could not be assigned to the R system. He proposed that these bands are due to transitions from the

$\tilde{X}\,^1\Sigma_g^+$ to hitherto unidentified other electronic states. It is possible that such transitions are present in the R system of CSe_2 also.

f) Perturbations in the vibrational and rotational structure of the bands of the system were observed, analogous to those in the bands of CS_2, in this work. These perturbations are probably due to the presence of states which are close in energy to the upper state of the R system.

The only features of dissimilarity between the two systems was the observation that there is no Zeeman effect observed in the rotational lines of the bands of the R system of CSe_2 . There are two ways in which this dissimilarity may be accounted for. Firstly, a Zeeman effect for the R system of CS_2 was observed only in the bands at the low energy end of the spectrum. Long path length cells were used to observe these bands. No Zeeman broadening was observed for the bands at the higher energy end. In CSe_2, much smaller path length cells were used since only small quantities of isotopes were available. Therefore, bands of the R system of CSe_2 could not be observed at the low energy end of the spectrum to check whether a Zeeman effect is observable in this region. Secondly, it is possible that the magnetic fields (of 25000 gauss) used for the CSe_2 molecule is not adequate. Douglas[39] was able to observe the Zeeman effect on CS_2 for much smaller fields. He showed that the observed Zeeman effect in the rotational (J) lines of the bands increases linearly with J. Such an increase is expected for a B_2 state, only if there is an interaction with a neighbouring state. The magnitudes of the interaction is dependent on the separation in energy between the interacting states. Hougen[118] has shown that an A_1, and B_1 components of a $^3A_2$ state could interact with the B_2 state of the CS_2 molecule; the B_2 upper state is the third component in this triplet state. It is possible that the A_1 and B_1 components of a $^3A_2$ state in CSe_2 interact less with the third B_2 state because of a larger energy separation. Much larger magnetic fields may then be necessary to observe a Zeeman effect.

It is concluded that the R system of CSe_2, like that of CS_2, is a spin multiplet component with B_2 symmetry. This B_2 state could be one of the components of a $^3A_2$ bent electronic state which correlates with a $^3\Delta_u$ or a $^3\Sigma_u^-$ state (refer Table 4-2) in the linear conformation of the molecule. The V system could arise from a transition to the upper component of a Renner-Teller $^3\Delta$ state and it is possible that this component is slightly bent. The A system could arise from a transition to the $^1\Sigma_u^+$ state of Table 4-2.

BIBLIOGRAPHY

1. Tinkham, M., "Group Theory and Quantum Mechanics", McGraw Book Co., New York, 1964.

2. Born, M., and Oppenheimer, J.R., Ann. Physik, 84, 457(1927)

3. Born, M., and Huang, K., in "Dynamical Theory of Crystal Lattices"., Oxford University Press, London and New York., (1954)., .

4. Liehr, A., Ann. Physik., 1., 221 (1957)

5. Slater, J. C., "Quantum Theory of Molecules and Solids", Vol. I., McGraw Hill (1963)., page 252.

6. Wilson, E. B., Decius, J.C., Cross, P. C., "Molecular Vibrations", McGraw Hill Book Co., New York, (1955)., page 273.

7. King, G. W., "Spectroscopy and Molecular Structure", Holt, Rinehart and Winston, Inc., New York (1964) page 57.

8. Herzberg, G., "Spectra of Polyatomic Molecules", D. Van Nostrand Co., (1966).

9. Messiah, A., "Quantum Mechanics" Vol. II, John Wiley & Sons, Inc. (1962)

10. Reference 7. Chapter 5

11. Hochstrasser, R. M., "Molecular Aspects of Symmetry", Benjamin Inc., (1966)

12. Eyring, H., Walter, J., and Kimball, G. E., "Quantum Chemistry", J. Wiley, New York, (1944)

13. Einstein, A., Z. Physik, 18, 121 (1917)

14. Herzberg, G. "Spectra of diatomic Molecules:, D. Van Nostrand Co., (1950)., page 20.

15. Hill, T. L., "Statistical Thermodynamics", Addison Wesley, (1960)

16. Harrison, G. R., Lord, R. C., and Loufbourow, J. R., "Practical Spectroscopy", Prentice-Hall, Inc., New Jersey (1948), page 363.

17. Robinson, G. W., in Marton, L., "Methods of Experimental Physics"., 3, Academic Press, New York (1962)., page 241.

18. Ibid., page 260.

19. Allen, H. C., and Cross, P. C., "Molecular Vib-Rotors", John Wiley And Sons., New York, 1963., Page 94.

20. Strandberg, M. W. P., Wentink, T., and Kyhl, R. L., Phys. Rev., 75, page 270, (1949).

21. Wentink, T., Koski, W.S., and Cohen, V. W., Phys. Rev. 81, 948 (1951).

22. Strandberg, M. W. P., Wentink, T., and Hill, A. G., Phys. Rev. 75, 827 (1949).

23. Wentink, T., J. Chem. Phys., 29, 188 (1958).

24. Wentink, T., J. Chem. Phys., 30, 105 (1959).

25. Townes, C. H., Holden, A. N., and Merritt. F. R., Phys. Rev., 74, 1113 (1948).

26. Bak, B., Sloan. R., and Williams, D., Phys. Rev., 80, 101, (1950).

27. Stoicheff, B. P., Can. J. Phys. 36, 218 (1958)

28. Rossman, K., Rao, K.N., and Nielsen, H. H., J. Chem. Phys. 27, 103, (1956)

29. Plyler, E. K., Blaine, L. R., and Tidwell, E. D., J. Res. Nat. Bur. Std., 55, 183 (1955)

30. Courtoy, C. P., Can. J. Phys., 35, 608 (1957)

31. Allen, H. C., Plyler, E. K., and Blaine. L. R., J. Am. Chem. Soc., 78, 4843 (1956)

32. Guenther, A. H., Wiggins, T. A., and Rank, D. H., J. Chem. Phys., 28, 682 (1958)

33. Lord, R. C., and McGubbin, T. K., J. Opt. Soc. Am. 47, 689 (1957)

34. Guenther, A. H., and Stoicheff, B. P., in private communication to Kleman. B., Ref. 37. (1963)

35. Stiles, D. A., Tyerman, W.J.R., Strawsz, O. P., and Gunning, H. E., Can. J. Chem., 44, 1677 (1966)

36. Callear, A. B., and Tyerman, W. J. R., Trans. Faraday, Soc., 61 , 2395 (1965)

37. Kleman. B., Can. J. Phys. 41 , 2034 (1963)

38. Liebermann, L. N., Phys. Rev., 55, 850, (1939)

39. a. Douglas, A. E., and Milton, E. R. V., J. Chem. Phys., 41., 357 (1964)
    b. Douglas, A. E., Can. J. Phys., 36, 147 (1958)

40. Ramasastry, C., and Rao. K. R., Indian J. Phys., 21, page 313 (1947)

41. Kusch. P., and Loomis. F. W., Phys. Rev., 55, 850 (1939)

42. Ramasastry. C., Proc. Nat. Inst. Sci. India, A., 18 page 177 (1952a)

43. Price, W. C., and Simpson, D. M., Proc. Roy. Soc (London) A, 165, page 272 (1938)

44. Hauptmann. E., Acta Phys. Pol. 7., page 86. (1938)

45. Douglas, A. E., and Zanon. I., Can. J. Phys. 42, 627(1964)

46. Brown. A. J., and Whalley, E., Inorganic Chemistry 7, 1254 (1968)

47. Herzberg.G., and Herzberg. L., J. Opt. Soc. Am., 43 , page 1037 (1953)

48. Herzberg. G., "Infrared and Raman Spectra", D. Van. Nostrand Co., (1945)

49. Silvey. G., Hardy, W. A., and Townes. C. H., Phys. Rev. 87, 236(A)., (1952)

50. Callear. A. B., Nature, 202, 1326, 1964

51. Grimm. H. G., and Metzger. H., Ber. dtsch. Chem. Ges., 69 , 1356 (1936)

52. Ives. D. J. G., Pittman. R. W., and Wardlaw. W., J. Chem. Soc. (London) 1947, page 1080.

53. "Tables of wavenumbers for the calibration of Infrared Spectrometers"., Butterworths, London (1961)

54. Douglas. A. E., Private Communication

55. White, J.U., J. Opt. Soc., Amer., 32, 285 (1942)

56. Bernstein. H. J., and Herzberg .G., J. Chem. Phys. 16. 30 (1948)

57. Warren.,C.H., and So., S. P., Private Communication

58. Edlen, B., J. Opt. Soc. Amer. 43, page 339 (1953)

59. Reference 7., page 106., page 82.

60. Koster. G. F., "Notes on Group Theory"., Technical Report Number 8.,Massachusetts Institute of Technology, (1956)

61. Reference 48., page 66

62. Landau L. D., and Lifshitz. E. M., "Quantum Mechanics", Pergamon, London, (1958). page 352.

63. Reference 48., page 274.

64. Reference 7., Section 9. 14

65. Reference 48., page 205

66. Nielsen. H. H., Phys. Rev. 60, 794 (1941)

67. Reference 6., page 198

68. Reference 48., page 251

69. Placzek. G., and Teller. E., Z Physik., 81 , 209 (1933)

70. Reference 48., Chapter 4., Section 1.

71. Reference 48., page 388

72. Reference 48., Chapter II., 6

73. Redlich. O., Z. Physik. Chem. B. 28, 371 (1935)

74. Rosenthal. J. E., Phys. Rev. 45, 426 (1934)

75. Plyler. E.J., and Humphreys. C. J., J. Research Nat. Bur. Standards 39 , 59, (1947)

76. Reference 48., p.391

77. Reference 48., p.168

78. Reference 48.,pp.169, 176.

79. Parr R. G., "Quantum Theory of Molecular Structure", Benjamin., Inc., New York (1963)

80. Shull. H., and Lowdin, P.o., Phys. Rev., 110, 1466 (1958)

81. Reference 8., page 299

82. Slater. J.C., Phys. Rev., 34, 1293 (1929)

83. Roothan, C.C.J., Rev. Mod. Physics. 23, 69, 1951

84. Reference 8, Chapter 5., Section 1

85. Fischer-Hjalmars. I., Arkiv. fur. Physik, 11, 529 (1957)

86. Walsh. A. D.., J. Chem. Soc. 2260., 1953

87. Peyerimhoff. S. D., and Bvenker. R. J., J.Chem. Phys., 47, 1953 (1967)

88. Mulliken. R. S., Physical Review, 60, 506 (1941)

89. Mulliken. R. S., Can. J. Chem, 36, 10, (1958)

90. Mulligan, J. [illegible]., J. Chem. Phys. 19, 1428 (1951)

91. Herzberg, G., and Teller, E., Z. Physik. Chem. B 21, 410, (1933)

92. Renner, R., Z. Physik., 92, 172, (1934)

93. Reference 7., page 415

94. Pople, J. A., and Longuet-Higgins, H. C., Mol. Phys. 1, page 372., (1958)

95. Reference 12., page 92

96. Dixon, R. N., Molecular Physics., 9, 357 (1965)

97. Merer, A. J., and Travis, D. N., Can. J. Phys. 44, page 1541; (1966)

98. Dixon, R. N., Trans. Far. Soc. 60, 1363 (1964)

99. Johns, J. W. C., Can. J. Phys. 45, page 2639 (1967)

100. Thorson, W., and Nakagawa, I., J. Chem. Phys. 33, 994 (1960)

101. Reference 9., page 454

102. Herzberg, G., and Innes, K. K., Can. J. Phys., 35, 842, (1957)

103. Reference 14., page 199

104. Reference 14.,page 226

105. Reference 8,page 107

106. Reference 14,page 237

107. Reference 8,page lo5

108. Polo,S.R.,Can. J.Phys.,35,880,(1957)

109. Reference 8,page 194

110. Reference 14,page 219

111. Herzberg,G.,"Atomic Spectra and Atomic Structure" Dover.,New York,(1944)

112a. Reference 14,page 299

112b. Reference 8

113. Townes,C.H.,and Schawlow,A.L.,"Microwave Spectroscopy" Mcgraw-Hill.,New York,(1955)

114. Reference 6,page 285

115. Reference 17,page 260

116. Kauzmann,W.,"Quantum Chemistry"Academic press.,(1957) page 581

117. Sadtler's "Standard Spectra".,Sadtler's Laboratories, Pa.

118. Hougen,J.T ,J.Chem.Phys.,41,363,(1964)

119. Callear,A.B.,Proc.Roy.Soc.,276A.,401,(1963)

120. Gordy,W.,Smith,W.V.,and Trambarulo,R,F.,"Microwave Spectroscopy" John Wiley& Sons.,New YOrk (1953).,page 307.

APPENDIX A

CHARACTER TABLE FOR $D_{\infty h}$ POINT GROUP

Species	E	$2C_{\infty}^{\phi}$	$\infty\sigma_v$	i	h	$2S_{\infty}^{\phi}$	∞C_2	
Σ_g^+	1	1	1	1	1	1	1	$\alpha_{xx}+\alpha_{yy}, \alpha_{zz}$
Σ_u^+	1	1	1	-1	-1	-1	-1	T_z
Σ_g^-	1	1	-1	1	1	-1	-1	R_z
Σ_u^-	1	1	-1	-1	-1	-1	1	
Π_g	2	2Cosθ	0	2	-2	-2Cosθ	0	R_x, R_y
Π_u	2	2Cosθ	0	-2	2	2Cosθ	0	T_x, T_y
Δ_g	2	2Cosθ	0	2	2	2Cos2θ	0	
Δ_u	2	2Cosθ	0	-2	-2	-2Cos2θ	0	

CHARACTER TABLE FOR C_{2v} POINT GROUP

Species	E	$C_2(z)$	$\sigma(xz)$	$\sigma(yz)$	
A_1	1	1	1	1	T_z
A_2	1	1	-1	-1	R_z
B_1	1	-1	1	-1	T_x, R_y
B_2	1	-1	-1	1	T_y, R_z

APPENDIX B

DIRECT PRODUCTS OF IRREDUCIBLE REPRESENTATIONS

$C_{\infty v}$ ($D_{\infty h}$) POINT GROUP

	Σ^{+}	Σ^{-}	Π	Δ	Φ
Σ^{+}	Σ^{+}	Σ^{-}	Π	Δ	Φ
Σ^{-}		Σ^{+}	Π	Δ	Φ
Π			$\Sigma^{+},[\Sigma^{-}]\Delta$	Π,Φ	Δ,Γ
Δ				$\Sigma,[\Sigma^{-}],\Gamma$	Π,H
Φ					$\Sigma,[\Sigma^{-}],I$

The above products are for the $C_{\infty v}$ group and may be used for the $D_{\infty h}$ group if gxu=u;gxg=g;uxu=g rules are used;

$C_{\infty v}$ POINT GROUP

	A_1	A_2	B_1	B_2
A_1	A_1	A_2	B_1	B_2
A_2		A_1	B_2	B_1
B_1			A_1	A_2
B_2				B_1

APPENDIX C

HÖNL - LONDON RULES

The intensity distribution in an absorption band is given by the relation

$$I_{KJ} = C \sigma A_{KJ} g_{KJ} e^{-F(K,J)/kT}$$

where A_{KJ} is the line strength, g_{KJ} the statistical weight of the lower state, σ the wavenumber of the line, k the Boltzman constant in cm^{-1}/degree, J is the rotational quantum number and K is the vibronic angular momentum quantum number (for linear molecule $K=l$). The line strengths for a symmetric rotor are given by the Honl-London formula[19] which are given by: for parallel bands ($\Delta K=0$)

R branches ($\Delta J = +1$): $A_{KJ} = \dfrac{(J+1)^2 - K^2}{(J+1)\ (2J+1)}$ (C.1a)

Q branches ($\Delta J = 0$): $A_{KJ} = \dfrac{K^2}{J(J+1)}$ (C.1b)

P branches ($\Delta J = -1$): $A_{KJ} = \dfrac{J^2 - K^2}{J(2J + 1)}$ (C.1c)

for perpendicular bands ($\Delta K = \pm 1$).

R branches ($\Delta J = +1$) $A_{KJ} = \dfrac{(J+2\pm K)(J+1\pm K)}{(J+1)(2J+1)}$ (C.2a)

Q branches ($\Delta J = 0$) $A_{KJ} = \dfrac{(J+1+K)(J+K)}{J(J+1)}$ (C.2b)

P branches ($\Delta J = -1$) $A_{KJ} = \dfrac{(J-1+K)(J+K)}{J(2J+1)}$ (C.2c)

These formulae have been arrived at by evaluating the transition moment due to symmetric rotor wavefunctions

$$\left\langle \Psi_{R'} \middle| \; \theta_{Fg} \; \middle| \Psi_{R''} \right\rangle$$

Here θ_{Fg} represent the direction cosines between the rotating molecule fixed coordinate system (g = x,y,z) and the space fixed coordinate system (F = X,Y,Z).

The matrix element is nonzero for the selection rules of a symmetric rotor and has a magnitude given by the Honl-London formulae, which are evaluated simply by the use of commutation relations. Each A_{KJ} have been weighted with respect to unresolved 2J+1 spatial degeneracy of the rotational J level.

APPENDIX D

FORCE CONSTANTS OF XCX MOLECULES

In terms of internal displacement coordinates R_1 R_2 and R_3 i.e. change in bond length r_{CX_1} change in band angle 2α, and change in bond length r_{CX_2} the valence force field expression for the potential energy is given by[77]

$$2V = k_1(R_1{}^2 + R_3)^2 + 2k_{12}R_1R_3 + k_\alpha R_2^2 \qquad \text{(D.1)}$$

where k_1 is the bond stretching force constant, k_α is the bending force constant and k_{12} is the interaction constant between R_1 and R_2 coordinates. . It can be shown[78] that the forceconstants and frequencies of vibration are related by the following expressions.

$$\lambda_1 + \lambda_2 = \left(1 + \frac{2m_X}{m_C}\cos^2\alpha\right)\frac{k_1 + k_{12}}{m_X} \qquad \text{(D.2a)}$$

$$\lambda_1\lambda_2 = \left(1 + \frac{2m_X}{m_C}\right)\left(\frac{k_1 + k_{12}}{m_X{}^2}\right)\frac{k_\alpha}{r_{12}{}^2} \qquad \text{(D.2b)}$$

$$\lambda_3 = \left(1 + \frac{2m_X}{m_C}\sin^2\alpha\right)\frac{k_1 - k_{12}}{m_X} \qquad \text{(D.2c)}$$

where m_C, m_X stands for the masses of C and X atoms, and $\lambda_k = 5.8894 \times 10^{-2}\omega_k^2$ and $r_{12} = r_1^2 + r_2{}^2 - 2r_1r_2\cos^2\alpha$. If the XCX molecule were linear i.e. $2\alpha = 180°$, (D.2) reduce to

$$\lambda_1 = \frac{k_1 + k_{12}}{m_X} \qquad \text{(D.3a)}$$

$$\lambda_2 = 2\left(1 + \frac{2m_X}{m_C}\right) \frac{k\alpha}{m_X r_{12}^2} \qquad \text{(D.3b)}$$

and

$$\lambda_3 = \left(1 + \frac{2m_X}{m_C}\right) \frac{k_1 - k_{12}}{m_C} \qquad \text{(D.3c)}$$

If λ_1, λ_2 and λ_3 are known, k_1, k_{12} and k_α can be calculated for a linear molecule. For a bent molecule, the angle 2α must also be known.

APPENDIX E

RESOLUTION OF SPECIES OF LINEAR MOLECULES OF $D_{\infty h}$ SYMMETRY INTO THOSE OF C_{2v} SYMMETRY

Change of axes:

$D_{\infty h}$	x	y	z
	$\downarrow$	$\downarrow$	$\downarrow$
C_{2v}	x	z	y

Species

	$D_{\infty h}$		C_{2v}
	Σ_g^+	—	A_1
	Σ_u^+	—	B_2
	Σ_g^-	—	B_1
	Σ_u^-	—	A_2
	Π_g	—	$A_2 + B_2$
	Π_u	—	$A_1 + B_1$
	Δ_g	—	$A_1 + B_1$
	Δ_u	—	$A_2 + B_2$
For S = 1	Σ_g^-	—	A_2
	Π_g	—	$B_1 + B_2$

APPENDIX F

DISTRIBUTION OF CSe_2 MOLECULES IN THE GROUND STATE v_2'' LEVELS

The fraction of CSe_2 molecules in v_2'' levels were calculated separately by the expression

$$\frac{Ni}{N} = \frac{d_i \exp(-G(v_i)/kT)}{\sum d_i \exp(-G(v_i)/kT)}$$

The fractions were calculated for four different temperatures used experimentally, assuming that $G(v_2)'' = \omega_2^{o}{}'' v_2$ The results are: for $\omega_2{}^0 = 313\ \mathrm{cm}^{-1}$

T	v_2''		
	0	1	2
-42°C	0.77	0.15	0.02
RT	0.66	0.22	0.06
100°C	0.59	0.28	0.10
200°C	0.50	0.33	0.15

If other factors in (1.22) are equal, the relative intensities of absorption transitions for $v_2''=0,1,2$ levels are proportional to their respective fractions given above at each temperature.

APPENDIX G

ROTATIONAL LEVELS OF A NEAR PROLATE TOP

Polo[108] obtained the expressions for the energy levels of a near symmetric rotor in terms of the parameter 'b' given in section 4.8. His formula can be written as

$$F_V(J,\ K) = 1/2\ (B_V + C_V)J(J+1) + \bar{A}_V$$
$$\times\left(1 - \frac{3}{8}b^2 - \frac{51}{512}b^4 - \ldots\right)K^2 + \Delta B^K\ J(J+1)$$
$$+ \Delta D^K\ J^2(J+1)^2 + \Delta H^K\ J^3(J+1)^3 + \ldots$$

where the coefficients ΔB^K, ΔD^K and ΔH^K are given by,

for K = 0:

$$\Delta B^0 = \bar{A}_V\left(\frac{1}{4}b^2 + \frac{9}{128}b^4 + \ldots\right)$$

$$\Delta D^0 = \bar{A}_V\left(-\frac{1}{8}b^2 - \frac{19}{128}b^4 + \ldots\right)$$

$$\Delta H^0 = \bar{A}_V\left(-\frac{3}{512}b^4 + \ldots\right) \qquad (G.1)$$

for K = 1:

$$\Delta B^1 = \bar{A}_V \times$$
$$\left(\pm\frac{1}{2}b + \frac{1}{4}b^2 \mp \frac{3}{128}b^3 + \frac{9}{128}b^4 \mp\right)$$

$$\Delta D^1 = \bar{A}_V\left(-\frac{1}{32}b^2 \pm \frac{1}{64}b^3 - \frac{35}{3072}b^4 \pm\right)$$

$$\Delta H^1 = \bar{A}_V\left(\pm\frac{1}{512}b^3 + \frac{1}{1536}b^4 \mp\right) \qquad (G.2)$$

for K = 2:

$$\Delta B^2 = \bar{A}_V\left(\frac{1}{8}(2 \pm 1)b^2 + \frac{1}{128}(9 \pm 4)b^4 + \ldots\right)$$

$$\Delta D^2 = \bar{A}_V \qquad \times$$
$$\left(\frac{1}{48}(2 \mp 1)b^2 + \frac{1}{2048}(23 \mp 32)b^4 + \ldots\right)$$

$$\Delta H^2 = \bar{A}_v \left(\frac{1}{18432}(57 \mp 64)\, b^4 + \ldots \right) \tag{G.3}$$

For K = 3

$$\Delta B^3 = \bar{A}_v \left(\frac{1}{4} b^2 \pm \frac{3}{128} b^3 + \frac{9}{128} b^4 \pm \ldots \right)$$

$$\Delta D^3 = \bar{A}_v \left(-\frac{1}{64} b^2 \mp \frac{1}{64} b^3 + \frac{61}{10240} b^4 \mp \right) \ldots$$

$$\Delta H^3 = \bar{A}_v \left(\pm \frac{1}{512} b^3 - \frac{3}{5120} b^4 \pm \right) \tag{G.4}$$

where $\bar{A}_v = (A_v - 1/2\ (B_v + C_v))$

APPENDIX H

Values of A, B and C Constants (in cm^{-1}) in a bent CSe_2 Molecule, for different Values of r_{CSe} (Å) and $\widehat{SeCSe}$ Angle (For method of calculation see reference 114)

r_{CSe}	$\widehat{SeCSe}$	Å	B	C	$K=2\frac{[B-1/2(A+C)]}{A-C}$
1.711Å	180°		0.0360	0.0360	-1.0000
	150°	7.6980	0.0386	0.0384	-0.9999
	*120°	2.0627	0.0480	0.0469	-0.9989
1.811Å	180°		0.0321	0.032	-1.0000
	150°	6.8914	0.0344	0.0342	-0.9999
	*120°	1.8412	0.0428	0.0418	-0.9989
1.911Å	180°		0.0288	0.0288	-1.0000
	150°	6.1710	0.0309	0.0308	-0.9999
	*120°	1.6536	0.0384	0.0376	-0.9989
2.011Å	180°		0.0260	0.0260	-1.0000
	150°	5.5726	0.0279	0.0278	-0.9999
	120°	1.4931	0.0347	0.0339	-0.9989
2.111Å	180°		0.0236	0.0236	-1.0000
	120°	1.3550	0.0315	0.0308	-0.9997
	150°	5.0571	0.0253	0.0252	-0.9984

---

* If a value of r_{CSe} = 1.711 Å is assumed for the linear molecule, then B" = 0.0360 cm^{-1}. For higher value of r_{CSe}, at angles marked by* (or angles close to it), B values are higher than 0.0360 cm^{-1}.

APPENDIX I

OSCILLATOR STRENGTHS OF THE R, V AND A ABSORPTIONS

The oscillator strengths of the three absorptions were obtained from the equation[17]

$$f_{nm} = 4.319 \times 10^{-9} \times \gamma \times \int \epsilon_\sigma d\sigma \ldots \quad (I.1)$$

where ϵ_σ is the extinction coefficient in litre mole^{-1} cm^{-1} at wavenumber σ, γ is a constant and the integration is over the entire absorption band. If the absorber is in the gas phase, γ is unity. If the absorber is in the solution phase, it is given by an expression[116] related to the refractive index of the solvent. The refractive index of methylene chloride at 25° C is 1.3348 (Handbook of Physics and Chemistry, 48th Ed.) and for this value, $\gamma = 0.84$.

The integral in (I.1) was not evaluated directly. Instead, the following approximation[17]

$$\int \epsilon_\sigma d\sigma = \varsigma\, \epsilon_{max} \Delta\sigma_{1/2} \quad \ldots \quad (I.2)$$

was used. ϵ_{max} is the maximum molar extinction co-efficient and $\Delta\sigma_{1/2}$ is the width at half height in cm^{-1}. A further simplification of (I.2) was obtained by assuming that the plot of ϵ_σ against σ is triangular in shape; for this assumed shape, the value of ς is unity.

The following form of the Beer - Lambert's law[16] is used to calculate ϵ_{max}

$$D = \log_{10} I_o/I = \epsilon_{max} \times c \times l \quad \ldots \quad (I.3)$$

I_o and I are the intensity of radiation incident on and transmitted by the sample, respectively. 'c' is the concentration of the sample in moles per litre and 'l' is the absorption path length in cm. D is the absorbance, measured off the Cary 14 spectrograms for each of the three absorptions.

The oscillator strengths of the R and V systems were calculated from the solution spectra of CSe_2 in methylene chloride. For the A system, the oscillator strength was obtained in the vapour phase. In each absorption band, $\Delta\sigma_{1/2}$ was obtained from the wavelengths measured at half the intensity height. The final form of the equation (I.1) used in the calculation is given by

$$f_{nm} = 4.319 \times 10^{-9} \times k \times \epsilon_{max} \times \Delta\sigma_{1/2} \ldots \quad (I.4)$$

The data used and results obtained are tabulated below:-

System	$c \times l$ $\frac{\text{moles} \times \text{cm}}{\text{litre}}$	D	ϵ_{max}	Mean $\Delta\sigma_{1/2}$	f_{nm}
	.002	0.14	-	-	-
R (CSe_2)	.001	0.09	55	2430	10^{-4}
	.0005	0.06			
	.002	1.08			
V (CSe_2)	.001	0.52	530	2300	10^{-3}
	.0005	0.31			
A (CSe_2)	.0025	1.85	7030	2300	10^{-1}
V (CS_2)	.325	1.84	53	2200	10^{-4}

The value of f_{nm} has been rounded off to the nearest power of 10. They are expected to be in error by a factor of 10. The maximum experimental uncertainty was in the concentrations of the absorber (refer to section 2.2). The f_{nm} value for CS_2 was obtained from the solution spectrum of CS_2 in cyclohexane given in Sadtler's charts[117].

APPENDIX J

ISOTOPIC SPECIES OF CSe_2

The number of isotopic species formed during the synthesis of CSe_2 from natural selenium is calculated thus :

a. No. of stable isotopics of Selenium = 6

b. No of available selenium positions in CSe_2 = 2

c. No. of species of CSe_2 which contain the same Se atoms .. = 6

d. No. of species of CSe_2 which contain different Se atoms . $= \frac{6!}{4!2!} = 15$

Total number of species of CSe_2 (c+d) = 21

The ratio of the number of molecules of one species with respect to that of another is determined from elementary considerations on probability. Let us assume that there are 100 atoms of natural selenium available. From percentage natural abundances given in Table 5-1, it is seen that there are 50 atom of Se^{80} among 100 atoms of Se^{nat}. Between the two positions in CSe_2, the probability of Se^{80} occupying the first position is 50/100; and the probability of Se^{80} occupying the second position is 49/99. The probability of Se^{80} occupying both is given by the product :

$$\frac{50}{100} \times \frac{49}{99} = 0.25 \qquad (J.1)$$

The result is the fraction of 80-80 molecules in CSe_2^{nat}. The molecular fraction of each of the 21 species were found in the same way; each fractionwas then multiplied by 400 and then entered in the last column of Table 5-1. It can be shown similarly that for a 1:1 w/w mixture of Se^{80} : Se^{78}, three species of CSe_2 are formed with a molecular ratio of 1:2:1.

THE (R) $\tilde{a} \leftarrow \tilde{X}$ SYSTEM OF CSe_2 (80-80) & (78-78) MOLECULES

Contact prints of spectrograms, recorded on a 35 ft. Eagle spectrograph (in the 3rd order), are reproduced in four successive panels of this Appendix.

1. Σ-Σ type bands of the 80-80 species and π-π type bands of the 78-78 species are marked. Connecting lines are shown between bands of isovibronic transitions. All assigned bands are not marked.
2. The quantum numbers v_1'', v_2'' are given at the end of each panel and v'_1, v'_2 are given for each band.
3. At the violet end of the spectrum, some weak bands of the V system are shown.

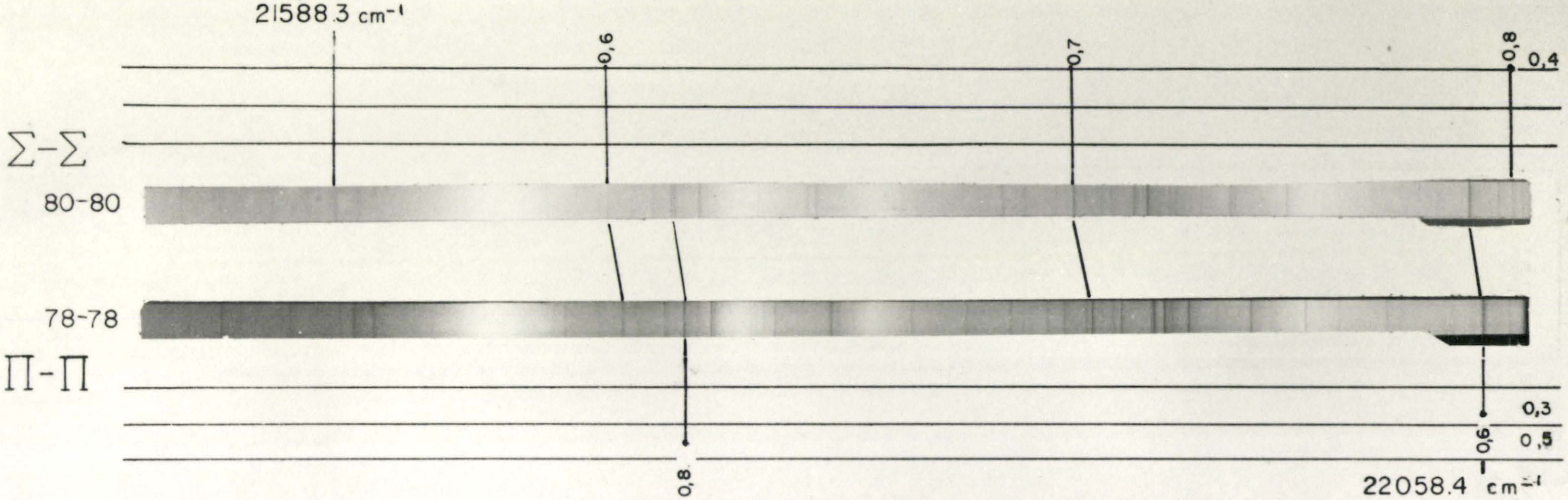

APPENDIX K — R system (4630- 4520 Å)

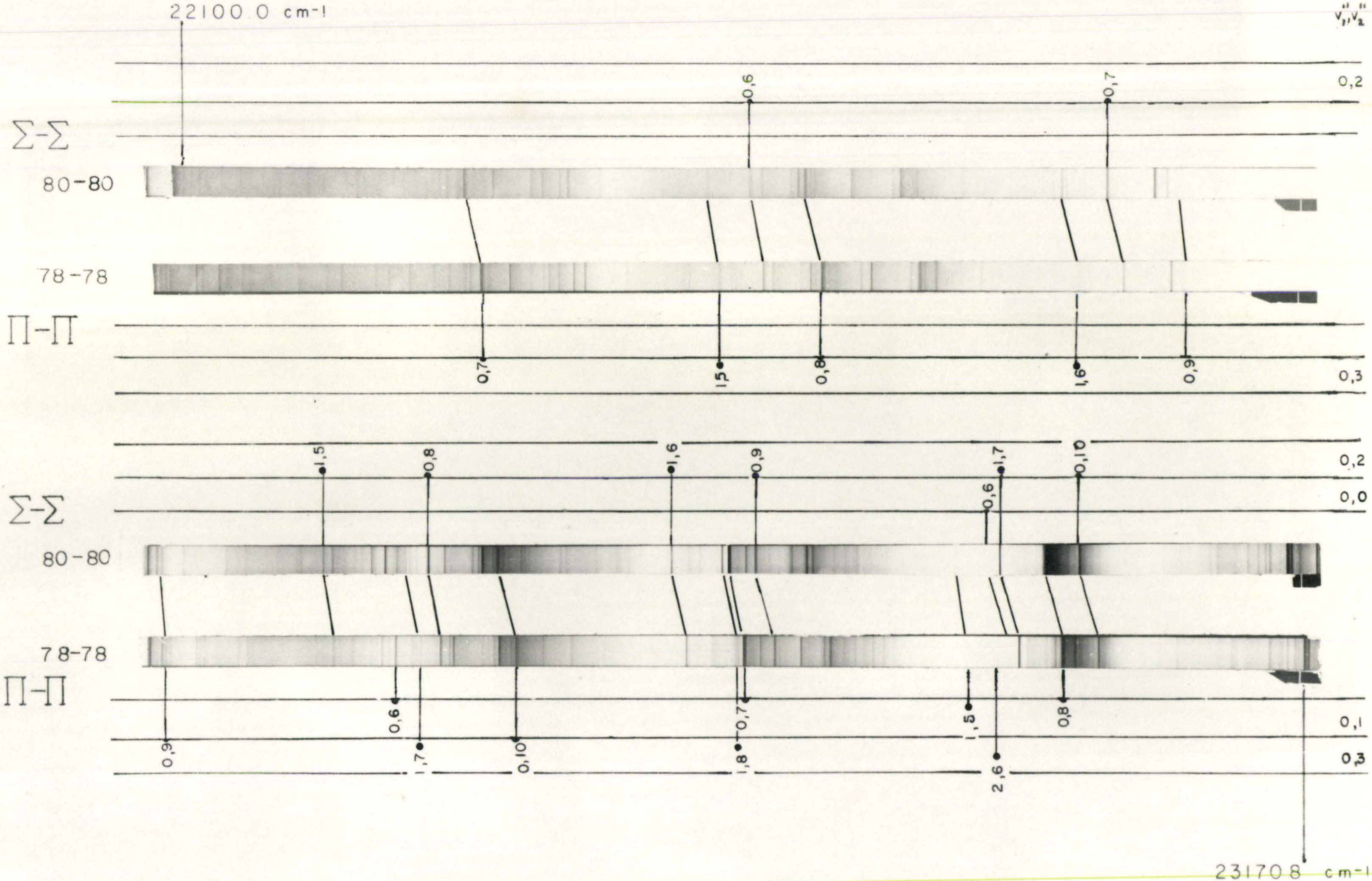

APPENDIX K—R system (4530-4310 Å)

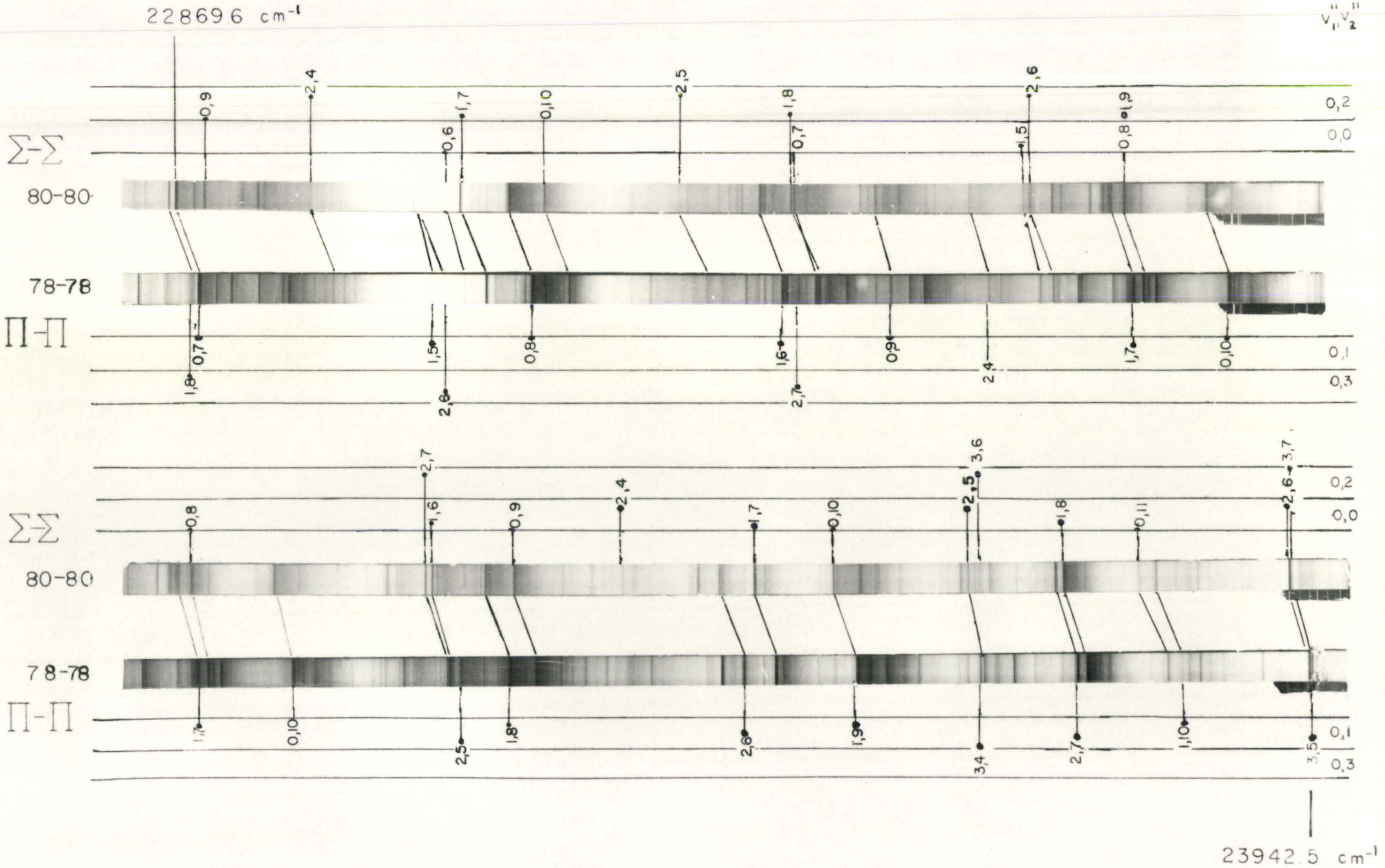

APPENDIX K.— R system (4370- 4170 Å)

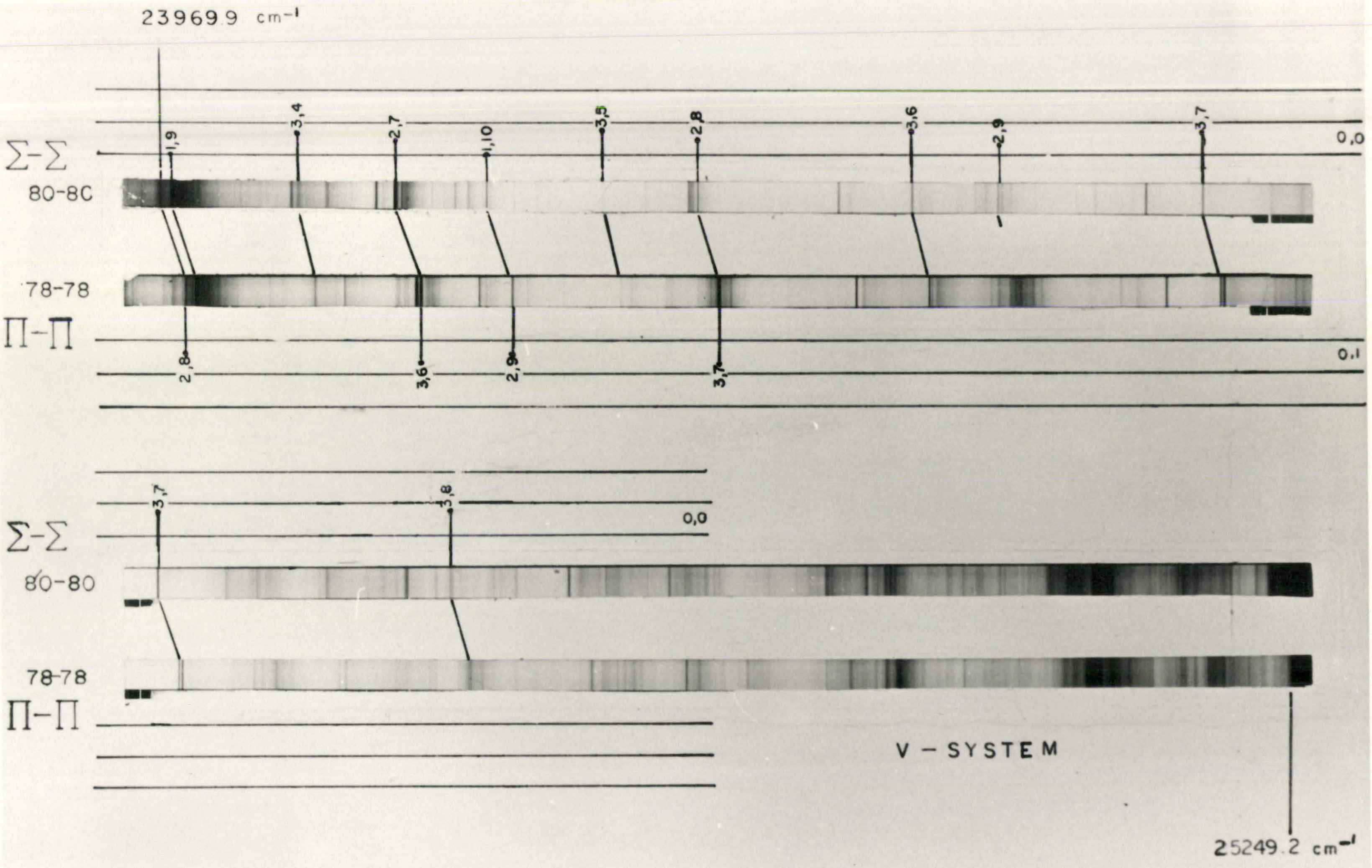

APPENDIX K.– R&V systems(4170-3940 Å)

APPENDIX L

BANDS OF CSe_2 IN THE 25251-21326 cm^{-1} REGION

1. Wavenumbers of observed band heads and measurable features are given below for both 80-80 and 78-78 molecules.

2. Intensities (I) are quoted relative to a maximum value of 100. If no value is quoted, the intensity of the band head or features must be assumed to be small.

3. Isotopic shifts for band heads, $\Delta\sigma_1 = \sigma_H(78\text{-}78) - \sigma_H(80\text{-}80)$ and $\Delta\sigma_2 = \sigma_H(78\text{-}80) - \sigma_H(80\text{-}80)$ are given for isovibronic transitions. The latter quantity is given only for the most intense bands.

4. Bands whose wavenumbers are greater than 24600 cm^{-1} may be due to both R and V systems.

5. The notations c = cold band; mc = possibly cold band; m = cold or hot band; mh = possibly hot band and h = hot band apply. These notations are given for the more intense bands.

6. Most of the bands below 22059 cm^{-1} are hot bands and are observed with greater intensity at higher temperatures. These bands are also observed in multiple reflection cells. Intensity values for these bands at room temperature are not given.

I	σ_{80-80}	$\Delta\sigma_1$	σ_{78-78}	I	$\Delta\sigma_2$
			25264.0		
70	25251.6	5.5	25257.1		
50	243.3	5.9	249.2		
30	237.1		221.8		
5	226.3		212.6		
25	181.4		206.6		
10	180.3		196.1		
40	137.5		188.4		
30	136.9		182.6		
30	134.2		179.9		
30	133.6		162.0		
60	125.5		159.9		
			147.0		
			141.7		
			136.3		
			129.0		
40	109.9		125.7		
25	098.7		121.0		
			25045.3		
30	25003.3		25038.4		
30	000.3		25020.2		
20	24997.3		25005.8		
40	985.8		24999.3		
25	960.8		24997.7		

			960.7	
			931.8	
			911.7	
25	24865.8	9.9	24875.7	
			845.2	
			844.4	
10	24827.7		838.9	
			834.3	
			825.2	
35	24805.2	13.6	24818.8	
10	24774.2			
5	760.8			
10	735.6		24753.9	
5	734.8		746.5	
5	732.4		745.4	
			743.7	
			725.7	
5	729.8		724.8	
25	709.1		721.8	25
10	707.9			
15	661.6	10.8	672.4	
10	657.6	11.6	669.2	
			24640.6	
	620.6		635.3	
	618.7		632.1	
10	603.0		619.3	
			607.1	

50c	24563.5	13.6	24577.1	50	
	562.9	12.4	575.3	50	
			570.4		
			566.2		
			544.0		
50c	24529.9	13.3	543.2	40	
	529.5	13.7			
	522.7				
10	500.3		527.0	10	
10	489.2		526.0		
			24516.7	10	
	466.1				
	450.9		24465.2		
15	446.6		465.5	10	
20mc	443.5		455.2	10	
10	436.3		452.3	20	
10	429.9		444.8	15	
	419.6		441.0	10	
	405.2				
	402.0		407.5		
	394.0	12.8	406.8		5.8
40	24393.5	11.7	24405.2	30	
10 <	377.1				
40	352.1		367.6	20	
40	24351.5	11.3	24362.8	30	
40	351.0		24346.6		
			324.0	5	

	318.3		24290.5	25	
60mc	24270.6	13.4	24284.0	25	6.2
60mc	264.9	19.1	284.0	80	
	256.5		283.7		
			271.9		
	249.7		266.5		
			258.3		
10	241.0	13.1	254.1	10	
			253.7		
10<	216.5		234.0	10	
10<	203.8				
10<	188.3		228.3	10	
	188.2				
	187.0		24195.6	5	
	179.5		24187.5		
10<	166.8		175.2		
15	151.3	15.8	167.1	25	7.7
	149.0	17.7	166.7	25	
10<	140.8	11.7	152.5	5	
	133.3	15.0	148.3		
	127.3		148.1	10	
	121.4				
	120.3				
15	24103.4	11.5	24114.9	80	
90m	24099.4	13.1	112.5	80	6.7
20	24089.2		103.4	10	
	073.5				
10<	24063.5	19.7	24083.2	15	

	063.0			
10	24046.1		073.0	5 <
	47.0			
	42.7			
15	24042.1	14.6	056.7	15
			24031.6	5 <
10 <	23987.5			
90	23976.2	14.6	23990.8	70
16	970.3		989.2	10
10	969.9		985.8	25
10 <	952.3		973.0	5 <
			23956.0	5 <
			944.2	50
70c	23930.4	12.9	943.3	50
	23932.7	12.1	942.5	60
			937.9	5 <
			936.8	5 <
			926.8	5 <
	23904.8	11.6	916.4	
	904.8*		914.1	
	894.5		911.4	
10	23880.6		895.6	10
			888.1	10 <
10 <	872.2		883.7	20
			883.3	
			877.8	
10	869.0		23876.8	10
			873.2	10

20	23858.4	7.2	865.6	20	
10	849.3				
	848.3				
10<	841.3	14.9	856.2	10<	6.8
15	819.2				
100c	23807.7	13.7	821.4	100	
70	23803.2	12.9	816.1	80	
	23801.6		814.8	10	
	799.5				
	792.1		807.8	10	
			801.7		
			798.8		
10	782.3		793.4	10	
			793.1		
20	23767.3	15.5	23782.8	50	
10	762.3	9.0	23771.3	10	
10	759.6				
25	23755.0	10.6	765.6	20	
15	23752.1	11.8	763.9	20	
			755.8	20	
	735.6		752.1		
10	719.5	11.2	23730.7		
	708.3				
20	706.8				
50	699.2	14.5	713.7	60	
50	23698.2		704.7	30	

70m	23683.7	14.2	697.9	90	
10 <	23676.3		686.1	10	
			676.7	10 <	
	647.6	10.6	658.2	25	
90mc	641.5	12.2	653.7	80	6.1
	23624.5		23647.6	15	
50mc	23623.3	14.1	23637.4	60	
			629.9	10 <	
40c	23611.8	13.8	625.6	60	
	607.8	11.8	619.6	10	
			618.3	10	
15	577.7				
20	571.8	16.0	23587.8	20	
10	561.6		577.8	10	
10	23556.1				
10	555.5	9.2	564.7	15	
15	23540.3	13.2	553.5	20	
			539.9	20	
100c	23514.7	12.4	23527.1	100	6.2
90mc	23499.4	14.0	23513.4	100	7.6
10	497.2		507.0	5	
10	488.7	10.7	499.4	15	
50m	474.5	13.0	23487.5	35	
60c	468.5	14.8	483.3		
70	471.6	9.0	480.6	25	5.2
50	468.2	13.4			
50	468.0	13.6	481.6	50	

			476.7	25	
15	453.1		459.8	10	
37	448.2	9.7	457.9	20	
			456.9	20	
10	446.4		455.6	20	
			448.2	10	
			445.4	10	
			23441.4		
10<	422.9		431.1	10 <	
			419.0	10 <	
			418.7		
10	23402.7	9.3	412.0	20	
	394.8				
70mh	23388.4	12.3	23400.7	90	6.7
			399.9	90	
	379.7				
	355.8	7.1	23362.9	70	
			359.2	25	
95mc	23347.4	8.9	356.3*	80	
60	340.9	15.4	356.3	80	5.2
50	335.8		350.8	80	
40	336.8	15.0	351.8	80	
40	335.4		347.4	20	
			342.5	5	
35	23329.8	11.1	340.9	15	
			324.5		
25	23314.7	9.6	324.3	25	

40	310.0	12.7	322.7	40	
35	23298.8	13.1	23311.9	25	
15	23297.5	14.9	23312.4	15	
	295.2	8.2	303.4	15	
			302.1	10	
			23283.8	10	
25	267.5	9.3	276.8	15	
	256.4	9.9	276.3	10	
			264.6	10 <	
10<	245.7	8.4	264.1	10 <	
10	249.6		253.4	10 <	
			244.8	70	
45	23231.7	11.8	243.5	70	
	225.1				
30	223.8	12.6	23236.4	50	
50h	220.1	6.7	226.8	40	
50	219.6		226.3	30	
7	215.9				
20	211.9	7.0	218.9	20	2.9
			23204.5		
30	184.5		204.1	50	
75c	178.2	9.9	188.1	75	
95c	176.5	13.1	189.6	75	
20	167.4		179.1	10	
75m	23163.3	9.9	173.2	85	
90m	23161.3	10.0	171.3	90	

90m	160.8	10.0	170.8	90	
			168.2	10	
15	149.7		166.0	15	
25	151.6	10.7	162.3	20	
10	145.5		159.3	10 <	
10	139.9		153.3	25	
			152.5	25	
	23124.1		132.4		
10	23096.2	8.0	23104.2	15	
55	23052.2	11.4	23063.6	35	
			051.6	30	
100m	23034.6	10.1	044.7	90	4.0
			044.3	90	4.1
10	23033.0		041.2	20	
			040.2		
			035.1		
			036.4		
			026.2	10	
65 m	23010.1	11.8	021.9	70	5.8
	10.0				
			016.6	10	
10 <	23003.5	7.4	010.9	15	
10 <	002.3				
			23000.6	10 <	
15	22987.4	7.5	22994.9	10	3.3
	986.7	7.4	994.1		
	942.6		22951.7	10	
8	938.9		945.9	10	

	22929.8		936.7	10	
			929.8	10 <	
40	910.6	13.5	924.1	30	
	10.1	13.6	923.7	30	
30	22913.1	7.9	921.0	20	
25h	902.7	6.3	909.0	45	
			908.7	45	
40	22883.8	11.7	895.5	50	
	883.5				
30	878.7	9.2	887.9	35	
85m	870.1	9.5	879.6	90	4.8
85	869.6	9.4	879.0	90	4.7
	866.8				
40	866.3		22876.9	15	
	863.8		22870.5		
15	22854.7	9.0	863.7	10	
5	849.3	13.1	862.4	10	
45	840.2	9.2	849.4	55	4.8
			845.0		
	818.4		825.9	10 <	
	801.6				
10	786.4				
15	22783.3	7.4	22790.7	20	
10	764.3				
	763.1		776.9	15	
	754.8				
30	752.2	11.0	763.2	35	

			754.5		
50	22744.0	11.3	755.3	60	5.5
	742.1		752.2		
20	739.1		746.3		
20	22724.6	6.6	731.2	40	
			22729.3	15	
50	715.1		22725.1	45	
50	22716.4	8.2	724.6	45	
10	705.2	9.7	714.9	10 <	
15	700.8		710.1	10	
45	22694.8	7.3	22702.1	50	
45	694.5	7.4	701.9	50	3.2
	689.8		698.8	15	
25	687.7	7.6	695.3	20	
	683.2				
20	668.5		22671.4	15	
20	22664.0	6.8	670.8		
10 <	625.8		628.5	10	
	616.0	8.0	624.0	10	
			607.0	10	
			604.9	10	
25	22594.5		603.2	15	
20	583.7		586.2	15	
25	581.0				
40	22576.8	9.1	585.9	25	
80mh	570.8	9.2	22580.0	75	4.6

80m	570.3		579.2	75	
60h	22547.2	9.3	556.5	55	
			553.1	20	
			537.0	15	
30h	22527.4	9.4	536.8	15	
40	22525.8	8.5	534.3	25	
40	25.2		533.9	25	
10	520.1				
20	476.6	9.6	22486.2	15	
	75.7				
5	22455.9	8.2	464.1	20	
35	22446.5				
35	445.5	9.8	456.3	35	
20	441.6	10.1	451.7	15	
25	422.4	9.9	432.3	30	
5	421.4	10.6	432.0	30	5.3
10	403.3				
20	401.2		427.0	15	
55	399.1	10.0	22409.1	60	4.9
55	398.9	9.2	22408.1	60	
30	395.4	6.8	22402.2	20	
20	391.7	5.9	22397.6	10 <	
15	377.9	5.9	383.8	15	
25	372.7				
25h	371.6	7.7	379.3	30	
15	351.1	9.3	360.4	15	
10	337.1		343.1	10 <	

10 <	329.4				
5 <	318.8				
15	306.3	6.3	22312.6	10	
15	298.7	8.3	307.0	10	
30	283.4	8.9	292.3	25	
15	279.5	8.4	287.9	20	
25	271.1	8.5	279.6	15	
15	265.7	9.5	275.2	15	
			266.5	10 <	
30	22247.7	8.7	256.4	25	4.2
50	234.1	9.0	243.1	45	4.4
50	233.5	8.8	242.3	45	4.1
10	230.8				
10	229.9	7.3	22237.2	15	
10	225.8				
15	221.0		22227.1	10	
5 <	215.2	6.8	212.0	10	
5 <	198.1	9.8	207.9	15	
5 <	196.4		192.0	10 <	
5	182.5		175.7	10 <	
15	158.9	9.7	168.6		
5 <	127.2		155.7	10	
5 <	118.2		122.6	10 <	
	22114.0				
5 <	107.5	10.9	118.4	15	
	103.6	6.9	22110.5	10	
	100.0		107.5		

10	085.1		22095.3		
10	080.0		094.0		
10	075.6				
30	22059.0	6.7	22065.7	30	
	058.4	6.7	22065.1	30	
	22046.3				
	22026.6				
	22021.4				
	22002.6				
15	21988.2	8.6	21996.8	20	
	21976.1				
	21967.1				
10	21966.8	9.3	21976.1	10	4.9
	955.4				
	945.6				
	942.5	4.9	947.4		
	934.7	8.0	942.7		4.1
	931.0				5.6
	929.8				
	917.4				
	21906.5	8.5	21915.0		4.3
	887.9				5.0
	21879.1				
	21862.0				
	21843.9				
	21816.1				
	809.1	7.0	816.1		3.3

21805.9			
21804.9			
21793.1			
21787.4			
21781.9			
21765.4			
21758.7			
21755.7	5.6	21761.3	3.0
21754.6			3.0
21748.3			
21747.0			
21732.2			
21730.1	8.1	21738.2	4.8
21716.9			
21708.1	8.8	21716.9	4.3
21677.0	4.5	21681.5	
21638.9			
21638.2			
21630.7	8.2	21638.9	
21629.9	8.3	21638.2	4.3
21607.4	7.9	21615.3	3.9
21589.4			
21588.3			
21585.9			3.5
21574.3			
21564.6			
21552.6			2.1

21533.6			
21526.5			4.3
21526.5			
21496.0	7.6	21503.6	3.6
21458.6			
21454.9			
21448.1			3.3
21445.8			
21429.7			
21414.2			
21413.5			
21343.6			
21343.3			
21326.5			4.2